General Disclaimer

One or more of the Following Statements may affect this Document

- This document has been reproduced from the best copy furnished by the organizational source. It is being released in the interest of making available as much information as possible.

- This document may contain data, which exceeds the sheet parameters. It was furnished in this condition by the organizational source and is the best copy available.

- This document may contain tone-on-tone or color graphs, charts and/or pictures, which have been reproduced in black and white.

- This document is paginated as submitted by the original source.

- Portions of this document are not fully legible due to the historical nature of some of the material. However, it is the best reproduction available from the original submission.

Produced by the NASA Center for Aerospace Information (CASI)

U-2037 36
c. 2.

400
NO

MSC INTERNAL NOTE NO. 65-FM-45

GENERAL PARAMETRIC REENTRY STUDY FOR NEAR EARTH ORBITS

By: Frank J. Suler

N70-35665 (ACCESSION NUMBER) (THRU) 1
181 (PAGES) (CODE) 30
TMX-64584 (NASA CR OR TMX OR AD NUMBER) (CATEGORY)
FACILITY FORM 602

RECEIVED
AUG 1970
NASA ST FACILITY
INPUT BRANCH

NATIONAL AERONAUTICS AND SPACE ADMINISTRATION

MANNED SPACECRAFT CENTER

HOUSTON, TEXAS

APRIL 29, 1965

[redacted]

MSC INTERNAL NOTE NO. 65-FM-45

GENERAL PARAMETRIC REENTRY STUDY FOR NEAR EARTH ORBITS

Prepared by: Frank J. Suler

Frank J. Suler

Approved: Carl R. Huss

Carl R. Huss
Chief, Flight Analysis Branch

Approved: John P. Mayer

John P. Mayer
Chief, Mission Planning and
Analysis Division

NATIONAL AERONAUTICS AND SPACE ADMINISTRATION

MANNED SPACECRAFT CENTER

HOUSTON, TEXAS

April 29, 1965

TABLE OF CONTENTS

Section		Page
1.0	Introduction	1
2.0	Discussion and results	1
	2.1 Method of calculation	1
	2.2 Geometry and assumed constants	2
	2.3 Examples	2
	2.3.1 Figures 1 and 2, elliptical orbit reentry	2
	2.3.2 Figure 39, circular orbit reentry . . .	3
	2.4 Converting given conditions to other reference altitudes	3
	2.5 Parking orbits as a function of cutoff conditions for various insertion altitudes . .	3
	2.6 Comments	4
3.0	Conclusions	4
4.0	References	4
5.0	Figures 1 through 40	5
6.0	Acknowledgment	45
7.0	Distribution	46

LIST OF FIGURES

Figure

1 Inertial flight-path angle versus inertial velocity (400000 feet) as a function of retrograde true anomaly, ΔV, and attitude for various elliptical orbits.

a. $h_p = 80$, $h_a = 100$ nm
b. $h_p = 80$, $h_a = 150$ nm
c. $h_p = 80$, $h_a = 200$ nm
d. $h_p = 85$, $h_a = 100$ nm
e. $h_p = 87$, $h_a = 100$ nm
f. $h_p = 87$, $h_a = 150$ nm
g. $h_p = 87$, $h_a = 161$ nm
h. $h_p = 87$, $h_a = 200$ nm
i. $h_p = 90$, $h_a = 100$ nm
j. $h_p = 90$, $h_a = 150$ nm
k. $h_p = 90$, $h_a = 200$ nm
l. $h_p = 100$, $h_a = 120$ nm
m. $h_p = 100$, $h_a = 150$ nm
n. $h_p = 100$, $h_a = 200$ nm
o. $h_p = 100$, $h_a = 250$ nm
p. $h_p = 100$, $h_a = 400$ nm
q. $h_p = 120$, $h_a = 140$ nm
r. $h_p = 120$, $h_a = 150$ nm
s. $h_p = 120$, $h_a = 200$ nm
t. $h_p = 120$, $h_a = 250$ nm
u. $h_p = 140$, $h_a = 150$ nm
v. $h_p = 140$, $h_a = 200$ nm
w. $h_p = 140$, $h_a = 250$ nm
x. $h_p = 140$, $h_a = 400$ nm

LIST OF FIGURES (Continued)

Figure

2 Inertial flight-path angle and velocity at 400000 feet as a function of retrograde true anomaly and a constant ΔV for an elliptical orbit where h_p = 80 nm and h_a = 100 nm.
a. ΔV = 100 fps
b. ΔV = 300 fps
c. ΔV = 500 fps
d. ΔV = 700 fps

3 Inertial flight-path angle and velocity at 400000 feet as a function of retrograde true anomaly and a constant ΔV for an elliptical orbit where h_p = 80 nm and h_a = 150 nm.
a. ΔV = 100 fps
b. ΔV = 300 fps
c. ΔV = 500 fps
d. ΔV = 700 fps

4 Inertial flight-path angle and velocity at 400000 feet as a function of retrograde true anomaly and a constant ΔV for an elliptical orbit where h_p = 80 nm and h_a = 175 nm.
a. ΔV = 80.5 fps
b. ΔV = 161.0 fps
c. ΔV = 241.5 fps
d. ΔV = 322.0 fps
e. ΔV = 402.5 fps

5 Inertial flight-path angle and velocity at 400000 feet as a function of retrograde true anomaly and a constant ΔV for an elliptical orbit where h_p = 80 nm and h_a = 200 nm.
a. ΔV = 100 fps
b. ΔV = 300 fps
c. ΔV = 500 fps
d. ΔV = 700 fps

6 Inertial flight-path angle and velocity at 400000 feet as a function of retrograde true anomaly and a constant ΔV for an elliptical orbit where h_p = 85 nm and h_a = 100 nm.
a. ΔV = 100 fps
b. ΔV = 300 fps
c. ΔV = 500 fps
d. ΔV = 700 fps

LIST OF FIGURES (Continued)

Figure

7 Inertial flight-path angle and velocity at 400000 feet as a function of retrograde true anomaly and a constant ΔV for an elliptical orbit where h_p = 87 nm and h_a = 100 nm.
a. ΔV = 100 fps
b. ΔV = 300 fps
c. ΔV = 500 fps
d. ΔV = 700 fps

8 Inertial flight-path angle and velocity at 400000 feet as a function of retrograde true anomaly and a constant ΔV for an elliptical orbit where h_p = 87 nm and h_a = 150 nm.
a. ΔV = 100 fps
b. ΔV = 300 fps
c. ΔV = 500 fps
d. ΔV = 700 fps

9 Inertial flight-path angle and velocity at 400000 feet as a function of retrograde true anomaly and a constant ΔV for an elliptical orbit where h_p = 87 nm and h_a = 161 nm.
a. ΔV = 80.5 fps
b. ΔV = 100. fps
c. ΔV = 161. fps
d. ΔV = 241.5 fps
e. ΔV = 300. fps
f. ΔV = 322. fps
g. ΔV = 402.5 fps
h. ΔV = 500. fps
i. ΔV = 700. fps

10 Inertial flight-path angle and velocity at 400000 feet as a function of retrograde true anomaly and a constant ΔV for an elliptical orbit where h_p = 87 nm and h_a = 200 nm.
a. ΔV = 100 fps
b. ΔV = 300 fps
c. ΔV = 500 fps
d. ΔV = 700 fps

11 Inertial flight-path angle and velocity at 400000 feet as a function of retrograde true anomaly and a constant ΔV for an elliptical orbit where h_p = 90 nm and h_a = 100 nm.
a. ΔV = 100 fps
b. ΔV = 300 fps
c. ΔV = 500 fps
d. ΔV = 700 fps

LIST OF FIGURES (Continued)

Figure

12 Inertial flight-path angle and velocity at 400000 feet as a function of retrograde true anomaly and a constant ΔV for an elliptical orbit where h_p = 90 nm and h_a = 150 nm.
a. ΔV = 100 fps
b. ΔV = 300 fps
c. ΔV = 500 fps
d. ΔV = 700 fps

13 Inertial flight-path angle and velocity at 400000 feet as a function of retrograde true anomaly and a constant ΔV for an elliptical orbit where h_p = 90 nm and h_a = 200 nm.
a. ΔV = 100 fps
b. ΔV = 300 fps
c. ΔV = 500 fps
d. ΔV = 700 fps

14 Inertial flight-path angle and velocity at 400000 feet as a function of retrograde true anomaly and a constant ΔV for an elliptical orbit where h_p = 100 nm and h_a = 120 nm.
a. ΔV = 100 fps
b. ΔV = 300 fps
c. ΔV = 500 fps
d. ΔV = 700 fps

15 Inertial flight-path angle and velocity at 400000 feet as a function of retrograde true anomaly and a constant ΔV for an elliptical orbit where h_p = 100 nm and h_a = 150 nm.
a. ΔV = 100 fps
b. ΔV = 300 fps
c. ΔV = 500 fps
d. ΔV = 700 fps

16 Inertial flight-path angle and velocity at 400000 feet as a function of retrograde true anomaly and a constant ΔV for an elliptical orbit where h_p = 100 nm and h_a = 200 nm.
a. ΔV = 100 fps
b. ΔV = 300 fps
c. ΔV = 500 fps
d. ΔV = 700 fps

LIST OF FIGURES (Continued)

Figure

17 Inertial flight-path angle and velocity at 400000 feet as a function of retrograde true anomaly and a constant ΔV for an elliptical orbit where h_p = 100 nm and h_a = 250 nm.
a. ΔV = 100 fps
b. ΔV = 300 fps
c. ΔV = 500 fps
d. ΔV = 700 fps

18 Inertial flight-path angle and velocity at 400000 feet as a function of retrograde true anomaly and a constant ΔV for an elliptical orbit where h_p = 100 nm and h_a = 400 nm.
a. ΔV = 100 fps
b. ΔV = 300 fps
c. ΔV = 500 fps
d. ΔV = 700 fps

19 Inertial flight-path angle and velocity at 400000 feet as a function of retrograde true anomaly and a constant ΔV for an elliptical orbit where h_p = 120 nm and h_a = 140 nm.
a. ΔV = 300 fps
b. ΔV = 500 fps
c. ΔV = 700 fps

20 Inertial flight-path angle and velocity at 400000 feet as a function of retrograde true anomaly and a constant ΔV for an elliptical orbit where h_p = 120 nm and h_a = 150 nm.
a. ΔV = 100 fps
b. ΔV = 300 fps
c. ΔV = 500 fps
d. ΔV = 700 fps

21 Inertial flight-path angle and velocity at 400000 feet as a function of retrograde true anomaly and a constant ΔV for an elliptical orbit where h_p = 120 nm and h_a = 200 nm.
a. ΔV = 100 fps
b. ΔV = 300 fps
c. ΔV = 500 fps
d. ΔV = 700 fps

LIST OF FIGURES (Continued)

Figure

22 Inertial flight-path angle and velocity at 400000 feet as a function of retrograde true anomaly and a constant ΔV for an elliptical orbit where h_p = 120 nm and h_a = 250 nm.
a. ΔV = 100 fps
b. ΔV = 300 fps
c. ΔV = 500 fps
d. ΔV = 700 fps

23 Inertial flight-path angle and velocity at 400000 feet as a function of retrograde true anomaly and a constant ΔV for an elliptical orbit where h_p = 140 nm and h_a = 150 nm.
a. ΔV = 300 fps
b. ΔV = 500 fps
c. ΔV = 700 fps

24 Inertial flight-path angle and velocity at 400000 feet as a function of retrograde true anomaly and a constant ΔV for an elliptical orbit where h_p = 140 nm and h_a = 200 nm.
a. ΔV = 300 fps
b. ΔV = 500 fps
c. ΔV = 700 fps

25 Inertial flight-path angle and velocity at 400000 feet as a function of retrograde true anomaly and a constant ΔV for an elliptical orbit where h_p = 140 nm and h_a = 250 nm.
a. ΔV = 300 fps
b. ΔV = 500 fps
c. ΔV = 700 fps

26 Inertial flight-path angle and velocity at 400000 feet as a function of retrograde true anomaly and a constant ΔV for an elliptical orbit where h_p = 140 nm and h_a = 400 nm.
a. ΔV = 300 fps
b. ΔV = 500 fps
c. ΔV = 700 fps

27 Inertial flight-path angle and velocity at 400000 feet as a function of retrograde true anomaly and a constant ΔV for an elliptical orbit where h_p = 153 nm and h_a = 180 nm.
a. ΔV = 300 fps
b. ΔV = 500 fps
c. ΔV = 700 fps

LIST OF FIGURES (Continued)

Figure

28 Inertial flight-path angle and velocity at 400000 feet as a function of retrograde true anomaly and a constant ΔV for an elliptical orbit where h_p = 153 nm and h_a = 200 nm.
a. ΔV = 300 fps
b. ΔV = 500 fps
c. ΔV = 700 fps

29 Inertial flight-path angle and velocity at 400000 feet as a function of retrograde true anomaly and a constant ΔV for an elliptical orbit where h_p = 153 nm and h_a = 250 nm.
a. ΔV = 300 fps
b. ΔV = 500 fps
c. ΔV = 700 fps

30 Inertial flight-path angle and velocity at 400000 feet as a function of retrograde true anomaly and a constant ΔV for an elliptical orbit where h_p = 153 nm and h_a = 400 nm.
a. ΔV = 300 fps
b. ΔV = 500 fps
c. ΔV = 700 fps

31 Inertial flight-path angle and velocity at 400000 feet as a function of retrograde true anomaly and a constant ΔV for an elliptical orbit where h_p = 160 nm and h_a = 180 nm.
a. ΔV = 300 fps
b. ΔV = 500 fps
c. ΔV = 700 fps

32 Inertial flight-path angle and velocity at 400000 feet as a function of retrograde true anomaly and a constant ΔV for an elliptical orbit where h_p = 160 nm and h_a = 200 nm.
a. ΔV = 300 fps
b. ΔV = 500 fps
c. ΔV = 700 fps

33 Inertial flight-path angle and velocity at 400000 feet as a function of retrograde true anomaly and a constant ΔV for an elliptical orbit where h_p = 160 nm and h_a = 250 nm.
a. ΔV = 300 fps
b. ΔV = 500 fps
c. ΔV = 700 fps

LIST OF FIGURES (Continued)

Figure

34 Inertial flight-path angle and velocity at 400000 feet as a function of retrograde true anomaly and a constant ΔV for an elliptical orbit where h_p = 160 nm and h_a = 400 nm.
a. ΔV = 300 fps
b. ΔV = 500 fps
c. ΔV = 700 fps

35 Inertial flight-path angle and velocity at 400000 feet as a function of retrograde true anomaly and a constant ΔV for an elliptical orbit where h_p = 180 nm and h_a = 200 nm.
a. ΔV = 300 fps
b. ΔV = 500 fps
c. ΔV = 700 fps

36 Inertial flight-path angle and velocity at 400000 feet as a function of retrograde true anomaly and a constant ΔV for an elliptical orbit where h_p = 180 nm and h_a = 250 nm.
a. ΔV = 300 fps
b. ΔV = 500 fps
c. ΔV = 700 fps

37 Inertial flight-path angle and velocity at 400000 feet as a function of retrograde true anomaly and a constant ΔV for an elliptical orbit where h_p = 180 nm and h_a = 300 nm.
a. ΔV = 300 fps
b. ΔV = 500 fps
c. ΔV = 700 fps

38 Inertial flight-path angle and velocity at 400000 feet as a function of retrograde true anomaly and a constant ΔV for an elliptical orbit where h_p = 180 nm and h_a = 400 nm.
a. ΔV = 300 fps
b. ΔV = 500 fps
c. ΔV = 700 fps

39 Reentry conditions at 400000 feet after retrograde from circular orbits.
a. Retrograde pitch angle, $\beta = 0^\circ$
b. Retrograde pitch angle, $\beta = 10^\circ$
c. Retrograde pitch angle, $\beta = 20^\circ$
d. Retrograde pitch angle, $\beta = 30^\circ$
e. Retrograde pitch angle, $\beta = 40^\circ$
f. Retrograde pitch angle, $\beta = 50^\circ$
g. Retrograde pitch angle, $\beta = 70^\circ$

LIST OF FIGURES (Concluded)

Figure

40 True anomaly, apogee altitude, perigee altitude and Keplerian period as a function of inertial velocity and inertial flight-path angle for various altitudes.
a. 70 nm altitude
b. 77 nm altitude
c. 85 nm altitude
d. 87 nm altitude
e. 90 nm altitude
f. 95 nm altitude
g. 100 nm altitude

1.0 INTRODUCTION

This paper presents results of a general parametric reentry study. Results are given in the form of inertial velocity and flight-path angle at 400,000 feet. For various elliptical parking orbits, the parameters varied were retrograde velocity change (ΔV), retrograde pitch angle and true anomaly. For circular orbits, ΔV and pitch angle were varied. Reference is made to existing data that can easily be used to convert the given 400,000 feet reentry conditions to other reference altitudes. In addition, important parking orbit parameters are given as a function of insertion conditions.

2.0 DISCUSSION AND RESULTS

Keplerian equations, a spherical earth, and the assumption of an instantaneous retro velocity change were assumed. To minimize the differences when comparing with integrated results the integrated ΔV should be taken as in plane along the local longitudinal body axis. The pitch angle (β) of the body axis should be with respect to the local horizontal. The true anomaly (θ) of the impulsive ΔV should coincide with the mid-burn position of the integrated burn, i. e., assume the ΔV to be split-burn.

2.1 Method of calculation. - The Keplerian solution of position and velocity in an elliptical orbit was obtained through use of a general elliptical orbital and reentry program; E042.[1] The parking orbit is defined with the initial input of either the apogee and perigee radii or an initial radius, velocity, and flight-path angle (R, V, γ).[2] As true anomaly is varied, the Keplerian equations give time-in-orbit and R, V, γ. After an impulsive ΔV, the velocity and flight-path angle are calculated trigonometrically. These new conditions define the transfer orbit which, in turn, allows velocity and flight-path angle for any transfer orbit position to be calculated .

---

[1] See reference 1. Good sources of elliptical expressions are the Martin "Orbital Flight Handbook" (reference 2) and the Langley "space notes."

[2] When the additional inputs of inclination, argument of perigee, and longitude of the ascending node are used, the program gives orbital and reentry conditions, time, and position with respect to a rotating earth.

2.2 Geometry and assumed constants. -

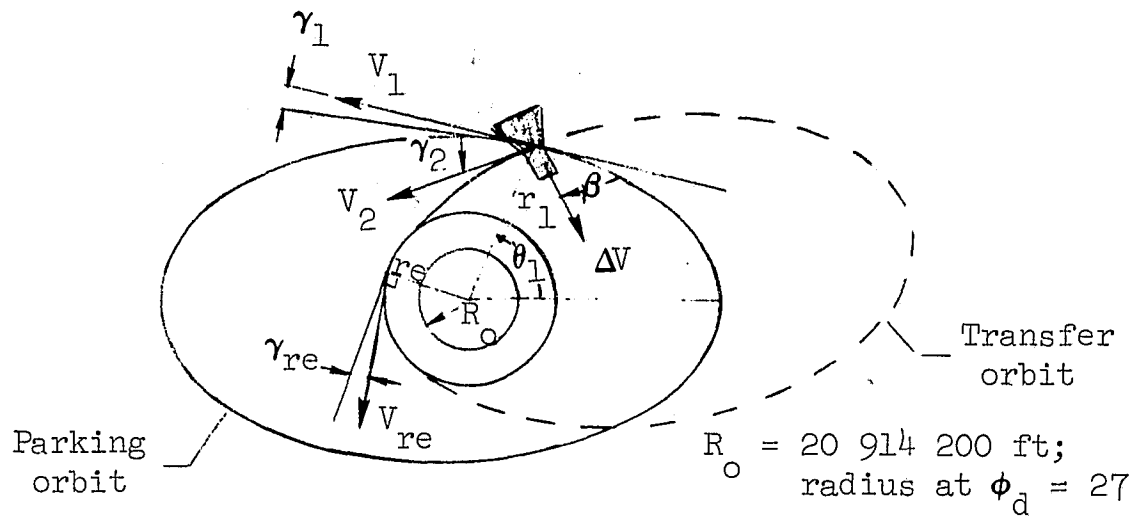

r_1, V_1, γ_1 is parking orbit position where ΔV is applied.

Flight-path angles measured with respect to local horizontal.

R_o = 20 914 200 ft; radius at $\phi_d = 27.5^o$

re = 21 314 200 ft

GM = 1.4077 (10^{16}) ft^3/sec^2

V_2 = inertial velocity after ΔV

V_{re} = inertial velocity at 400 000 ft

γ_{re} = flight-path angle at 400 000 ft

θ_1 = parking orbit true anomaly of retrograde

ΔV = retrograde ΔV

2.3 Examples. -

2.3.1 Figures 1 and 2, elliptical orbit reentry. - Figure 1 shows the effect on reentry conditions when varying the parameters ΔV, β , and θ for particular elliptical orbits. Refer to Figure 1 (a), for hp/ha = 80/100 nm. For a given ΔV and pitch angle, the effect of varying the retrograde true anomaly, θ, is indicated by moving vertically on the figure. Thus, for ΔV = 700 ft/sec and $\beta = 0^o$ the reentry flight-path angle varies from -1.17^o to -1.86^o with a reentry velocity of about 25090 fps. This same information is given by Figure 2 (d).

Again using Figure 1 (a) for the 80/100 orbit:

a. What are the reentry V, γ ranges for ΔV = 500 fps and $\beta = 0^o$?
Range of γ_i is from $-.96^o$ to -1.55^o.
Reentry velocity is about 25290 ft/sec.

b. What are the reentry conditions after apogee and perigee reentries using a ΔV of 340 ft/sec applied at an angle of 25°?
For $\theta = 0^o$ Vi = 25480 ft/sec $\gamma_i = -.79^o$
For $\theta = 180^o$ Vi = 25480 ft/sec $\gamma_i = -1.22^o$

Figures 3 through 38 give similar information for other elliptical orbits.

2.3.2 Figure 39, circular orbit reentry. - Figure 39 gives circular orbit reentry conditions for various retrograde attitudes. For example, what are the reentry conditions following a 330 ft/sec retrograde from a 160 nm circular orbit for $\beta = 20^{\circ}$? How much will these conditions change if the pitch angle is decreased to zero?

For the 20° pitch angle, Figure 39 (c) gives Vi = 25727 ft/sec and $\gamma_i = -1.38^{\circ}$. From Figure 39 (a), decreasing the pitch angle to zero results in Vi = 25710 ft/sec (-17 ft/sec) and $\gamma_i = -1.46^{\circ}$ ($-.8^{\circ}$).

2.4 Converting given conditions to other reference altitudes. - Converting given Vi, γ_i reentry conditions at 400,000 feet to another altitude, say 350,000 feet, is easily accomplished by noting the variation of velocity and flight-path angle in a Keplerian ellipse. Reference 3 gives these V, γ variations in a useful format. Assume 350 K feet reentry conditions are desired for the above circular orbit reentry example in paragraph 2.3.2, where at 400 K feet Vi = 25727 ft/sec and $\gamma_i = -1.38^{\circ}$. From reference 3, Figure 4 (d), the V, γ 400 K feet values define a transfer ellipse where hp/ha = -13/159 nm. Figure 4 (c), for an altitude of 350 K feet, shows that for hp/ha = -13/159 nm, Vi = 25787 ft/sec and $\gamma_i = -1.36^{\circ}$.

2.5 Parking orbits as a function of cutoff conditions for various insertion altitudes. - Figure 40 gives apogee and perigee altitude (ha, hp), true anomaly (θ), and period (τ), as a function of the cutoff parameters h, V, γ.[3] These graphs also allow a quick estimation of time to go to apogee and perigee since the insertion true anomaly is indicated. For this estimate, assume the orbital travel to be $360/\tau$ deg/min. These data are the result of the general Keplerian relation of ha, hp, θ, and τ with h, V, γ and are plotted in the given "insertion conditions" format for usage and compatibility with other flight control displays.

Refer to Figure 40 (d), which is for an insertion attitude of 87 nm. Assume cutoff occurred at Vi = 25775 ft/sec and $\gamma_i = +1.85^{\circ}$. The following is indicated:

hp/ha = 5/250 nm
initial true anomaly = 73°
period, τ = 89.2 min
time to go to apogee = 26.6 min
time to go to perigee = 71.2 min

---

[3]From reference 4. See also reference 5 for additional data covering wider ranges in altitude.

For this example, if no spacecraft propulsion capability is used, the subsequent reentry conditions can be obtained by the preceding method. Hence, from Figure 1 (c) of reference 3, at 350 K feet Vi = 25983 ft/sec and $\gamma_i = -1.62^{\circ}$ for hp/ha = 5/250 nm.

2.6 Comments. - These, and the referenced data, represent a growing amount of useful mission planning data. These data should be thought of as related puzzle pieces that are to be fitted together for the purpose of simplifying the mission planning/evaluating task. In this regard, familiarity with this data will be beneficial in relating it to future data as it becomes available.

3.0 CONCLUSIONS

Inertial velocity and flight-path angle at 400,000 feet are given for reentries from near earth circular and elliptical parking orbits. The relationship of important parking orbit parameters to conditions at insertion is made in addition to pointing out the pertinent usefulness of existing data.

4.0 REFERENCES

4.1 MSC Memorandum, "Elliptical Orbital and Reentry Program E042," by Frank J. Suler, Flight Analysis Branch, MPAD, to be published.

4.2 "Orbital Flight Handbook," Martin Company, Space Systems Division, (Baltimore) ER12684, 1963.

4.3 MSC Internal Note No. 64-FM-23, "Graphical Determination of Reentry Conditions," by Sandra A. Yates, Mathematical Physics Branch, MPAD, July 16, 1964.

4.4 MSC Internal Note No. 65-FM-23, "Preflight Orbital and Reentry Data for the First Manned Gemini Flight (GT-3)," by Bobbie D. Weber and Frank J. Suler, Flight Analysis Branch, MPAD, March 3, 1965.

4.5 MSC Memorandum, "Results of a Two-Body Parametric Study," by Sandra A. Yates, Mathematical Physics Branch, MPAD, September 18, 1963.

4.6 MSC Internal Note No. 64-FM-10, "Change in Velocity Magnitude and Direction Due to Applying an Incremental Velocity Instantaneously at any Angle," by Sandra A. Yates, Mathematical Physics Branch, MPAD, June 10, 1964.

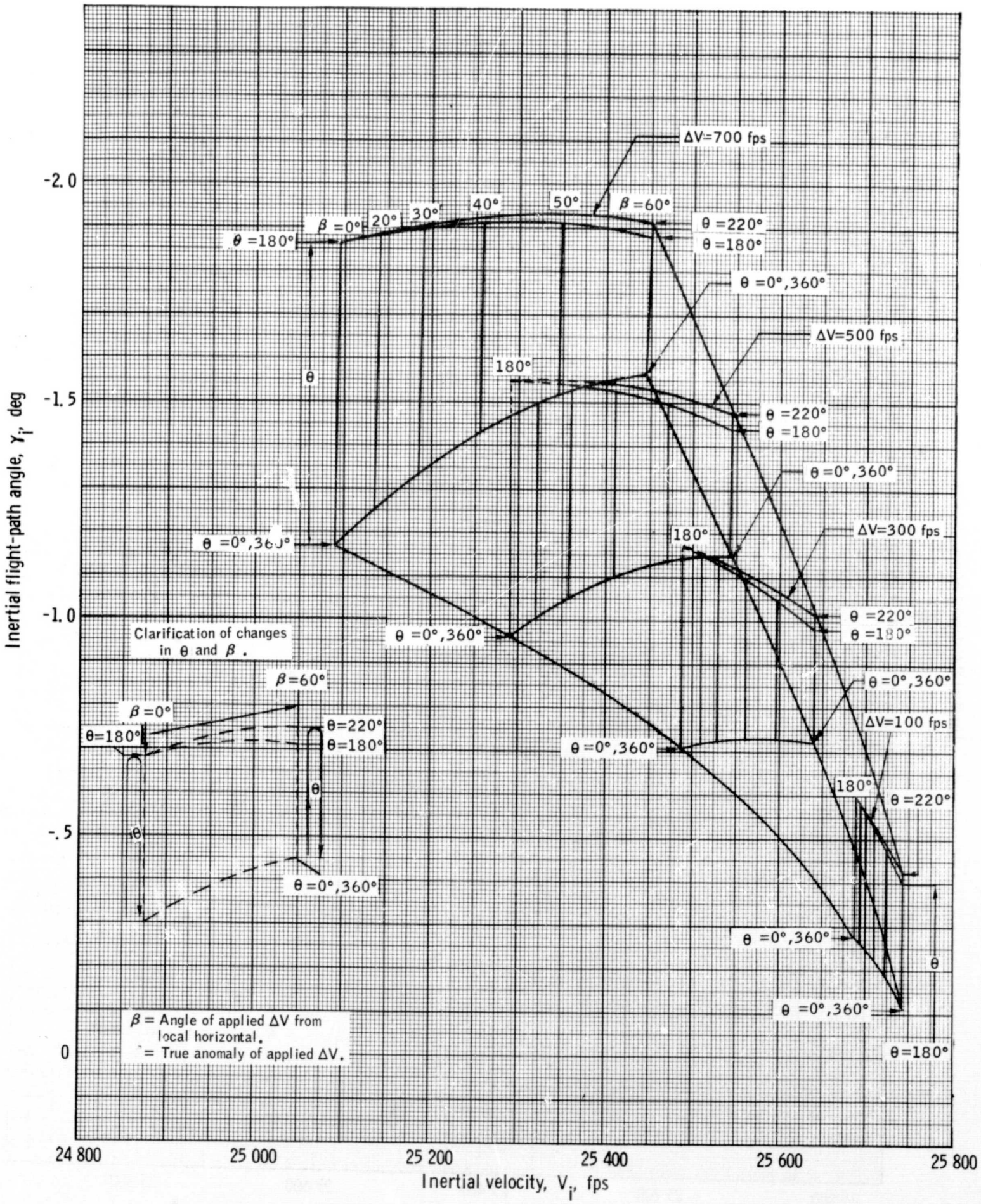

(a) hp = 80, ha = 100 n. mi.

Figure 1. - Inertial flight-path angle versus inertial velocity (400 000 feet) as a function of retrograde true anomaly, ΔV, and attitude for various elliptical orbits.

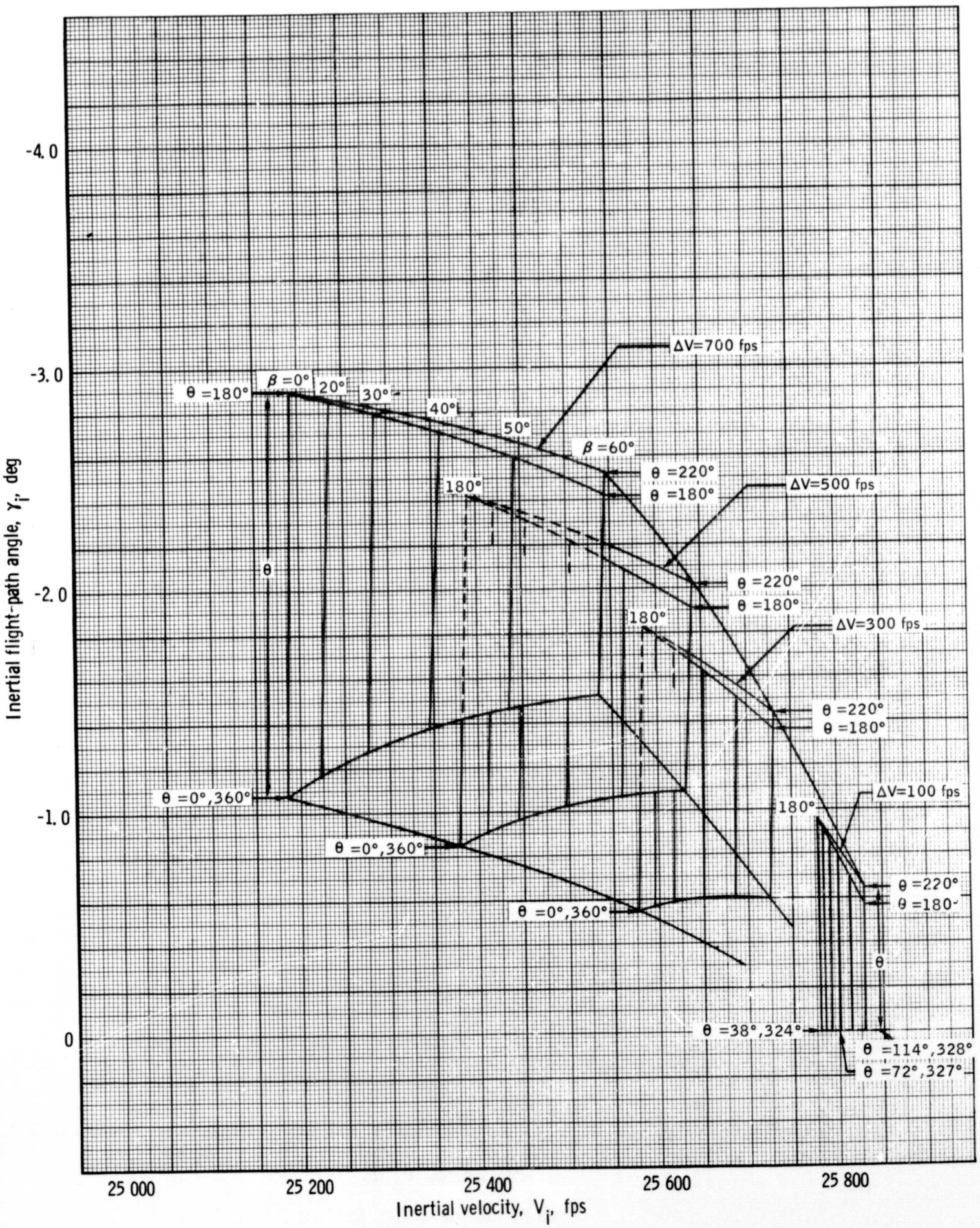

(b) hp = 80, ha = 150 n. mi.

Figure 1. - Continued.

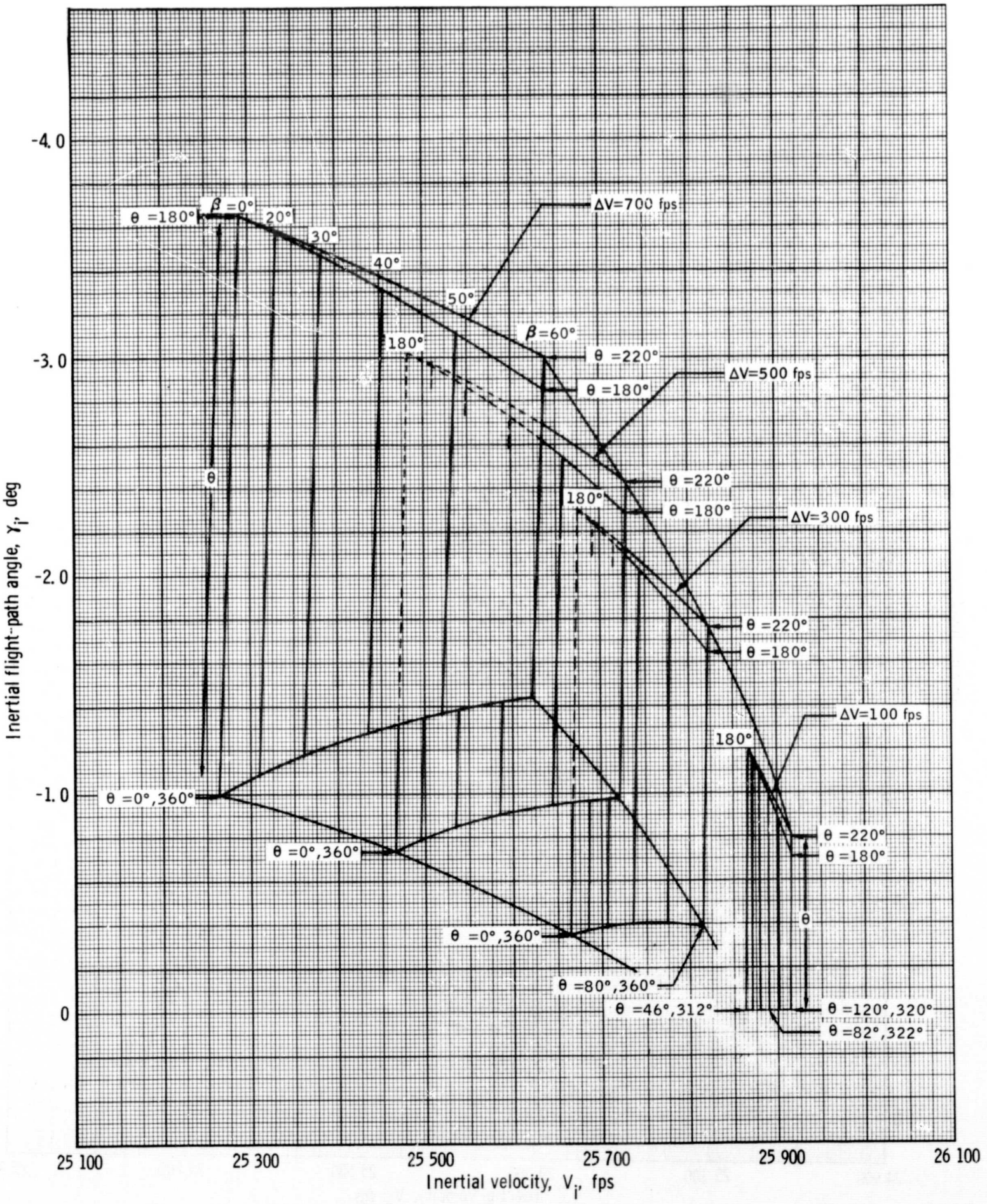

(c) hp = 80, ha = 200 n. mi.

Figure 1. - Continued.

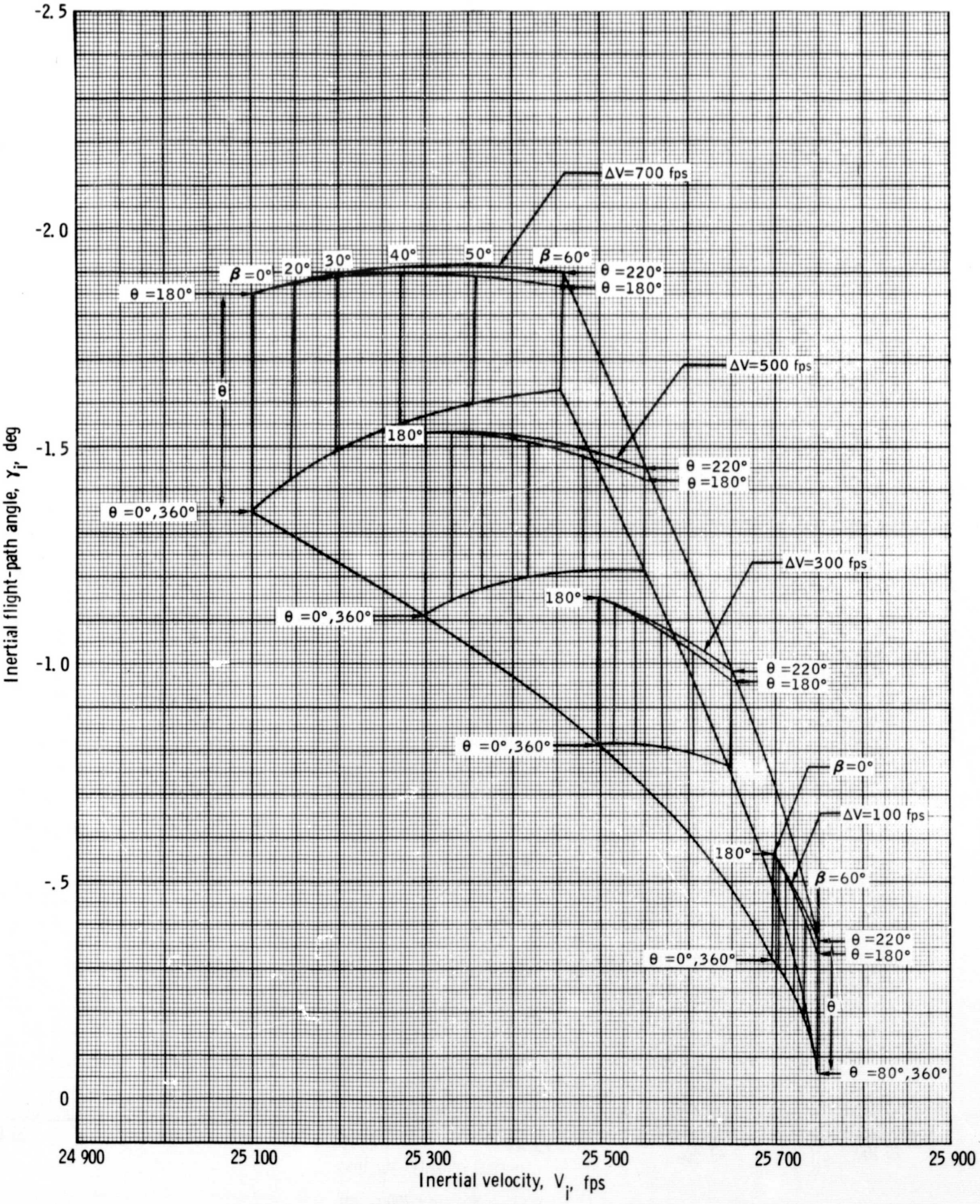

(d) hp = 85, ha = 100 n. mi.

Figure 1. - Continued.

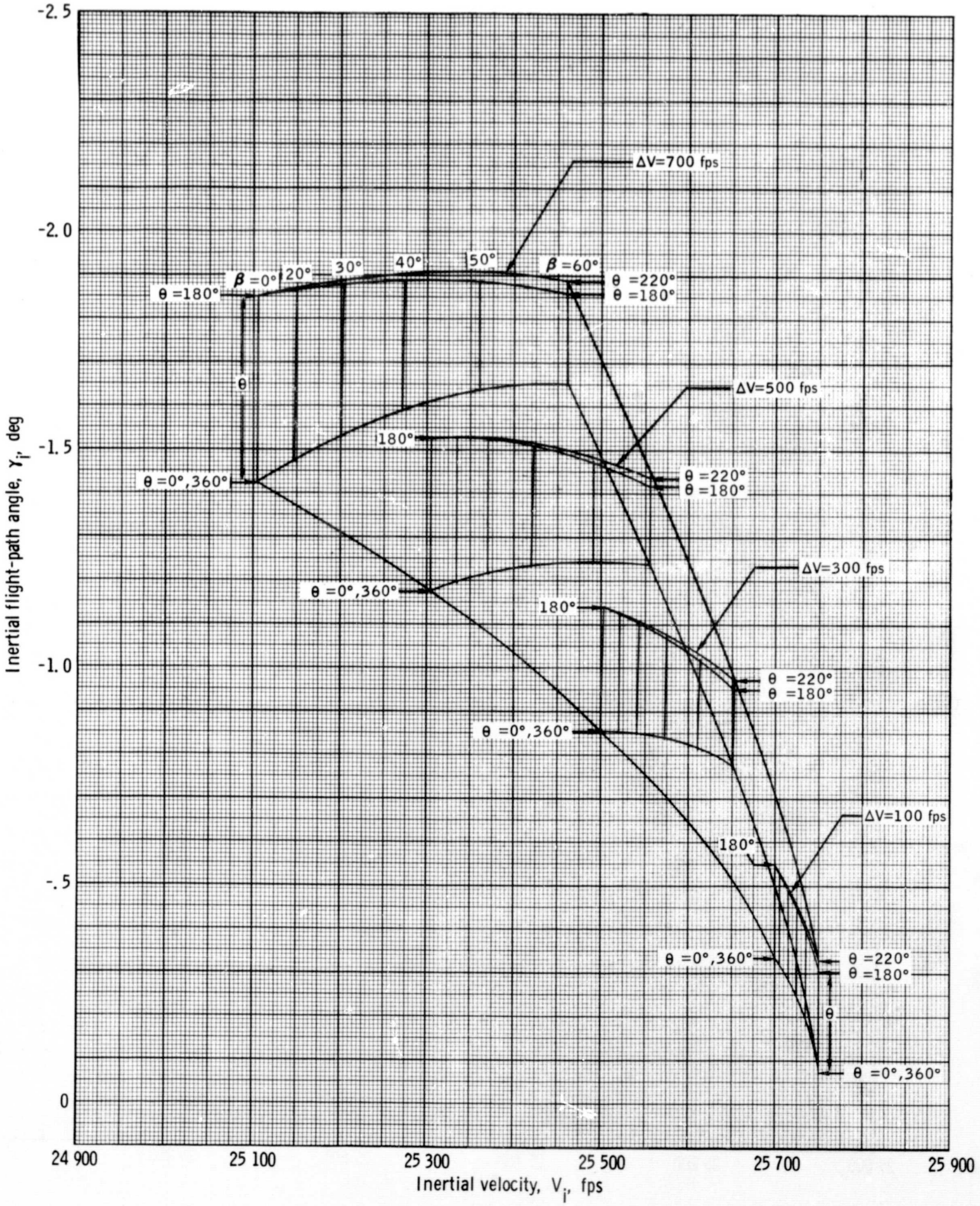

(e) hp = 87, ha = 100 n. mi.

Figure 1. - Continued.

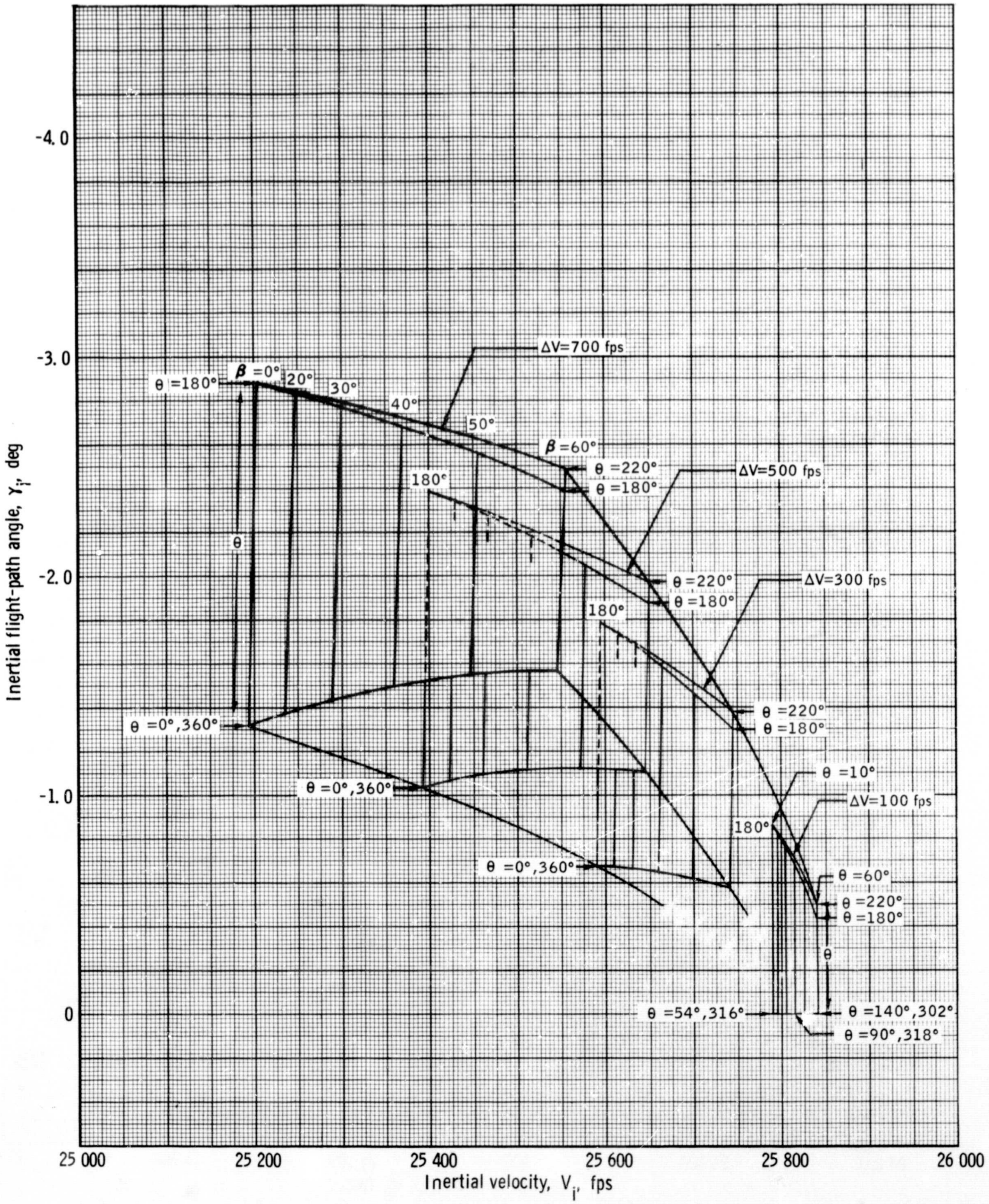

(f) hp = 87, ha = 150 n. mi.

Figure 1. - Continued.

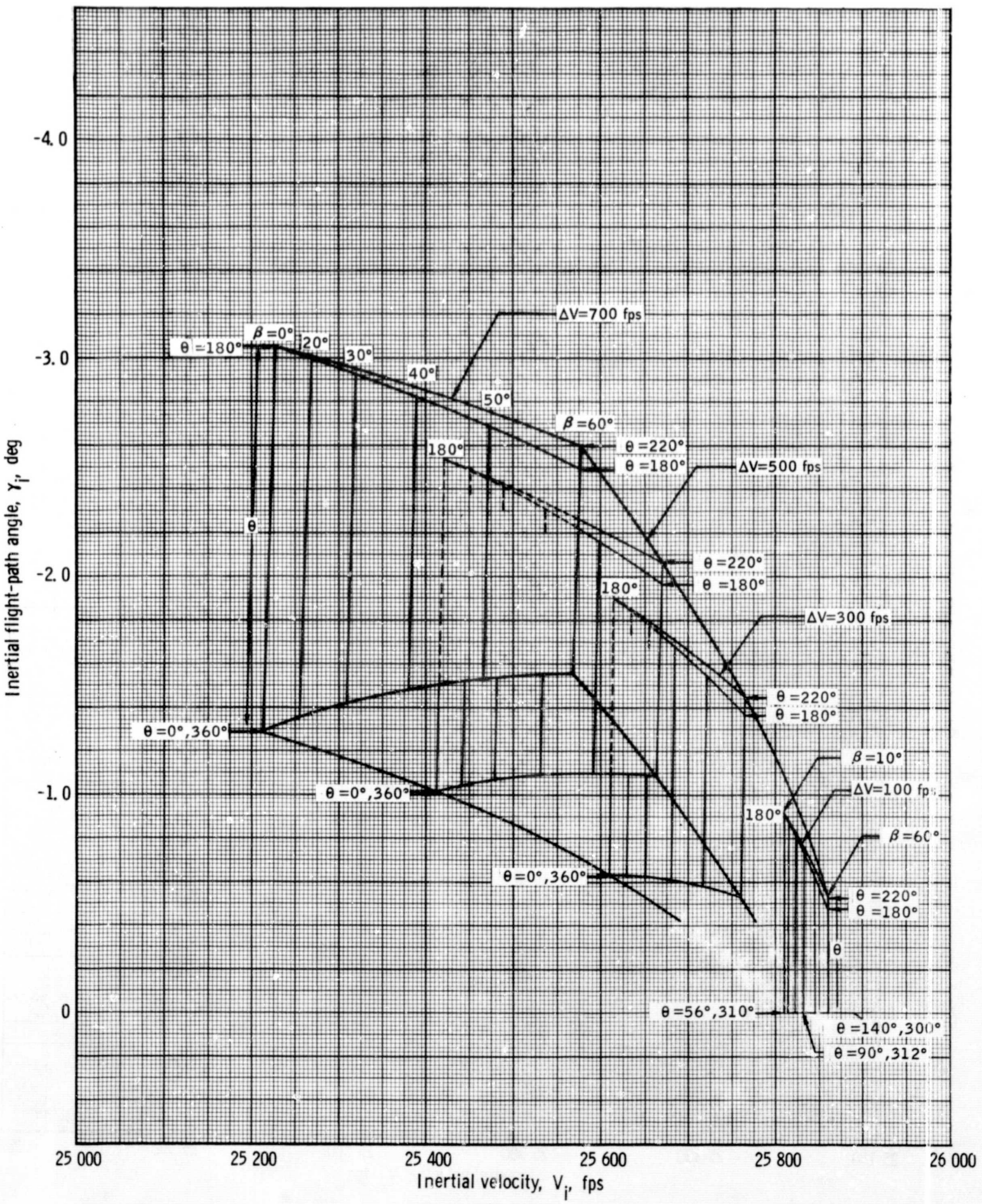

(g) hp = 87, ha = 161 n. mi.

Figure 1. - Continued.

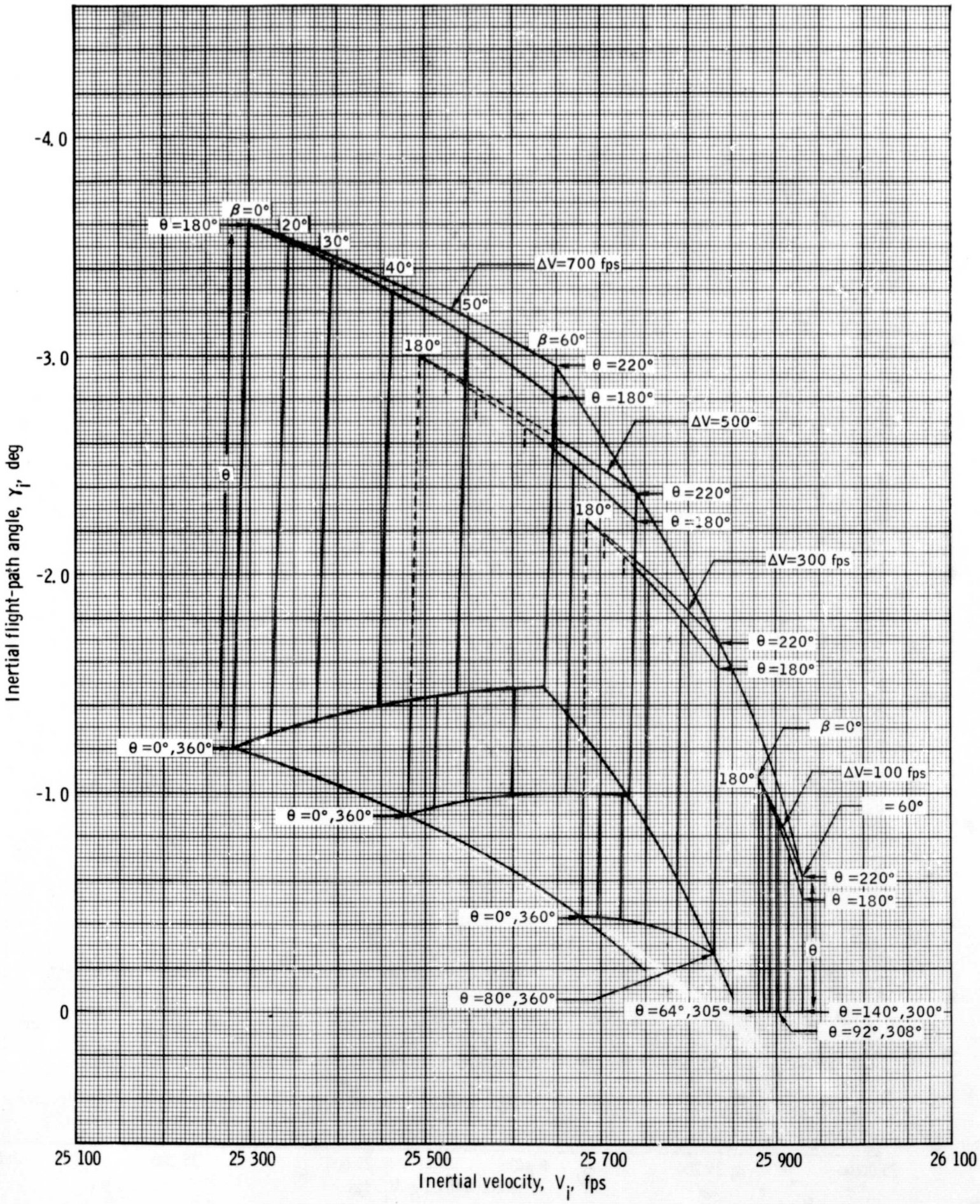

(h) hp = 87, ha = 200 n. mi.

Figure 1. - Continued.

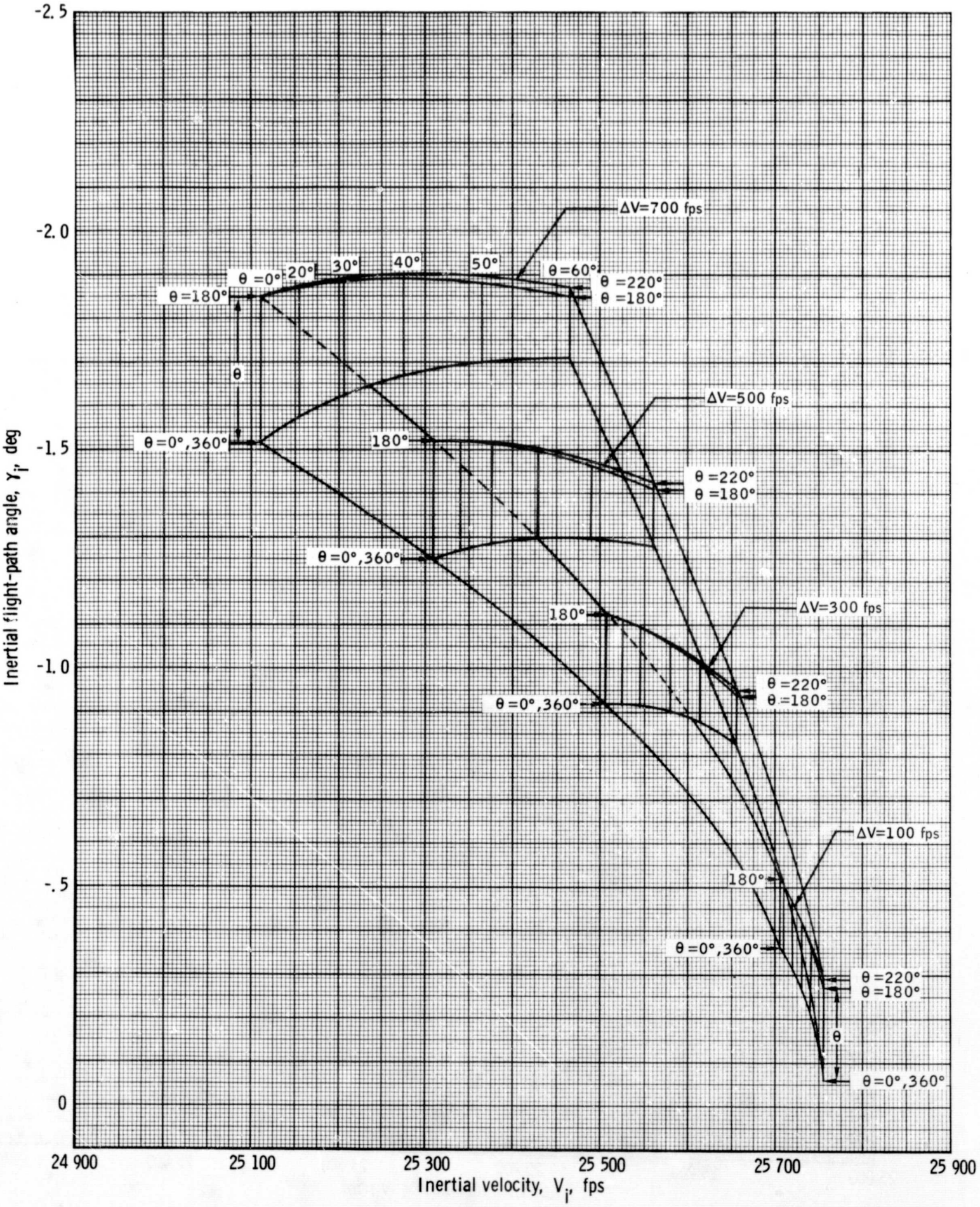

(i) hp = 90, ha = 100 n. mi.

Figure 1. - Continued.

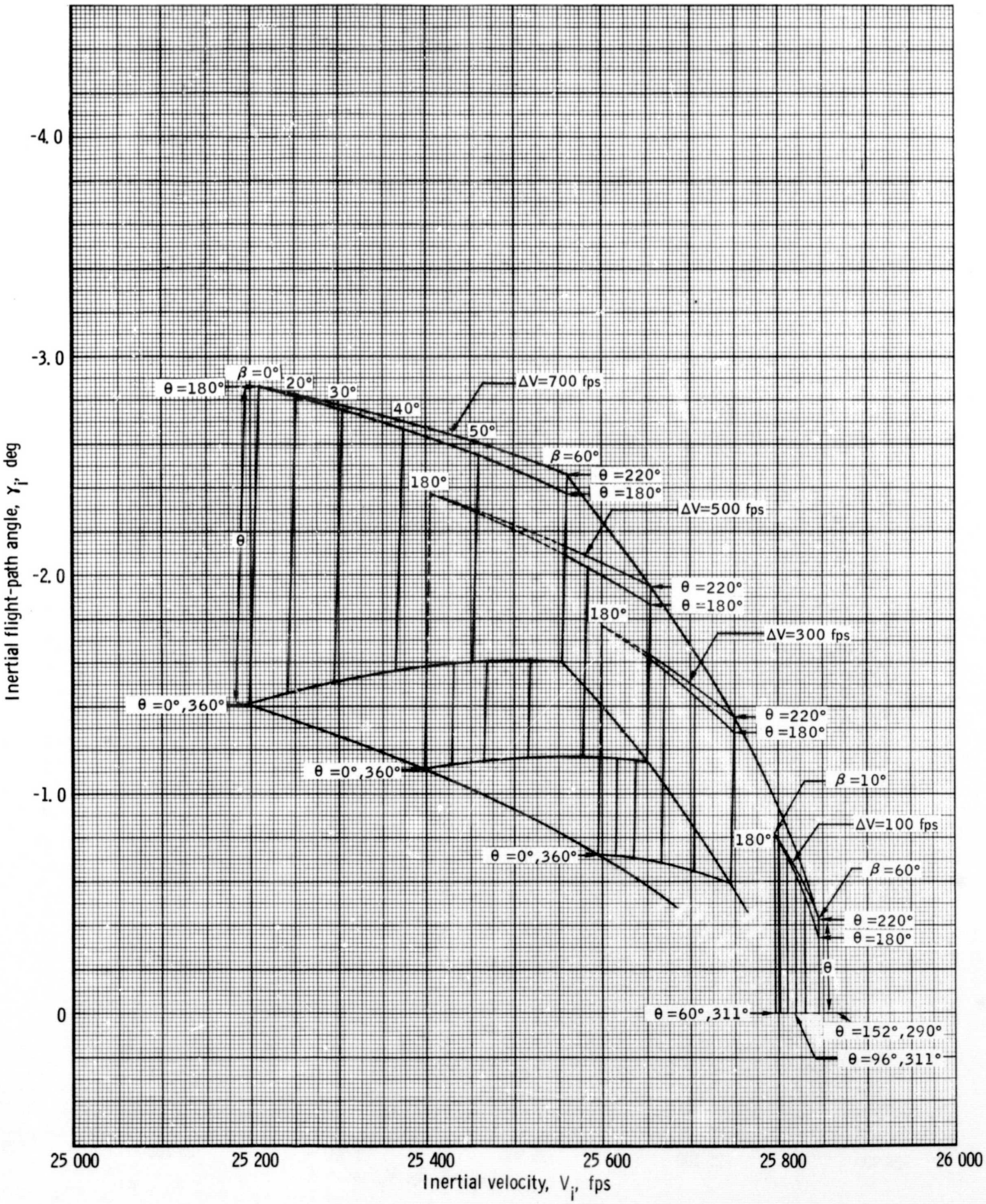

(j) hp = 90, ha = 150 n. mi.

Figure 1. - Continued.

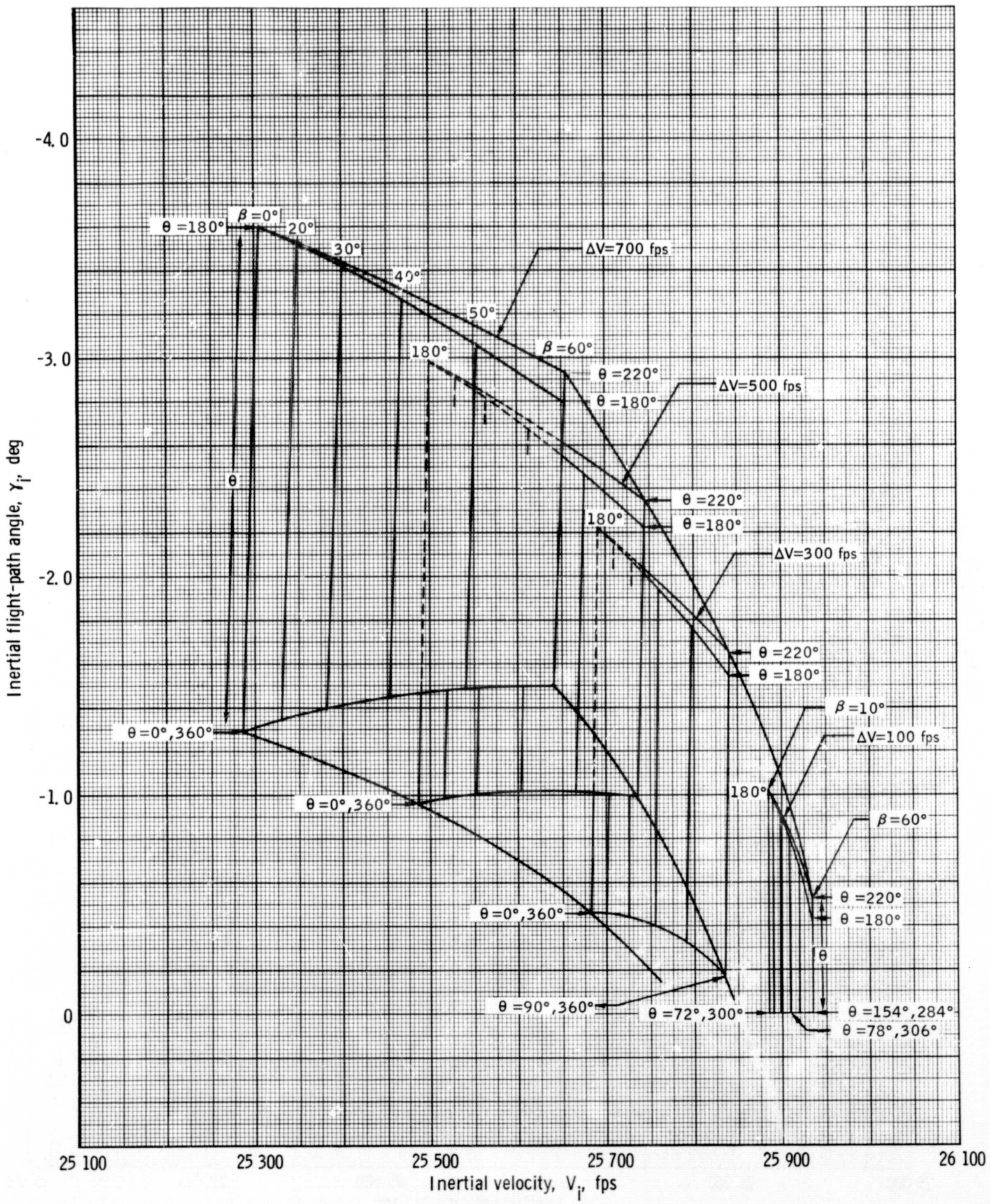

(k) hp = 90, ha = 200 n. mi.

Figure 1. - Continued.

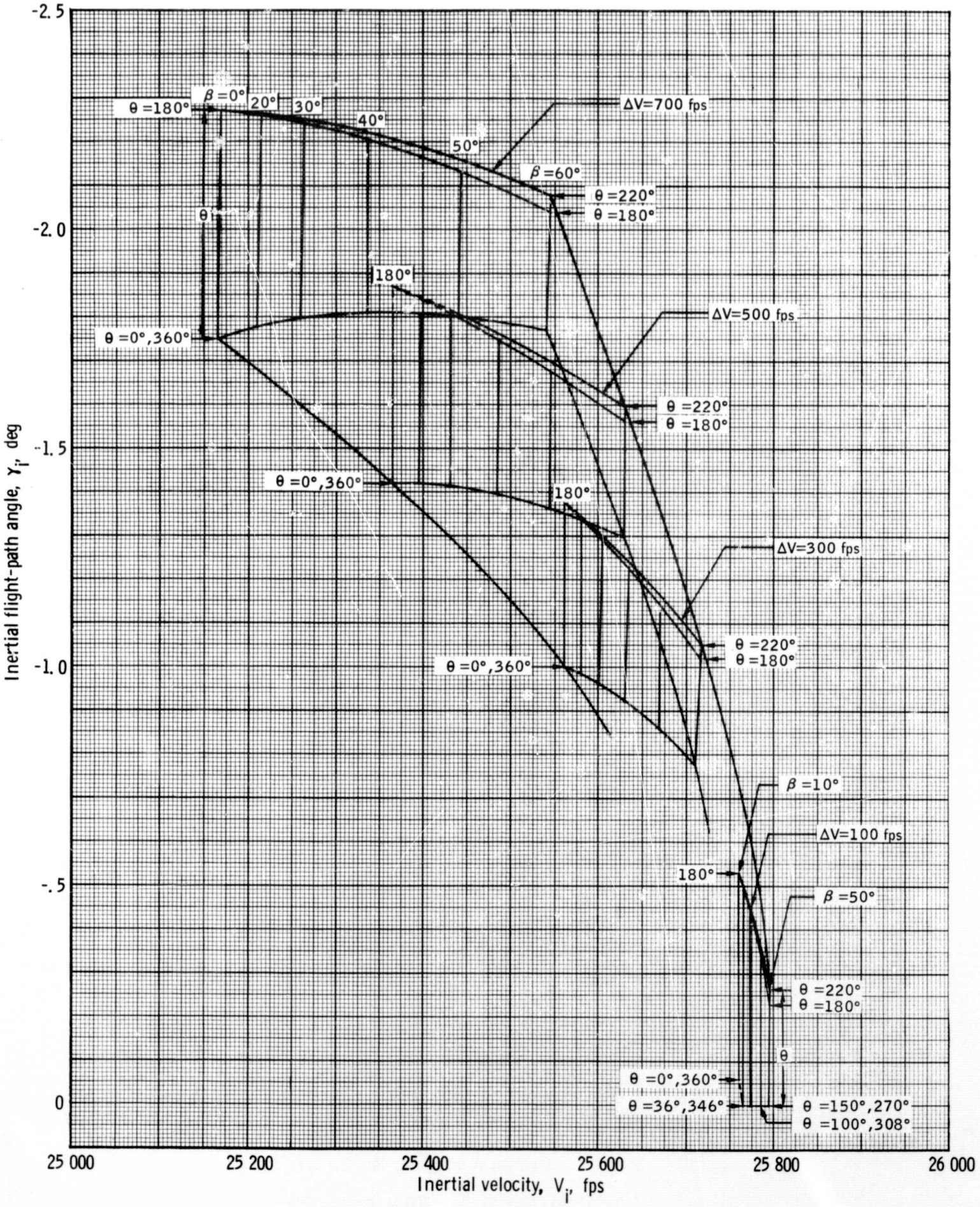

(l) hp = 100, ha = 120 n. mi.

Figure 1. - Continued.

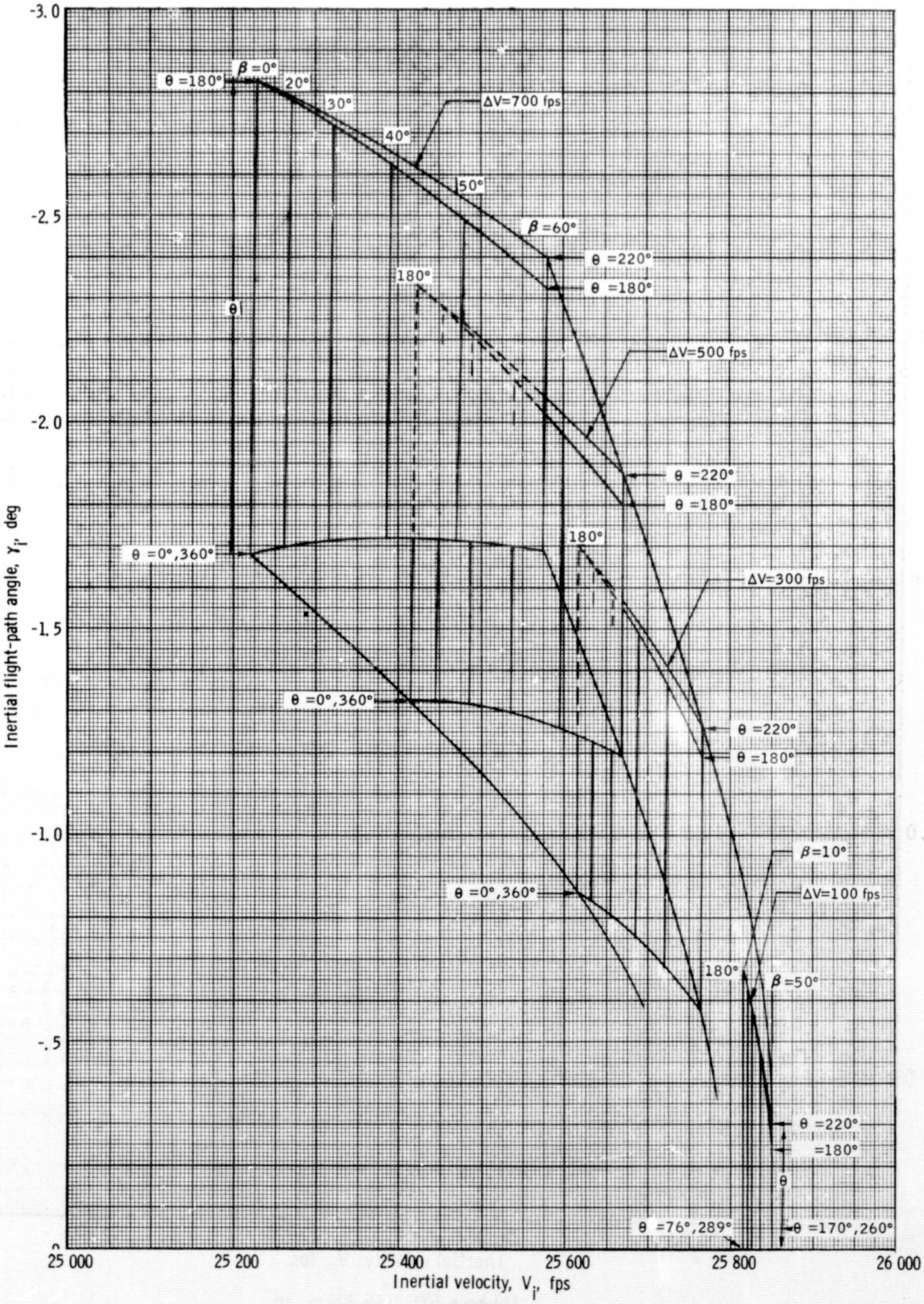

(m) hp = 100, ha = 150 n. mi.

Figure 1. - Continued.

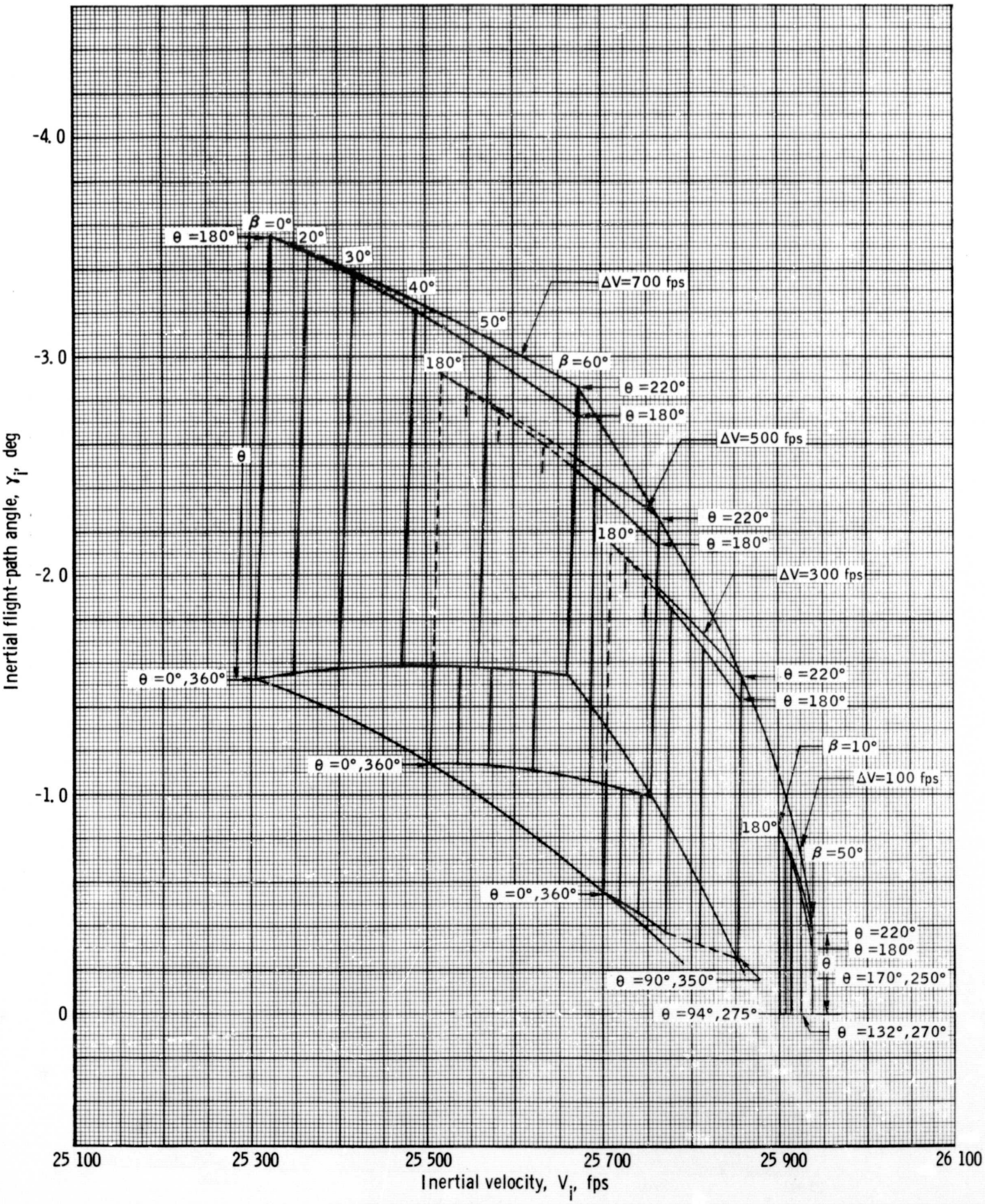

(n) hp = 100, ha = 200 n. mi.

Figure 1. - Continued.

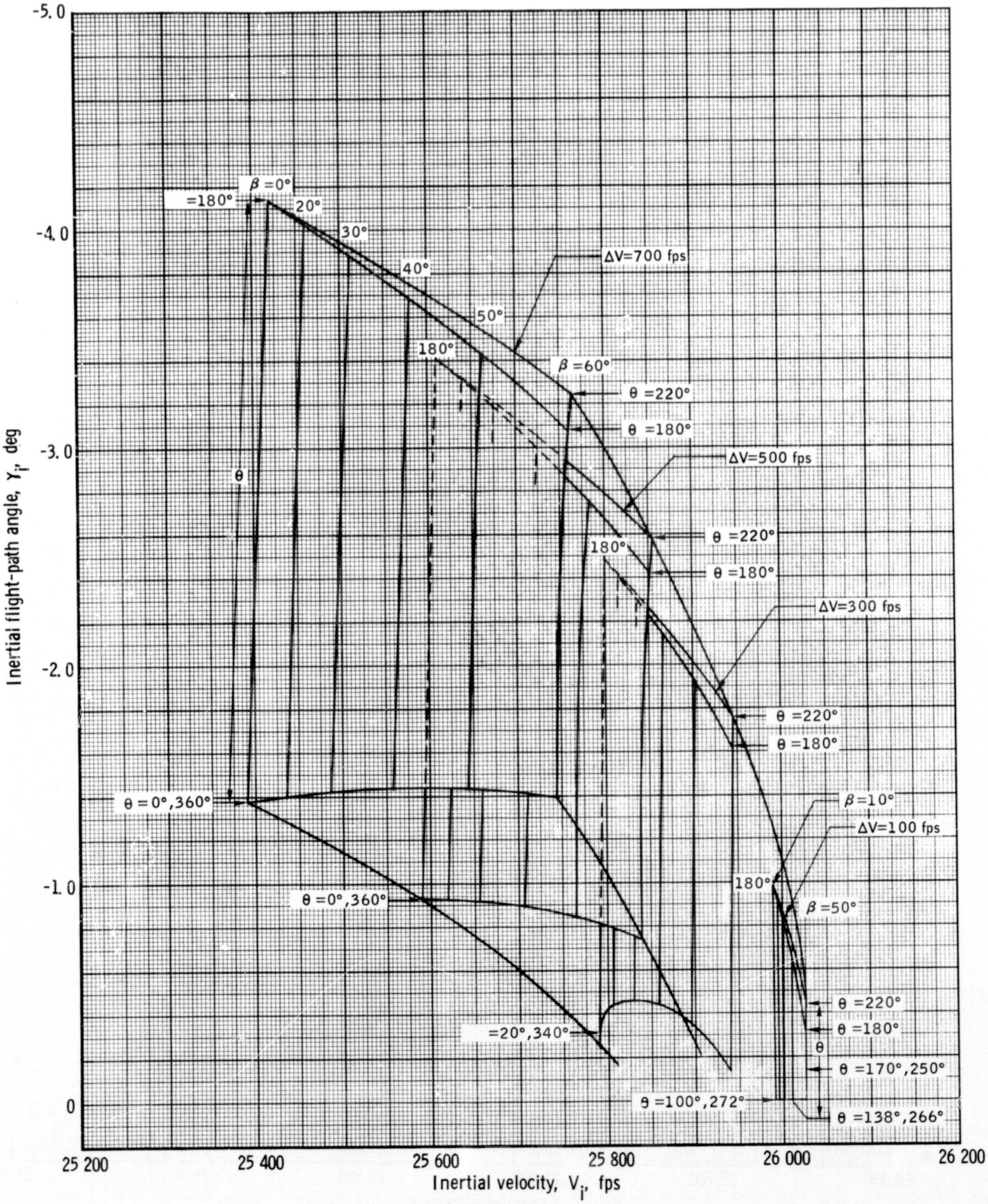

(o) hp = 100, ha = 250 n. mi.

Figure 1. - Continued.

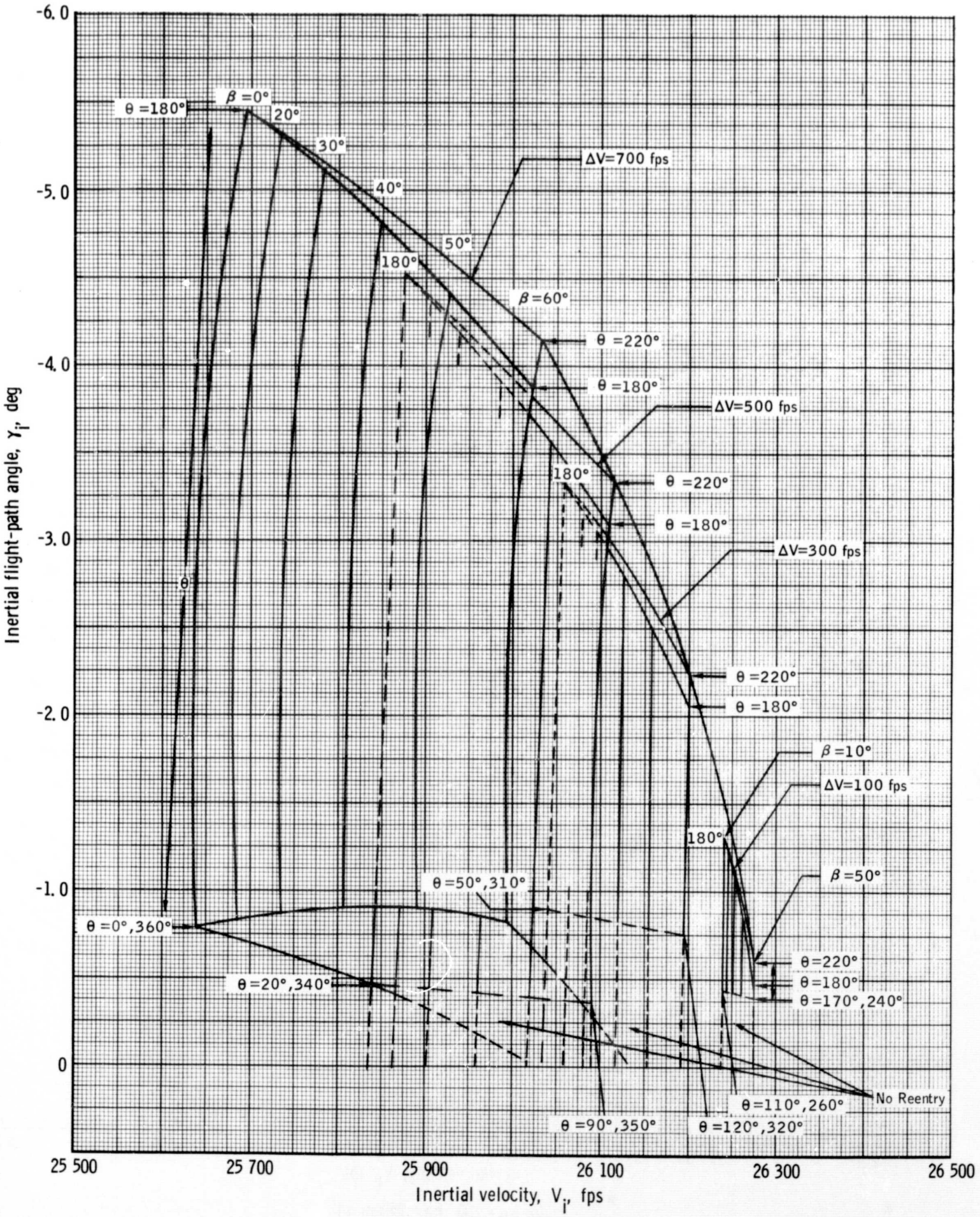

(p) hp = 100, ha = 400 n. mi.

Figure 1. - Continued.

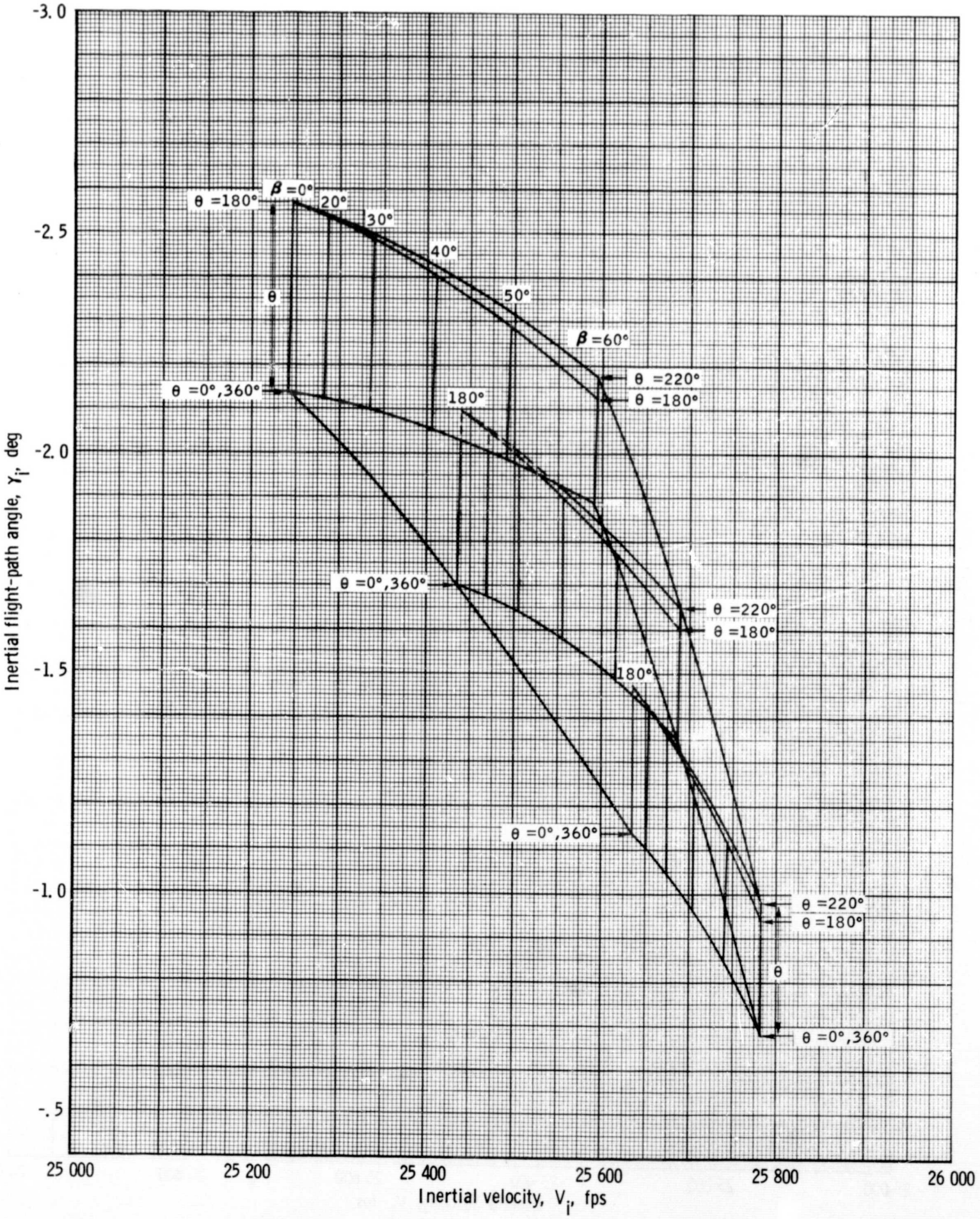

(q) hp = 120, ha = 140 n. mi.

Figure 1. - Continued.

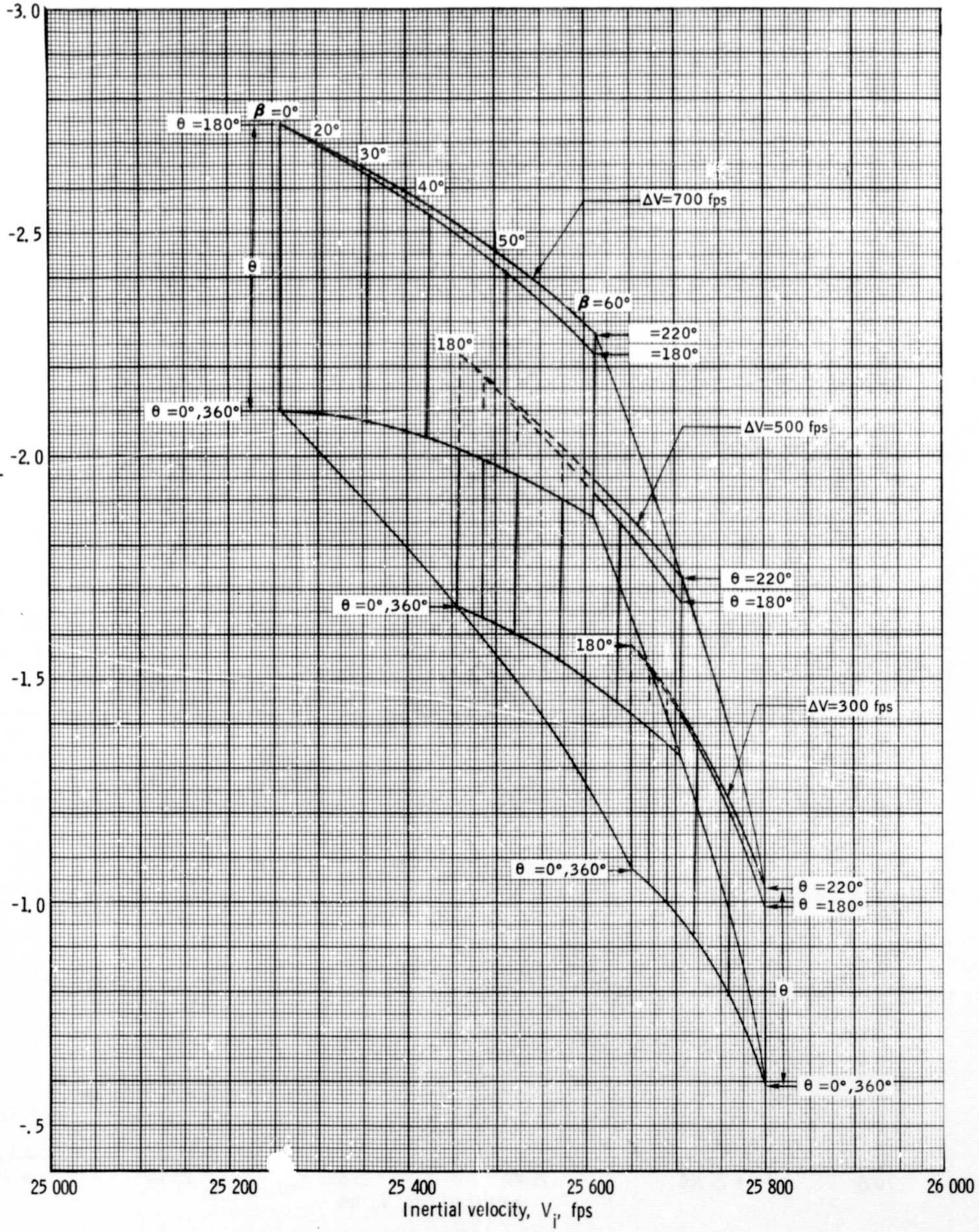

(r) hp = 120, ha = 150 n. mi.

Figure 1. - Continued.

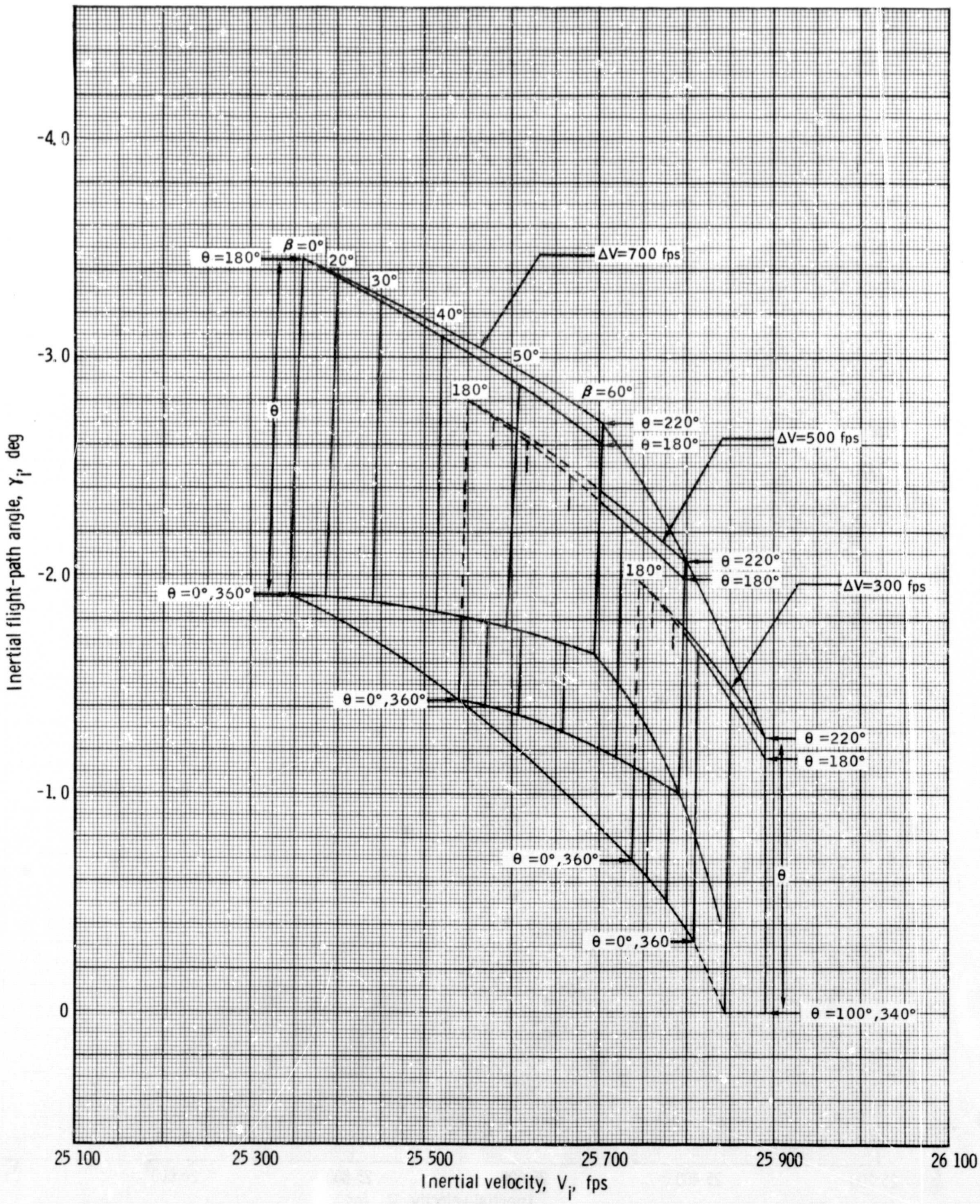

(s) hp = 120, ha = 200 n. mi.

Figure 1. - Continued.

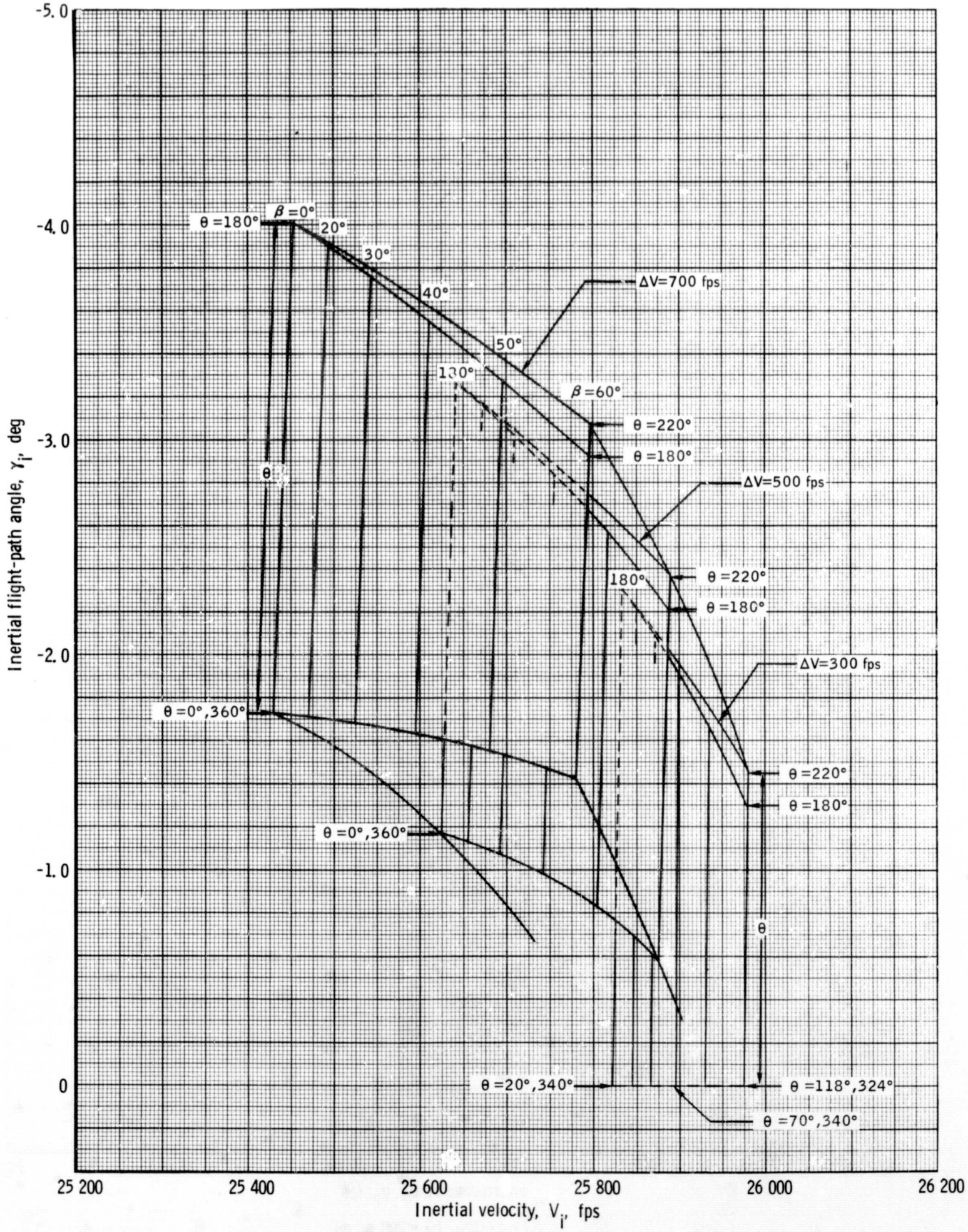

(t) hp = 120, ha = 250 n. mi.

Figure 1. - Continued.

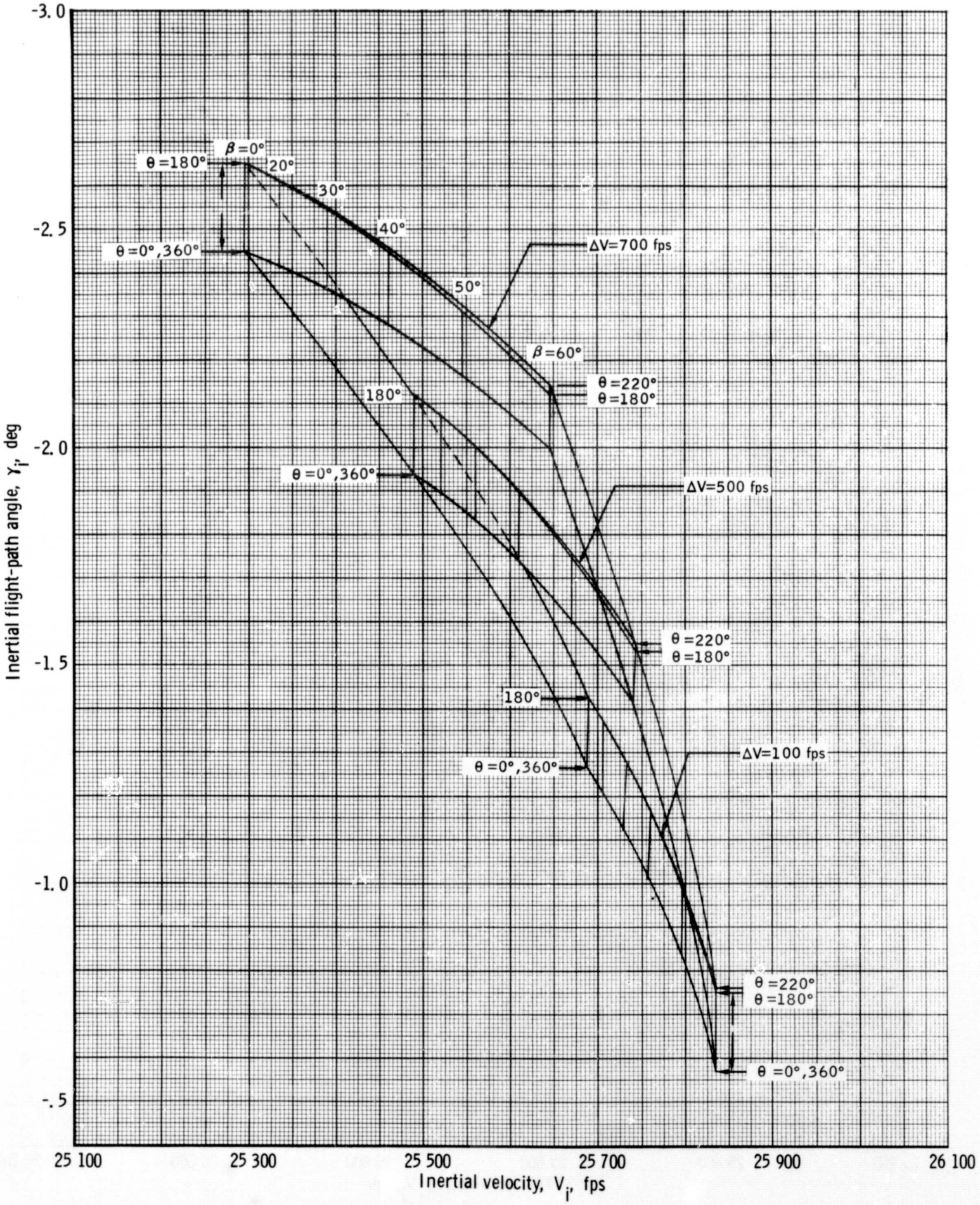

(u) hp = 140, ha = 150 n. mi.

Figure 1. - Continued.

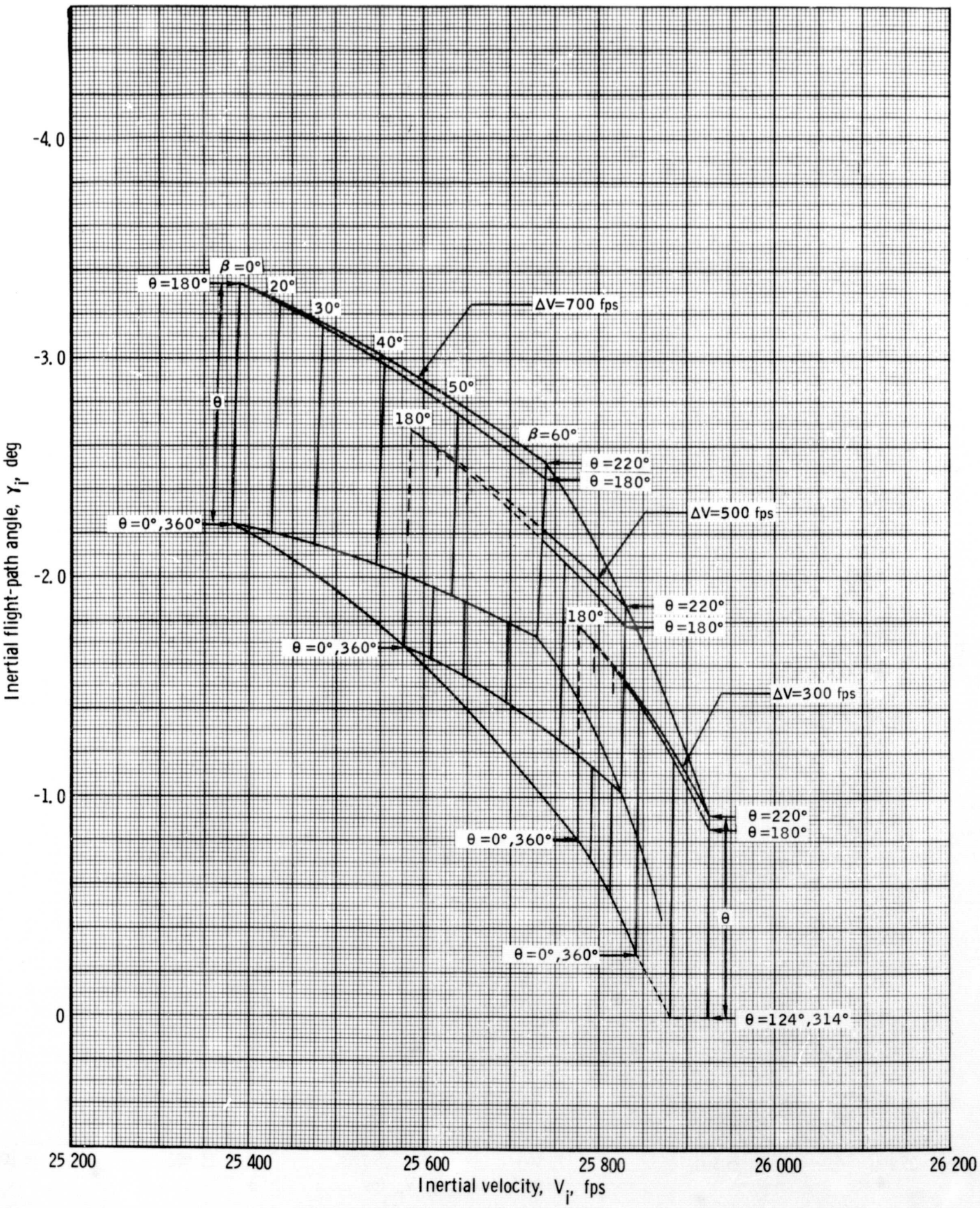

(v) hp = 140, ha = 200 n. mi.

Figure 1. - Continued.

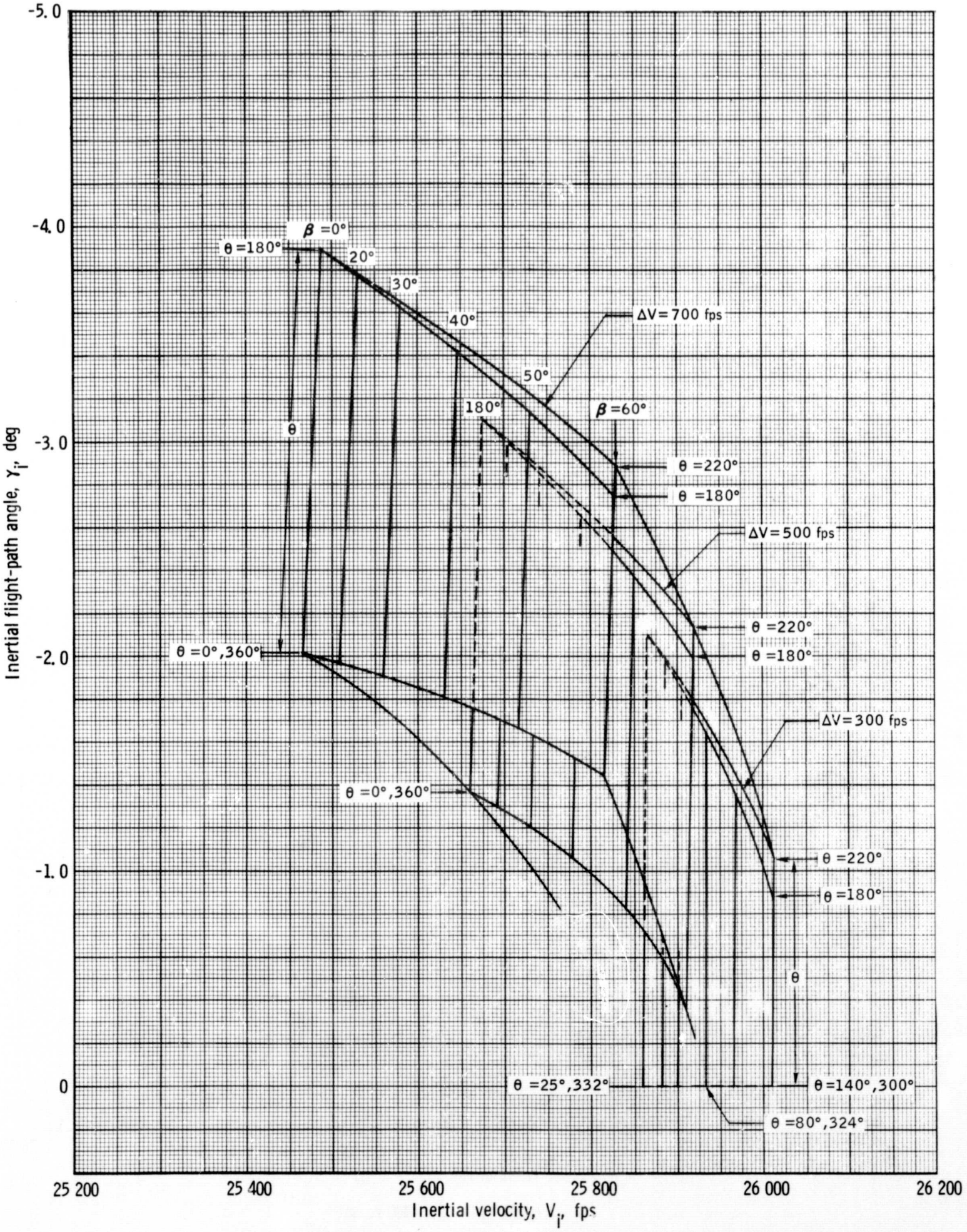

(w) hp = 140, ha = 250 n. mi.

Figure 1. - Continued.

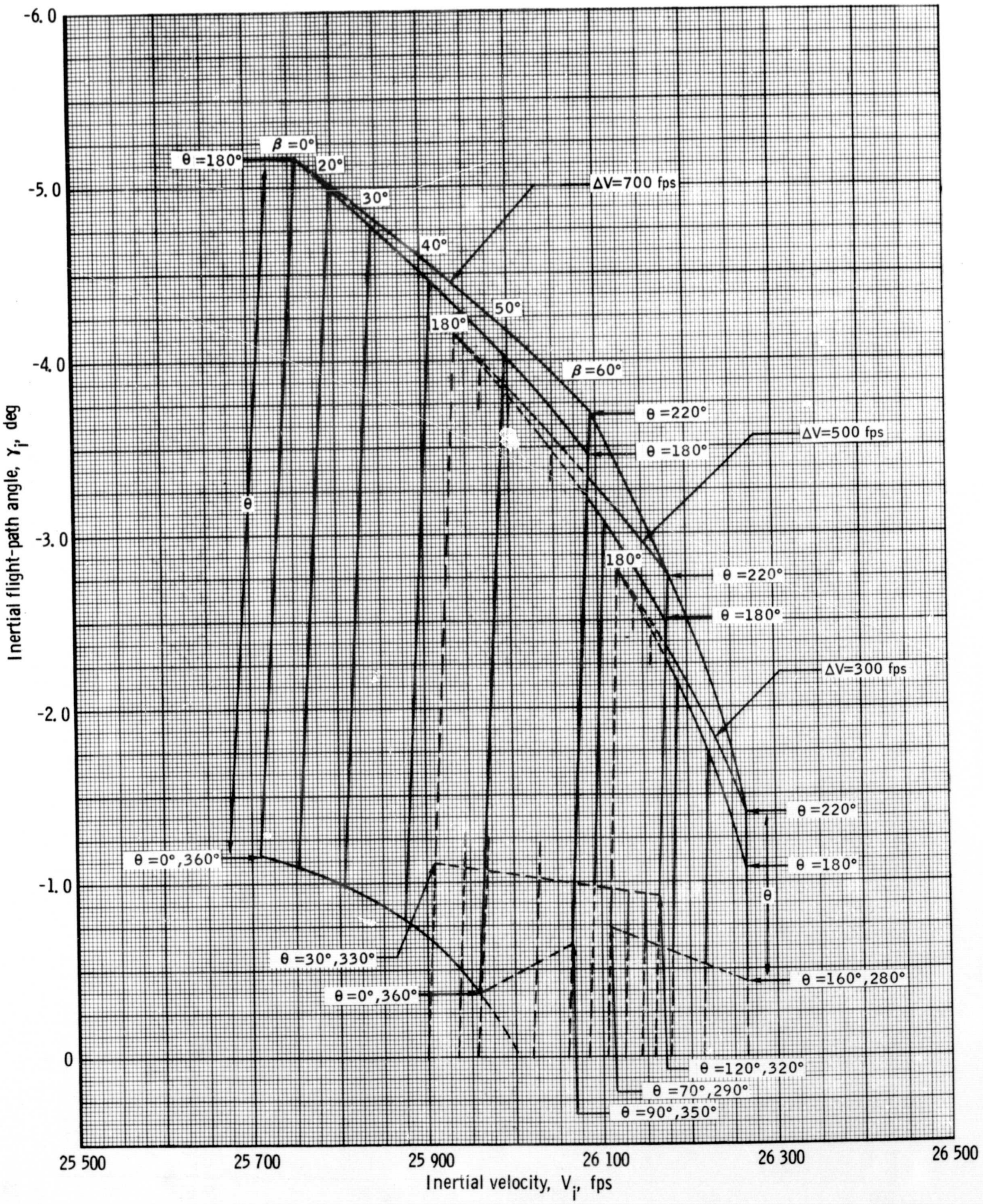

(x) hp = 140, ha = 400 n. mi.

Figure 1. - Concluded.

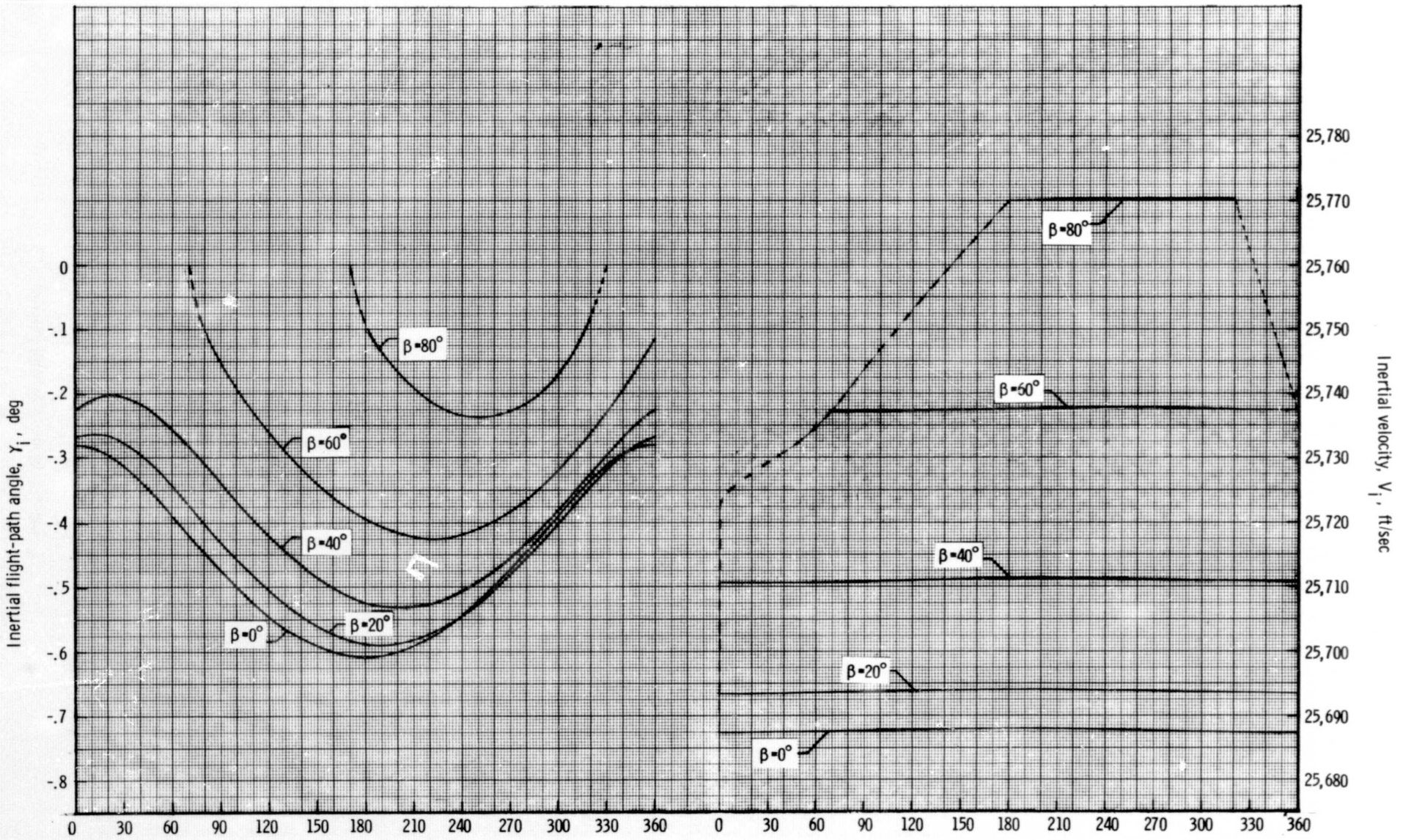

(a) ΔV = 100 fps

Figure 2. - Inertial flight-path angle and velocity at 400 000 feet as a function of retrograde true anomaly and a constant ΔV for an elliptical orbit where h_p = 80 nautical miles and h_a = 100 nautical miles.

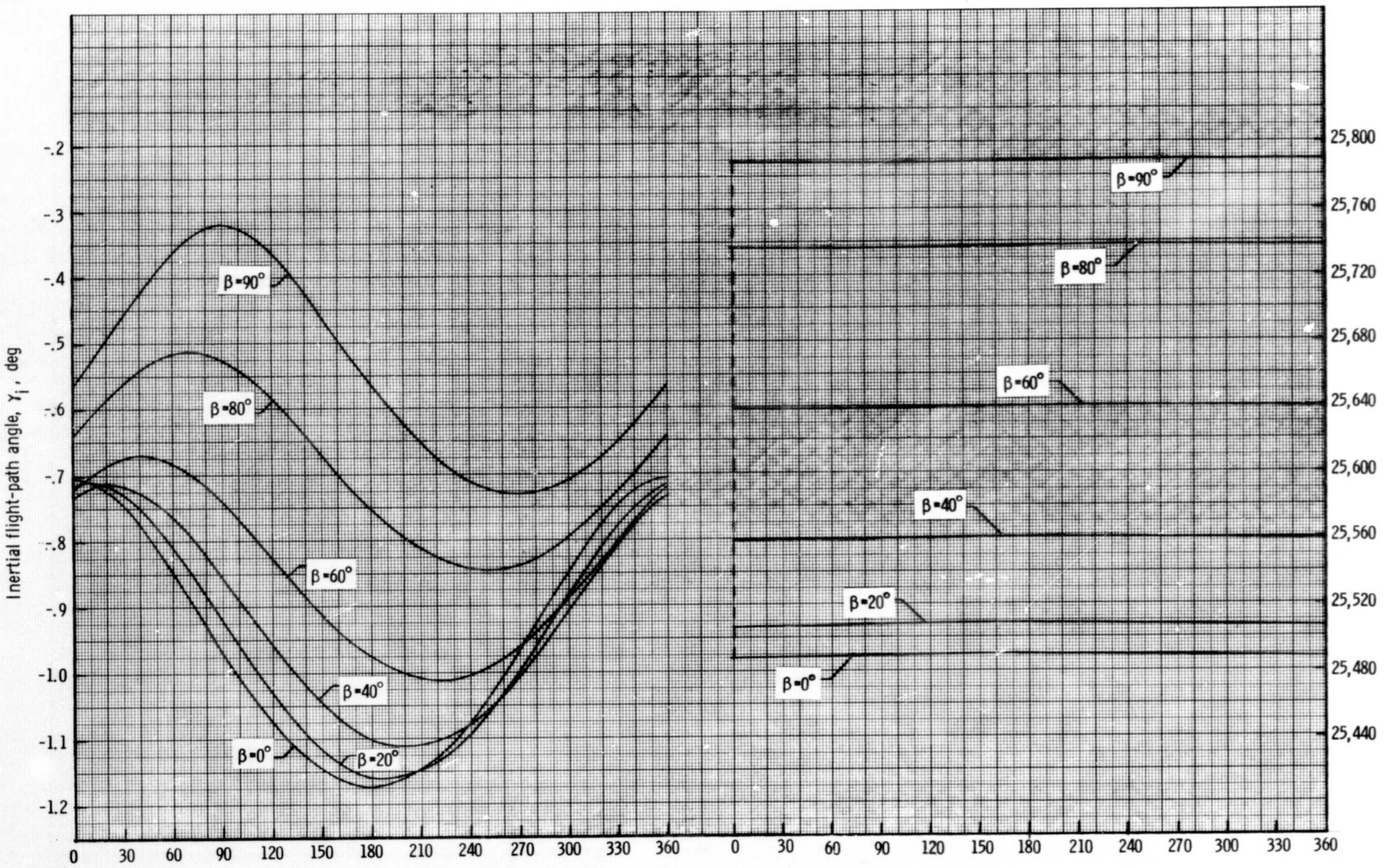

(b) ΔV = 300 fps

Figure 2. - Continued.

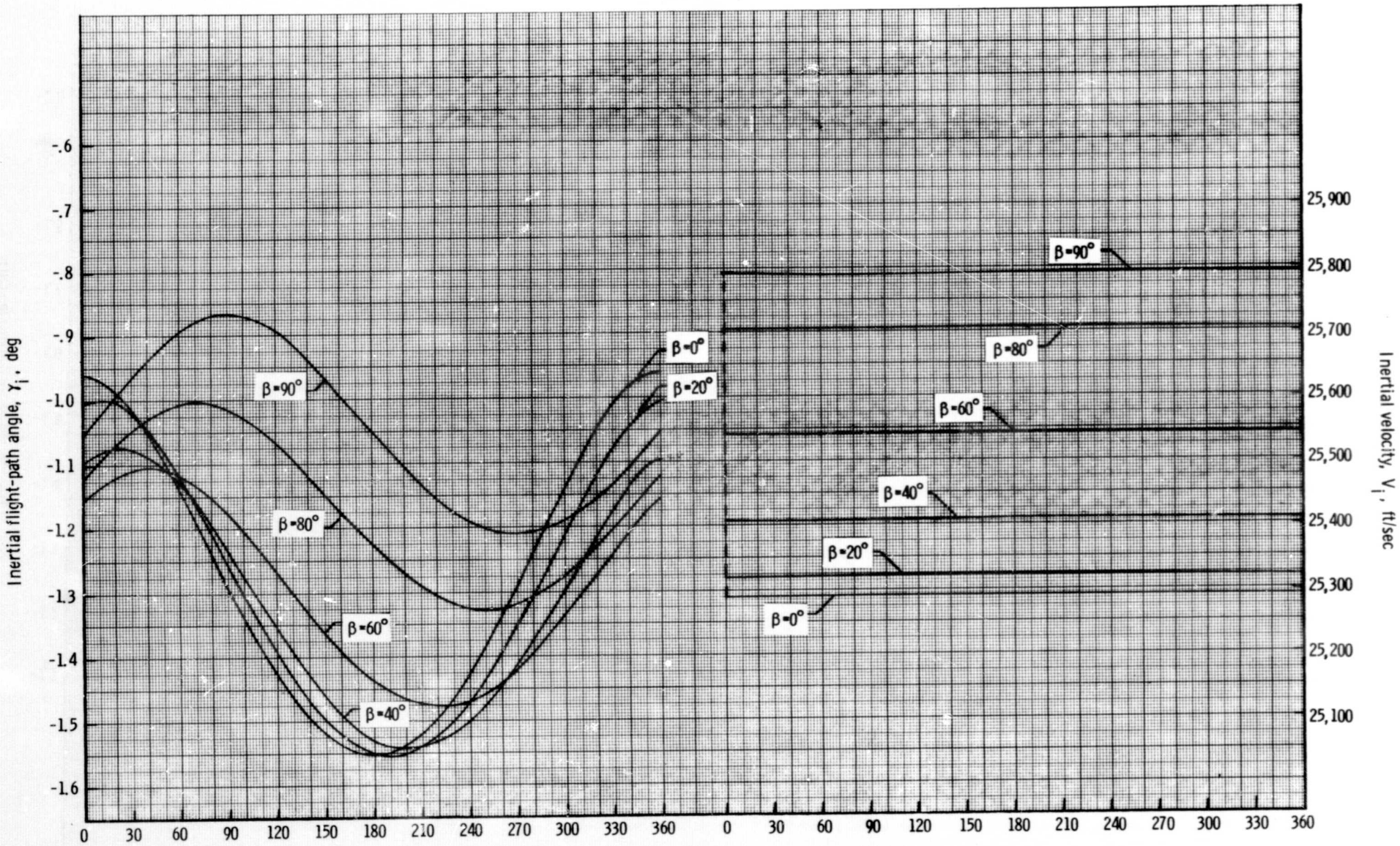

(c) ΔV = 500 fps

Figure 2. - Continued.

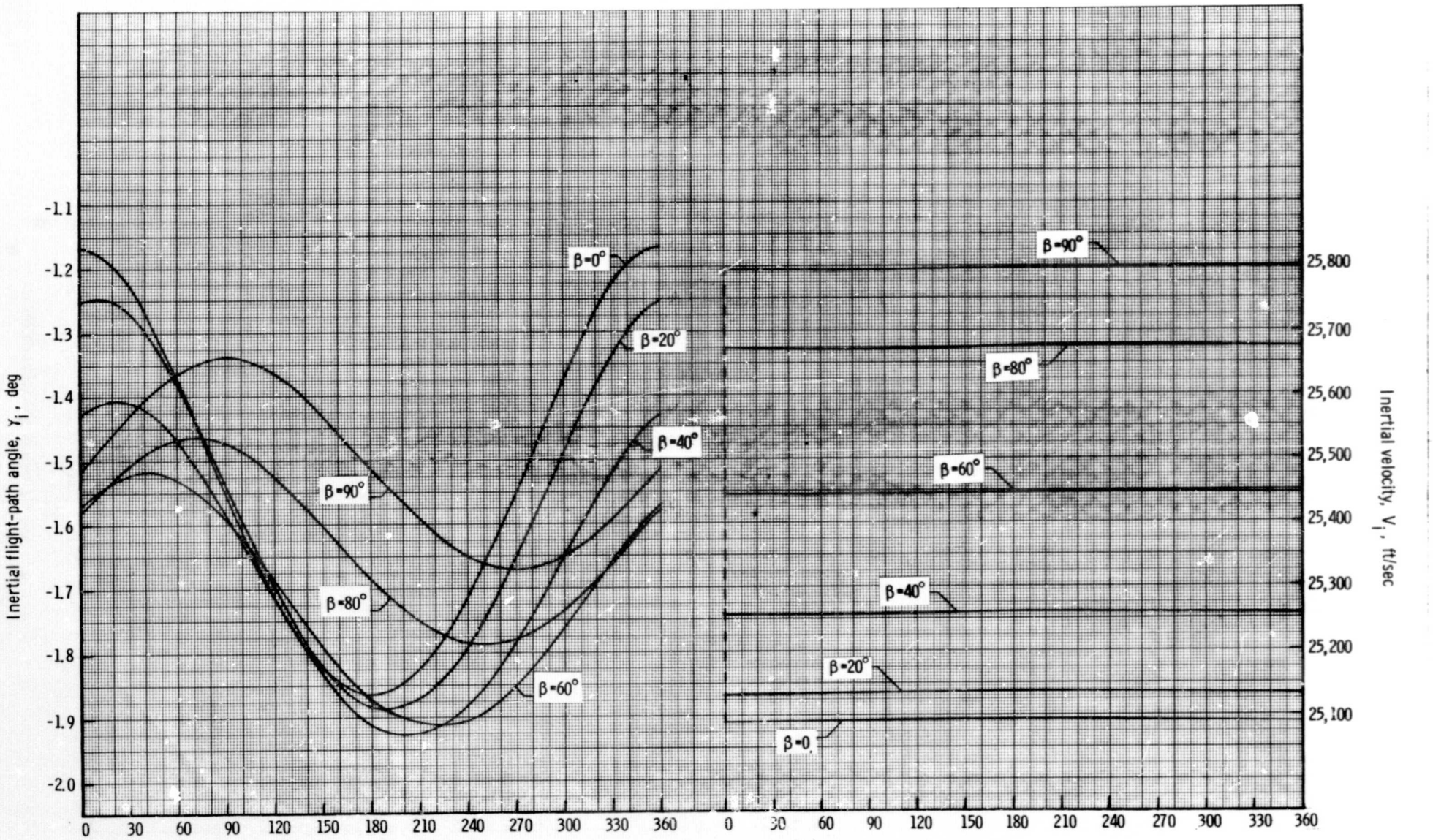

(d) ΔV = 700 fps

Figure 2. - Concluded.

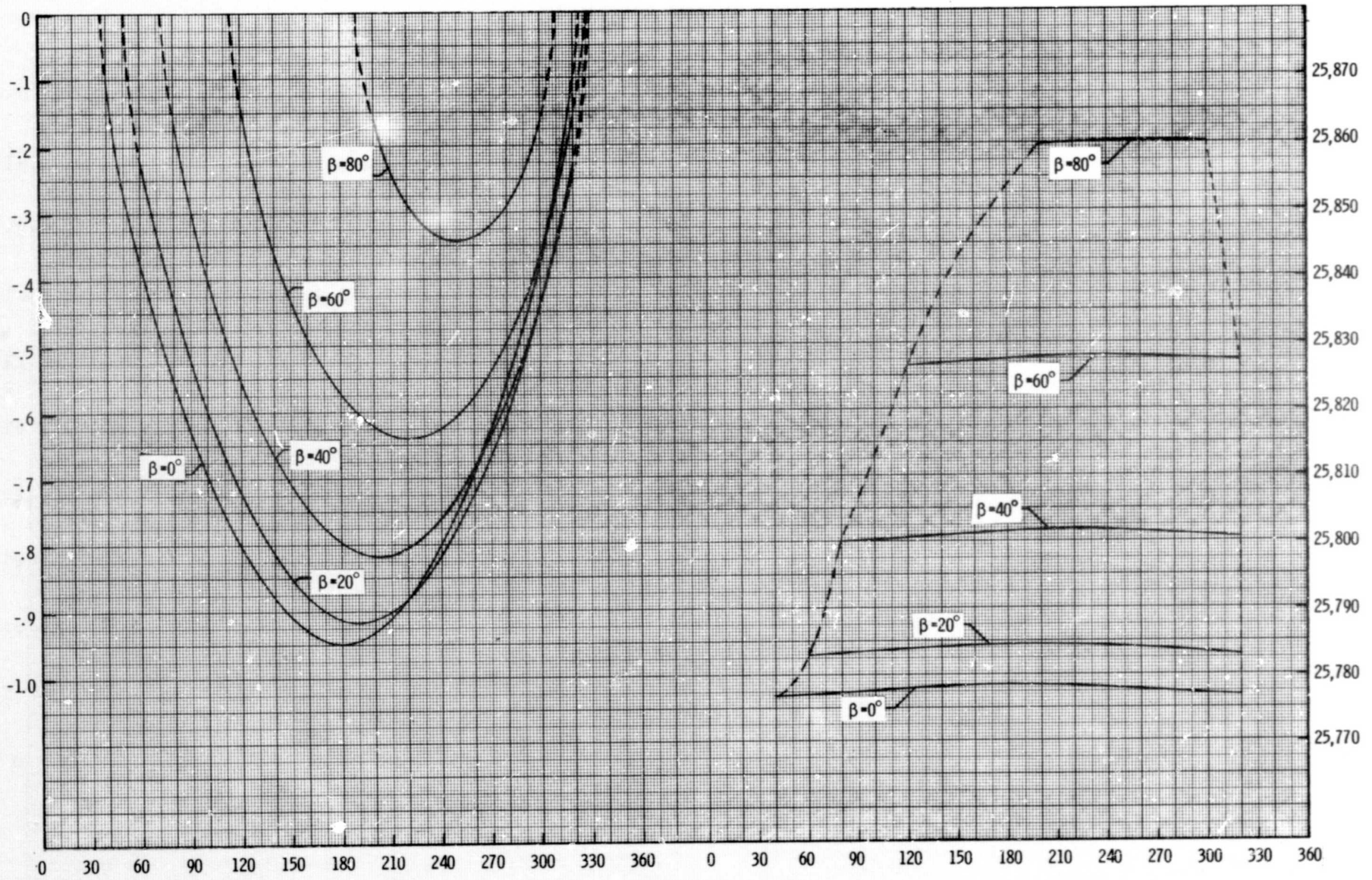

(a) ΔV = 100 fps

Figure 3. - Inertial flight-path angle and velocity at 400 000 feet as a function of retrograde true anomaly and a constant ΔV for an elliptical orbit where h_p = 80 nautical miles and h_a = 150 nautical miles.

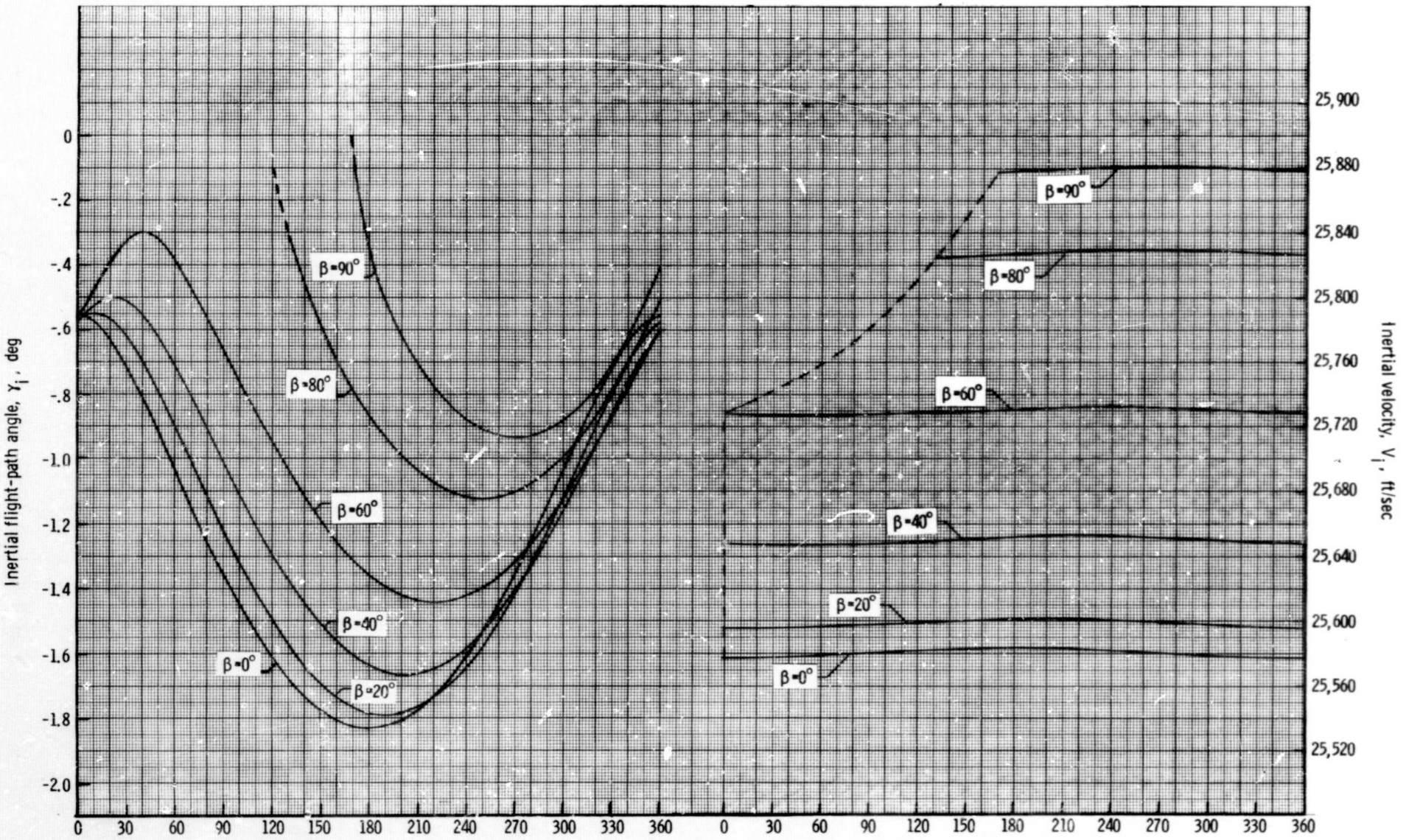

(b) ΔV = 300 fps

Figure 3. - Continued.

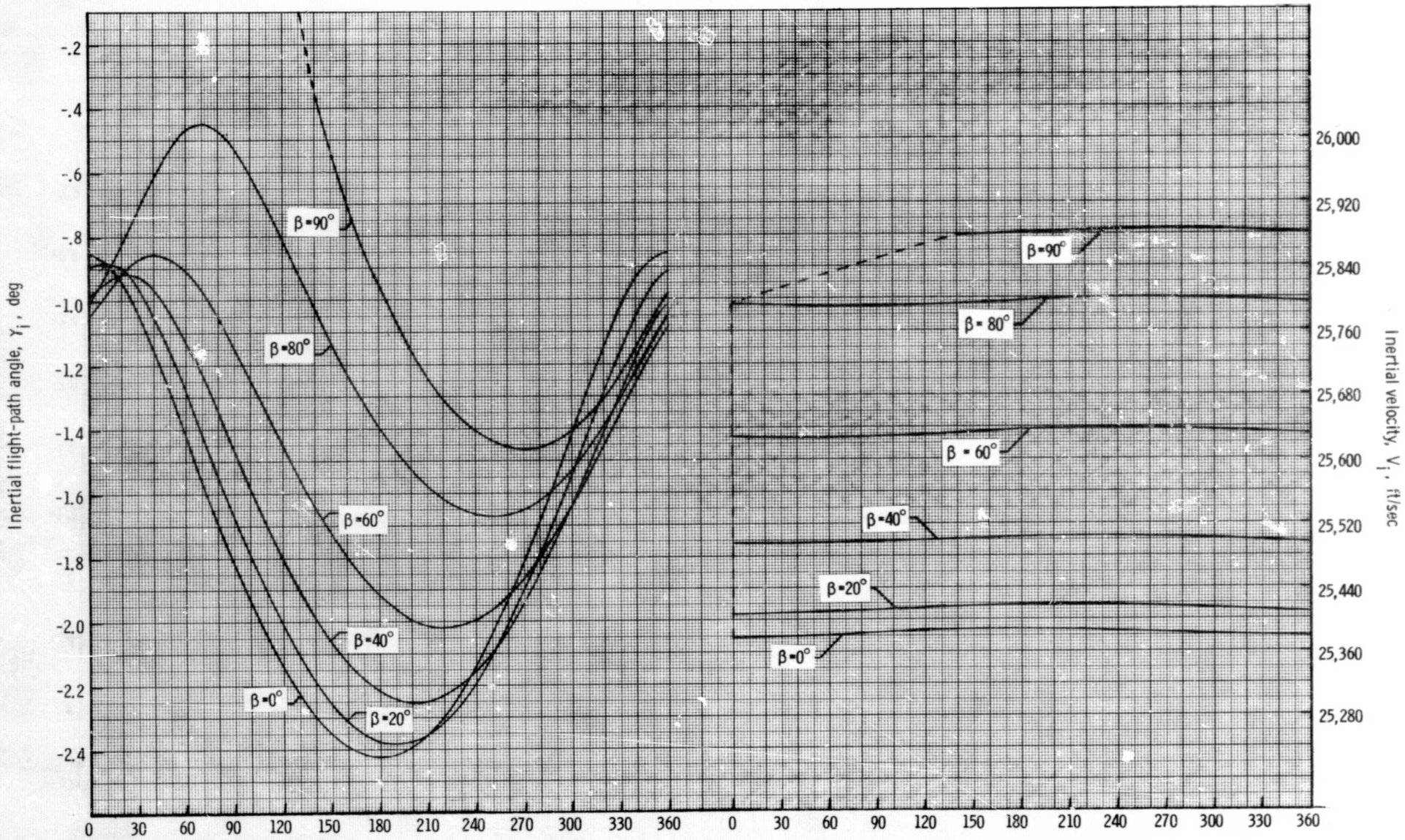

(c) ΔV = 500 fps

Figure 3. - Continued.

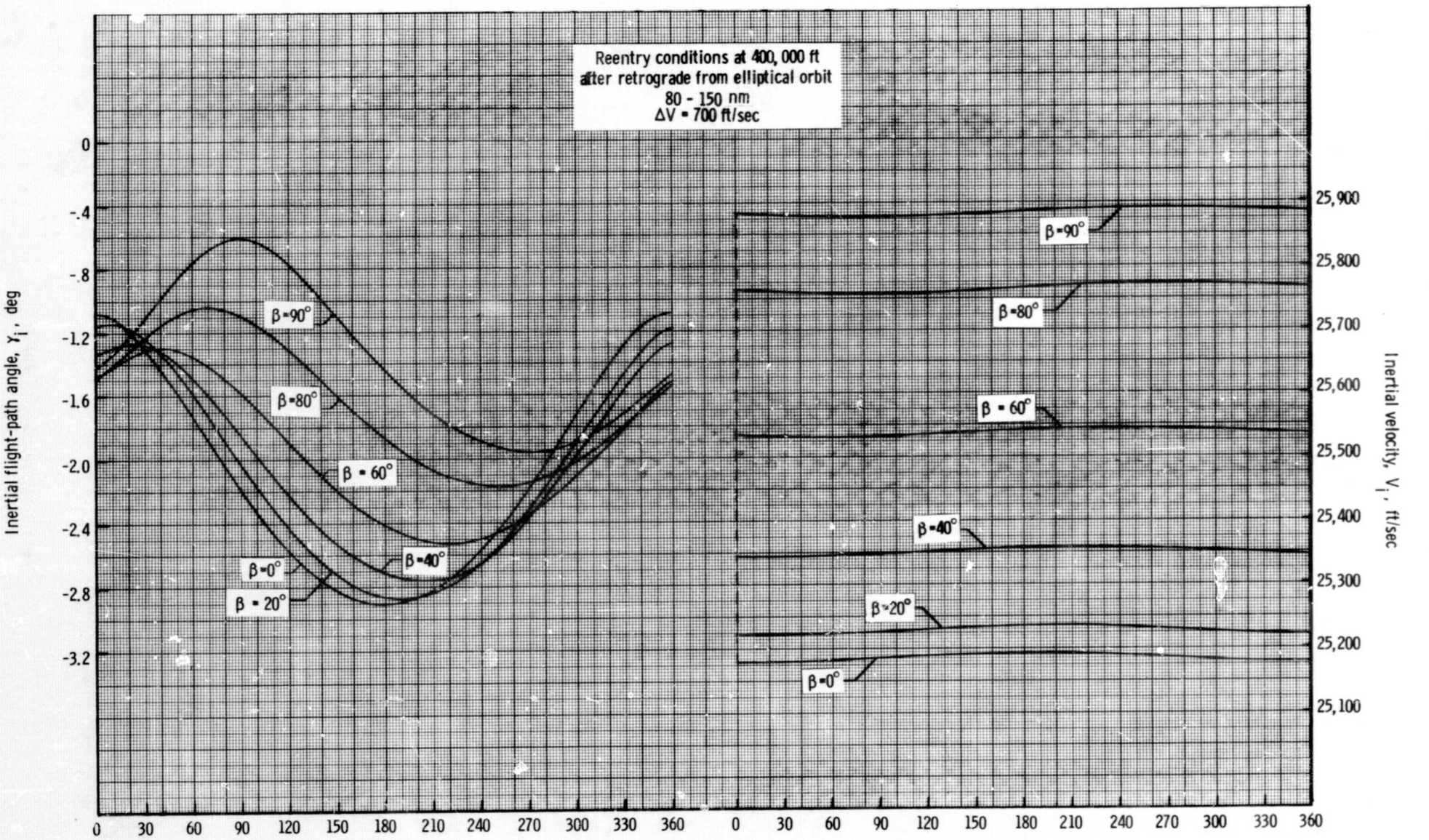

(d) ΔV = 700 fps

Figure 3. - Concluded.

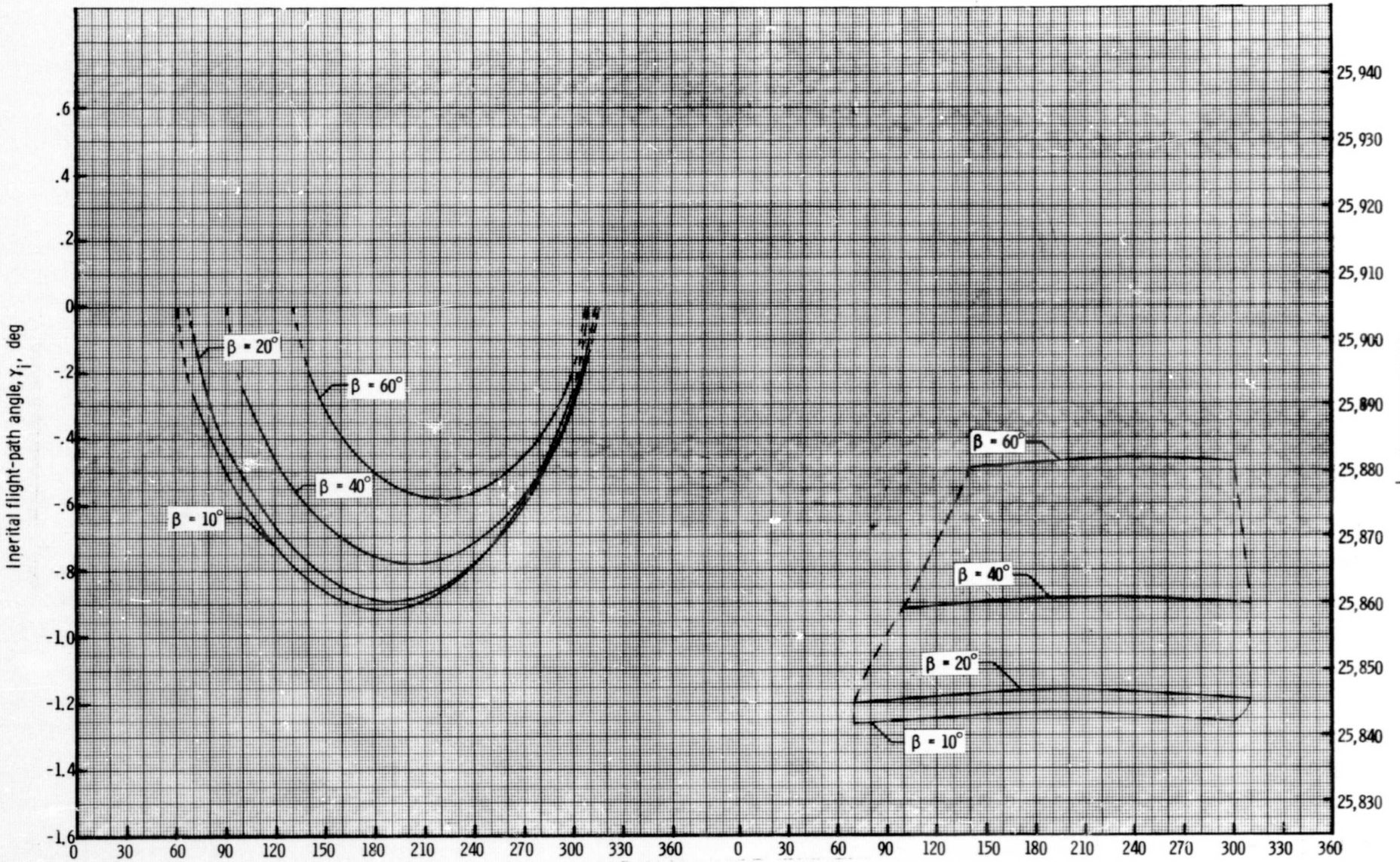

(a) ΔV = 80.5 fps

Figure 4. - Inertial flight-path angle and velocity at 400 000 feet as a function of retrograde true anomaly and a constant ΔV for an elliptical orbit where h_p = 80 nautical miles and h_a = 175 nautical miles.

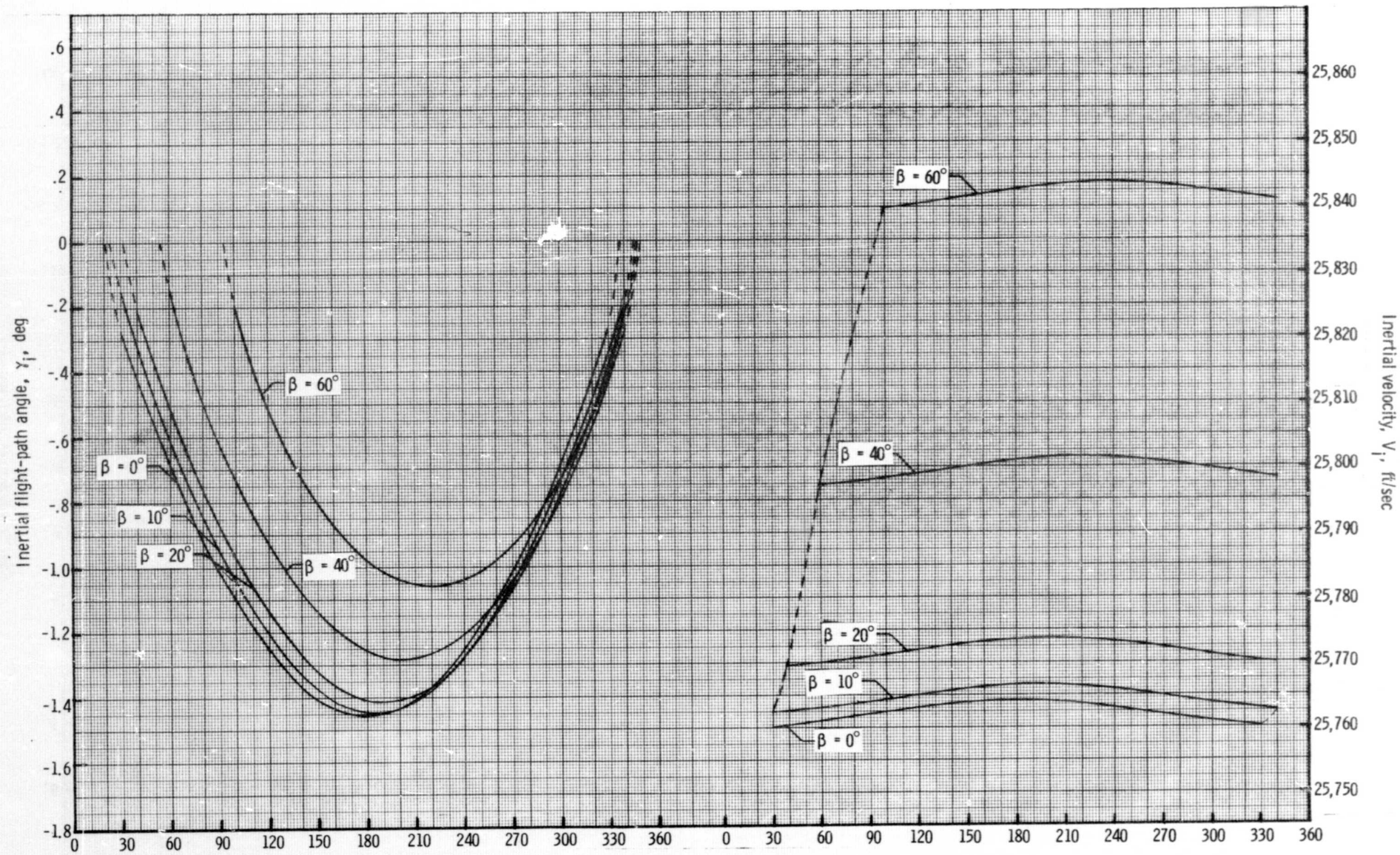

(b) ΔV = 161 fps

Figure 4. - Continued.

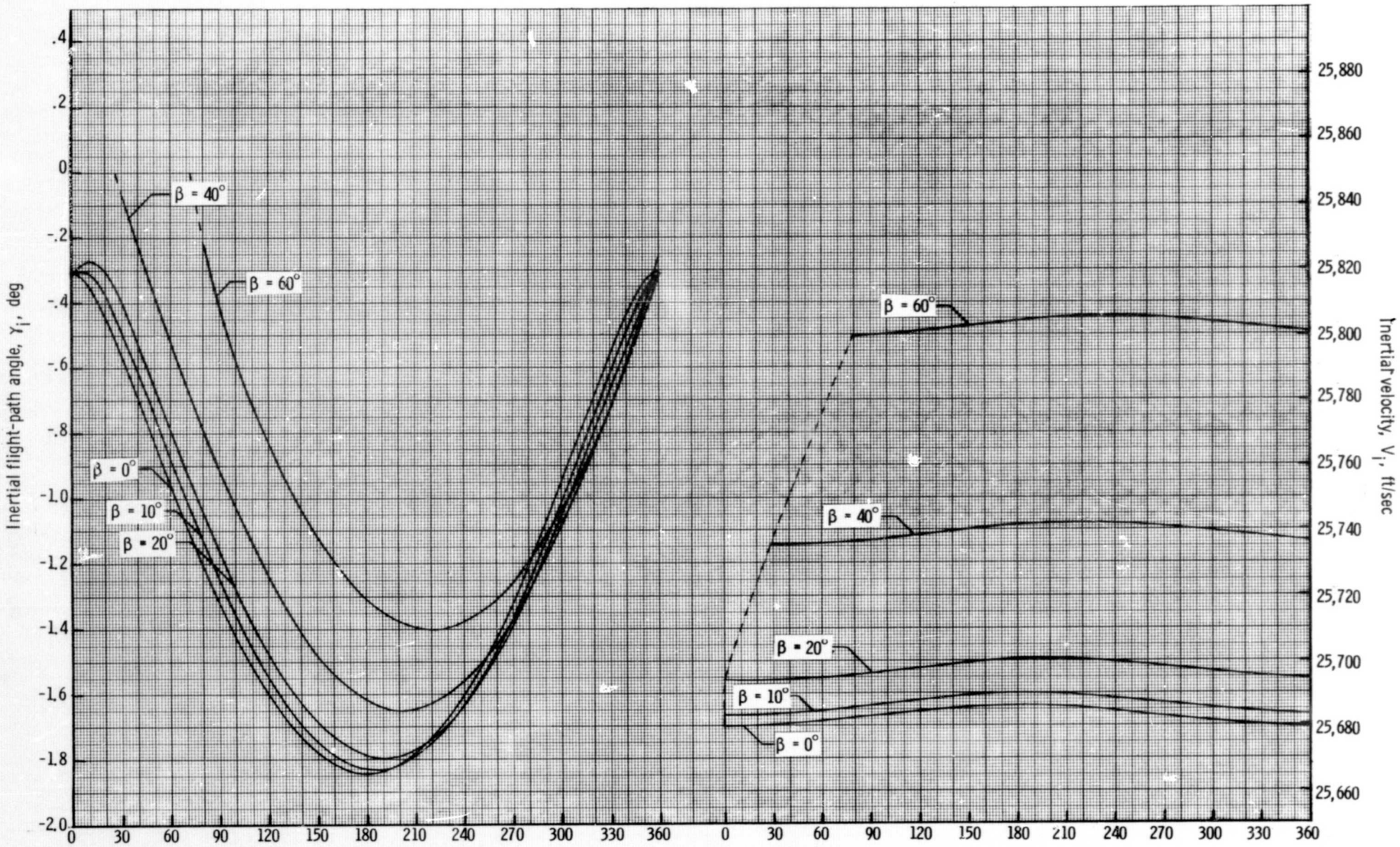

(c) ΔV = 241.5 fps

Figure 4. - Continued.

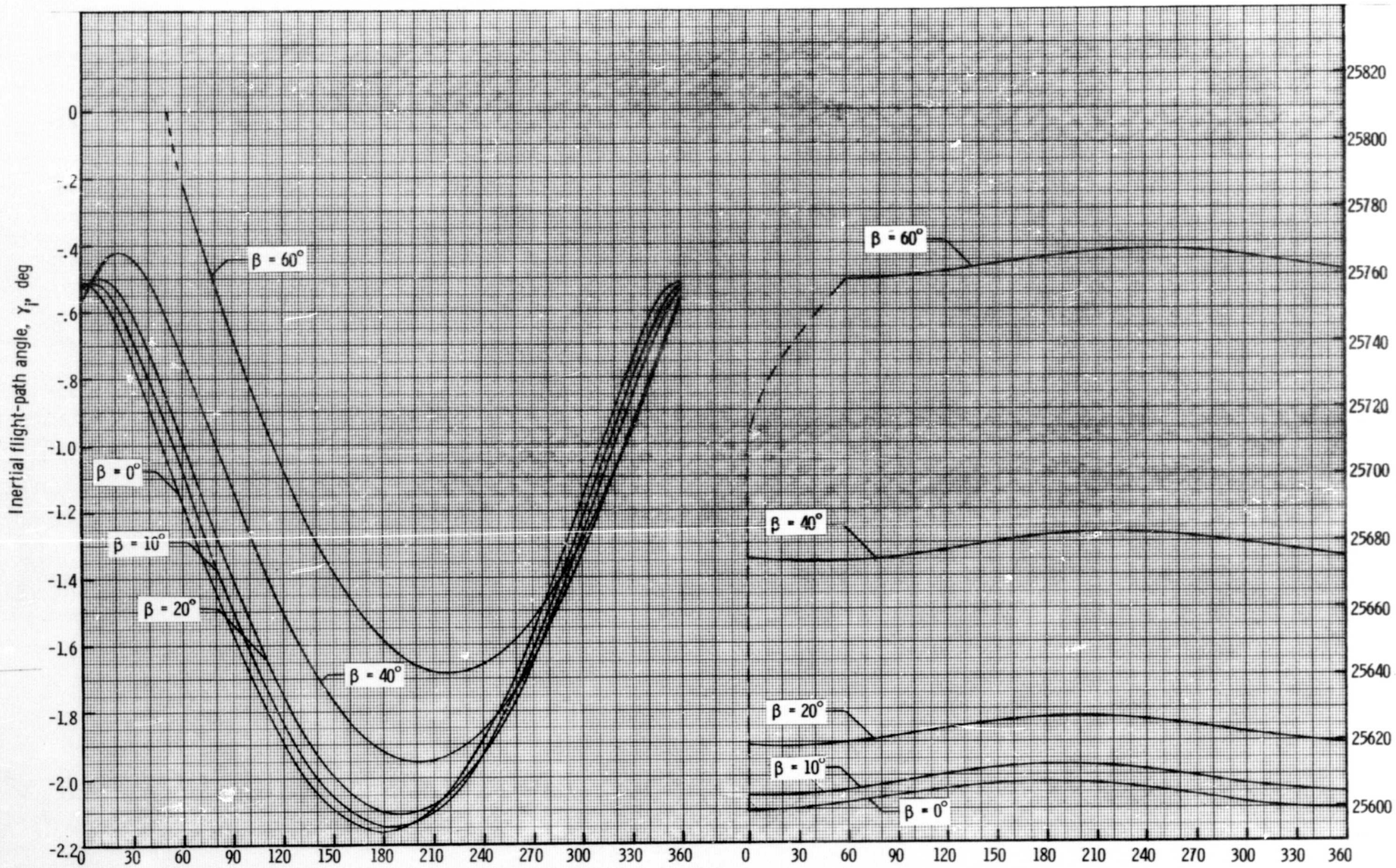

(d) ΔV = 322 fps

Figure 4. - Continued.

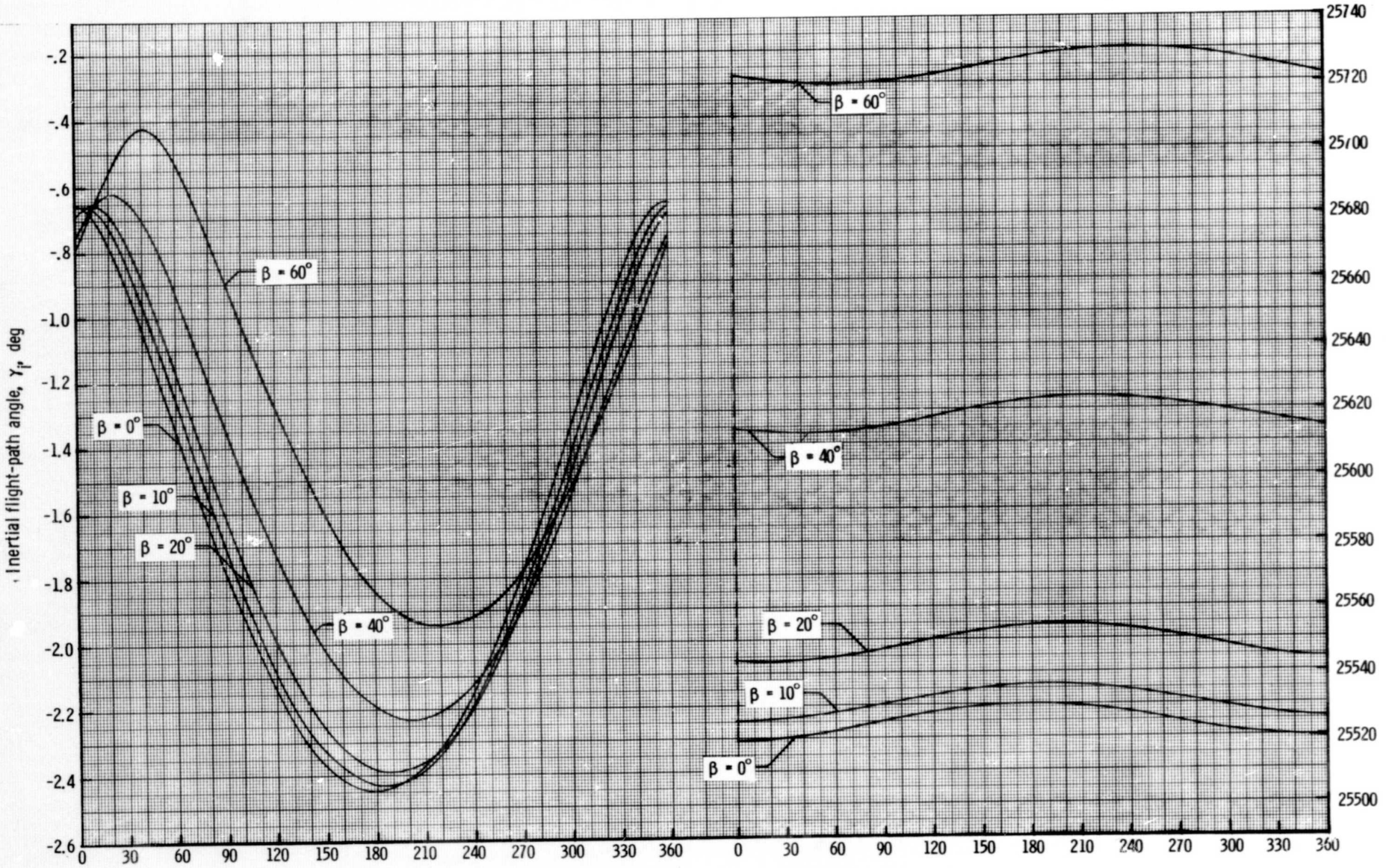

(e) ΔV = 402.5 fps

Figure 4. - Concluded.

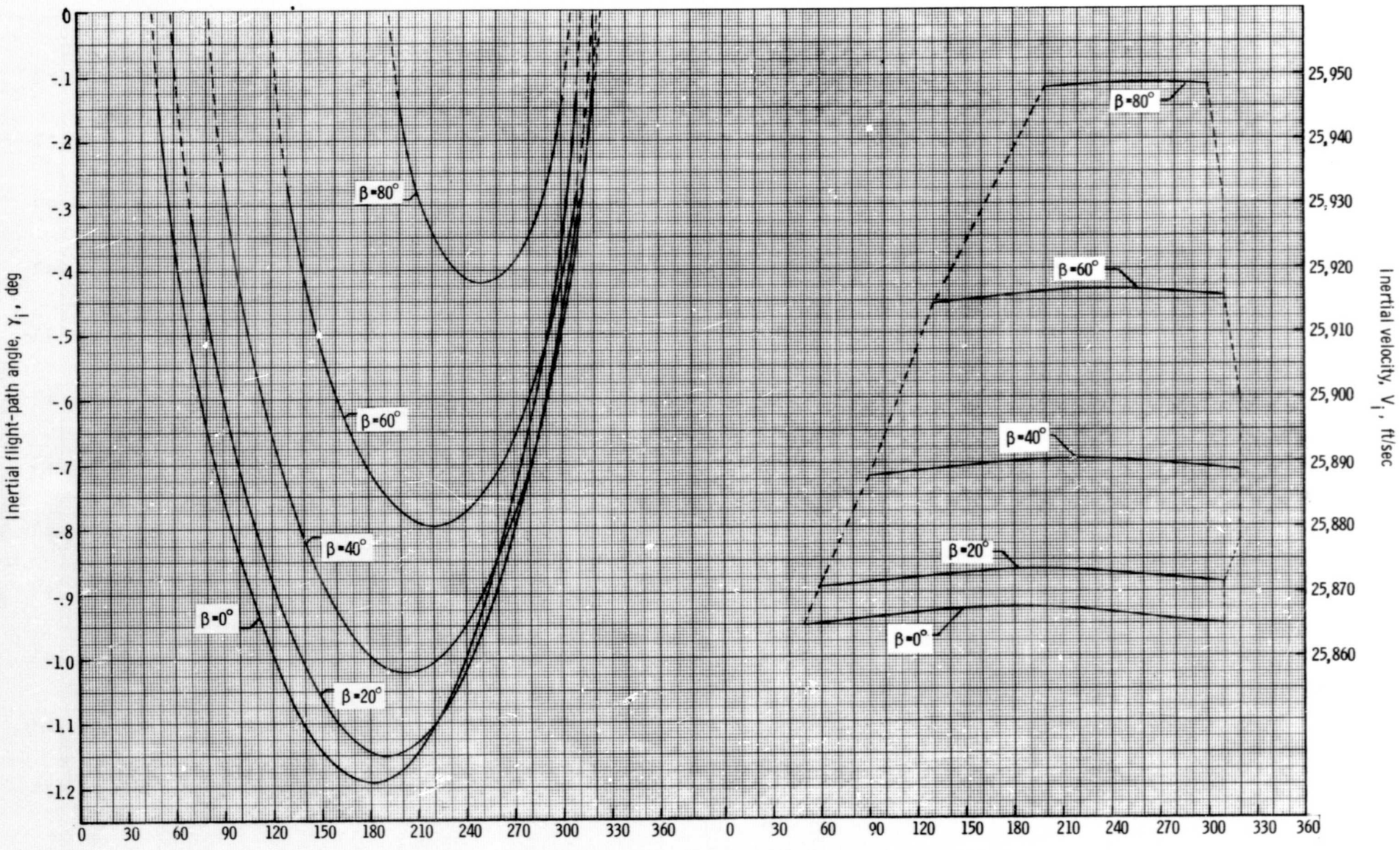

(a) ΔV = 100 fps

Figure 5. - Inertial flight-path angle and velocity at 400 000 feet as a function of retrograde true anomaly and a constant ΔV for an elliptical orbit where h_p = 80 nautical miles and h_a = 200 nautical miles.

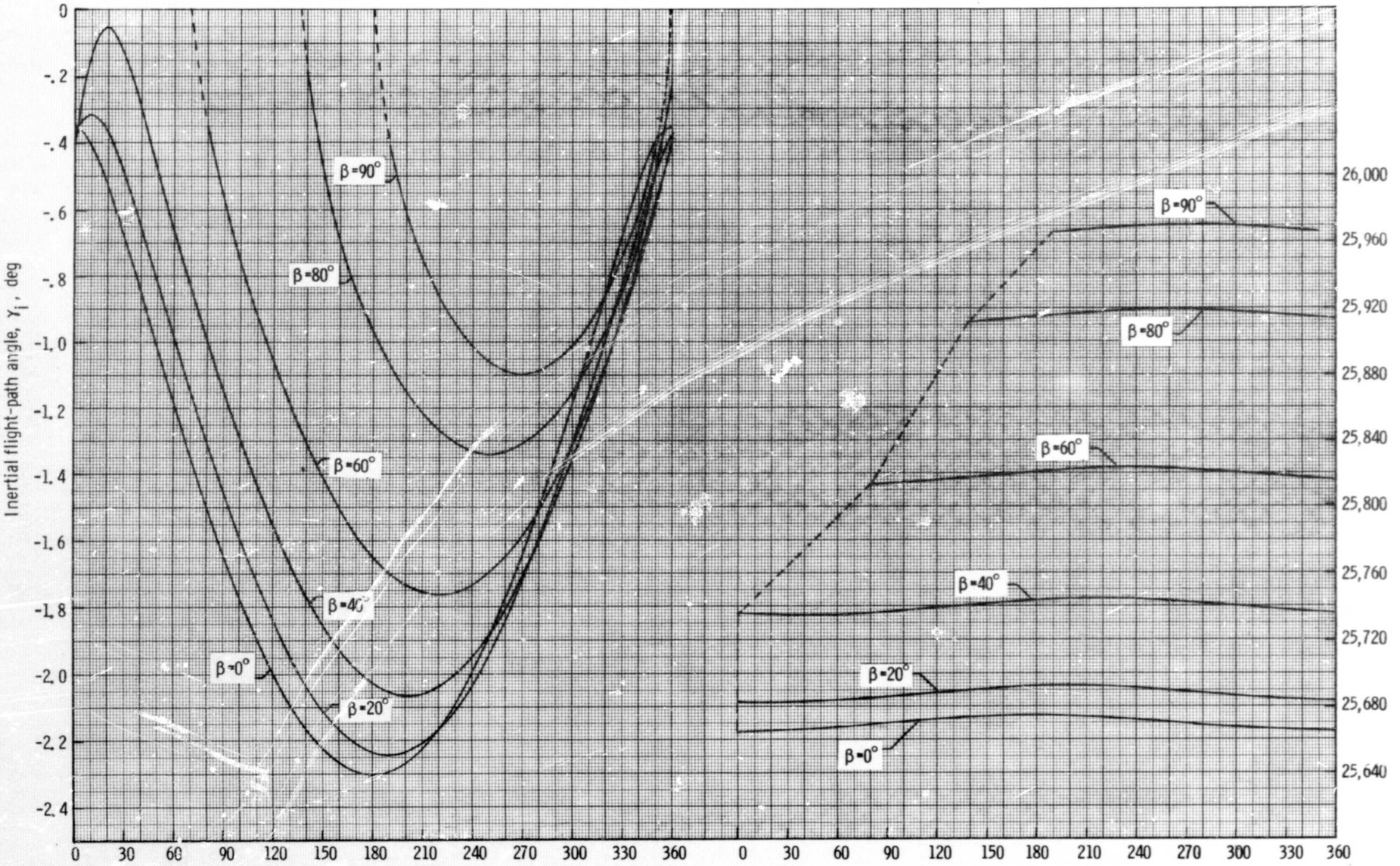

(b) ΔV = 300 fps

Figure 5. - Continued.

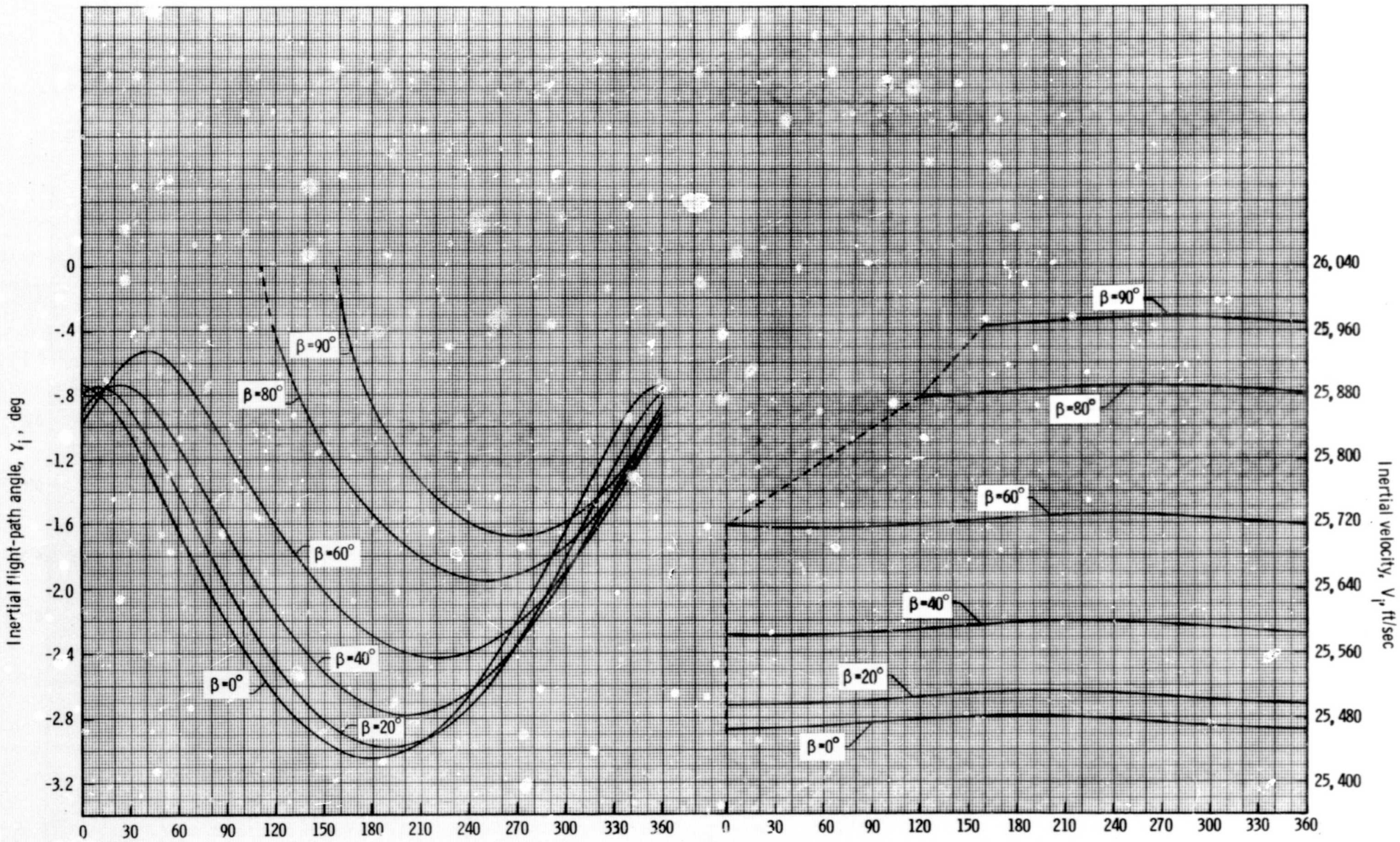

(c) $\Delta V = 500$ fps

Figure 5. - Continued.

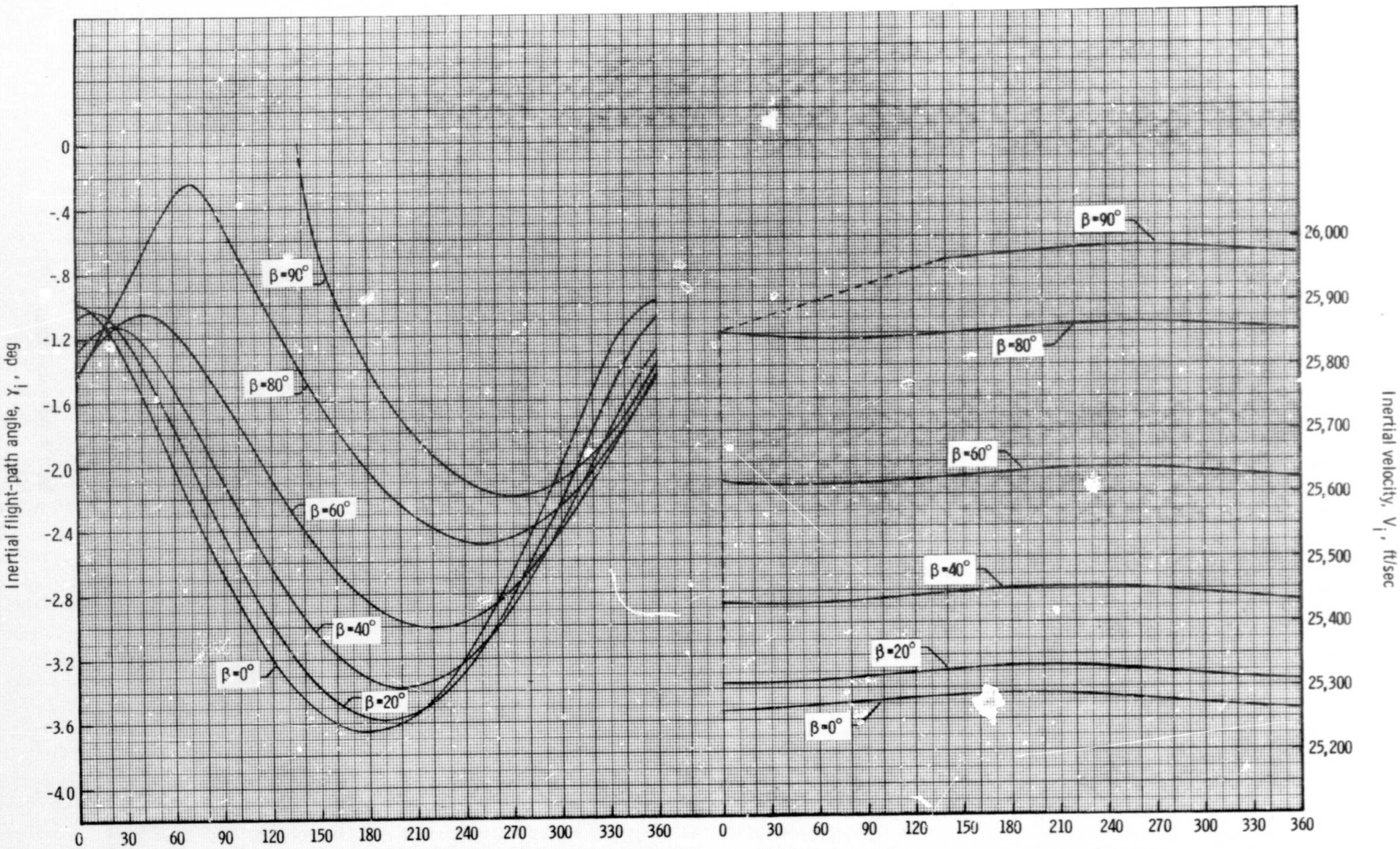

(d) ΔV = 700 fps

Figure 5. - Concluded.

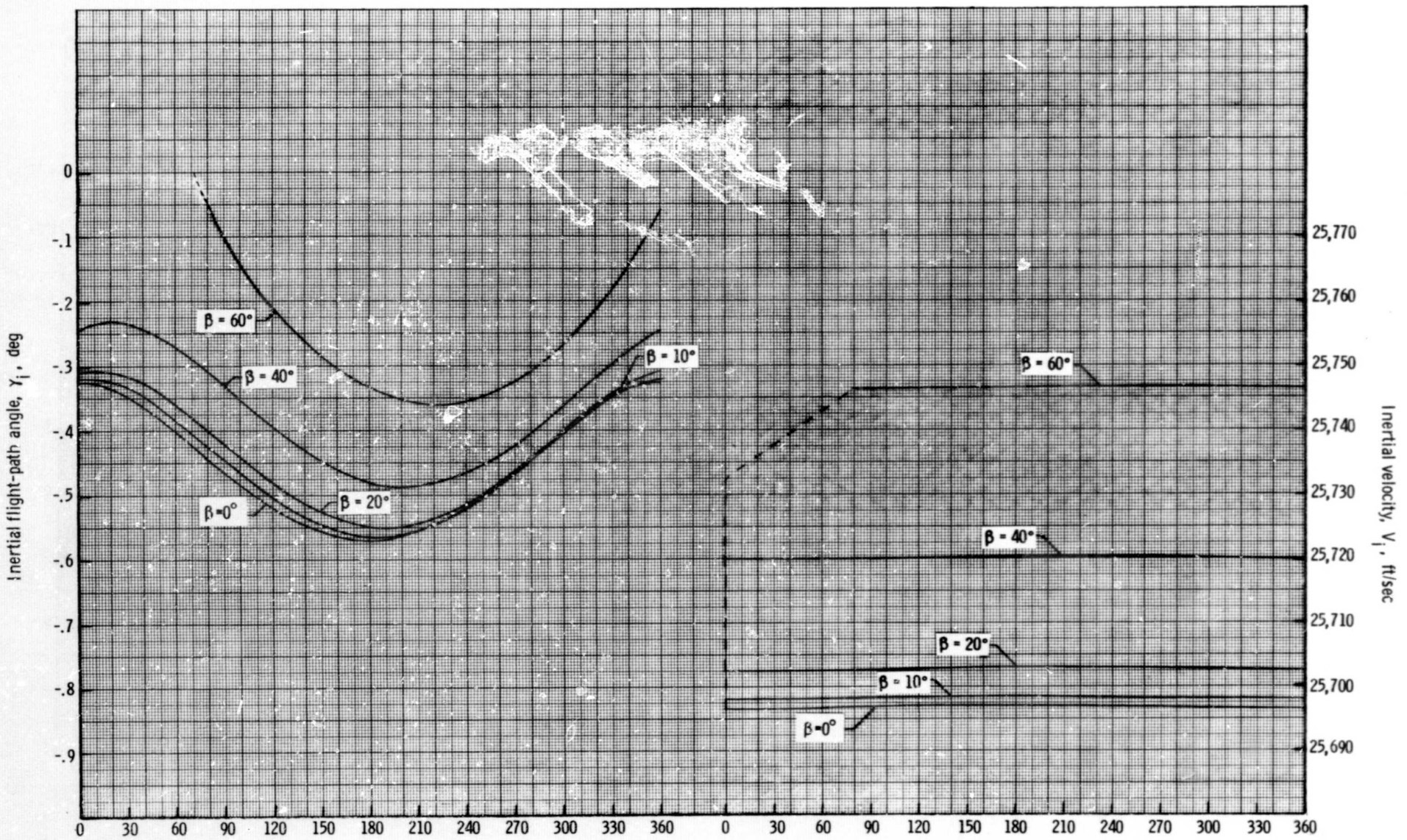

(a) ΔV = 100 fps

Figure 6. - Inertial flight-path angle and velocity at 400 000 feet as a function of retrograde true anomaly and a constant ΔV for an elliptical orbit where h_p = 85 nautical miles and h_a = 100 nautical miles.

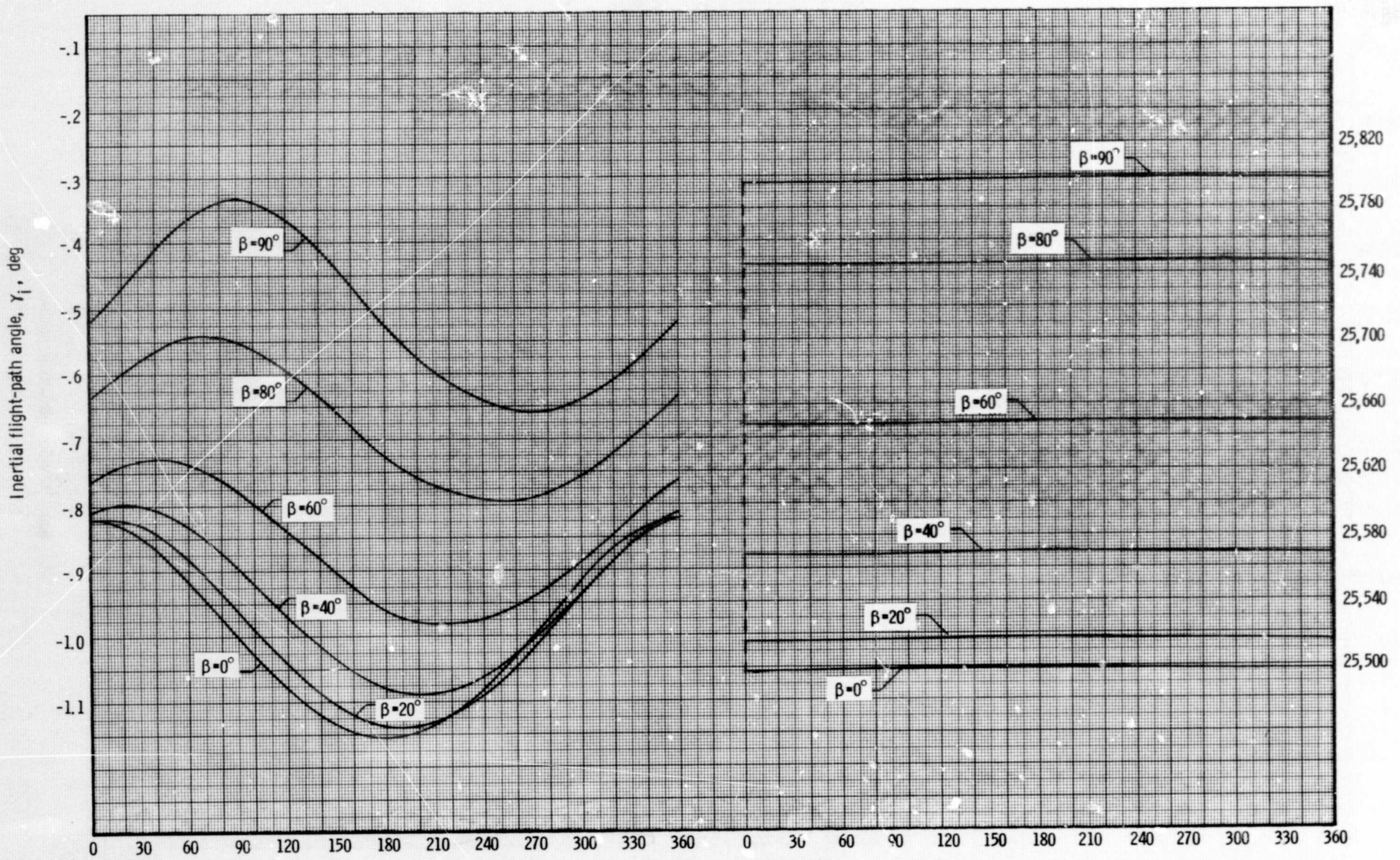

(b) ΔV = 300 fps

Figure 6. - Continued.

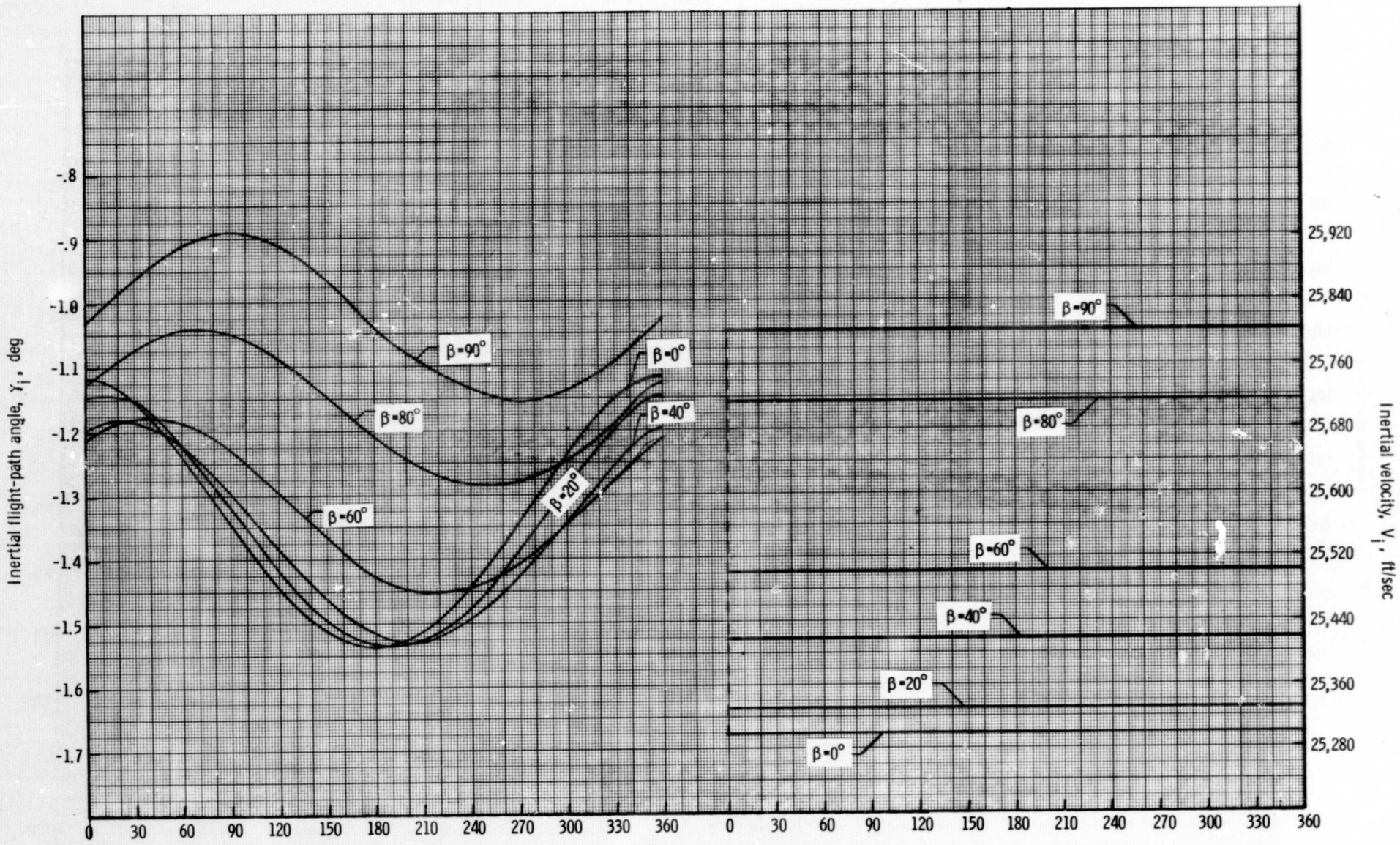

(c) ΔV = 500 fps

Figure 6. - Continued.

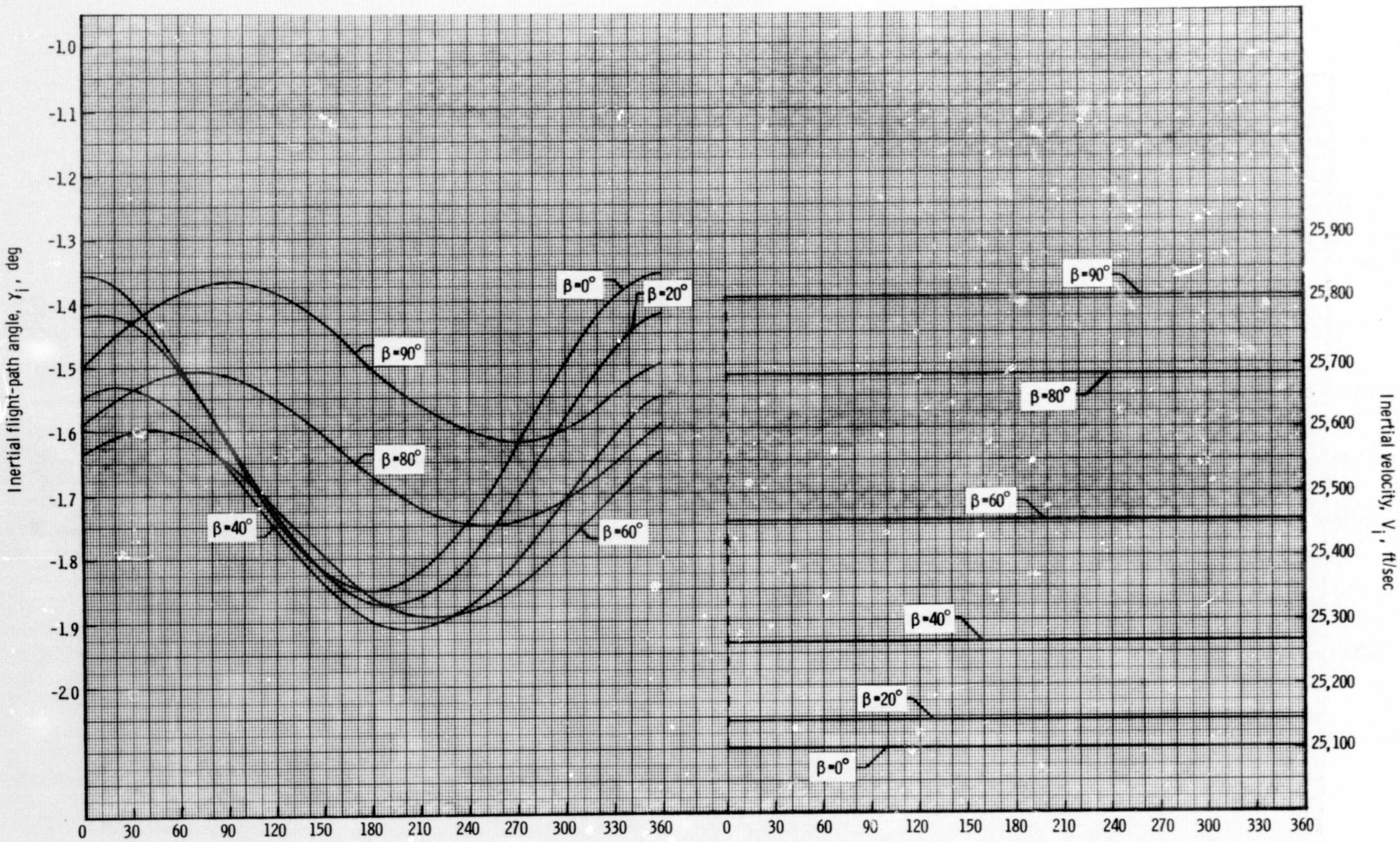

(d) ΔV = 700 fps

Figure 6. - Concluded.

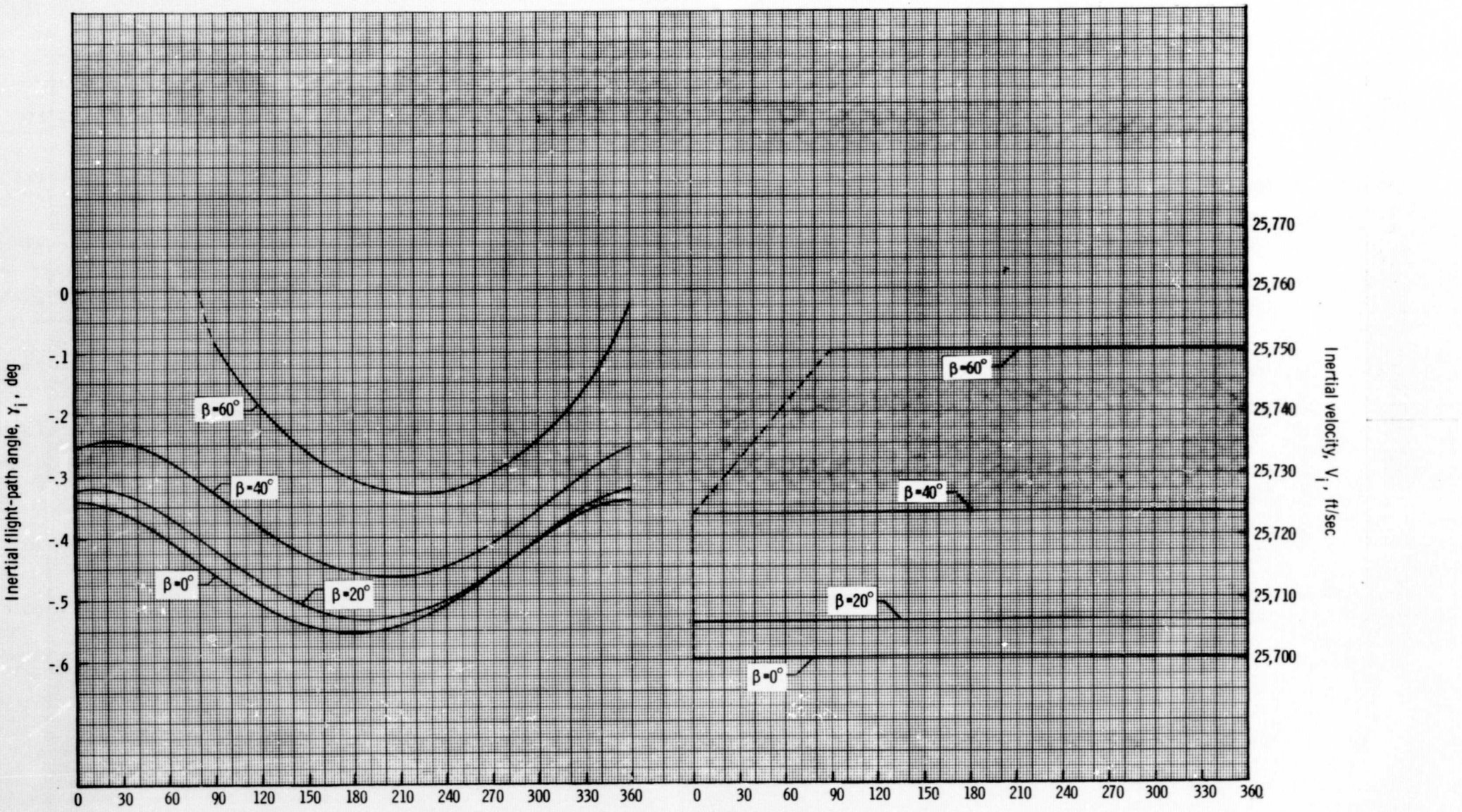

(a) ΔV = 100 fps

Figure 7. - Inertial flight-path angle and velocity at 400 000 feet as a function of retrograde true anomaly and a constant ΔV for an elliptical orbit where h_p = 87 nautical miles and h_a = 100 nautical miles.

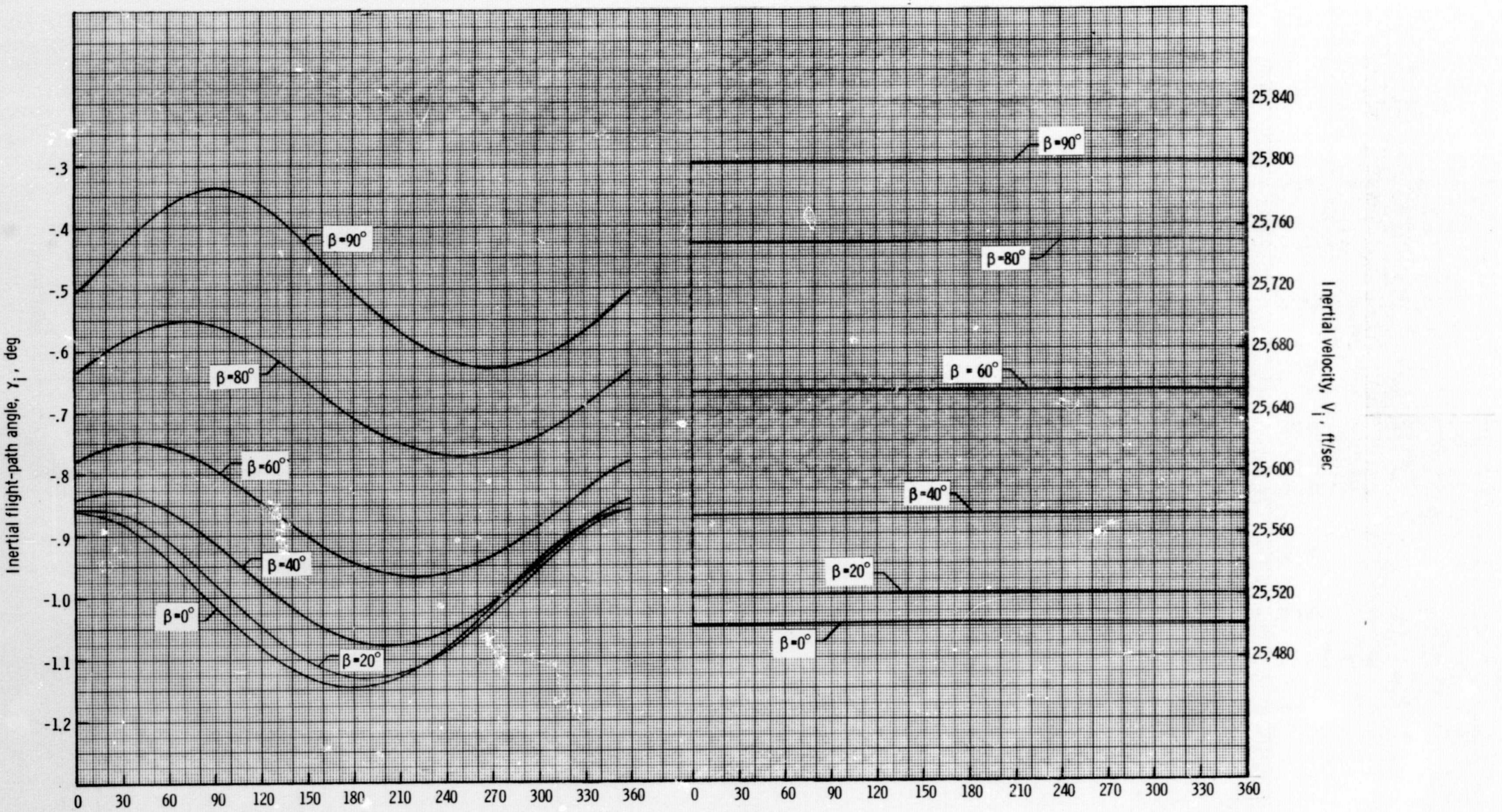

(b) ΔV = 300 fps

Figure 7. - Continued.

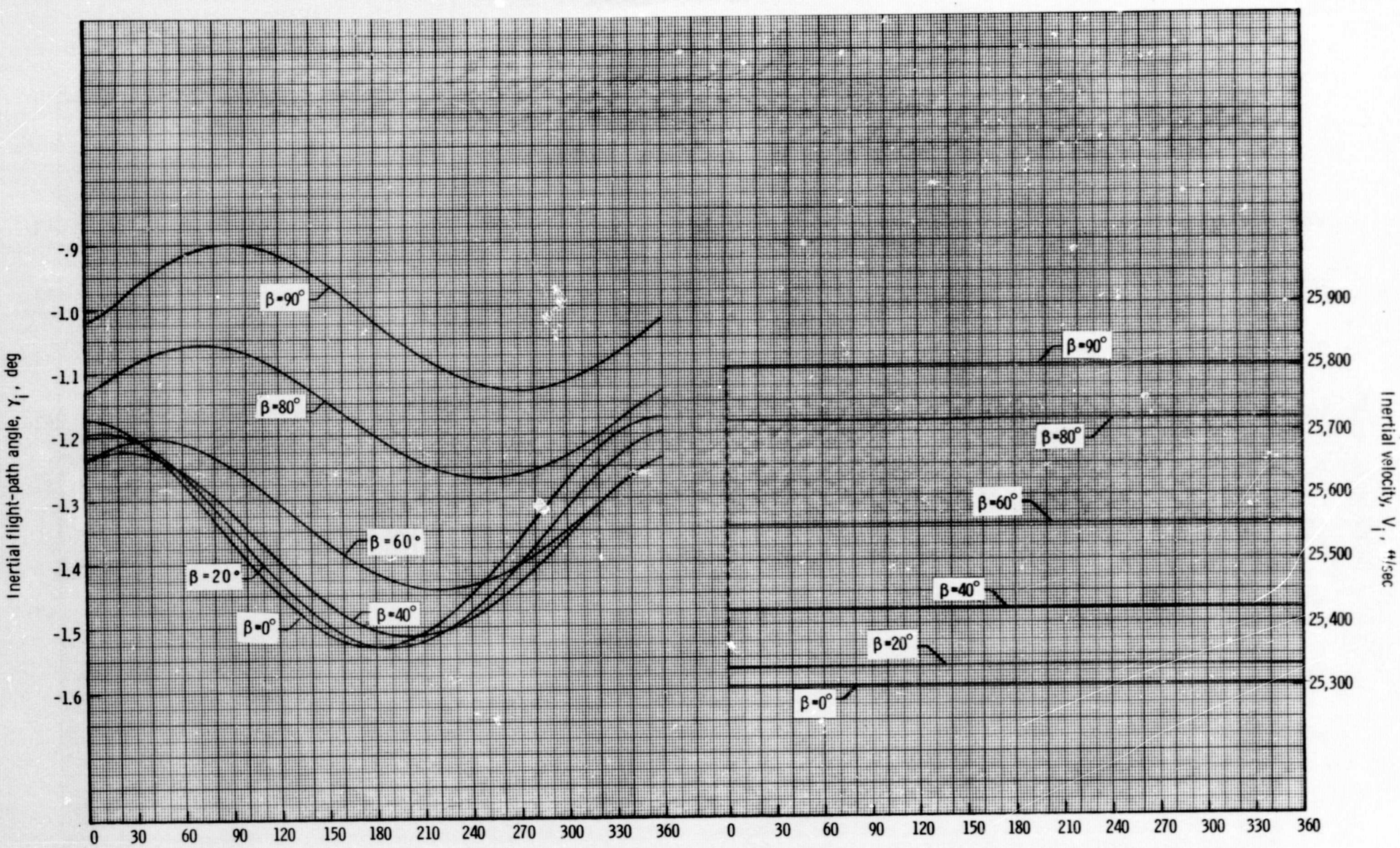

(c) ΔV = 500 fps

Figure 7. - Continued.

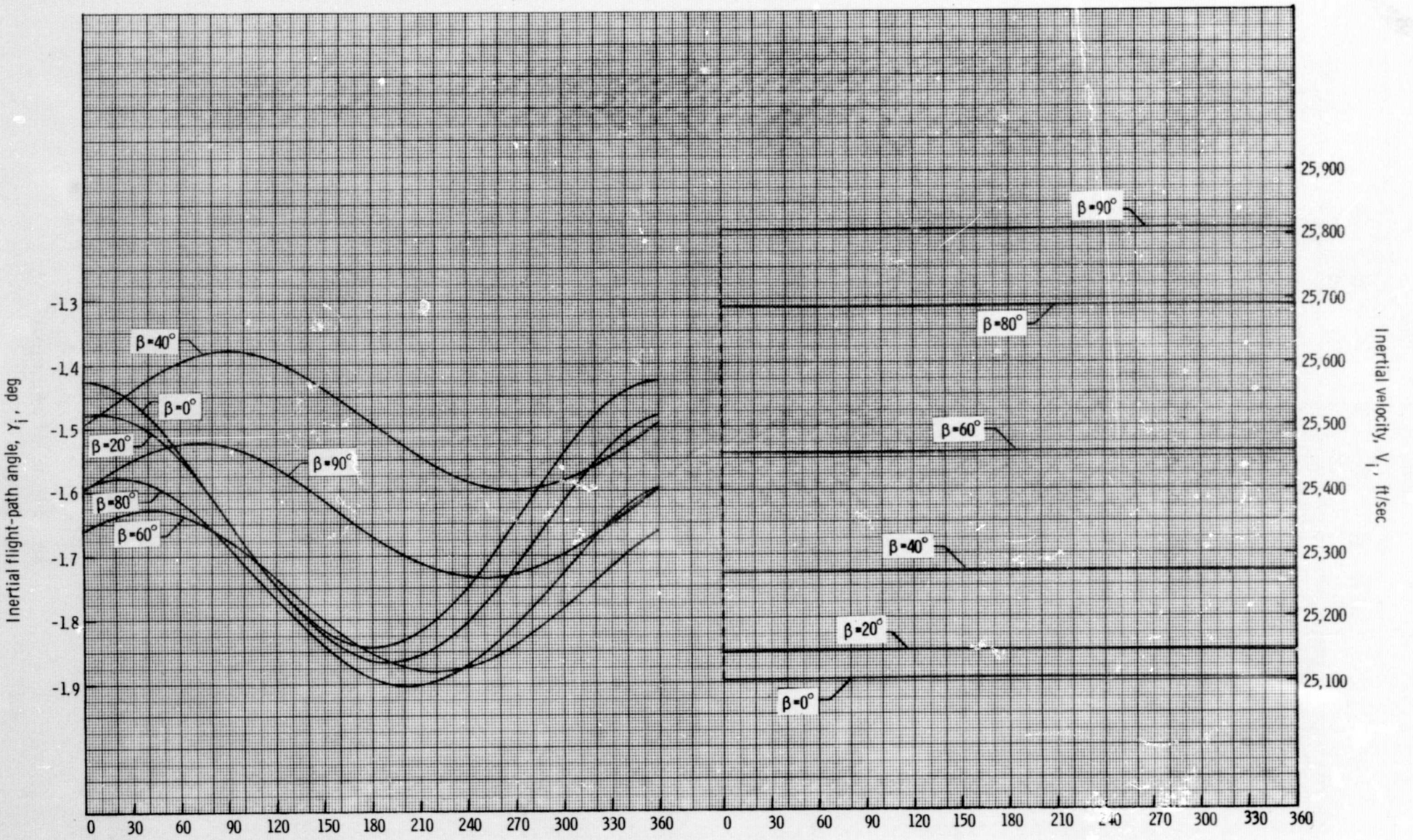

(d) ΔV = 700 fps

Figure 7. - Concluded.

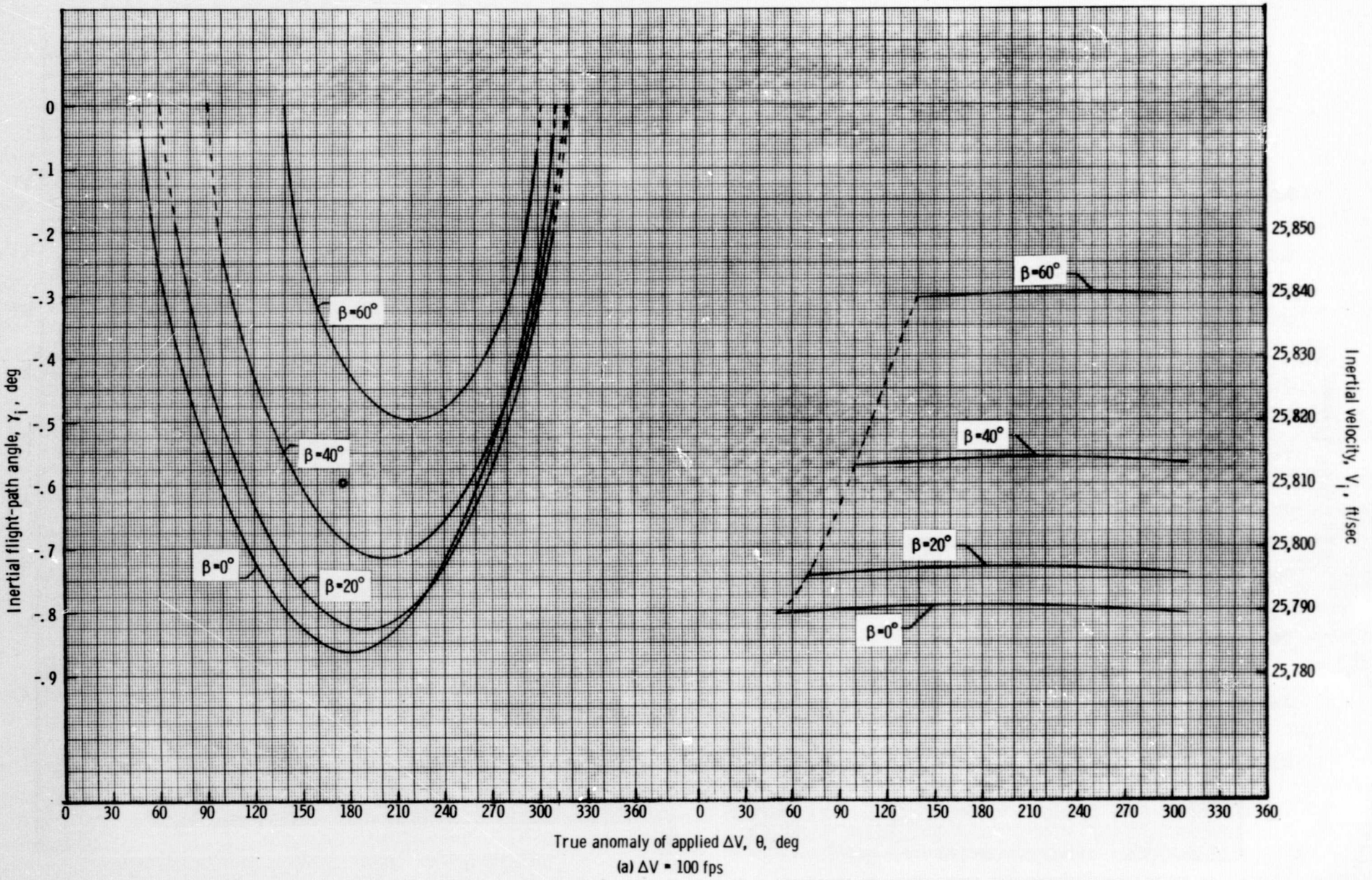

(a) ΔV = 100 fps

Figure 8. Inertial flight-path angle and velocity at 400 000 feet as a function of retrograde true anomaly and a constant ΔV for an elliptical orbit where h_p = 87 nautical miles and h_a = 150 nautical miles.

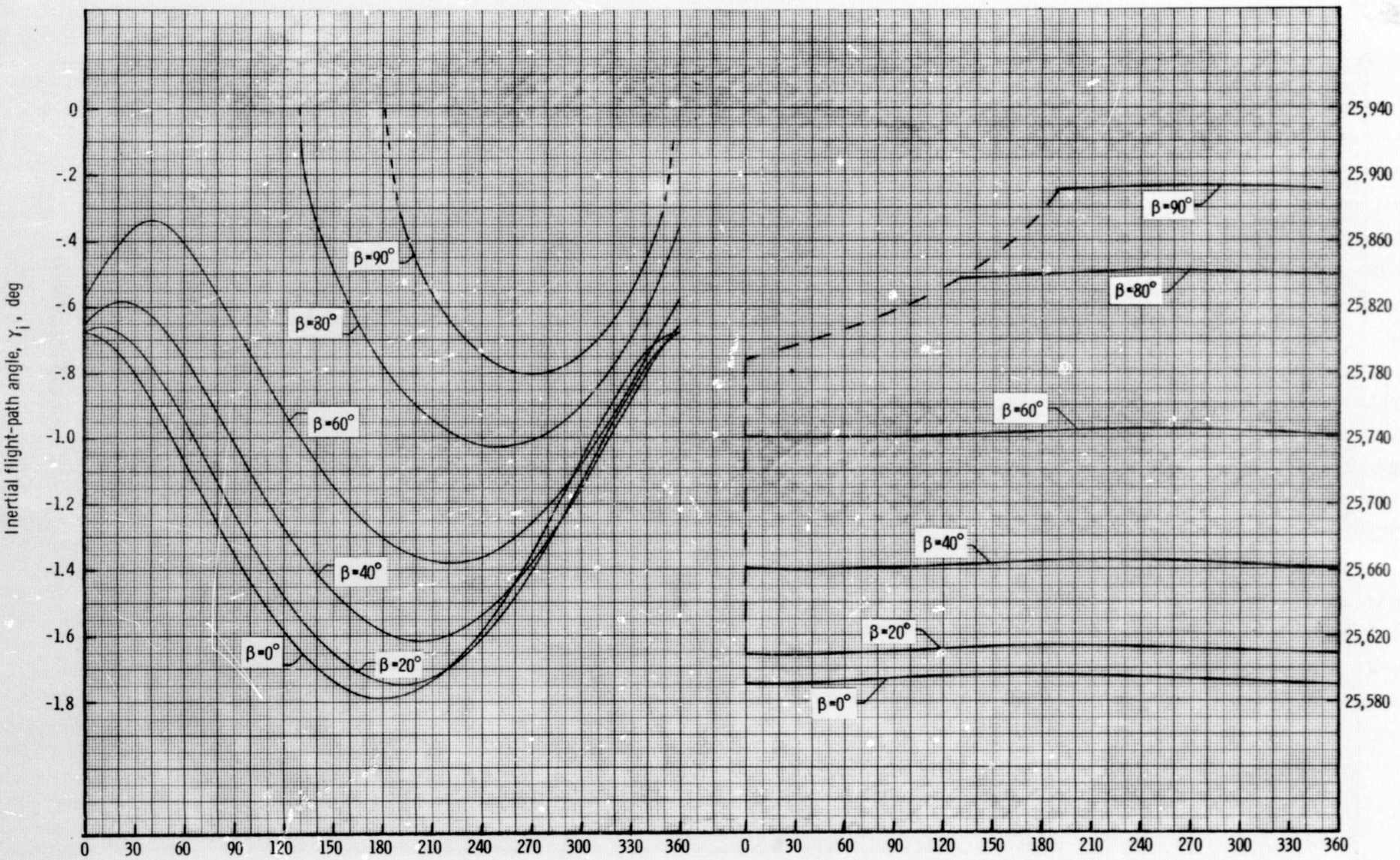

(b) ΔV = 300 fps

Figure 8. - Continued.

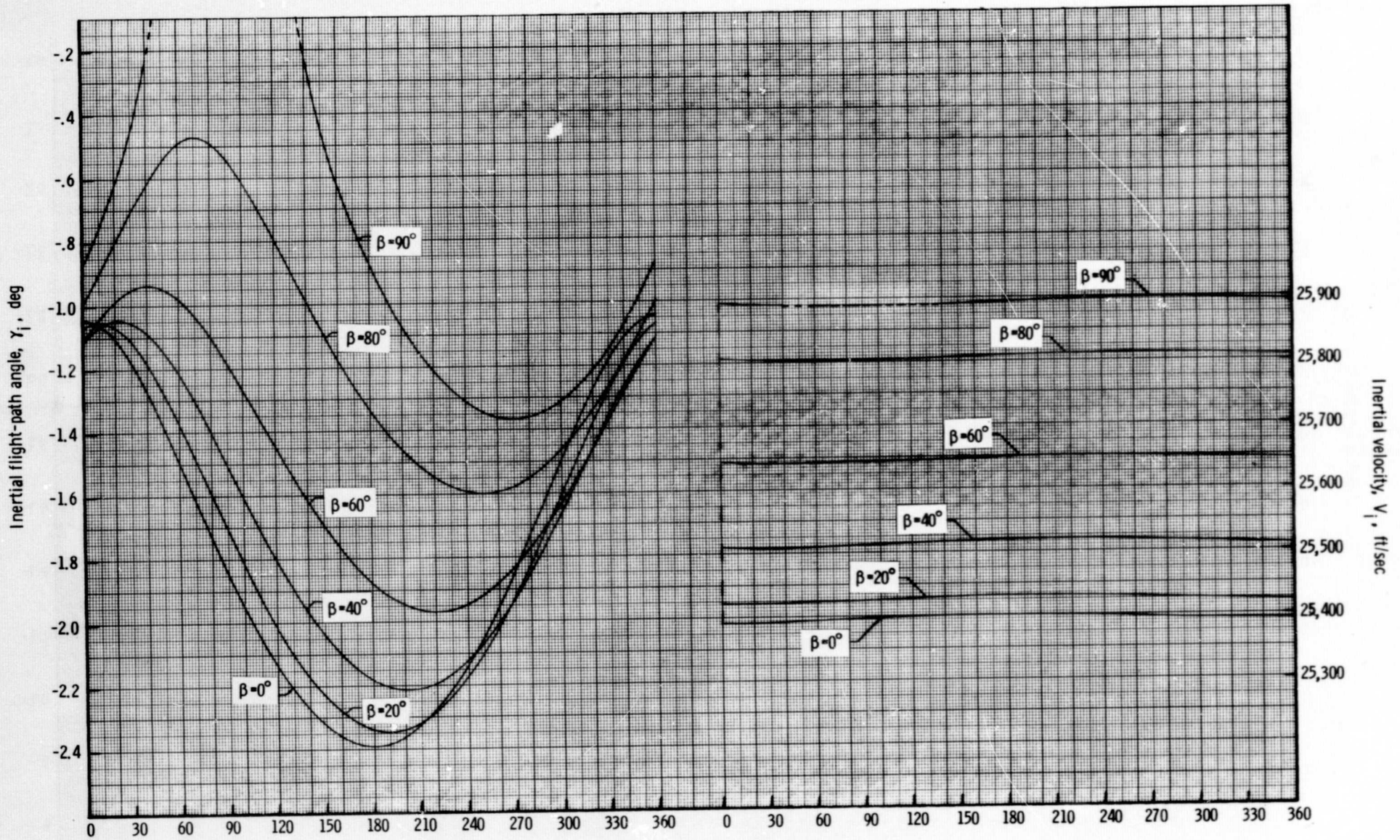

(c) ΔV = 500 fps

Figure 8. - Continued.

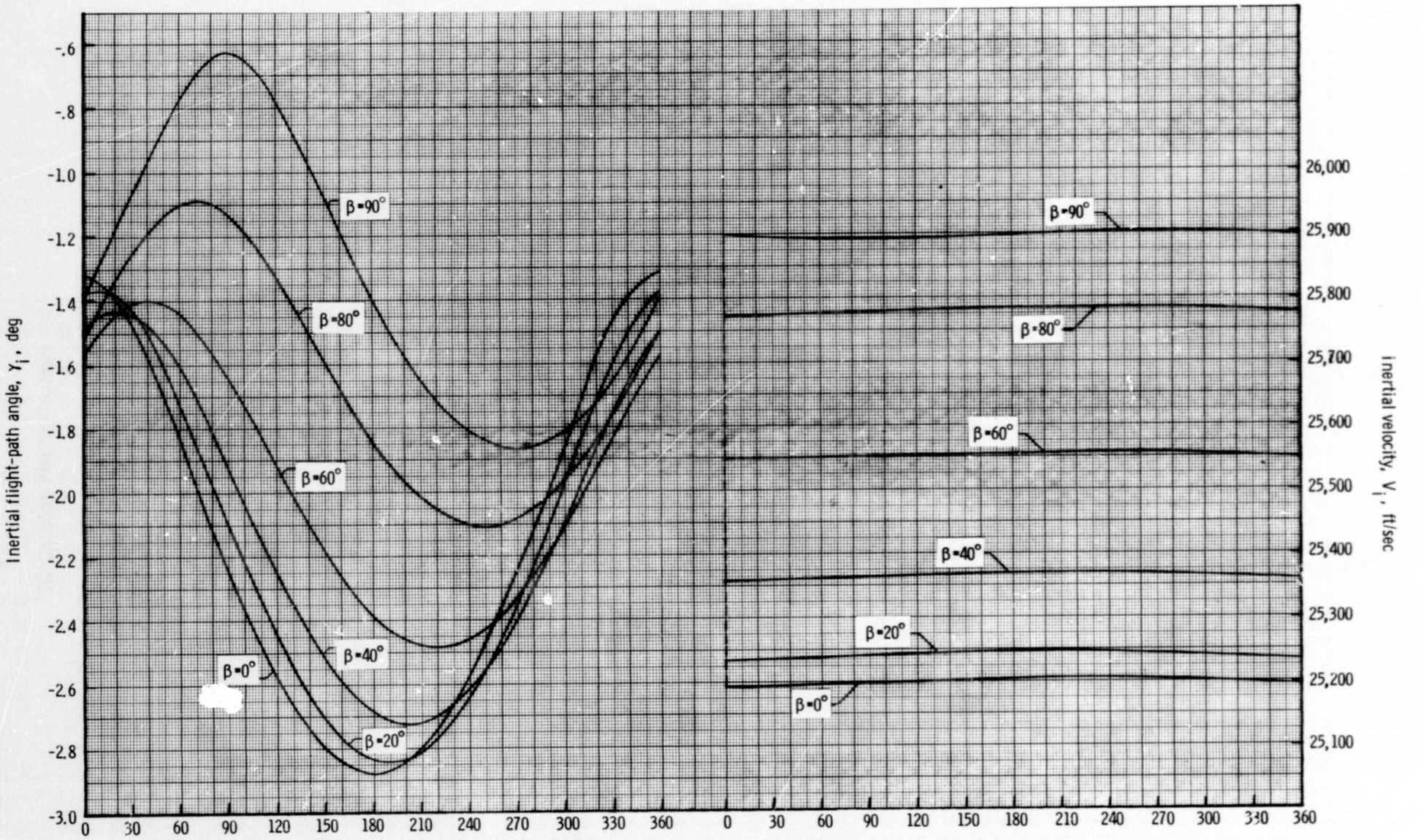

(d) ΔV = 700 fps

Figure 8. - Concluded.

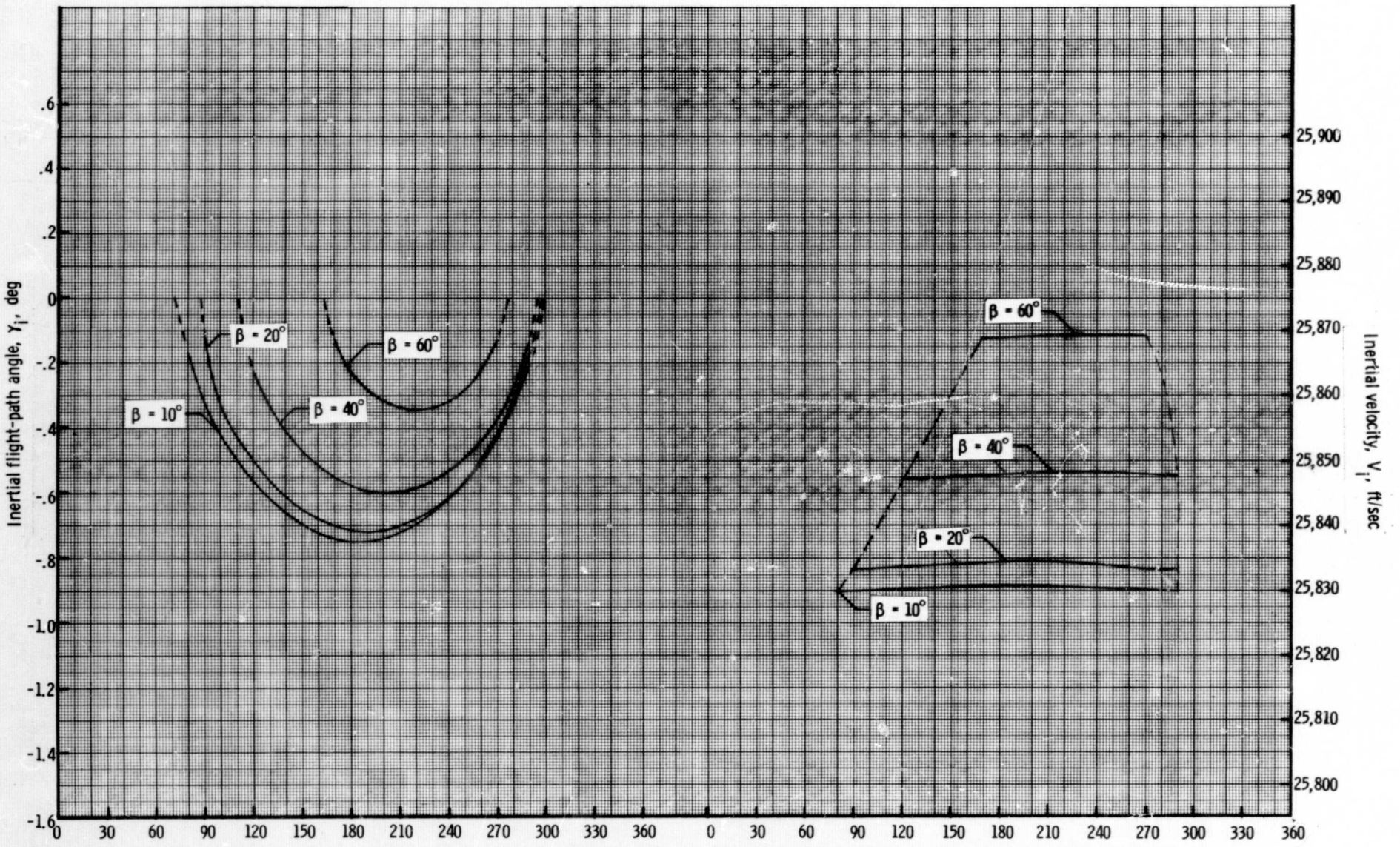

(a) ΔV = 80.5 fps

Figure 9. - Inertial flight-path angle and velocity at 400 000 feet as a function of retrograde true anomaly and a constant ΔV for an elliptical orbit where h_p = 87 nautical miles and h_a = 161 nautical miles

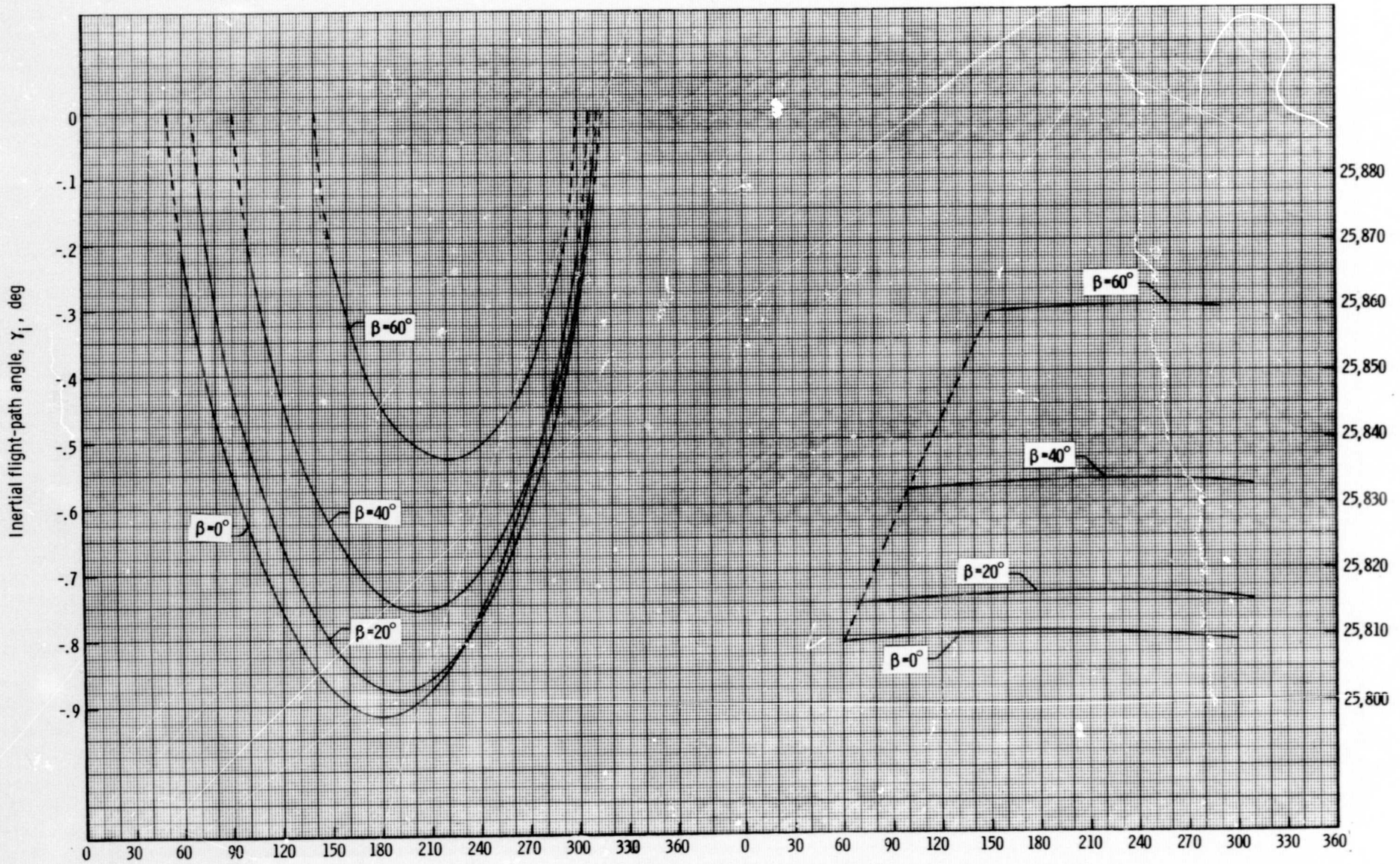

(b) ΔV = 100 fps

Figure 9. - Continued.

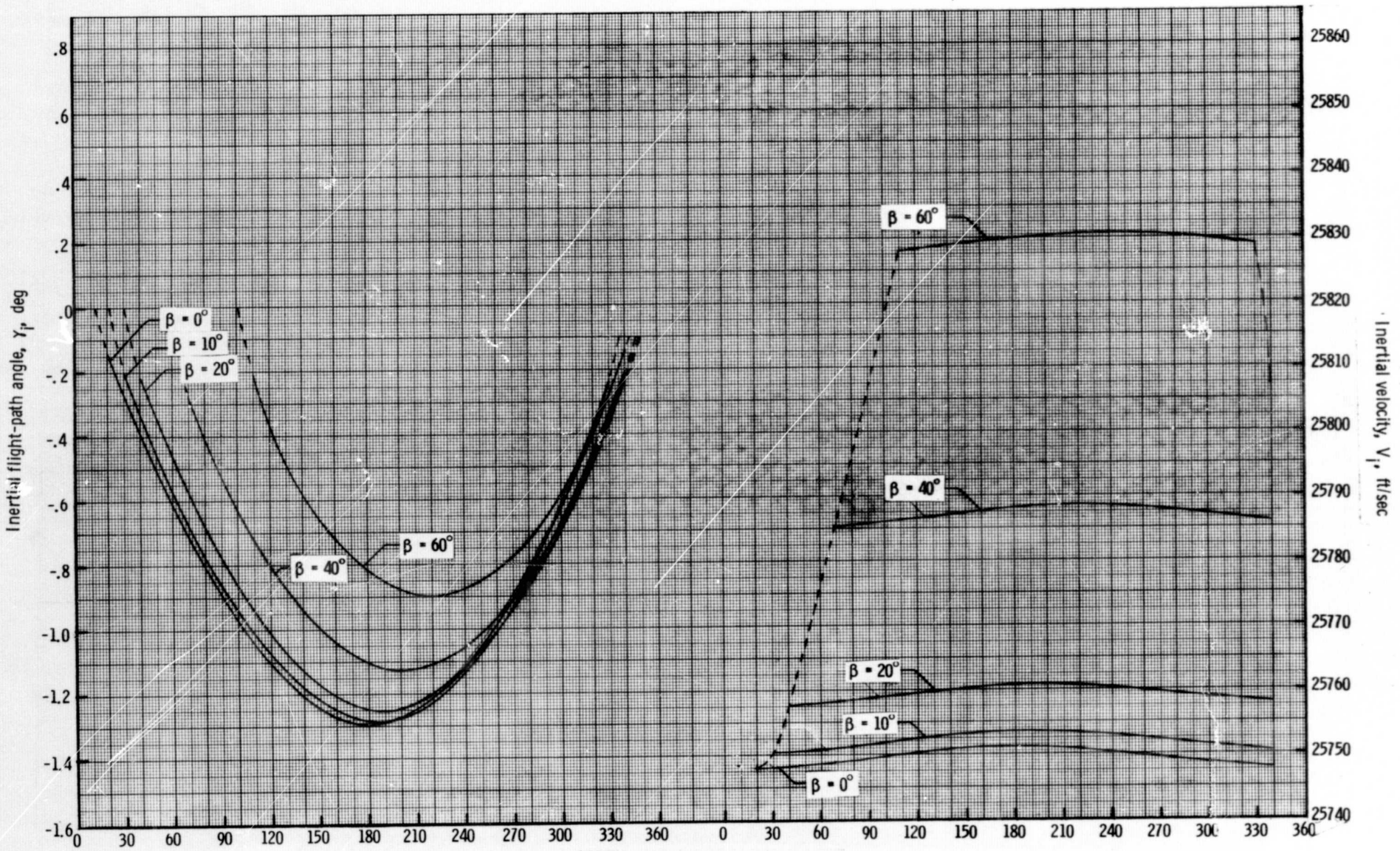

(c) ΔV = 161 fps

Figure 9. - Continued.

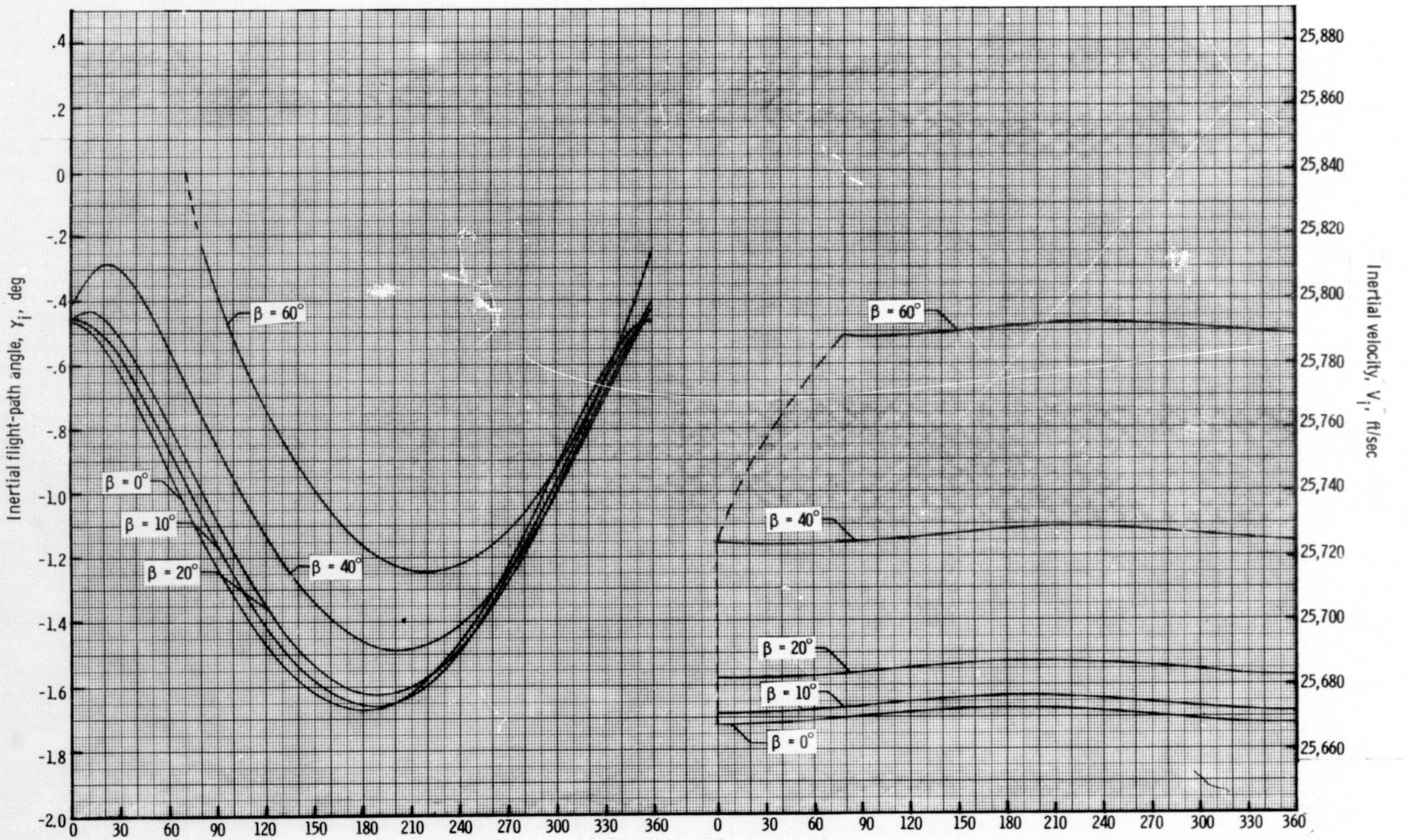

(d) ΔV = 241.5 fps

Figure 9. - Continued.

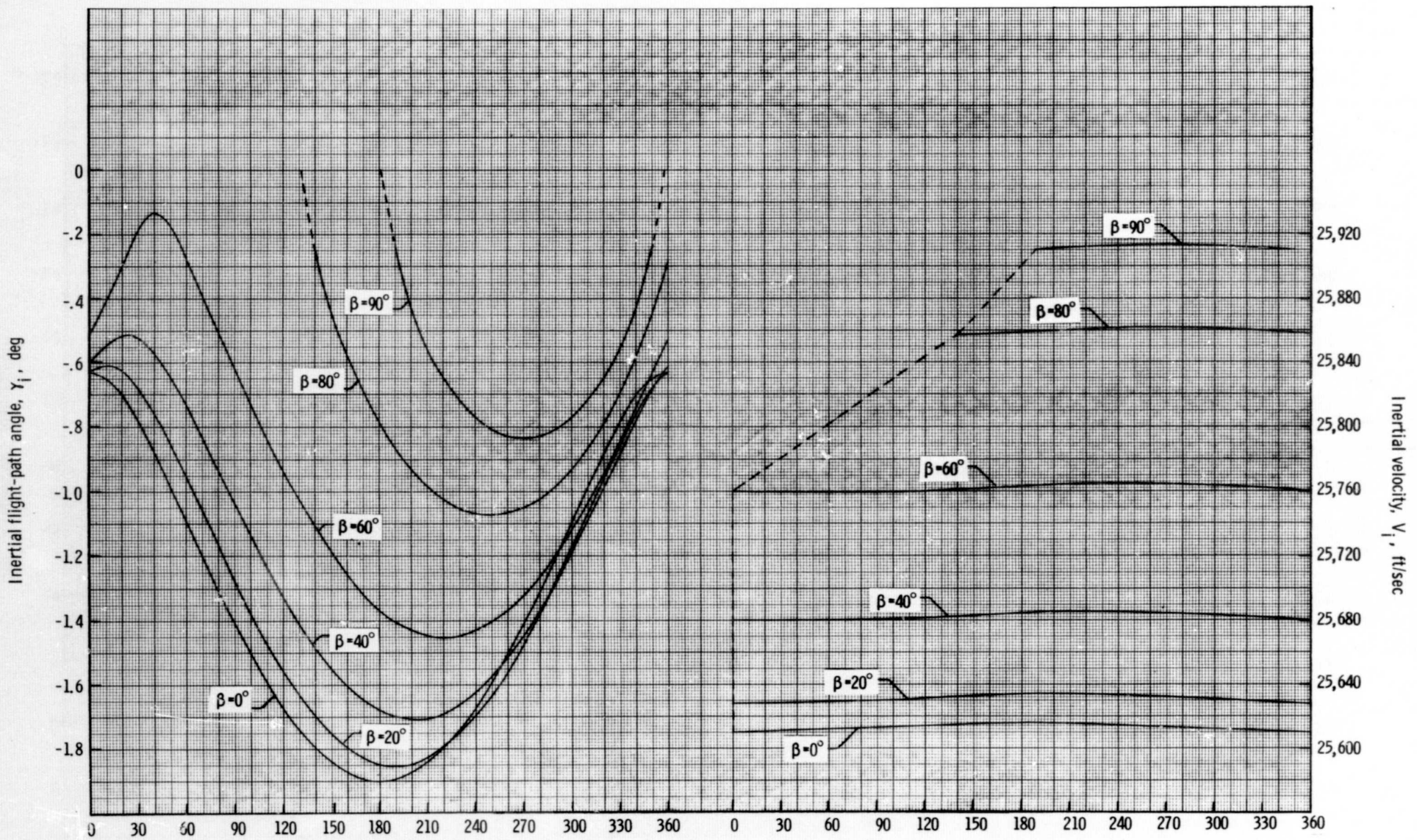

(e) ΔV = 300 fps

Figure 9. - Continued.

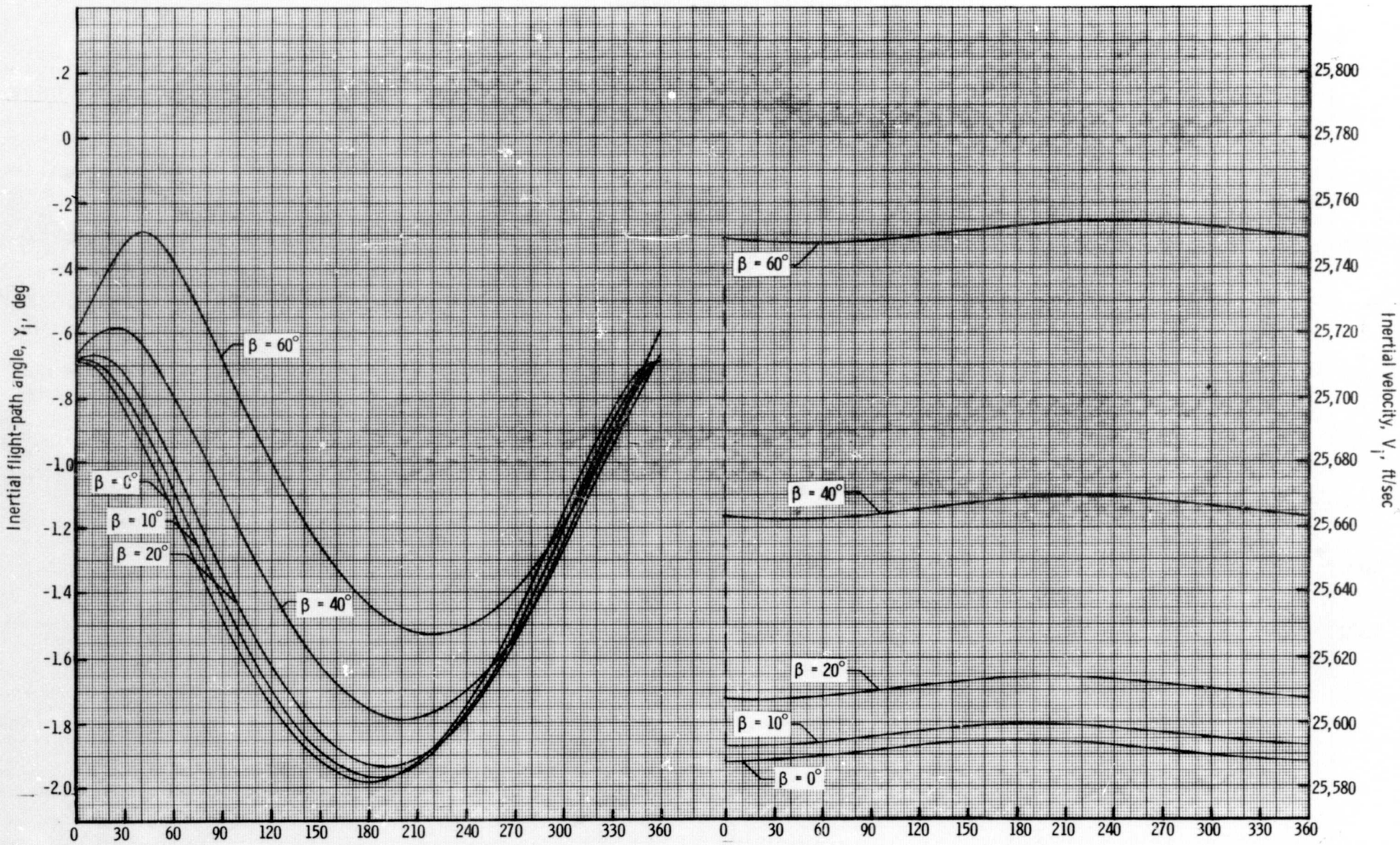

(f) ΔV = 322 fps

Figure 9. - Continued.

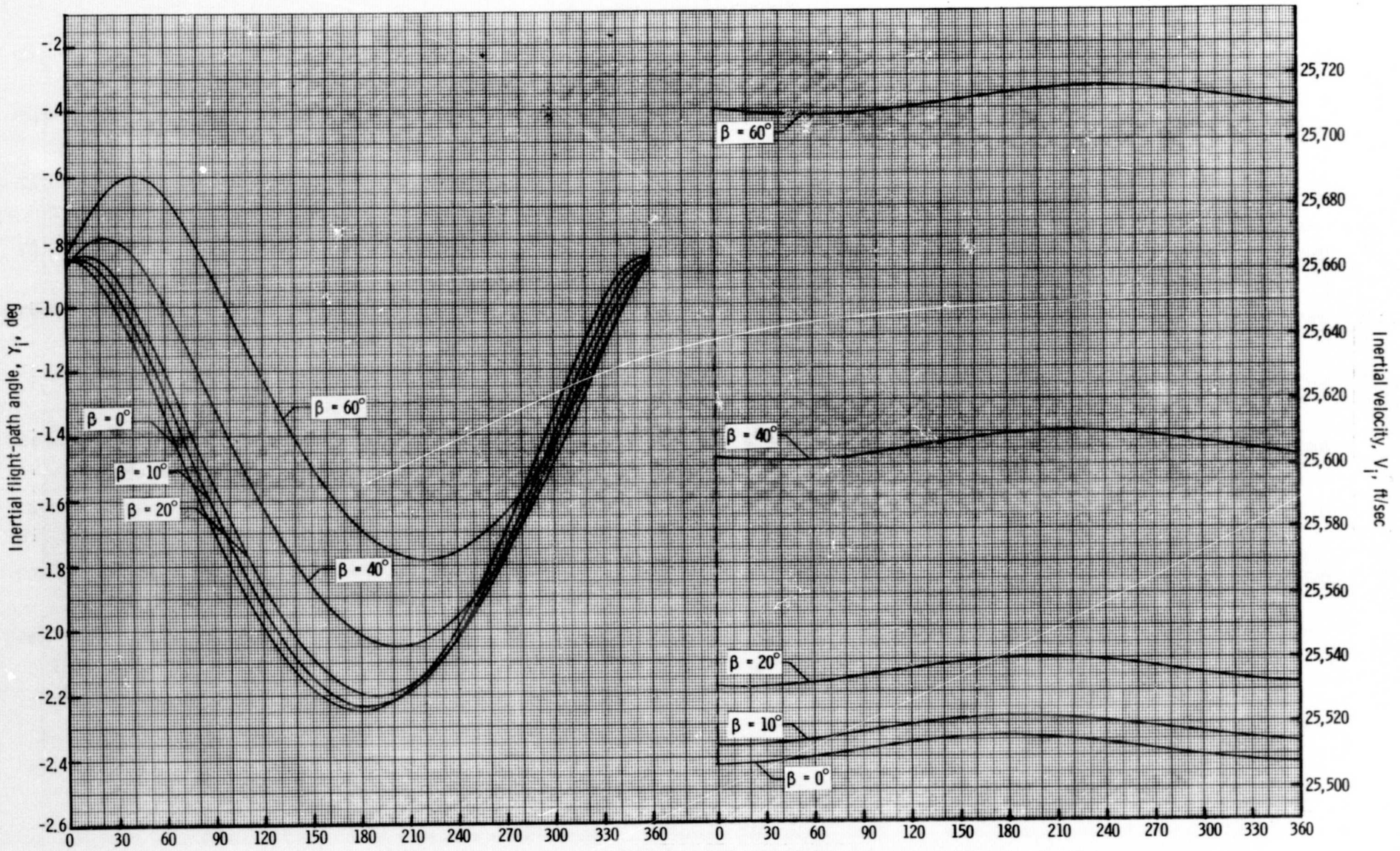

(g) ΔV = 402.5 fps

Figure 9. - Continued.

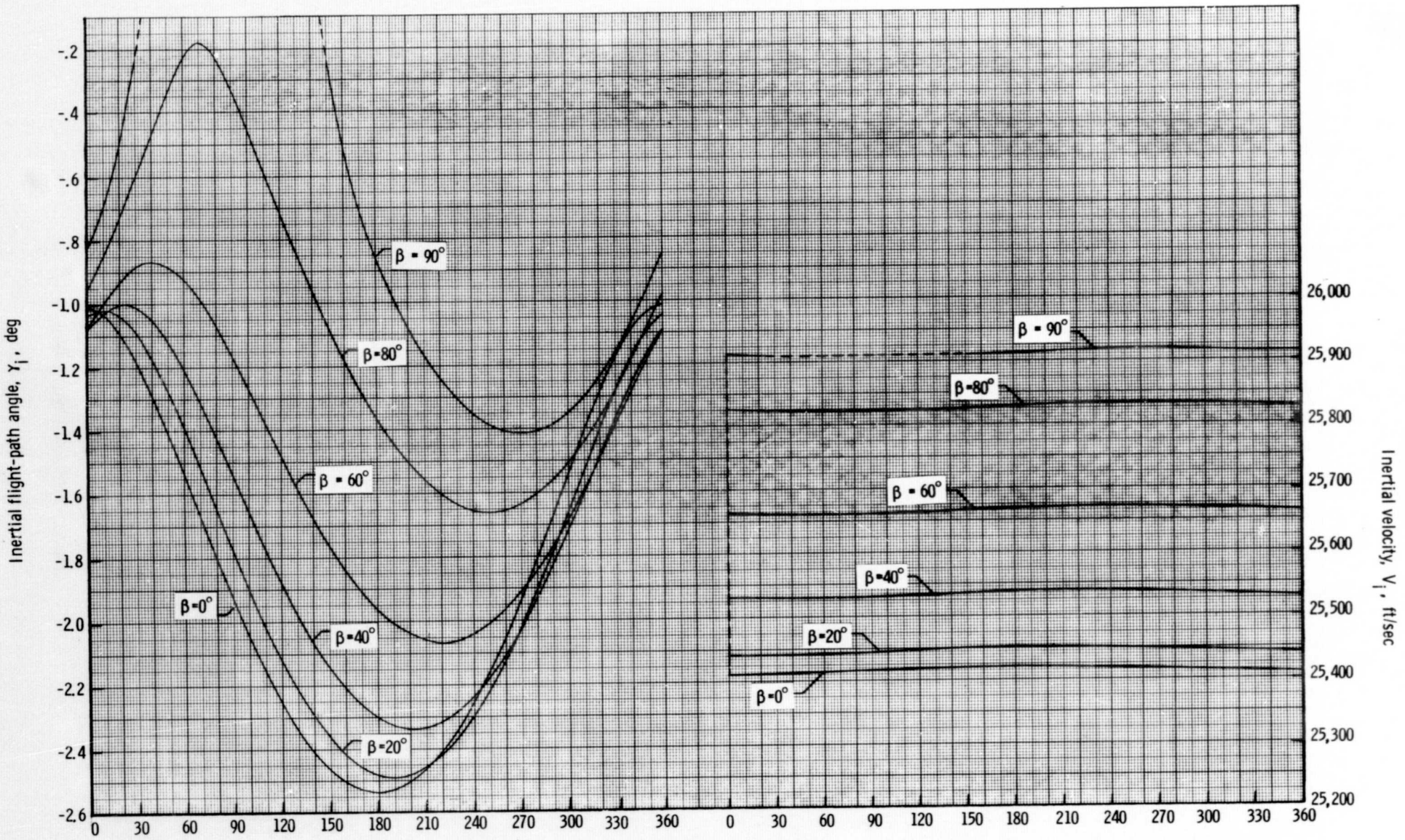

(h) ΔV = 500 fps

Figure 9. - Continued.

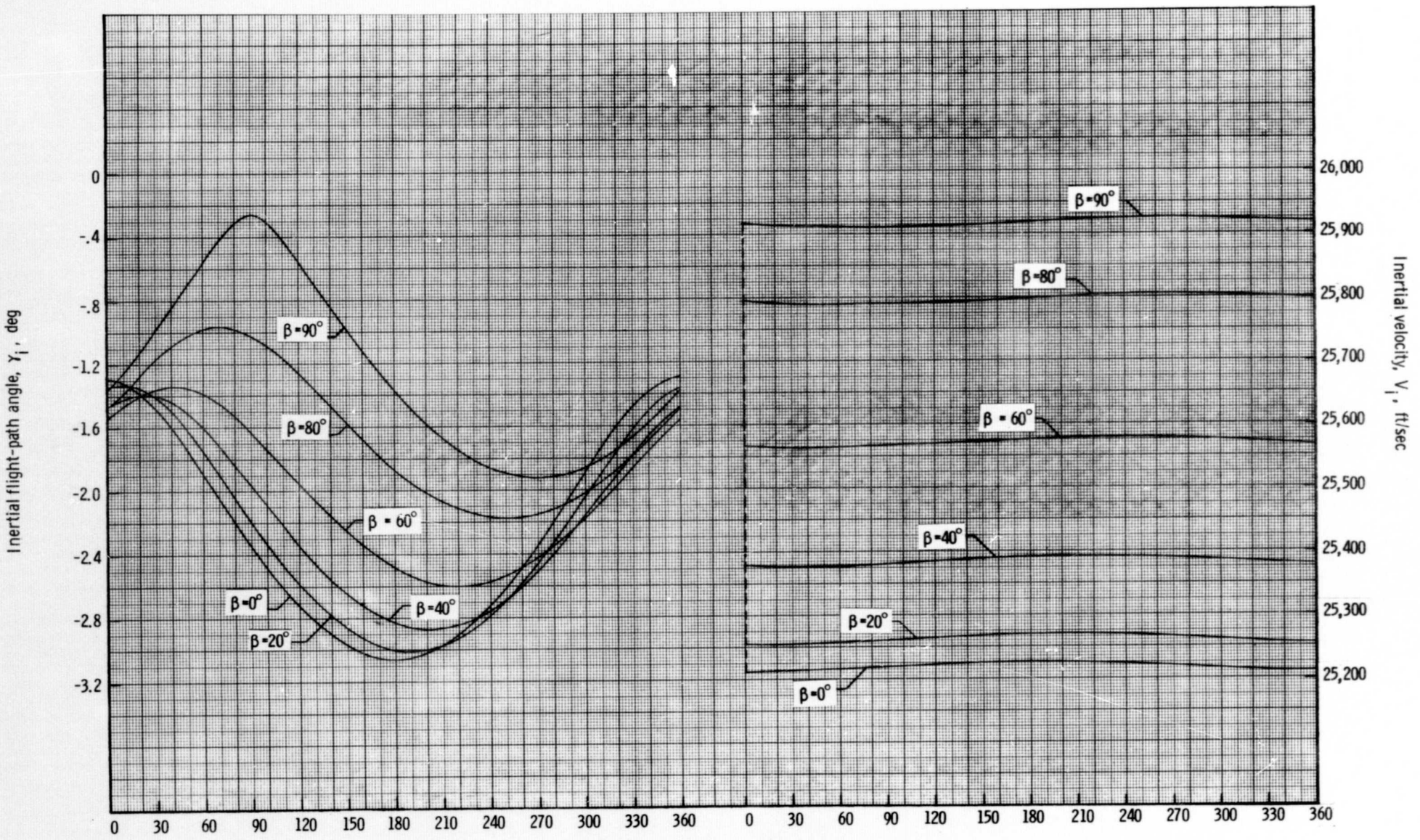

(i) ΔV = 700 fps

Figure 9. - Concluded.

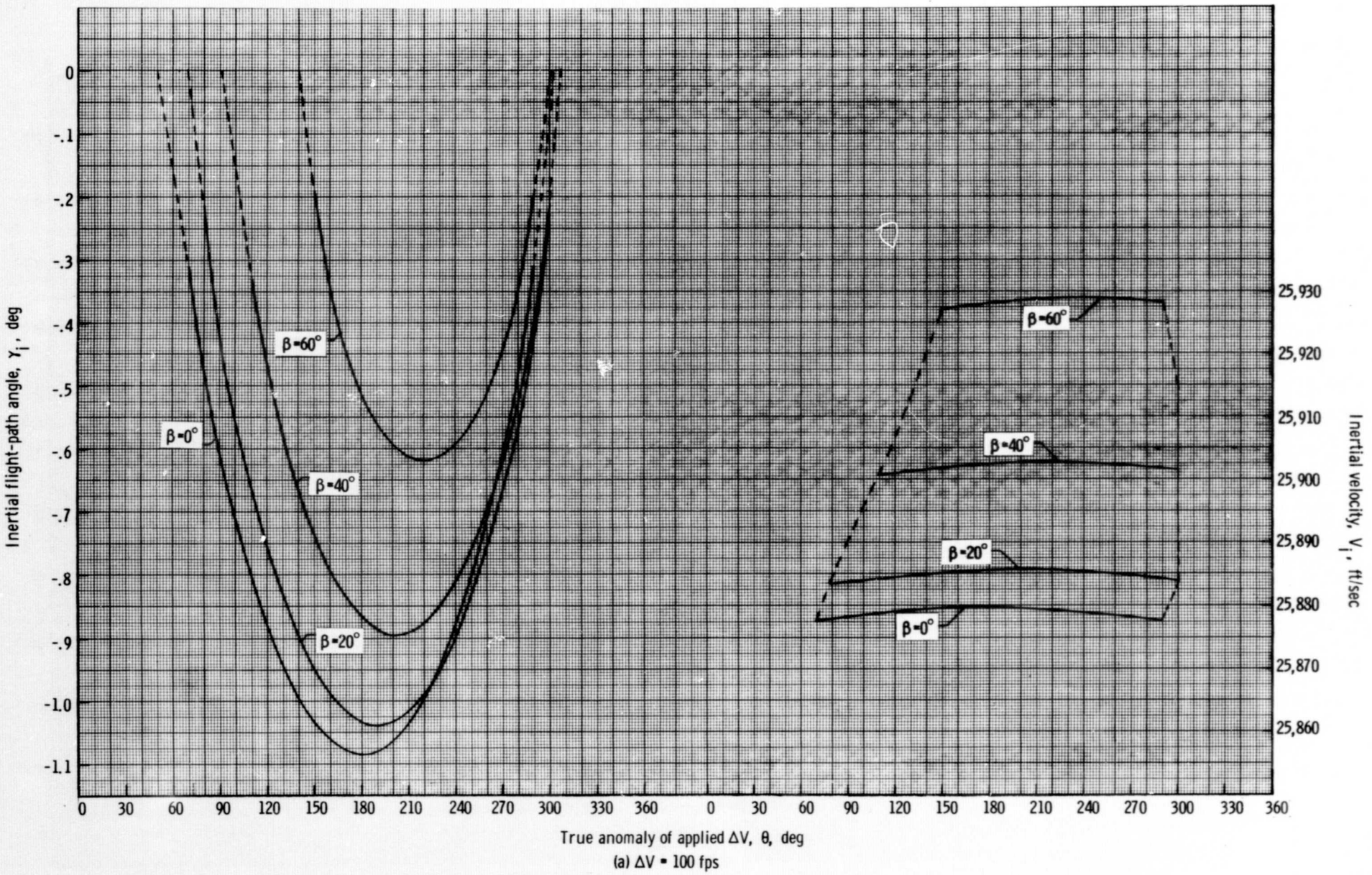

(a) ΔV = 100 fps

Figure 10. - Inertial flight-path angle and velocity at 400 000 feet as a function of retrograde true anomaly and a constant ΔV for an elliptical orbit where h_p = 87 nautical miles and h_a = 200 nautical miles.

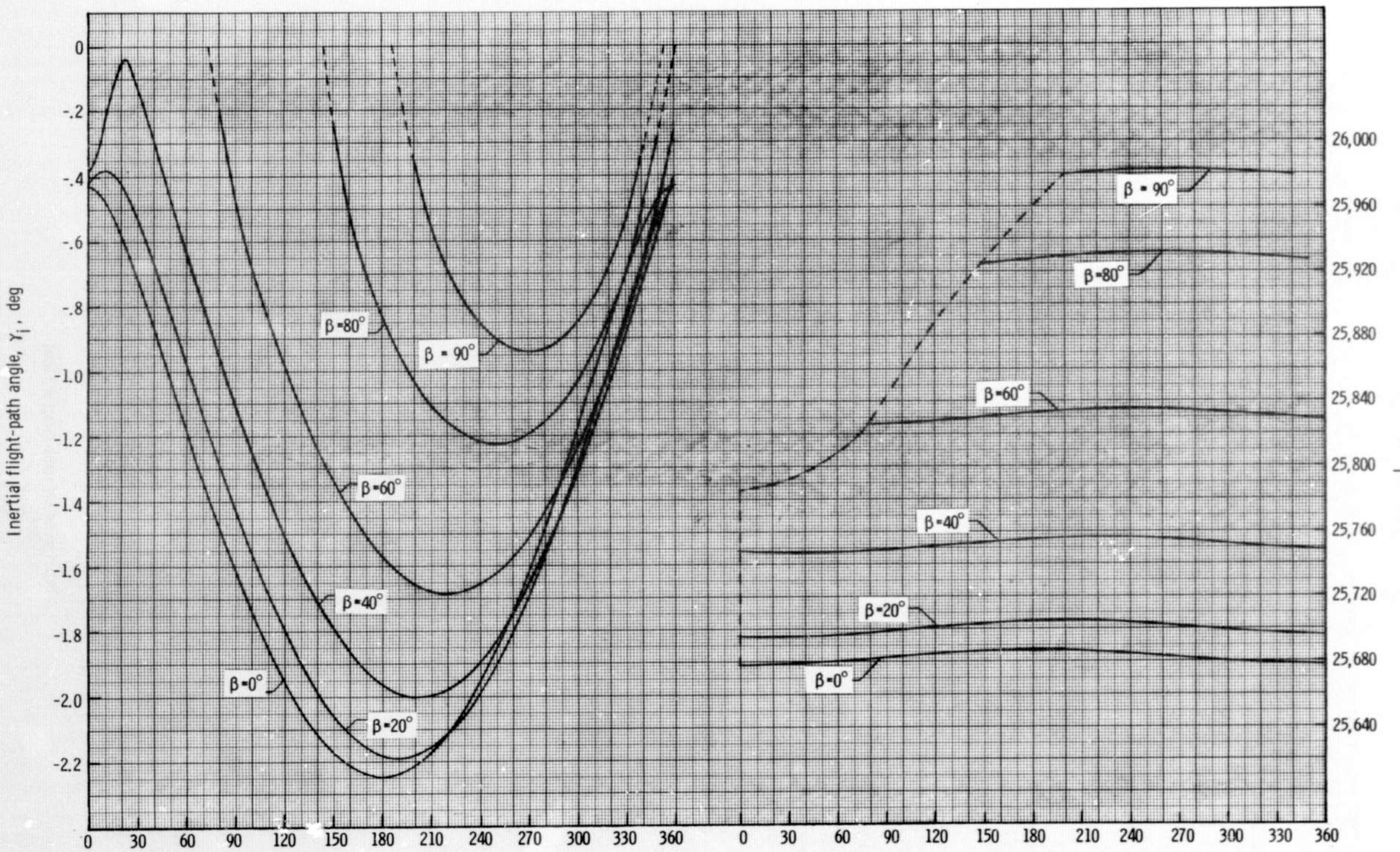

(b) ΔV = 300 fps

Figure 10. - Continued.

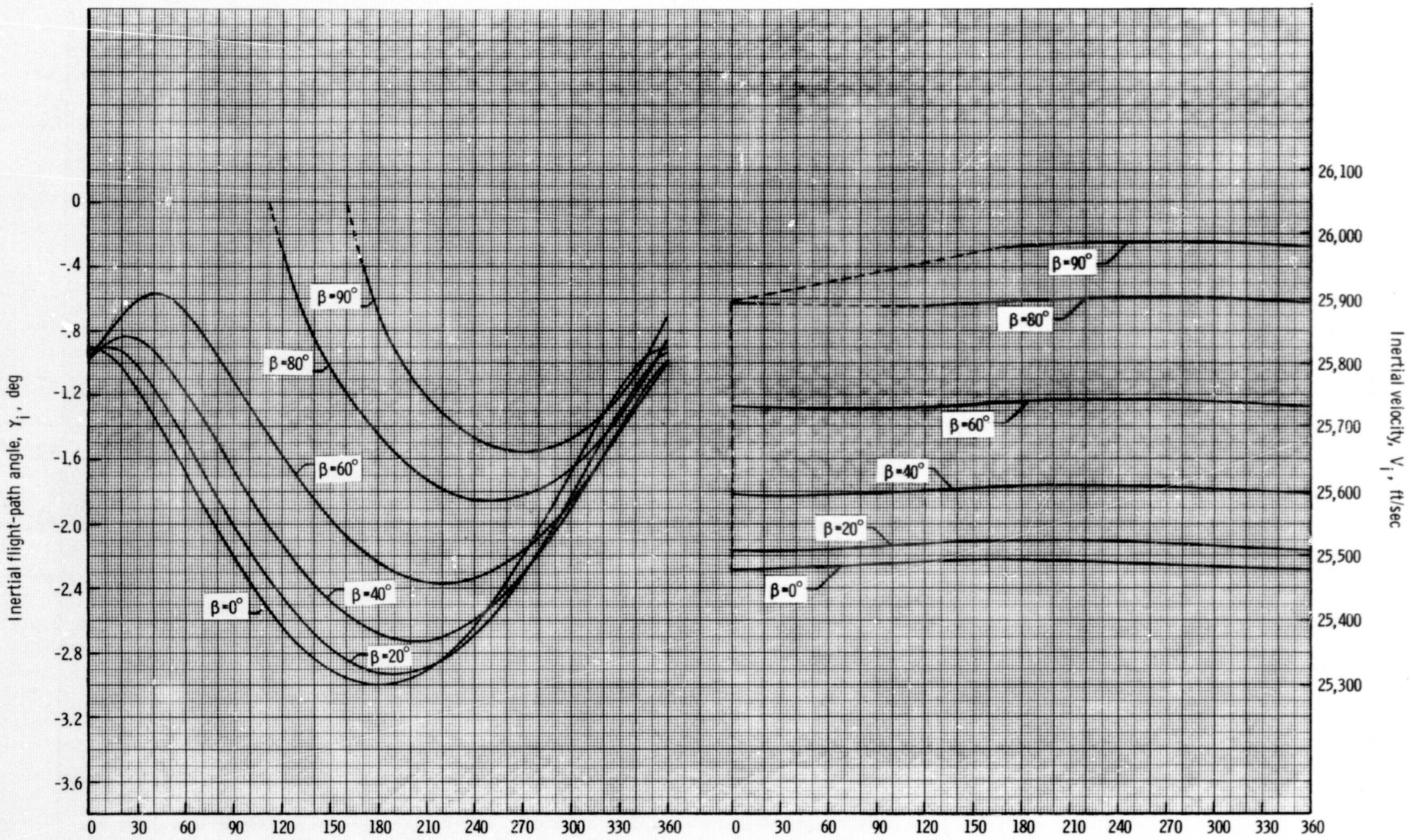

(c) ΔV = 500 fps

Figure 10. - Continued.

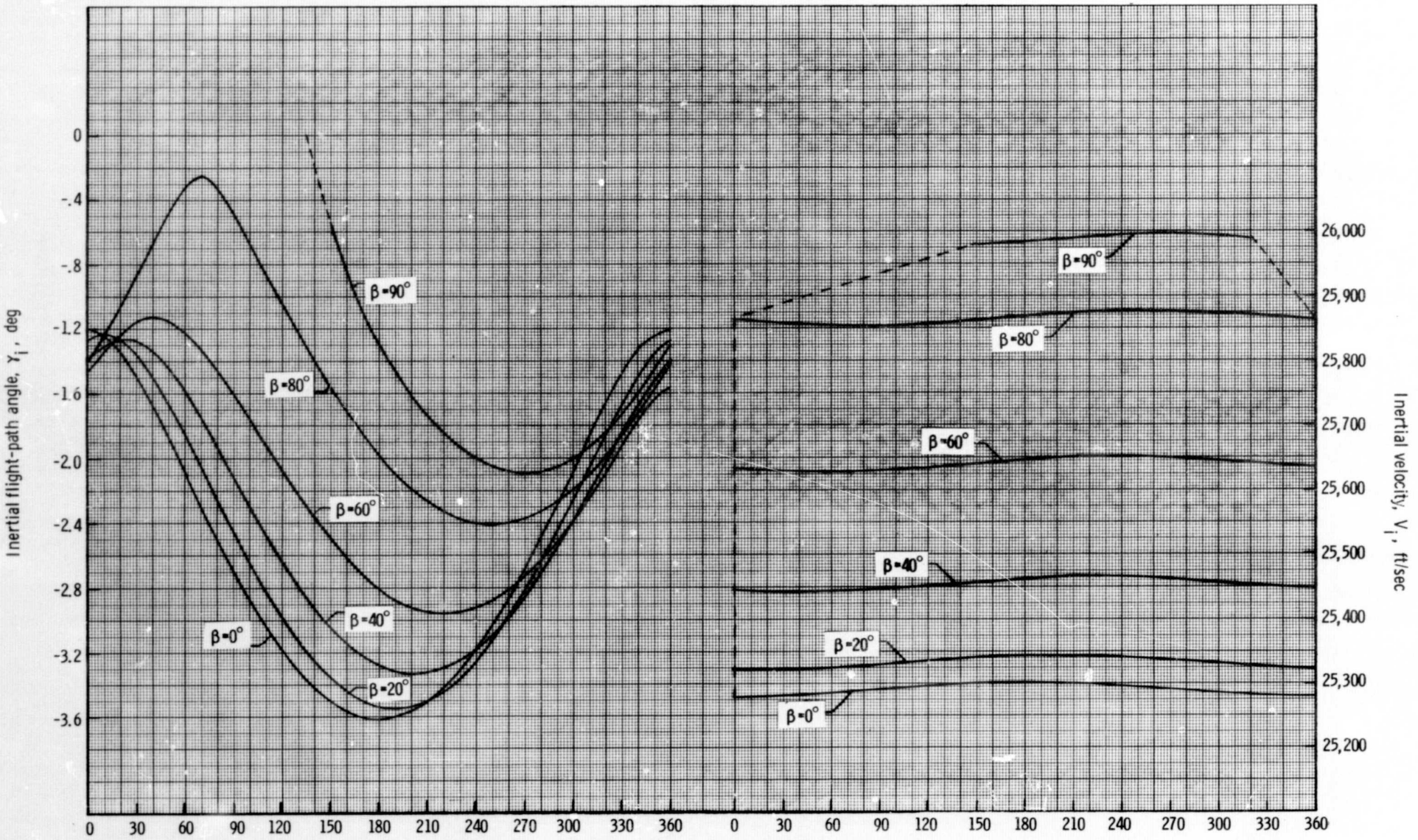

(d) ΔV = 700 fps

Figure 10. - Concluded.

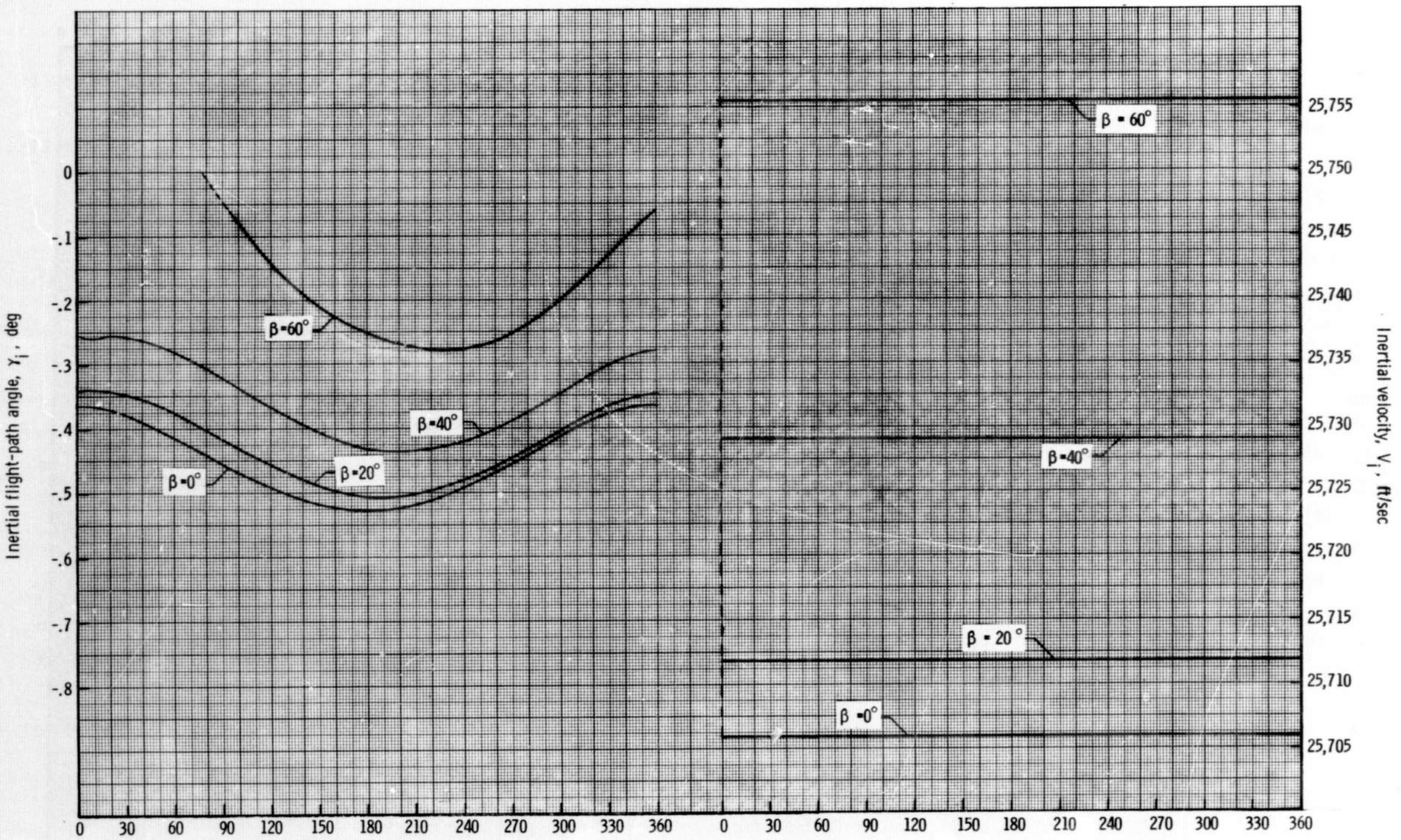

(a) ΔV = 100 fps

Figure 11. - Inertial flight-path angle and velocity at 400 000 feet as a function of retrograde true anomaly and a constant ΔV for an elliptical orbit where h_p = 90 nautical miles and h_a = 100 nautical miles.

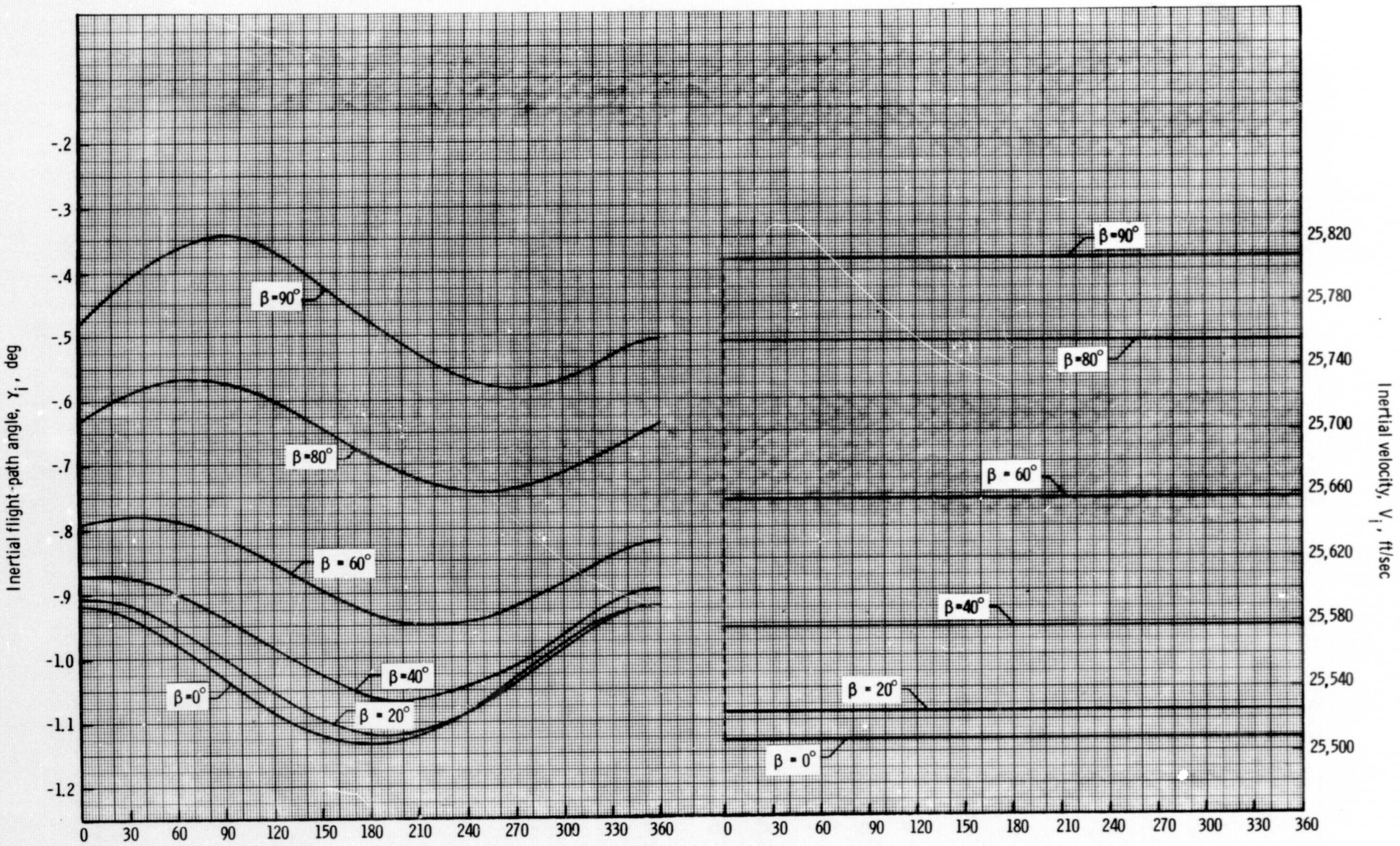

(b) ΔV = 300 fps

Figure 11. - Continued.

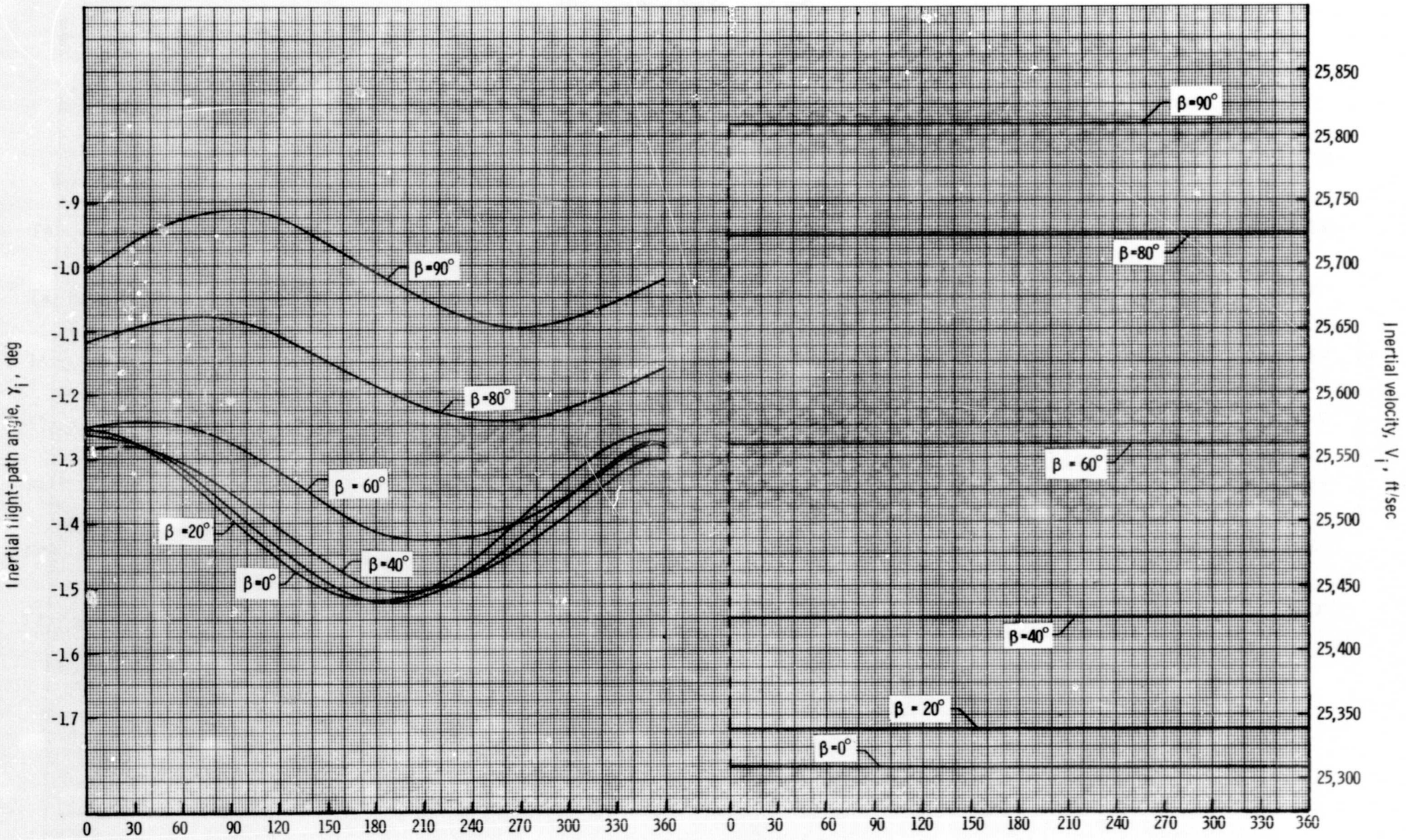

(c) ΔV = 500 fps

Figure 11. - Continued.

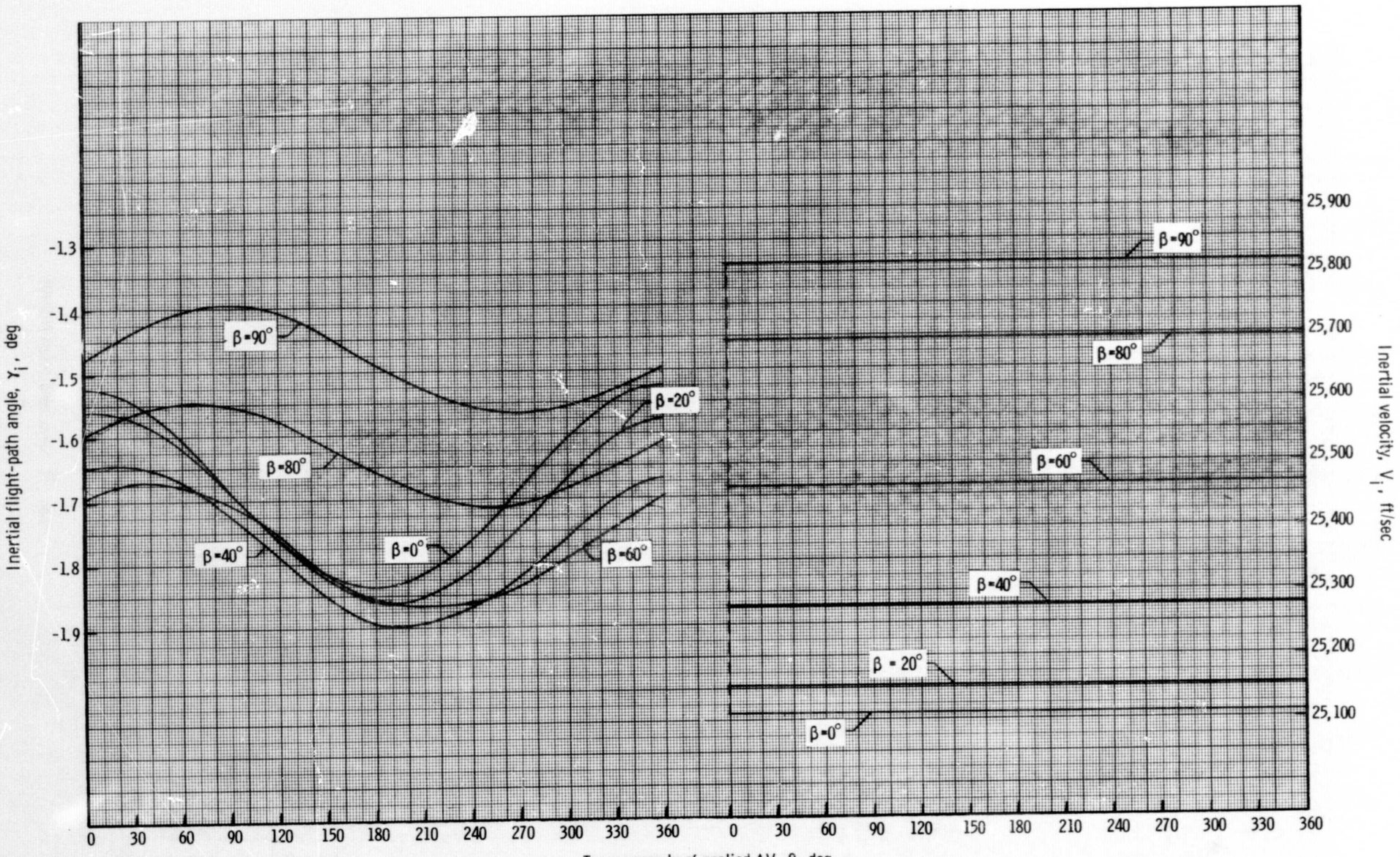

(d) ΔV = 700 fps

Figure 11. - Concluded.

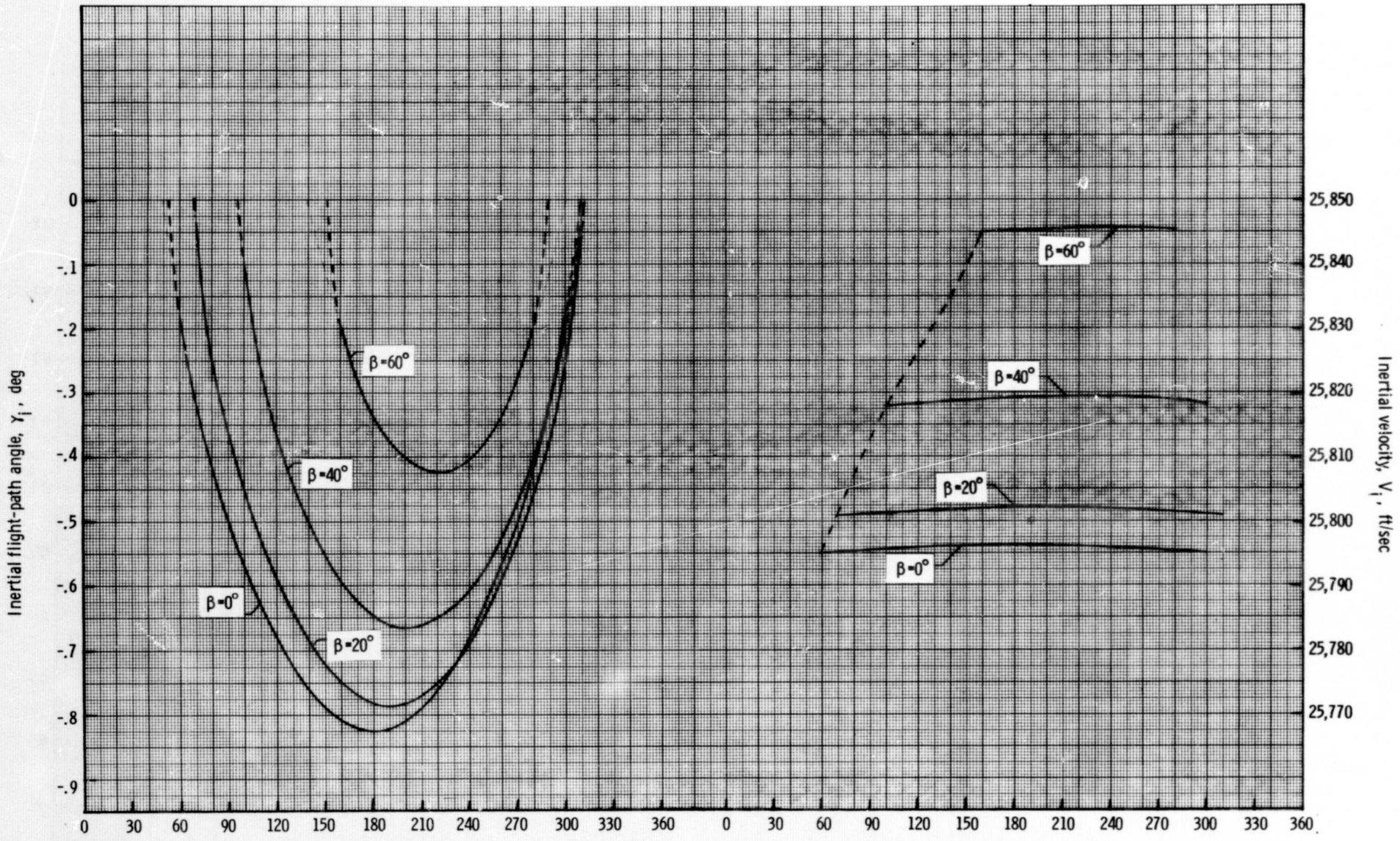

(a) ΔV = 100 fps

Figure 12. - Inertial flight-path angle and velocity at 400 000 feet as a function of retrograde true anomaly and a constant ΔV for an elliptical orbit where h_p = 90 nautical miles and h_a = 150 nautical miles.

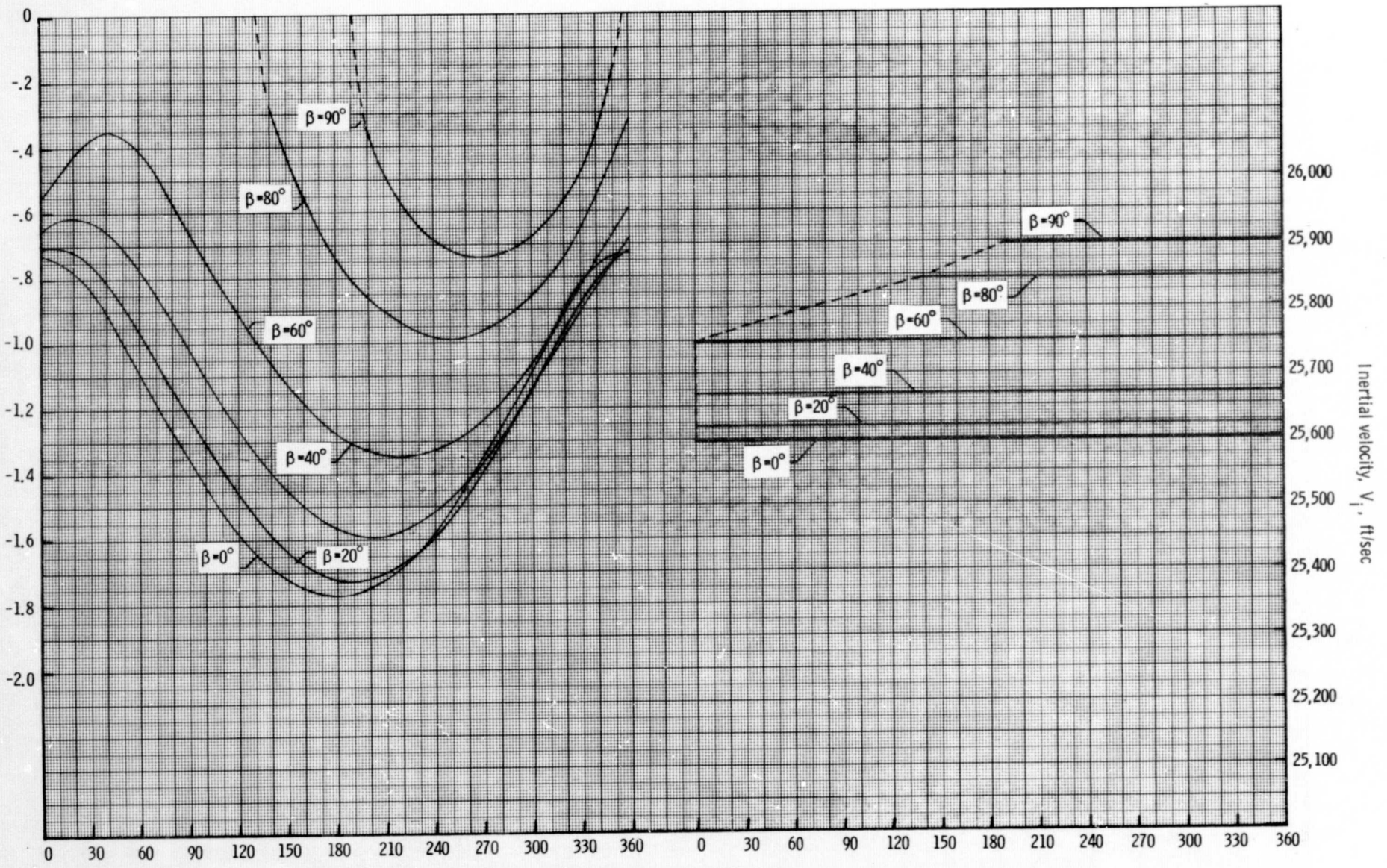

(b) ΔV = 300 fps

Figure 12. - Continued.

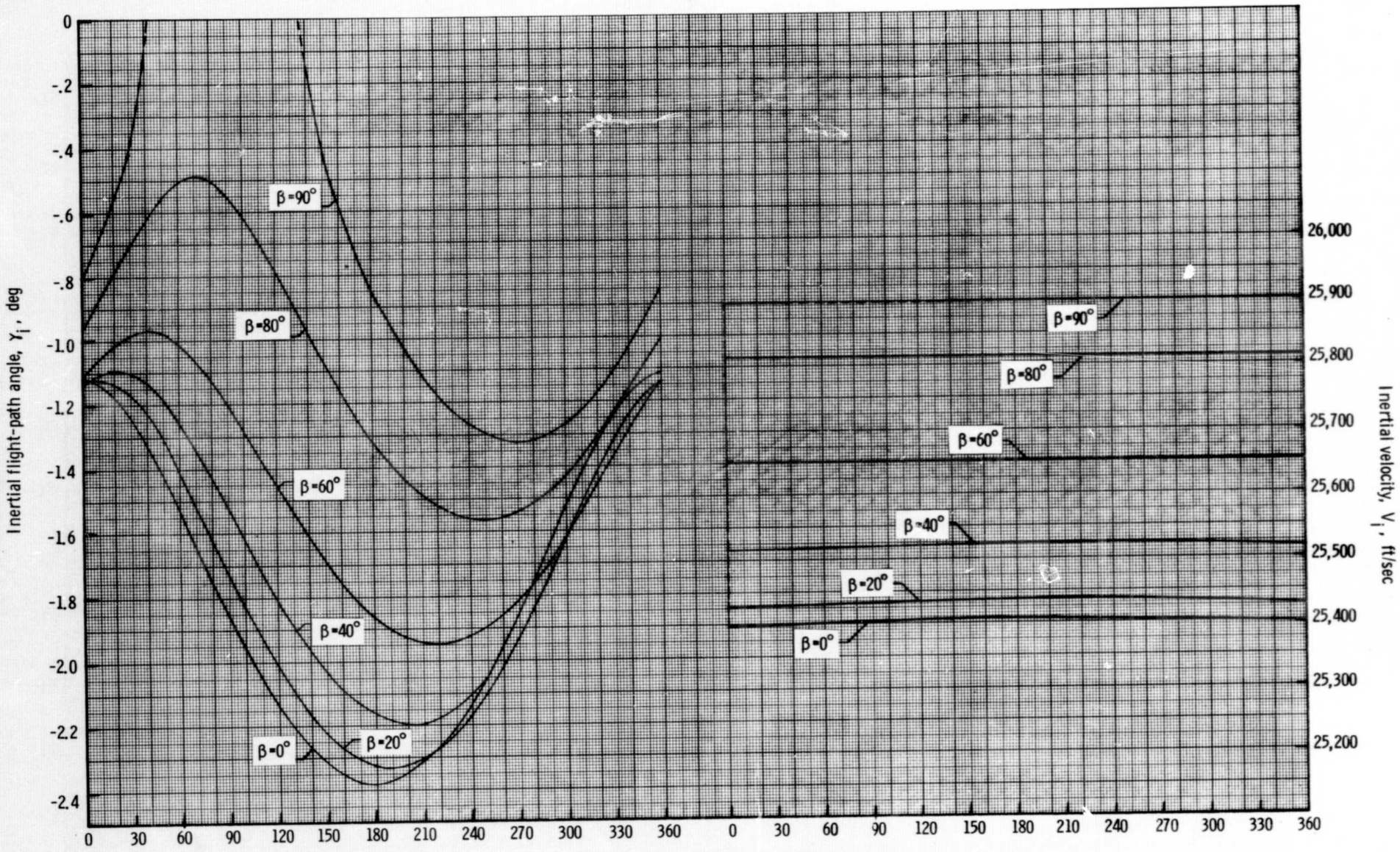

(c) ΔV = 500 fps

Figure 12. - Continued.

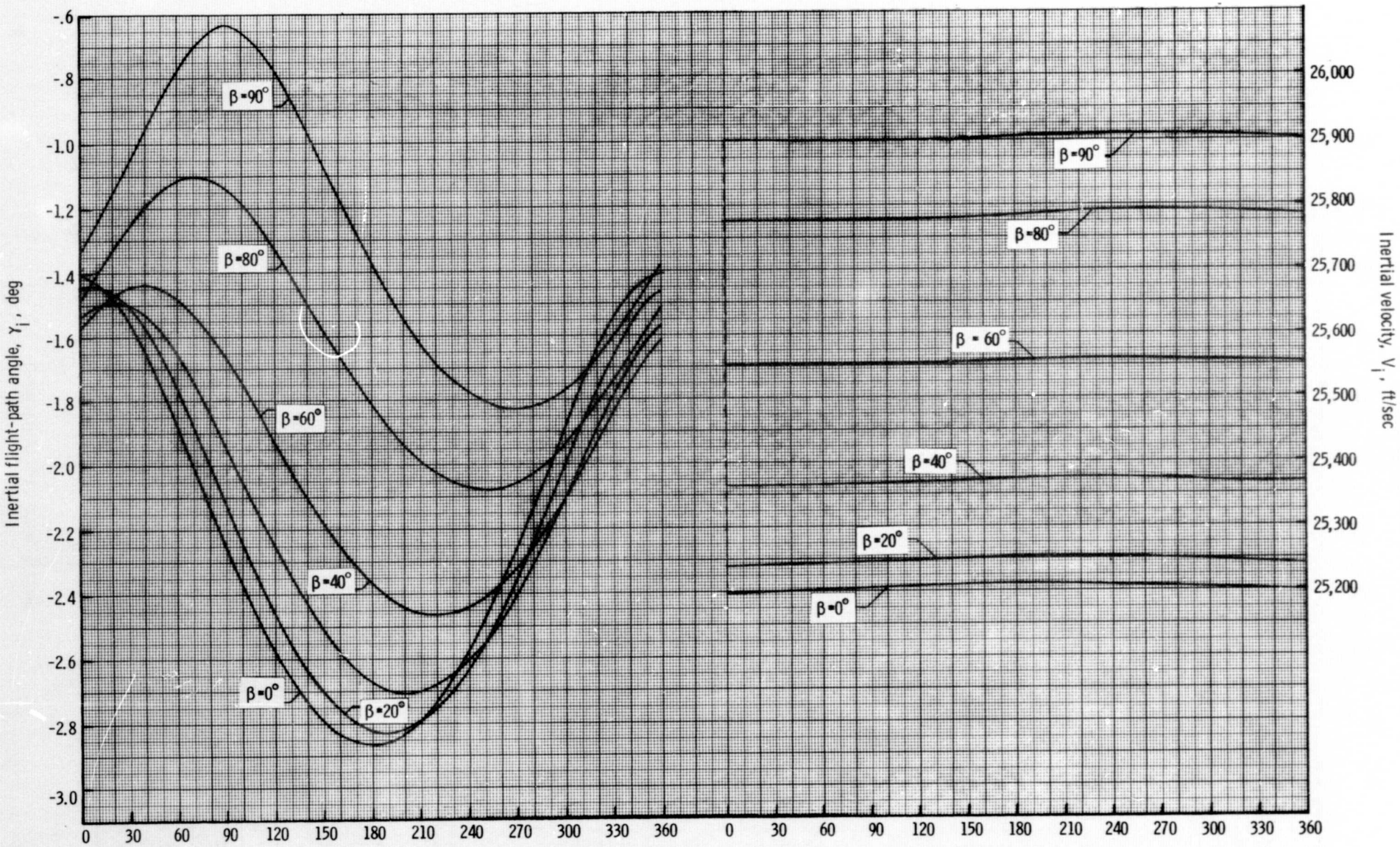

(d) ΔV = 700 fps

Figure 12. - Concluded.

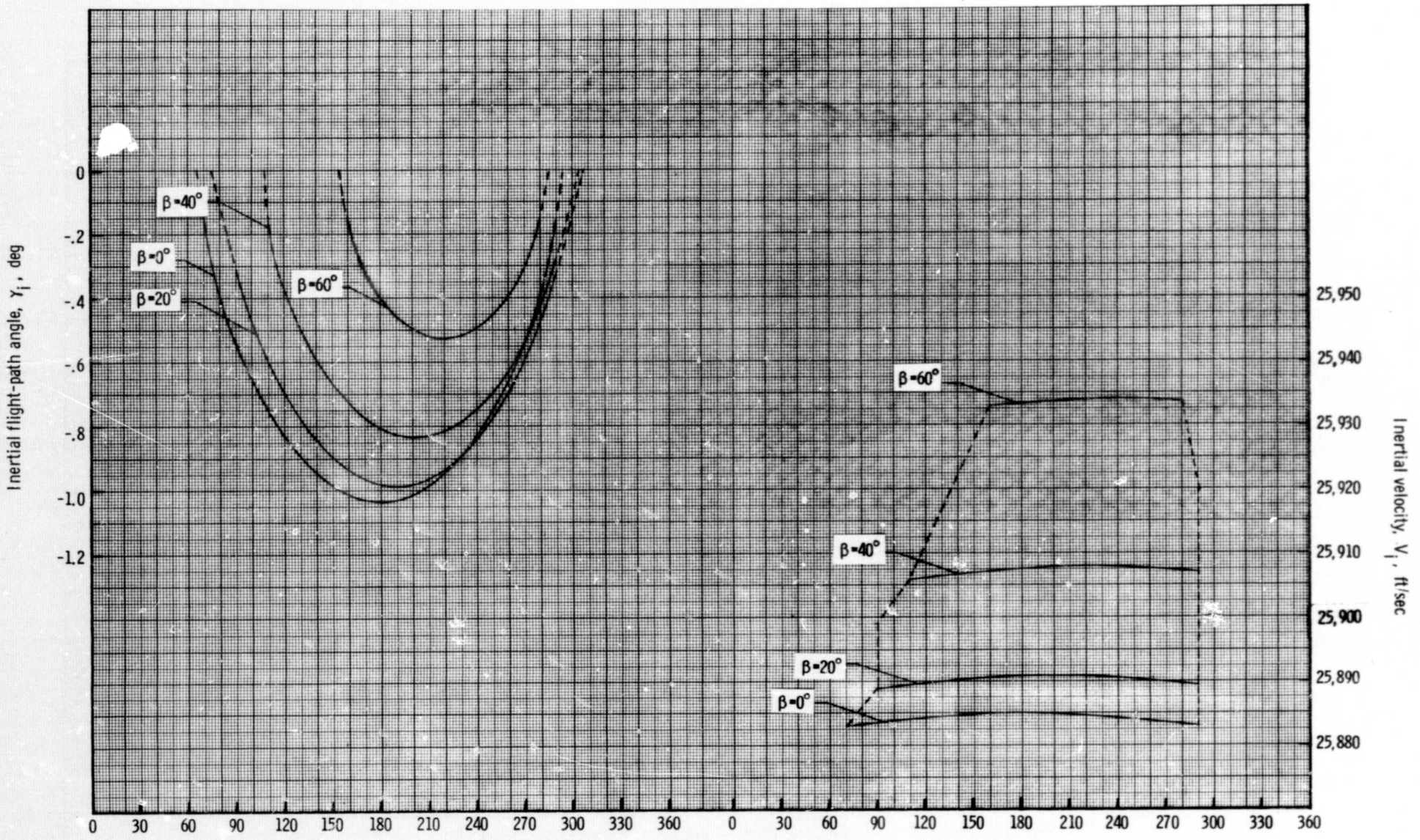

(a) ΔV = 100 fps

Figure 13. - Inertial flight-path angle and velocity at 400 000 feet as a function of retrograde true anomaly and a constant ΔV for an elliptical orbit where h_p = 90 nautical miles and h_a = 200 nautical miles.

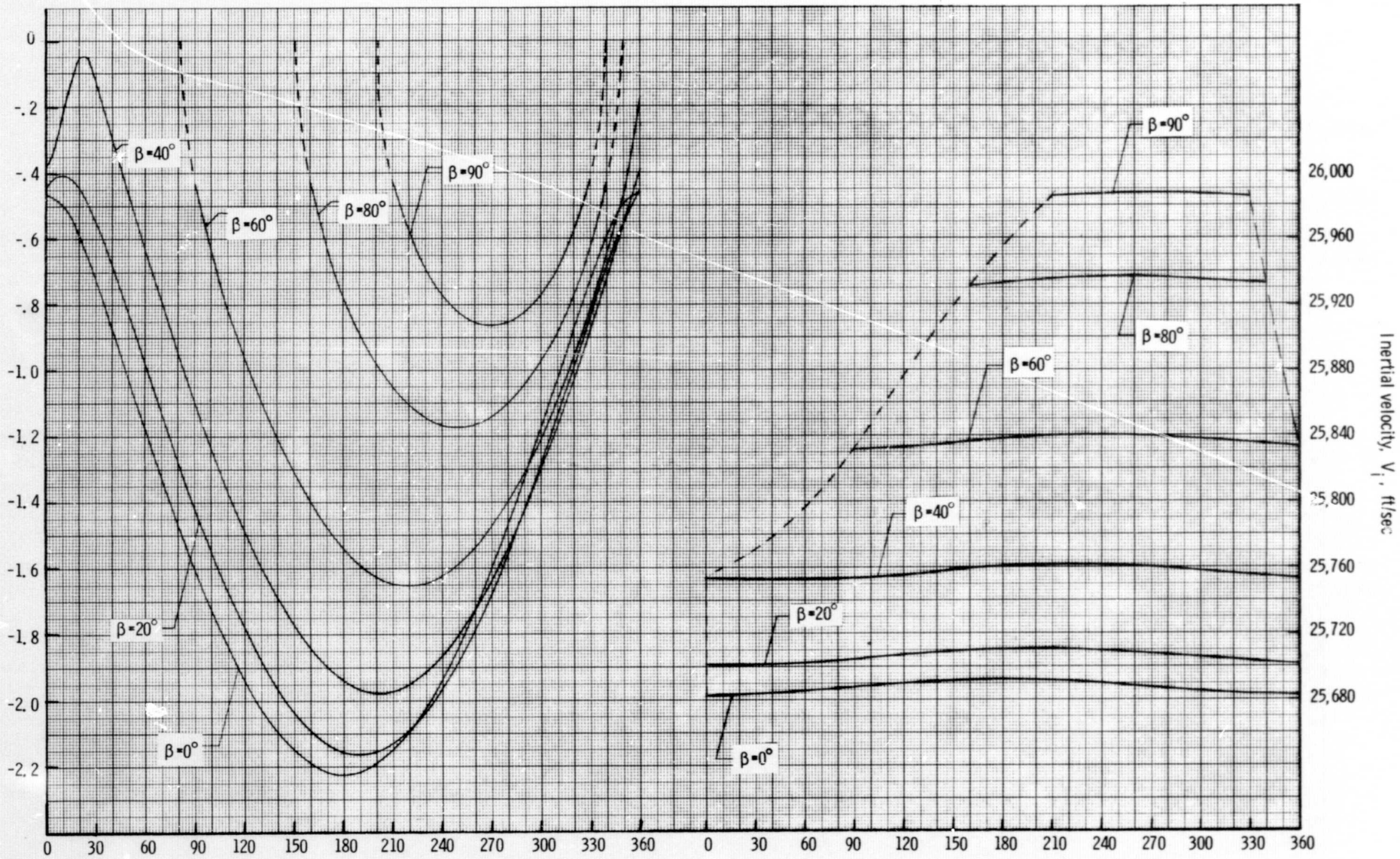

(b) ΔV = 300 fps

Figure 13. - Continued.

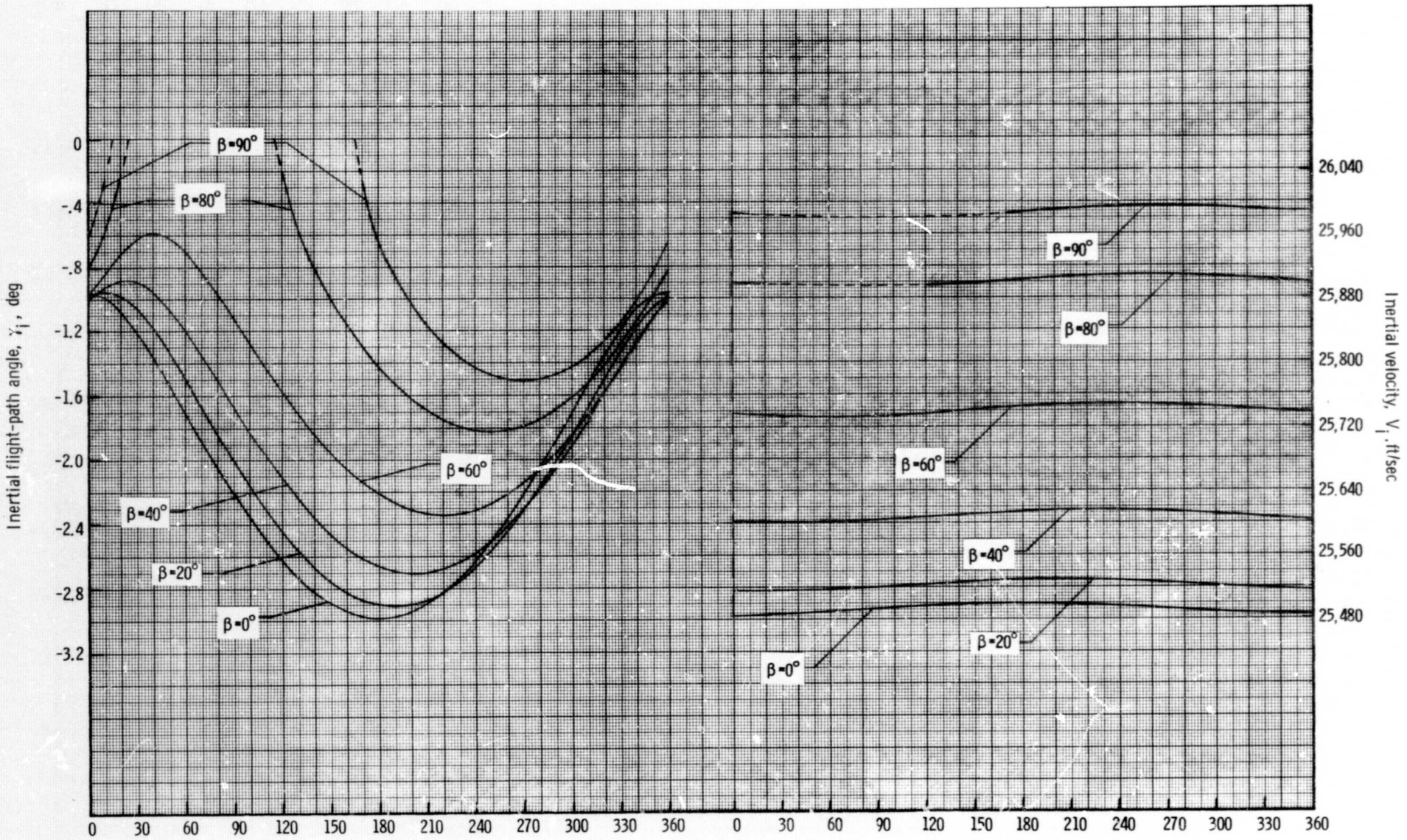

(c) ΔV = 500 fps

Figure 13. - Continued.

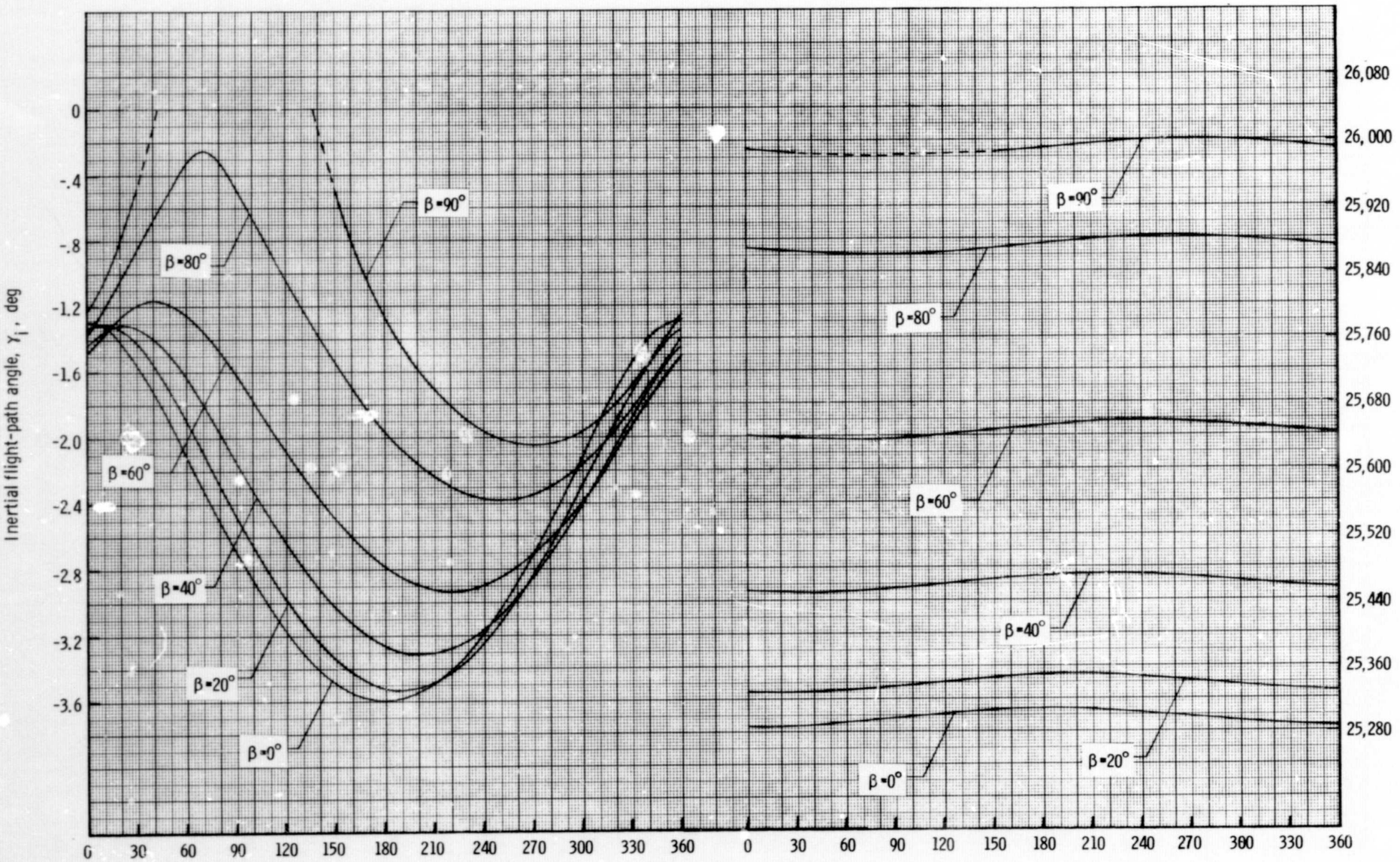

(d) ΔV = 700 fps

Figure 13. - Concluded.

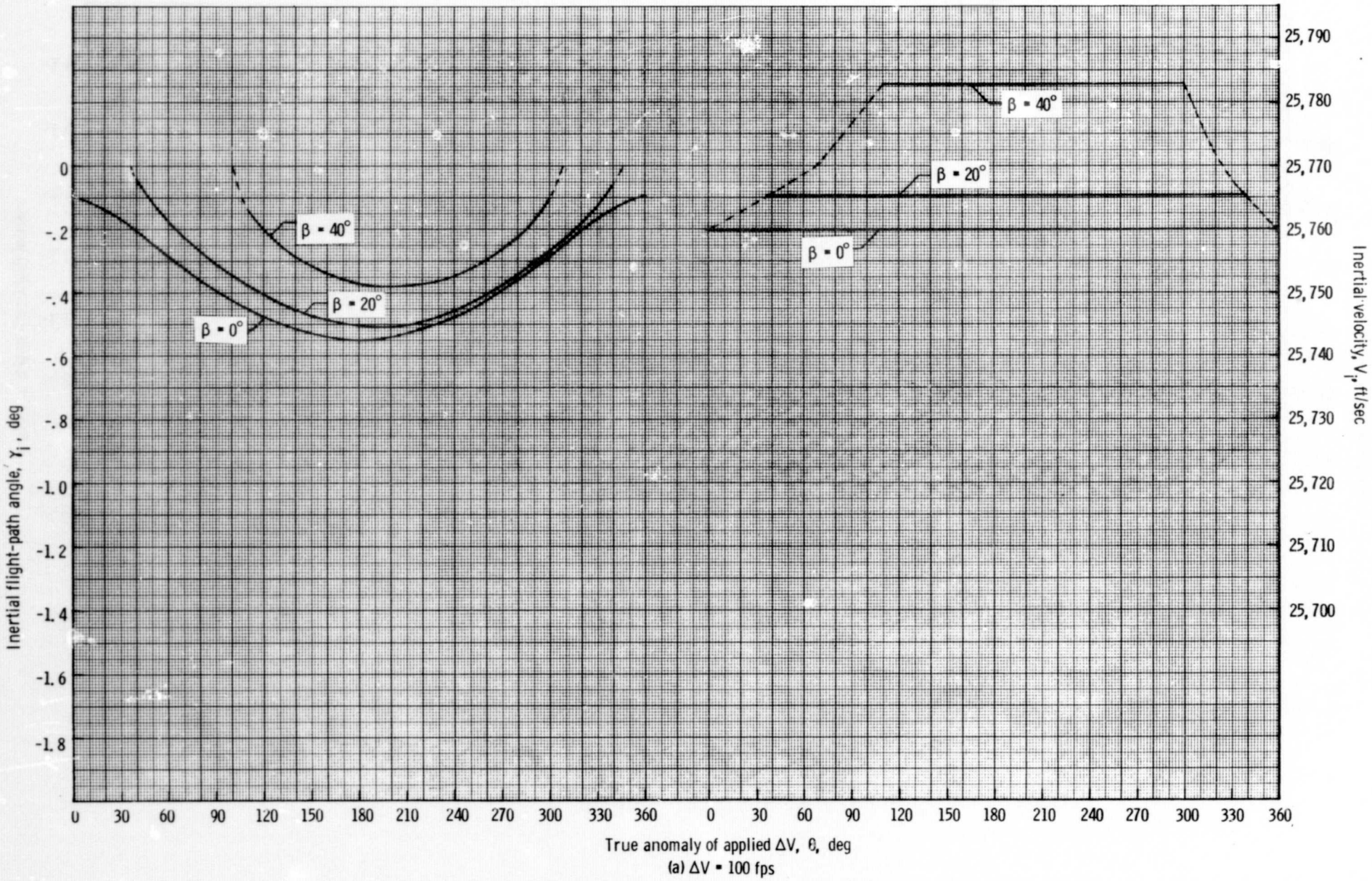

(a) ΔV = 100 fps

Figure 14. - Inertial flight-path angle and velocity at 400 000 feet as a function of retrograde true anomaly and a constant ΔV for an elliptical orbit where h_p = 100 nautical miles and h_a = 120 nautical miles.

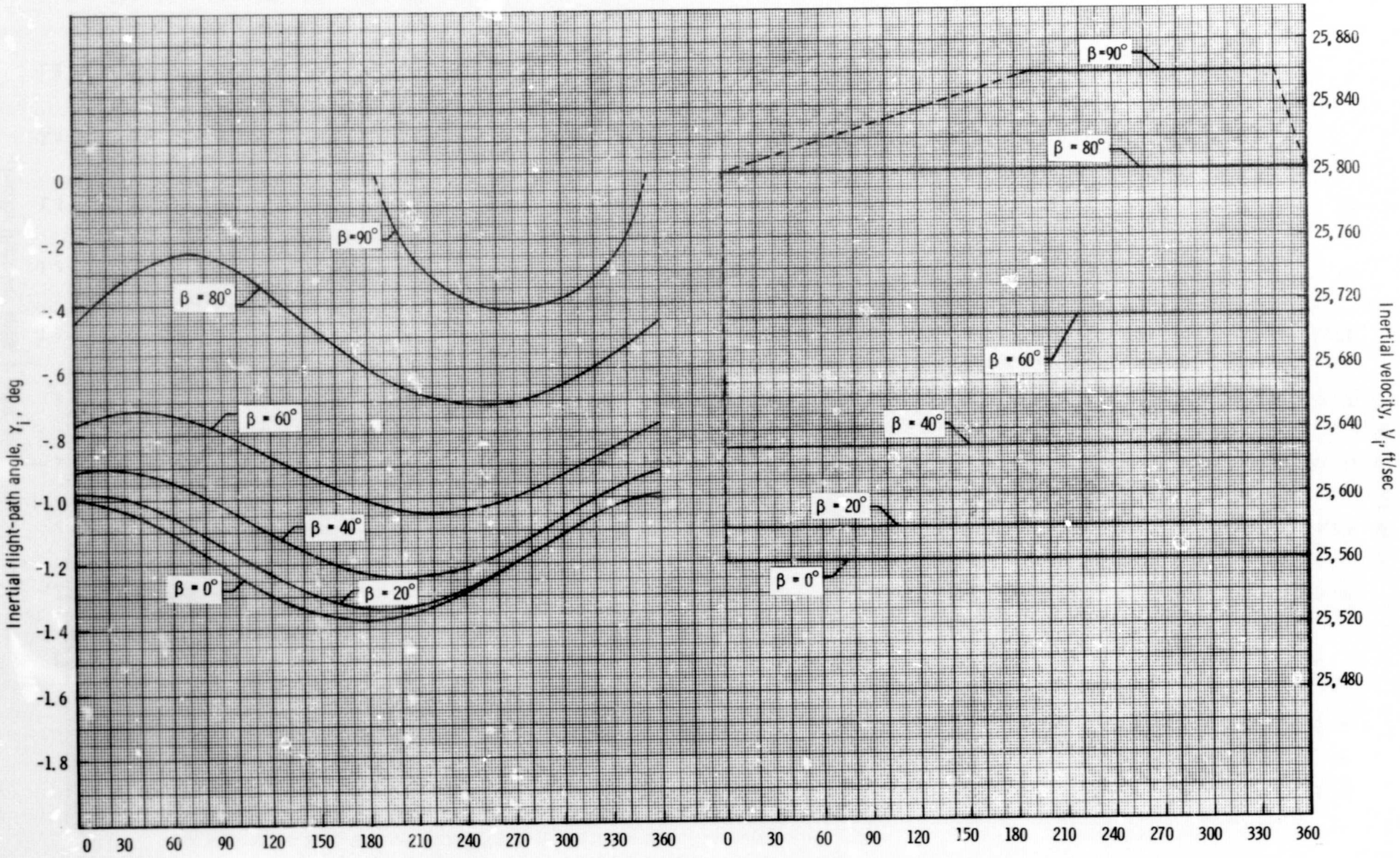

(b) ΔV = 300 fps

Figure 14. - Continued.

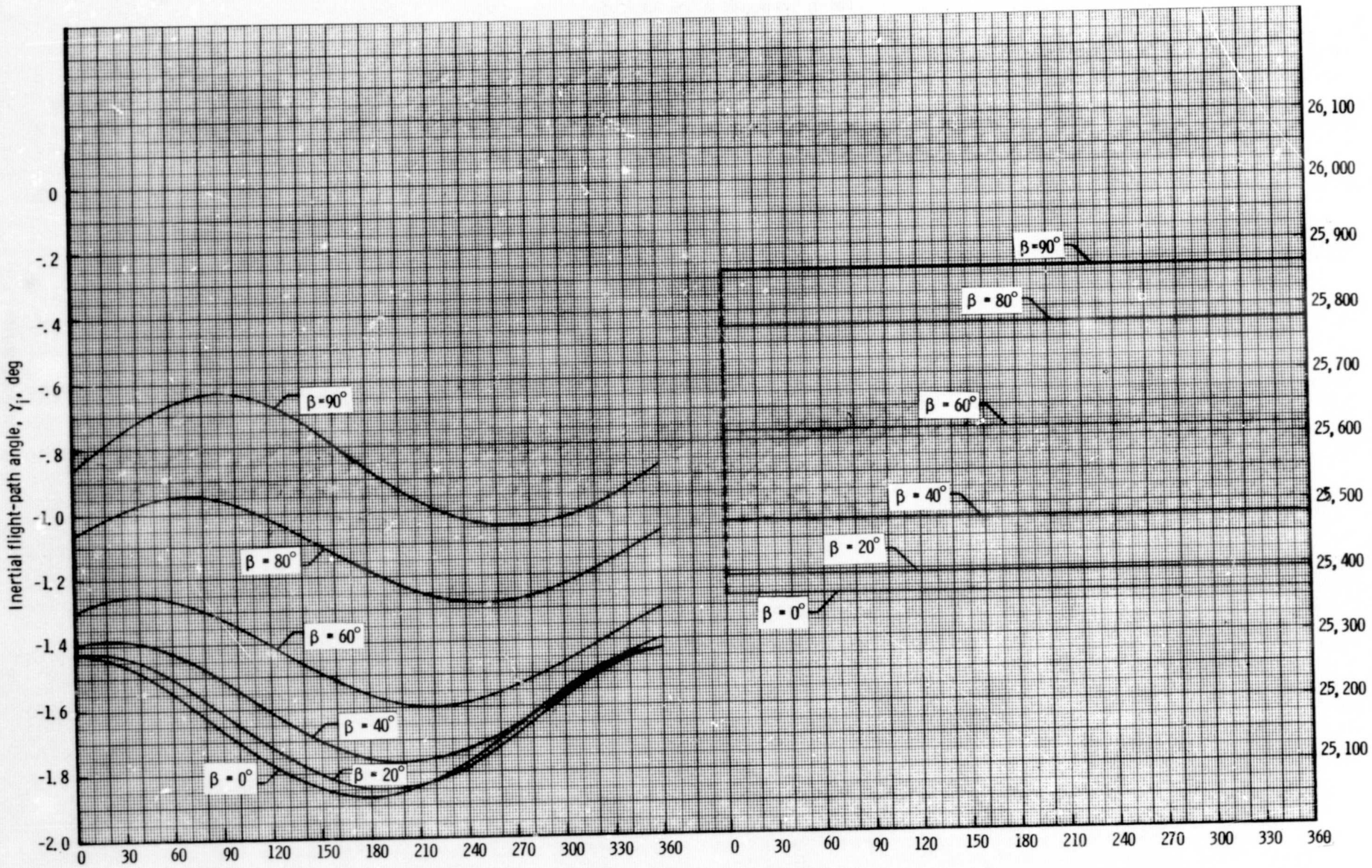

(c) ΔV = 500 fps

Figure 14. - Continued.

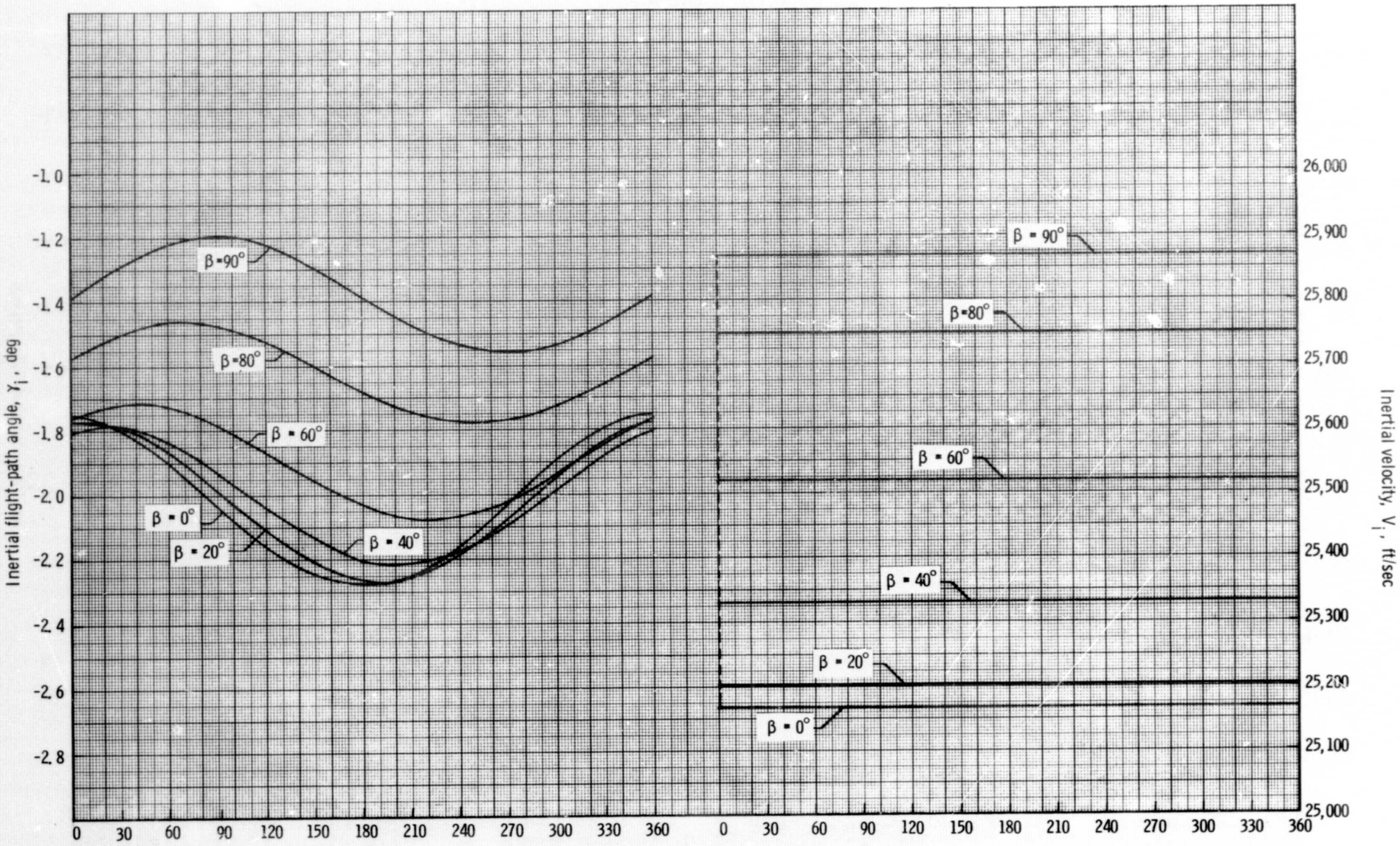

(d) ΔV = 700 fps

Figure 14. - Concluded.

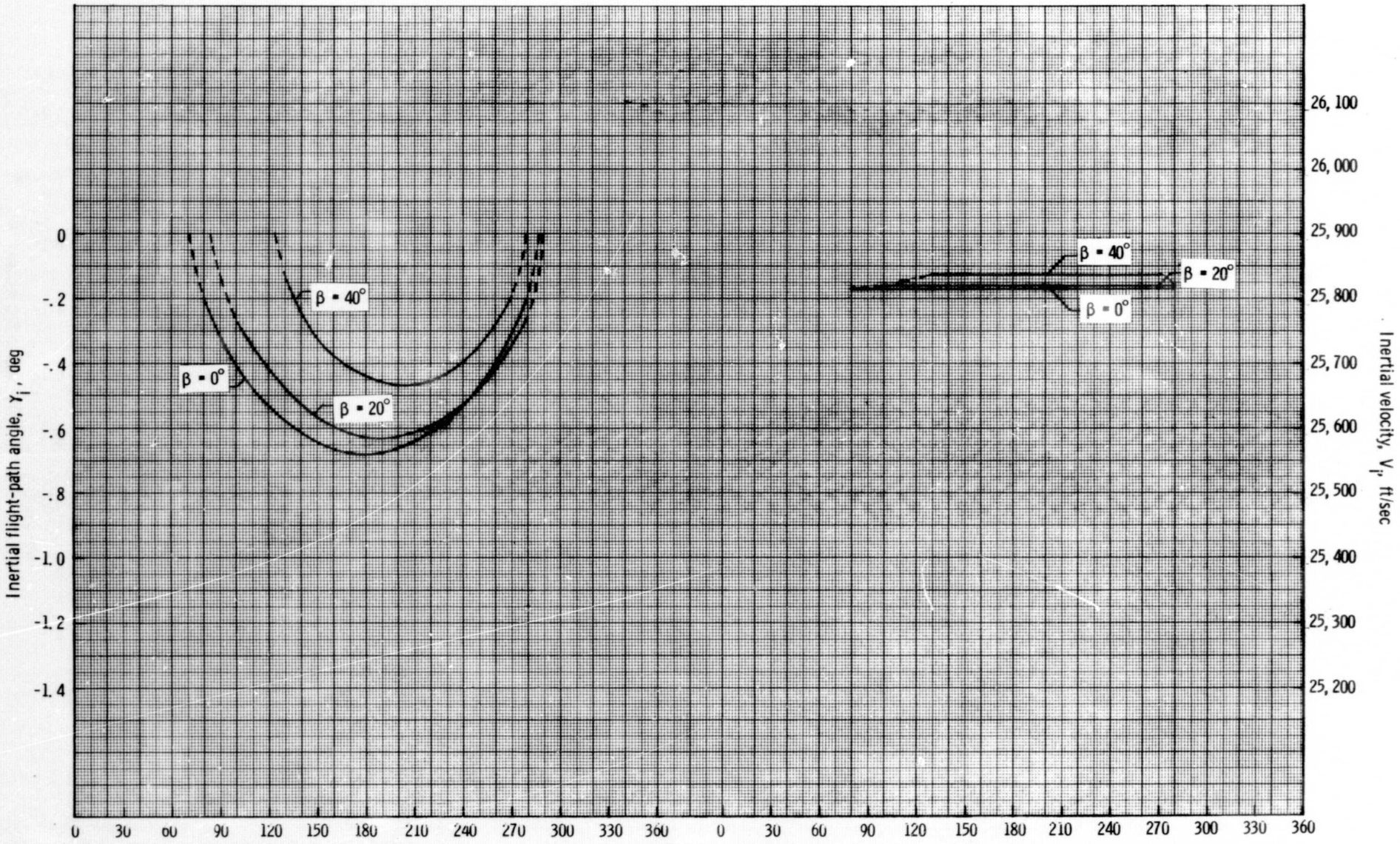

(a) ΔV = 100 fps

Figure 15. - Inertial flight-path angle and velocity at 400 000 feet as a function of retrograde true anomaly and a constant ΔV for an elliptical orbit where h_p = 100 nautical miles and h_a = 150 nautical miles.

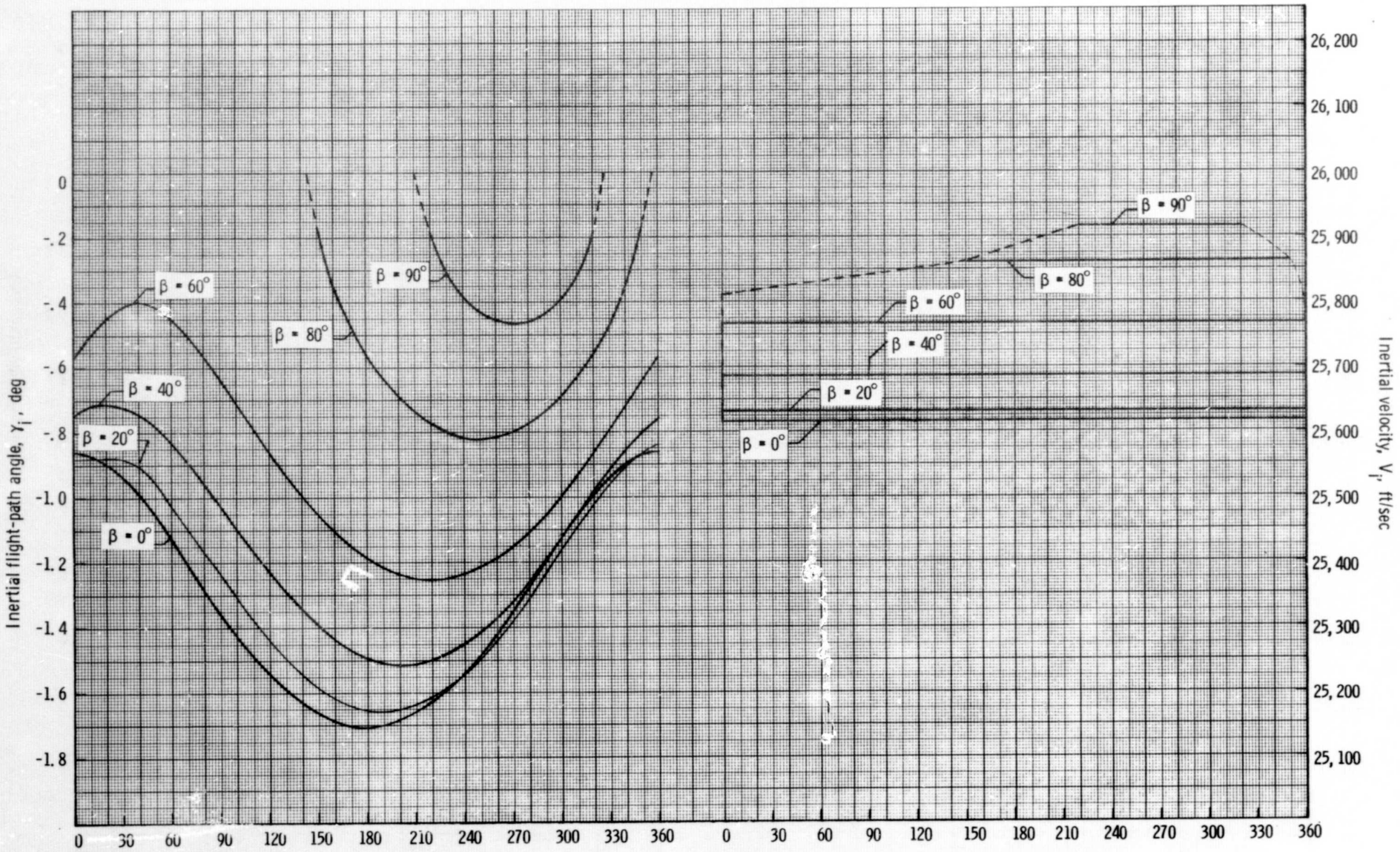

(b) ΔV = 300 fps

Figure 15. - Continued.

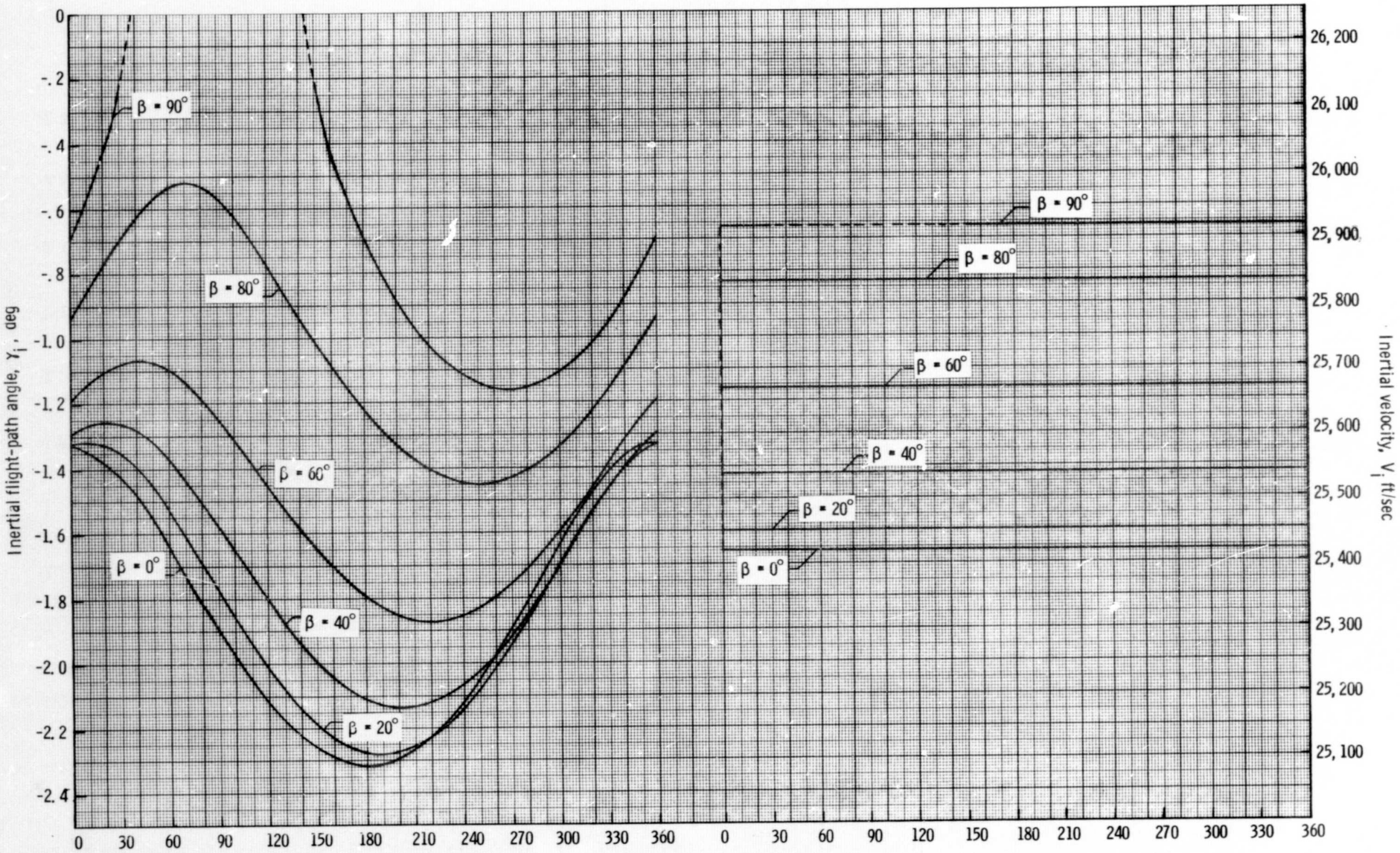

(c) ΔV = 500 fps

Figure 15. - Continued.

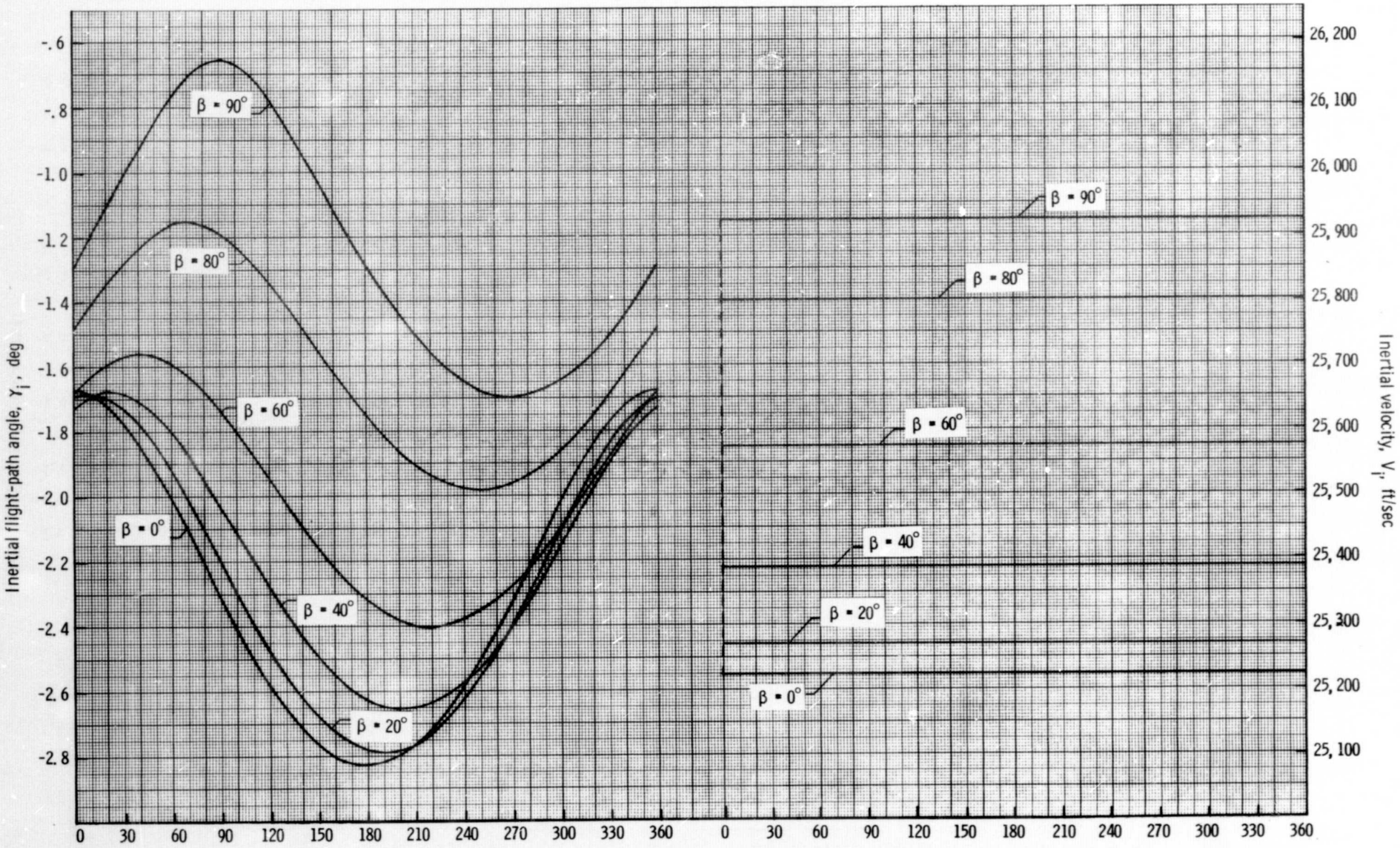

(d) ΔV = 700 fps

Figure 15. - Concluded.

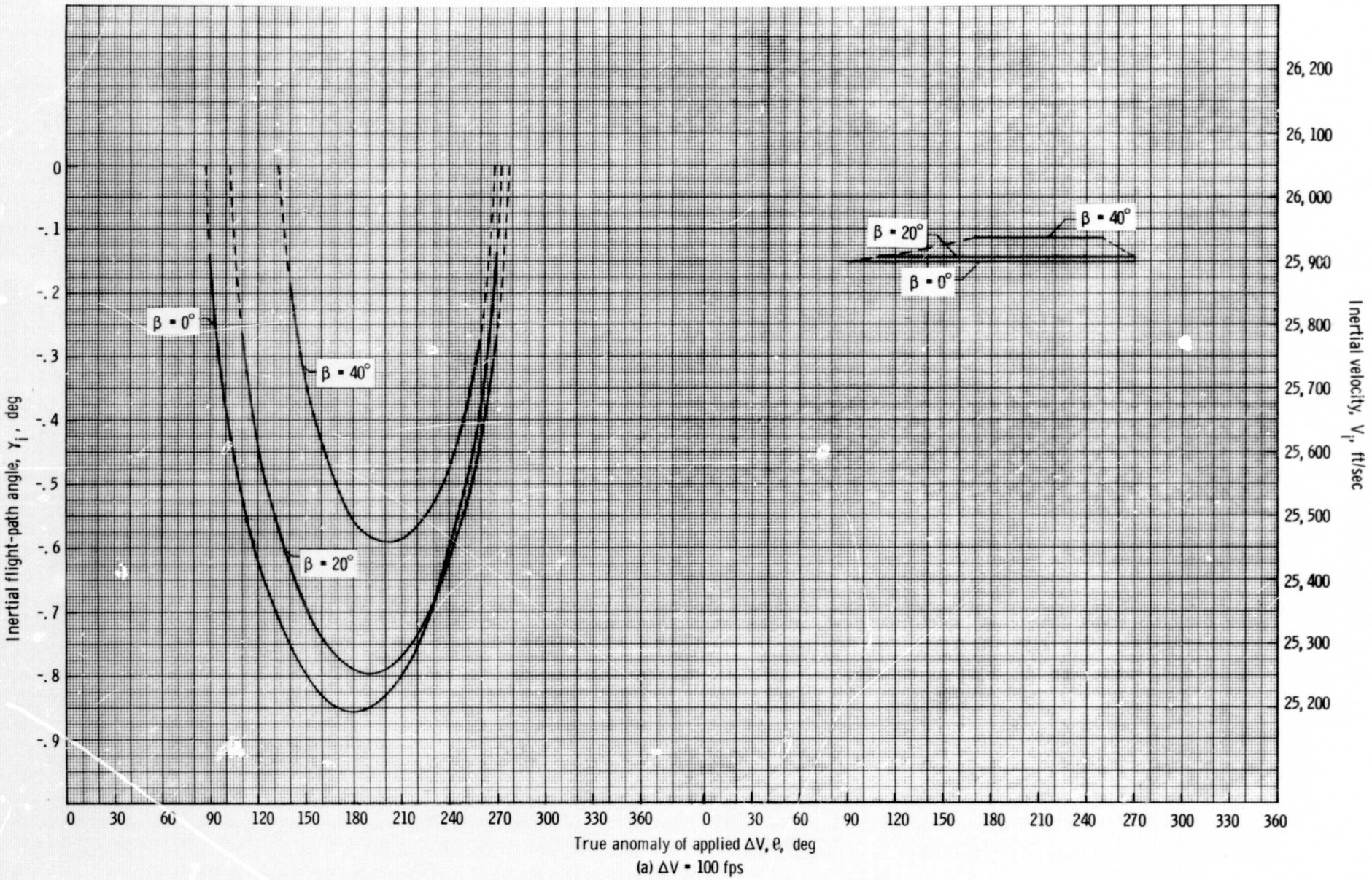

(a) ΔV = 100 fps

Figure 16. - Inertial flight-path angle and velocity at 400 000 feet as a function of retrograde true anomaly and a constant ΔV for an elliptical orbit where h_p = 100 nautical miles and h_a = 200 nautical miles.

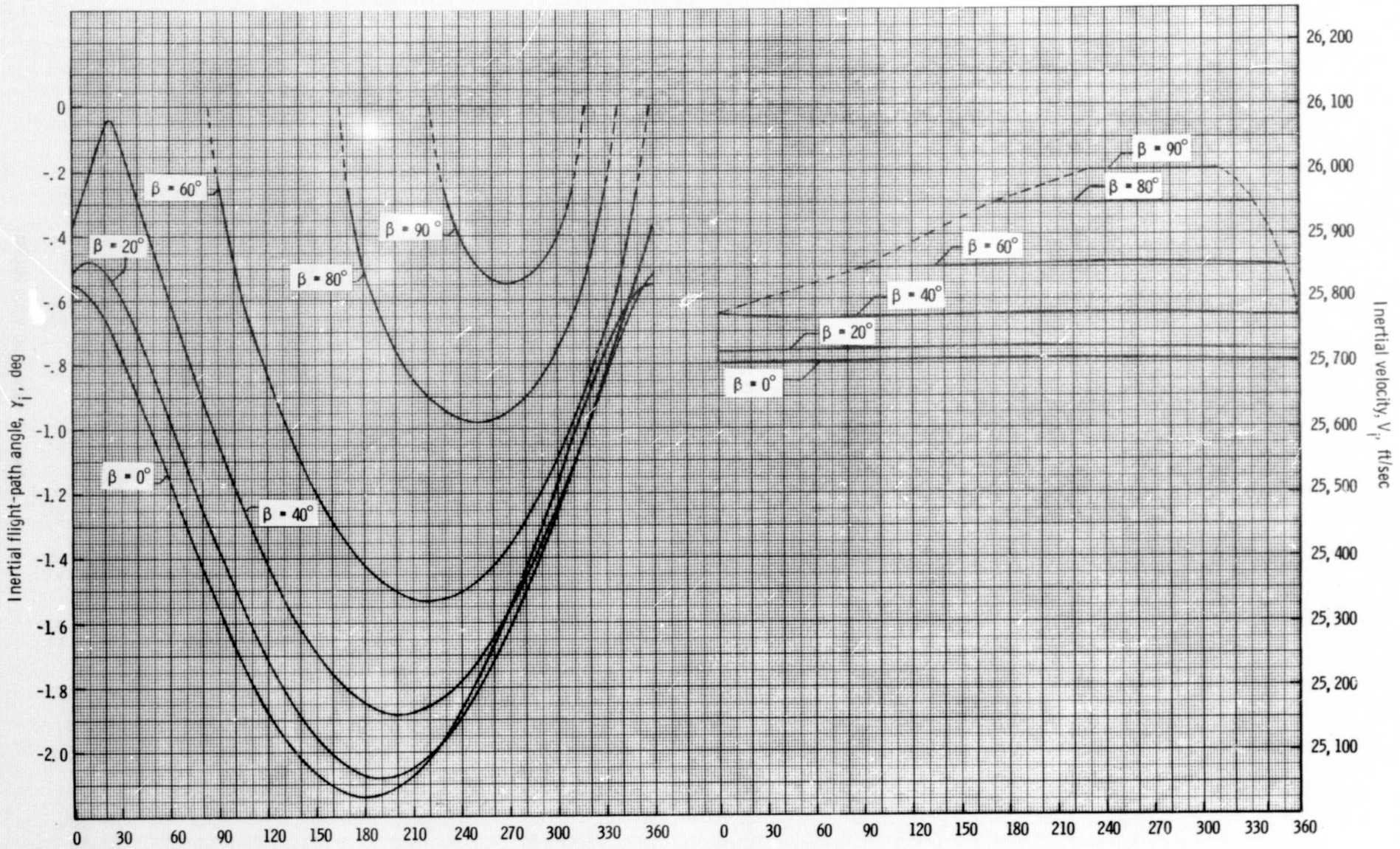

(b) ΔV = 300 fps

Figure 16. - Continued.

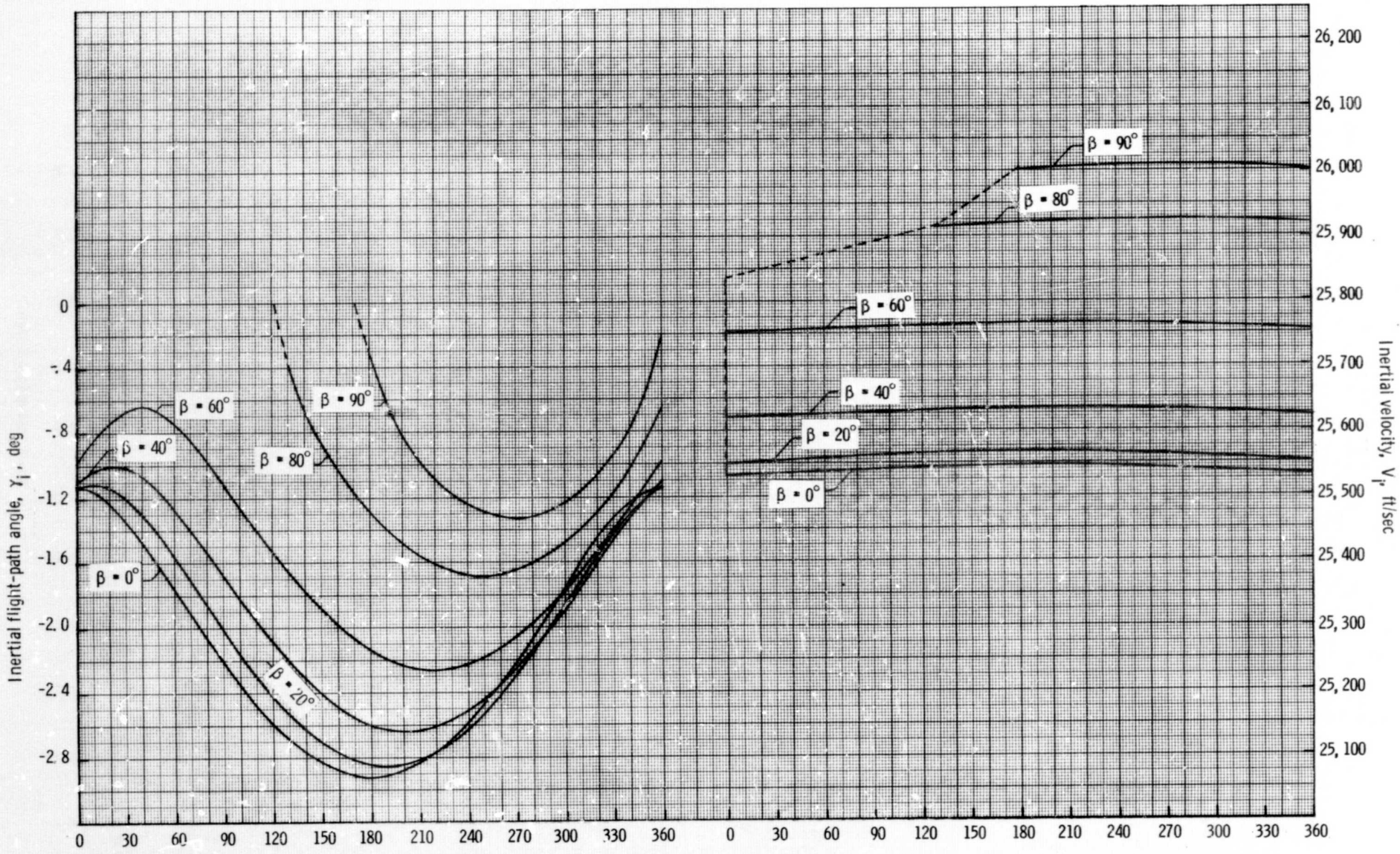

(c) ΔV = 500 fps

Figure 16. - Continued.

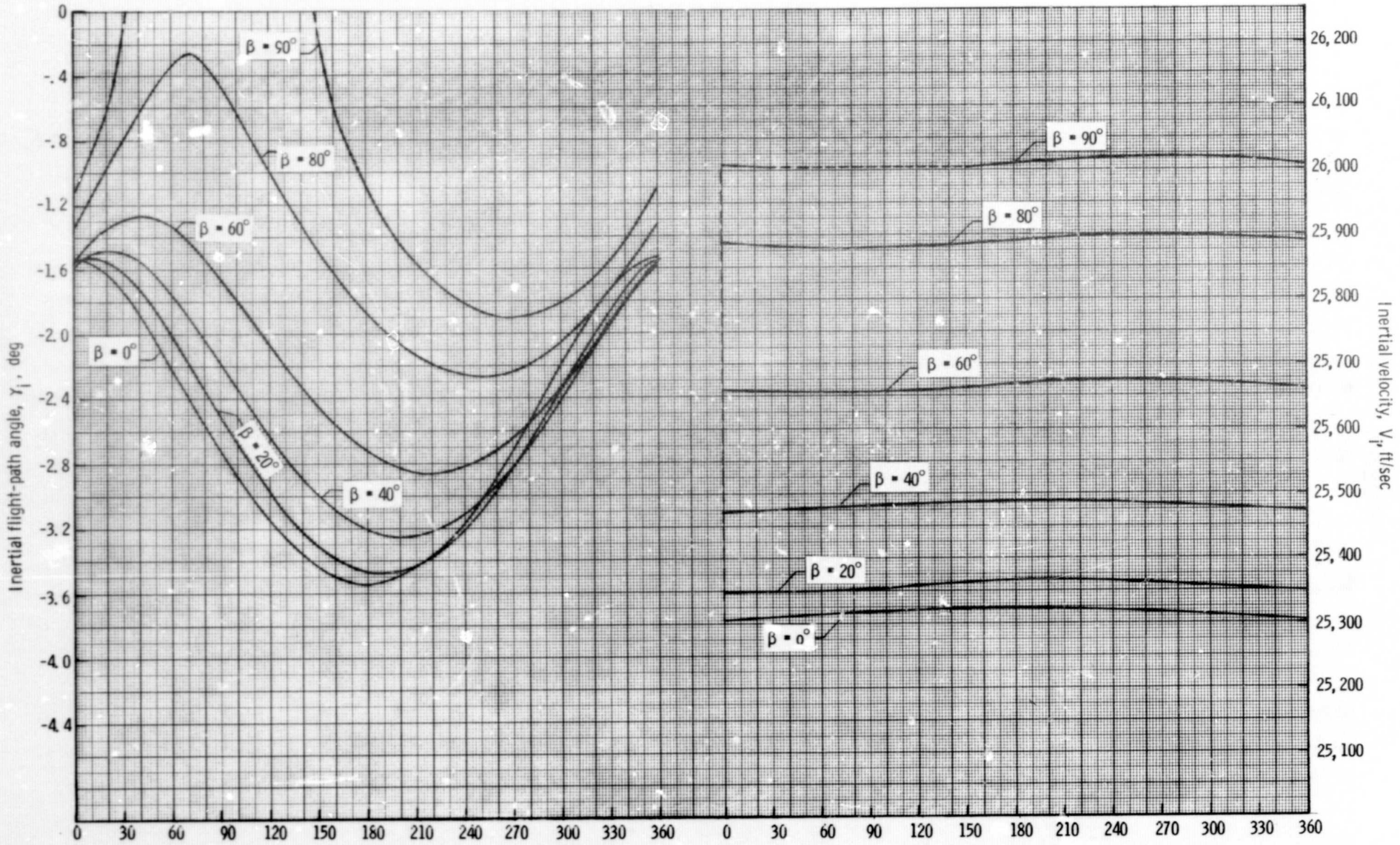

(d) ΔV = 700 fps

Figure 16. - Concluded.

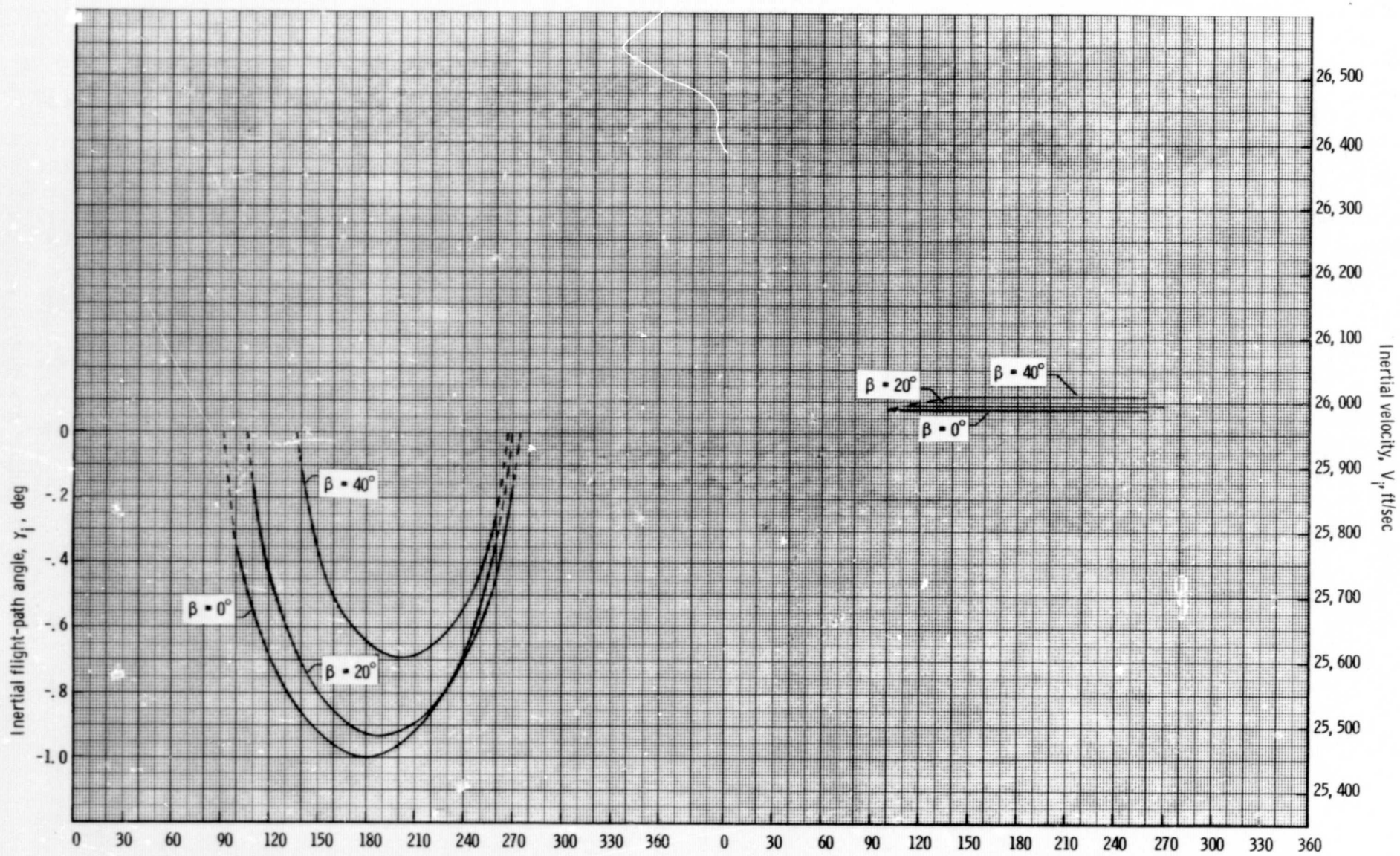

(a) ΔV = 100 fps

Figure 17. - Inertial flight-path angle and velocity at 400 000 feet as a function of retrograde true anomaly and a constant ΔV for an elliptical orbit where h_p = 100 nautical miles and h_a = 250 nautical miles.

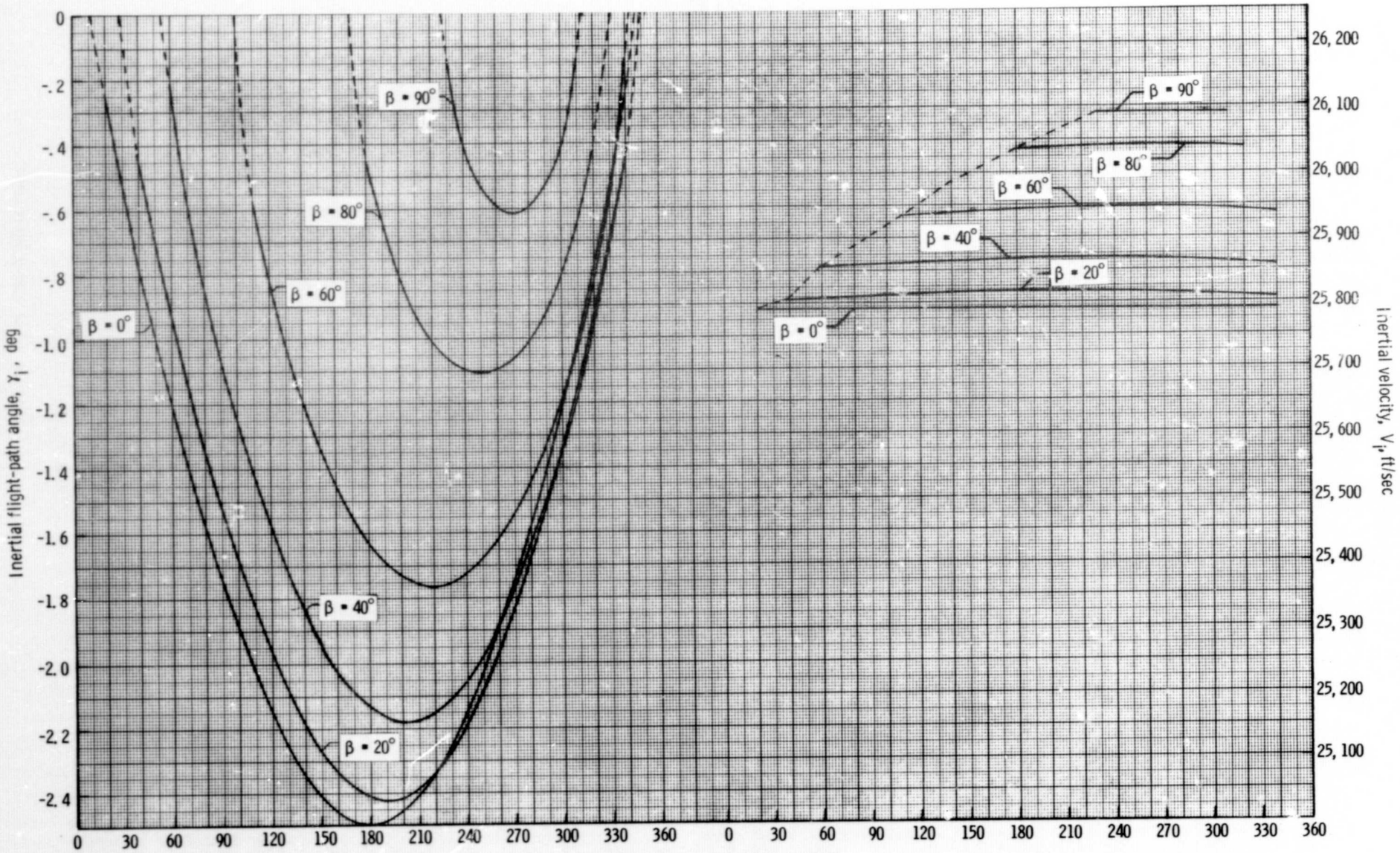

(b) ΔV = 300 fps

Figure 17. - Continued.

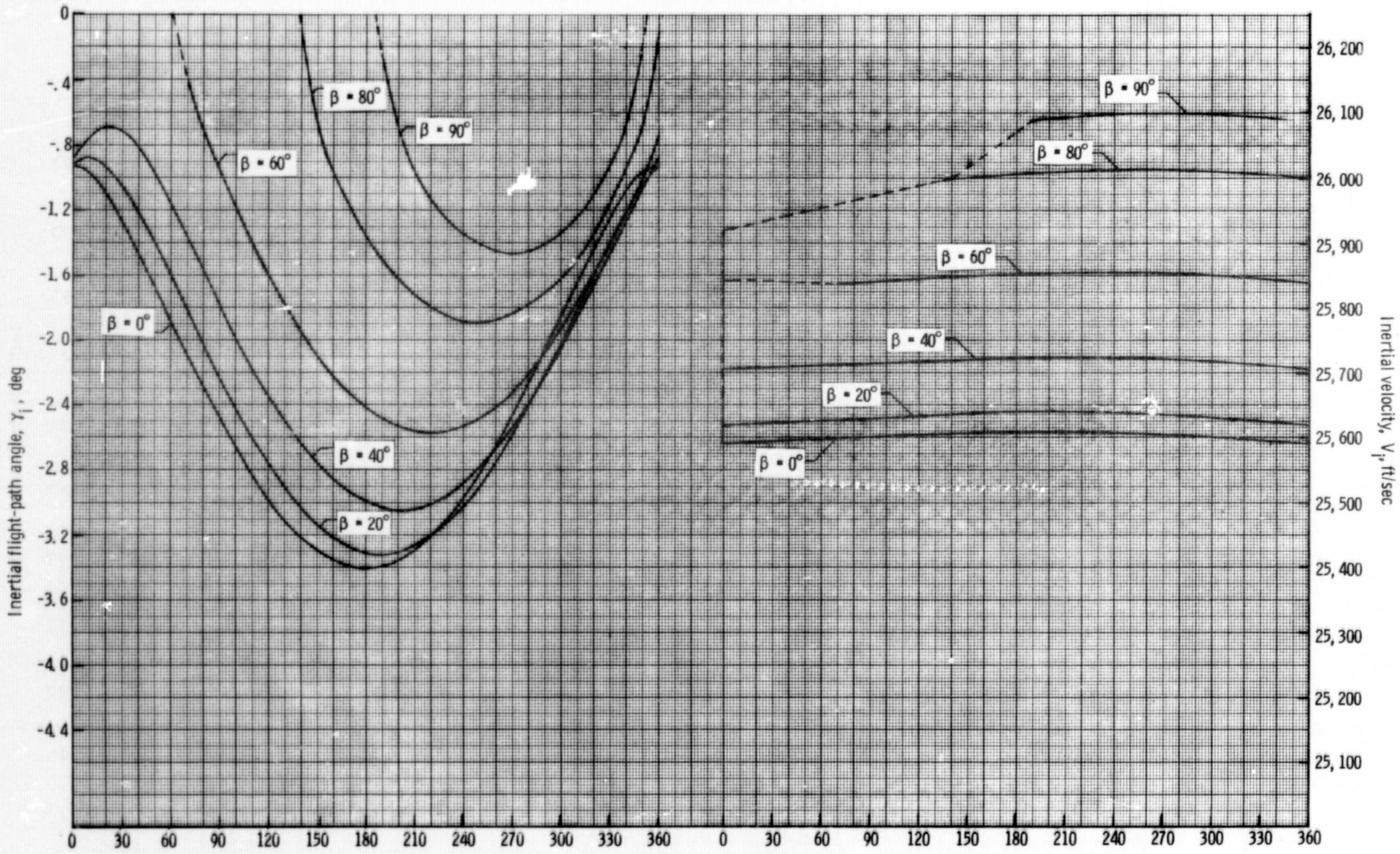

(c) $\Delta V = 500$ fps

Figure 17. - Continued.

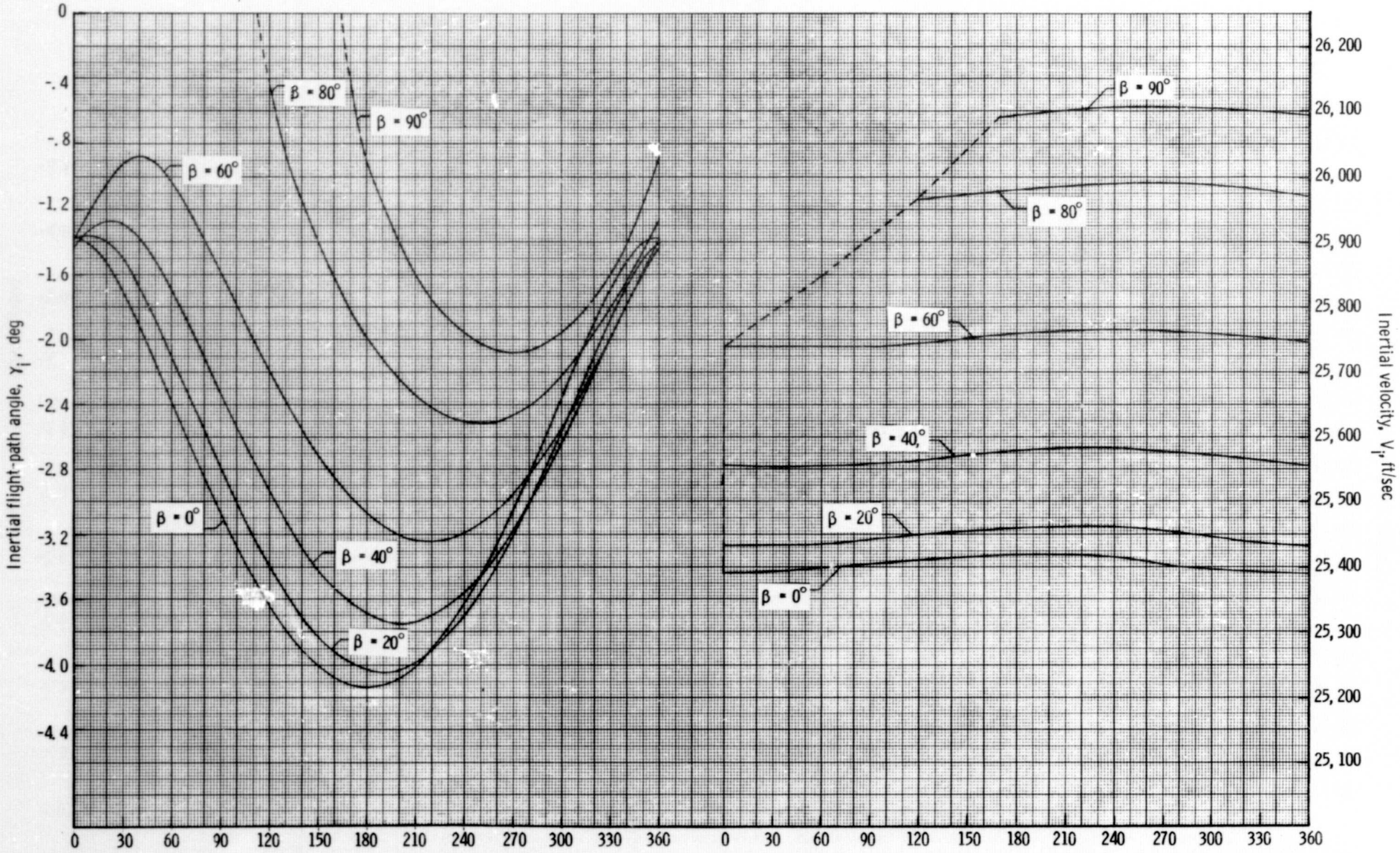

(d) ΔV = 700 fps

Figure 17. - Concluded.

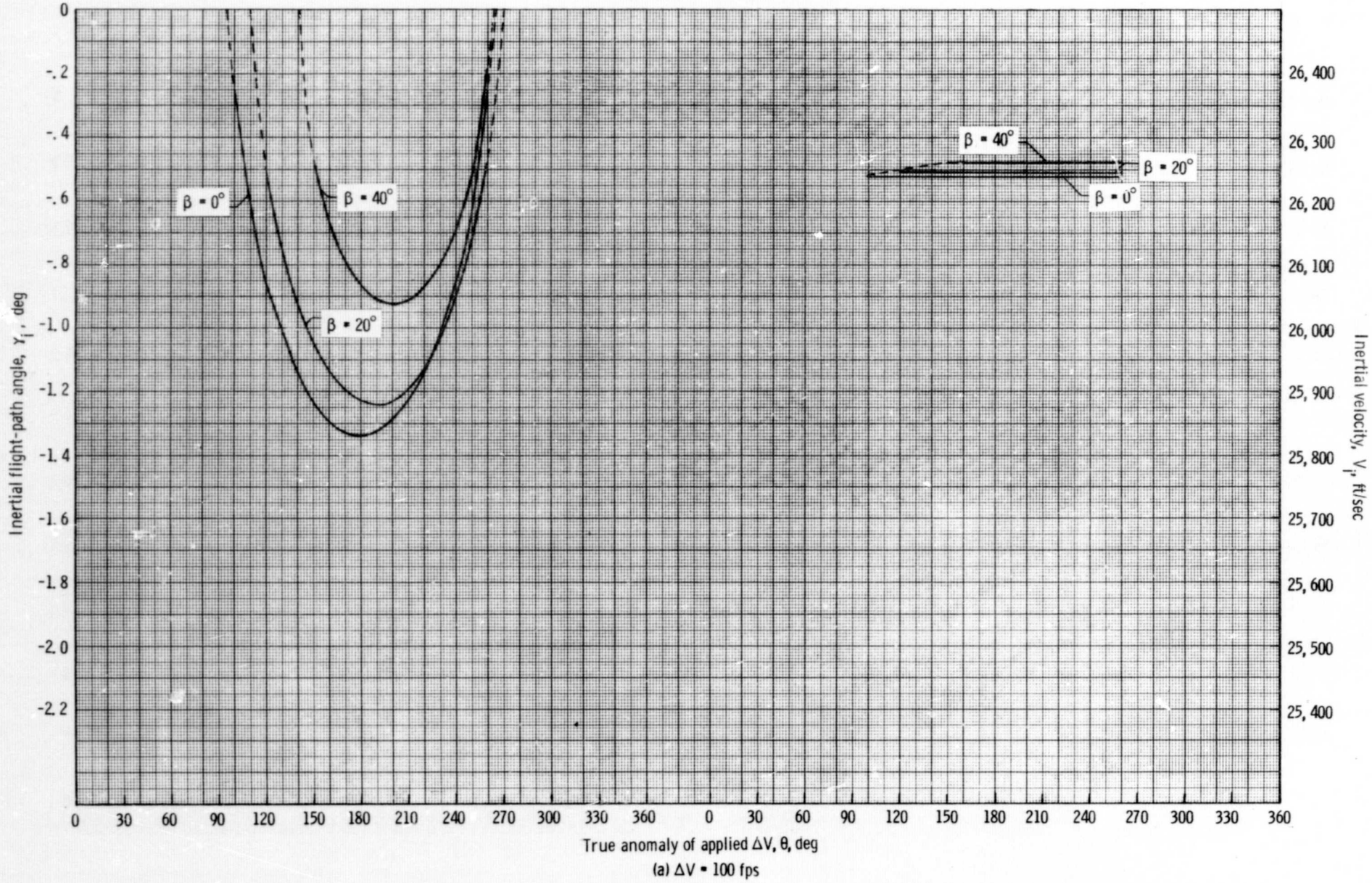

(a) ΔV = 100 fps

Figure 18. - Inertial flight-path angle and velocity at 400 000 feet as a function of retrograde true anomaly and a constant ΔV for an elliptical orbit where h_p = 100 nautical miles and h_a = 400 nautical miles.

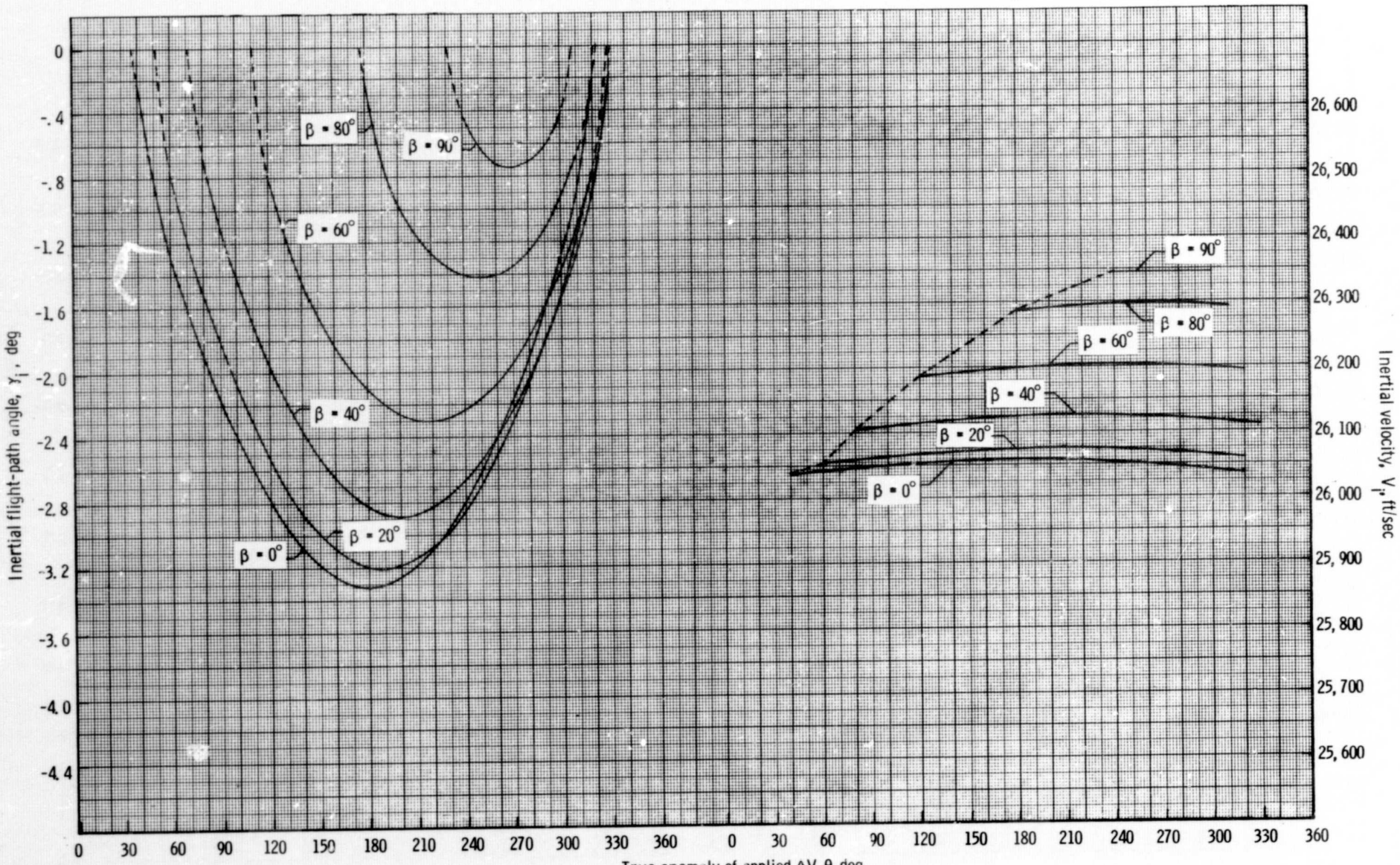

(b) ΔV = 300 fps

Figure 18. - Continued.

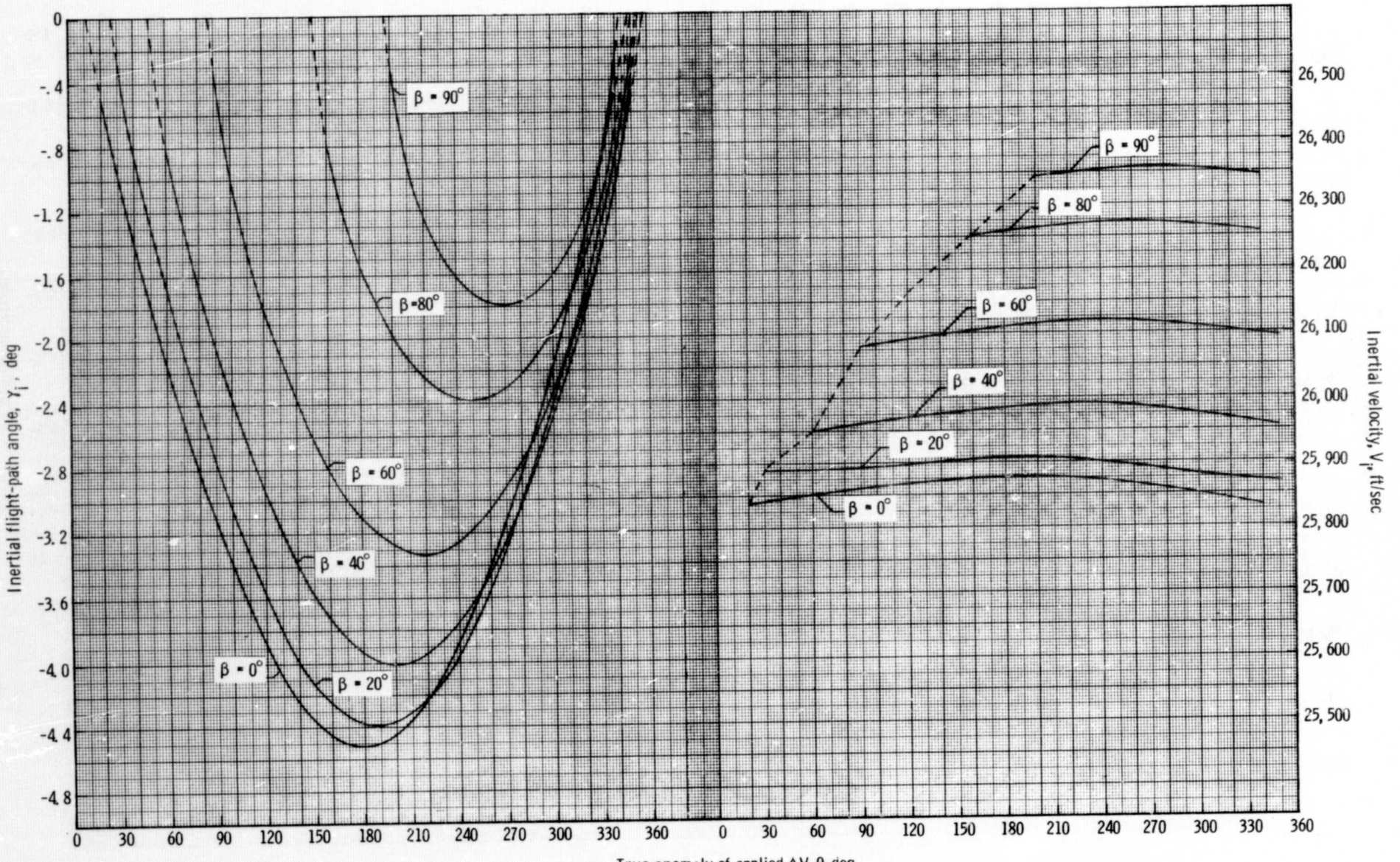

(c) ΔV = 500 fps

Figure 18. - Continued.

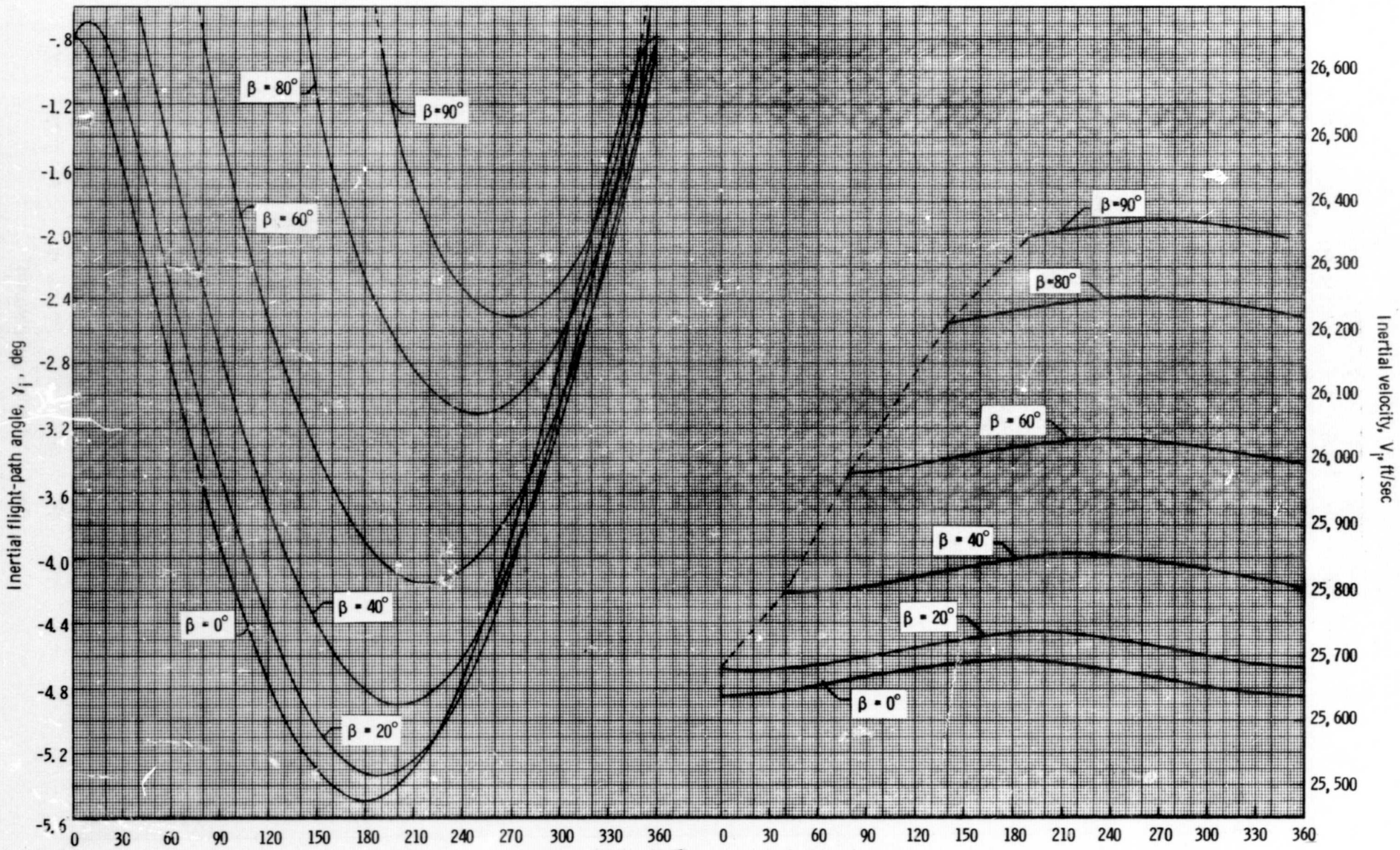

(d) $\Delta V = 700$ fps

Figure 18. - Concluded.

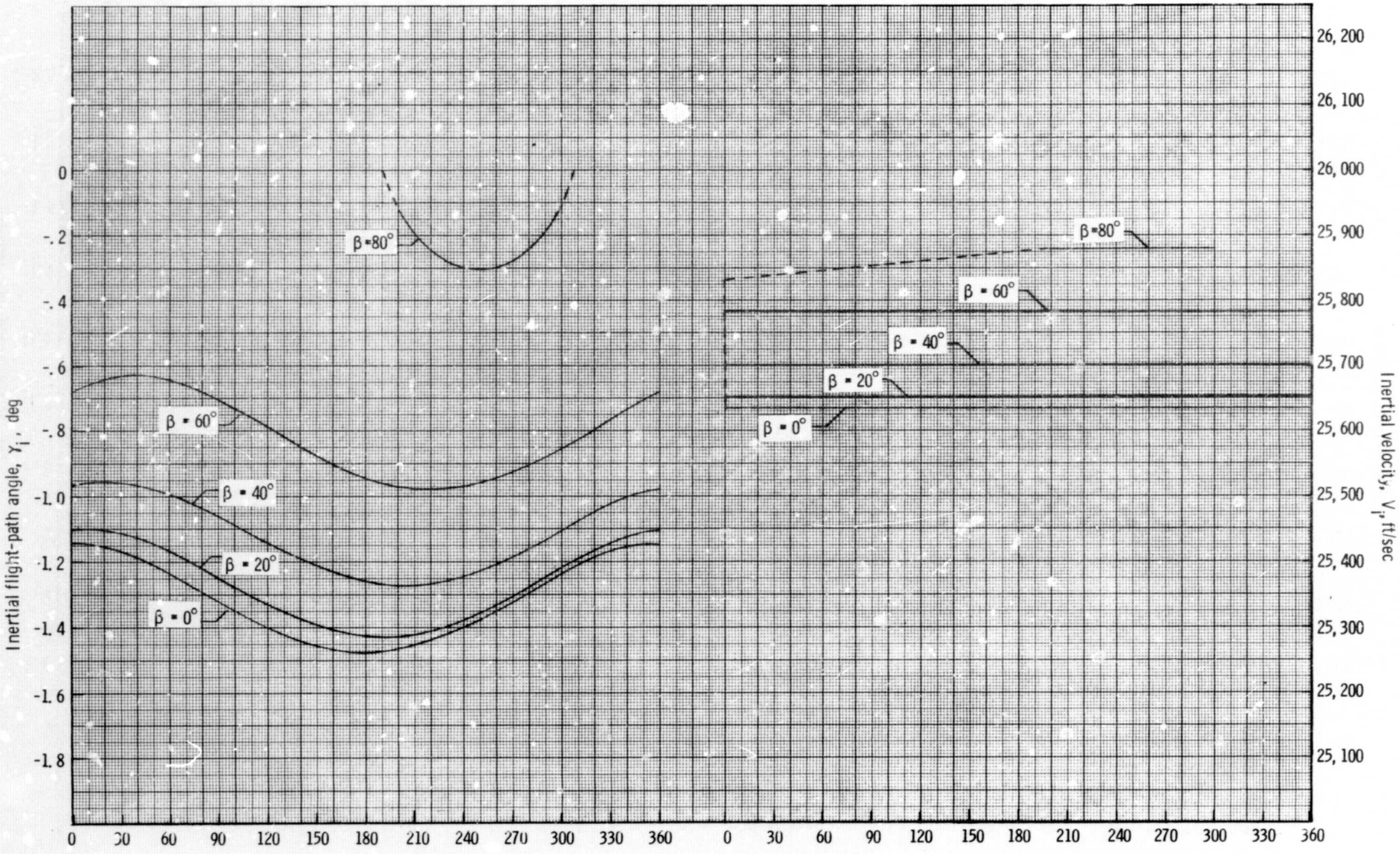

(a) ΔV = 300 fps

Figure 19. - Inertial flight-path angle and velocity at 400 000 feet as a function of retrograde true anomaly and a constant ΔV for an elliptical orbit where h_p = 120 nautical miles and h_a = 140 nautical miles.

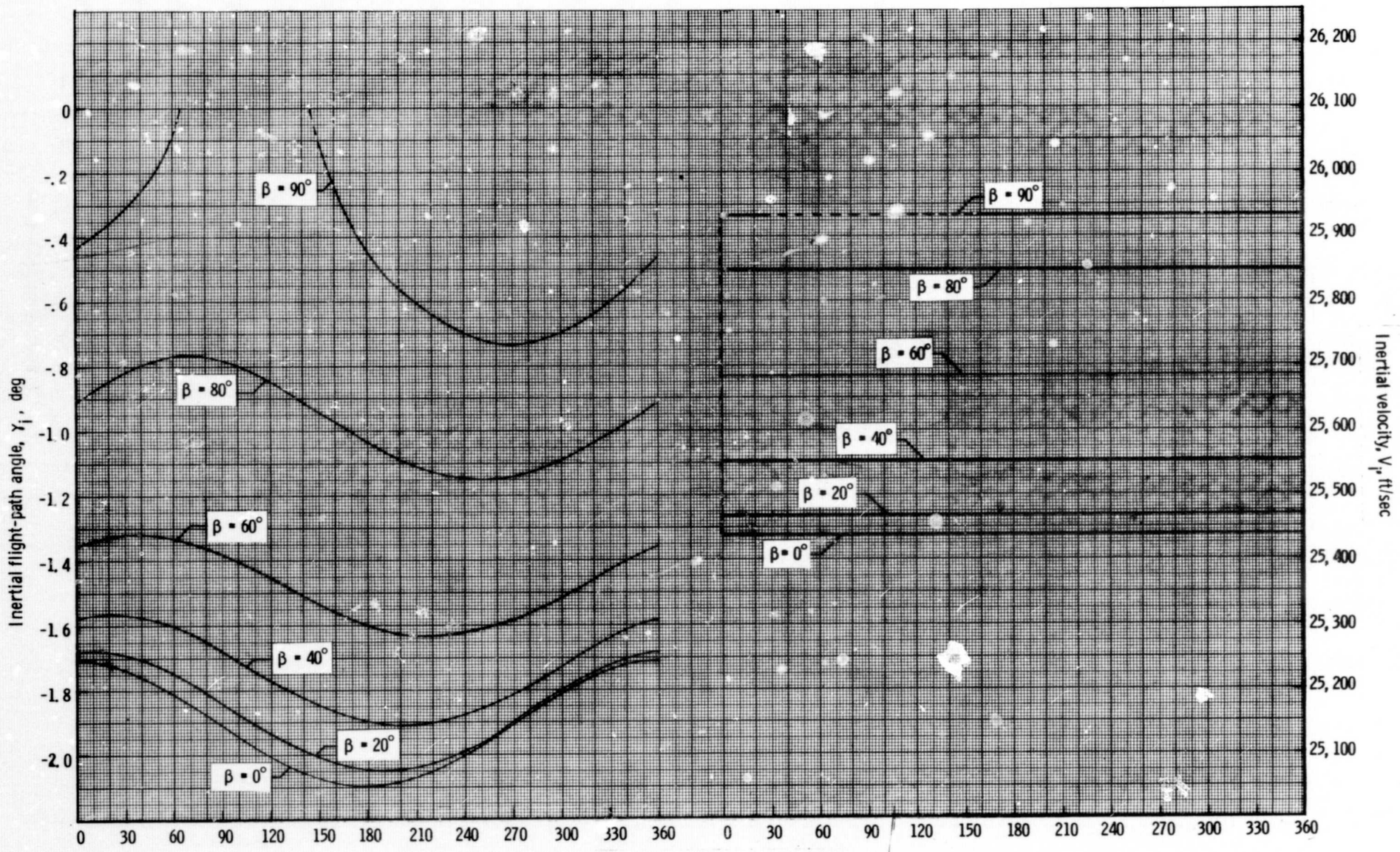

(b) ΔV = 500 fps

Figure 19. - Continued.

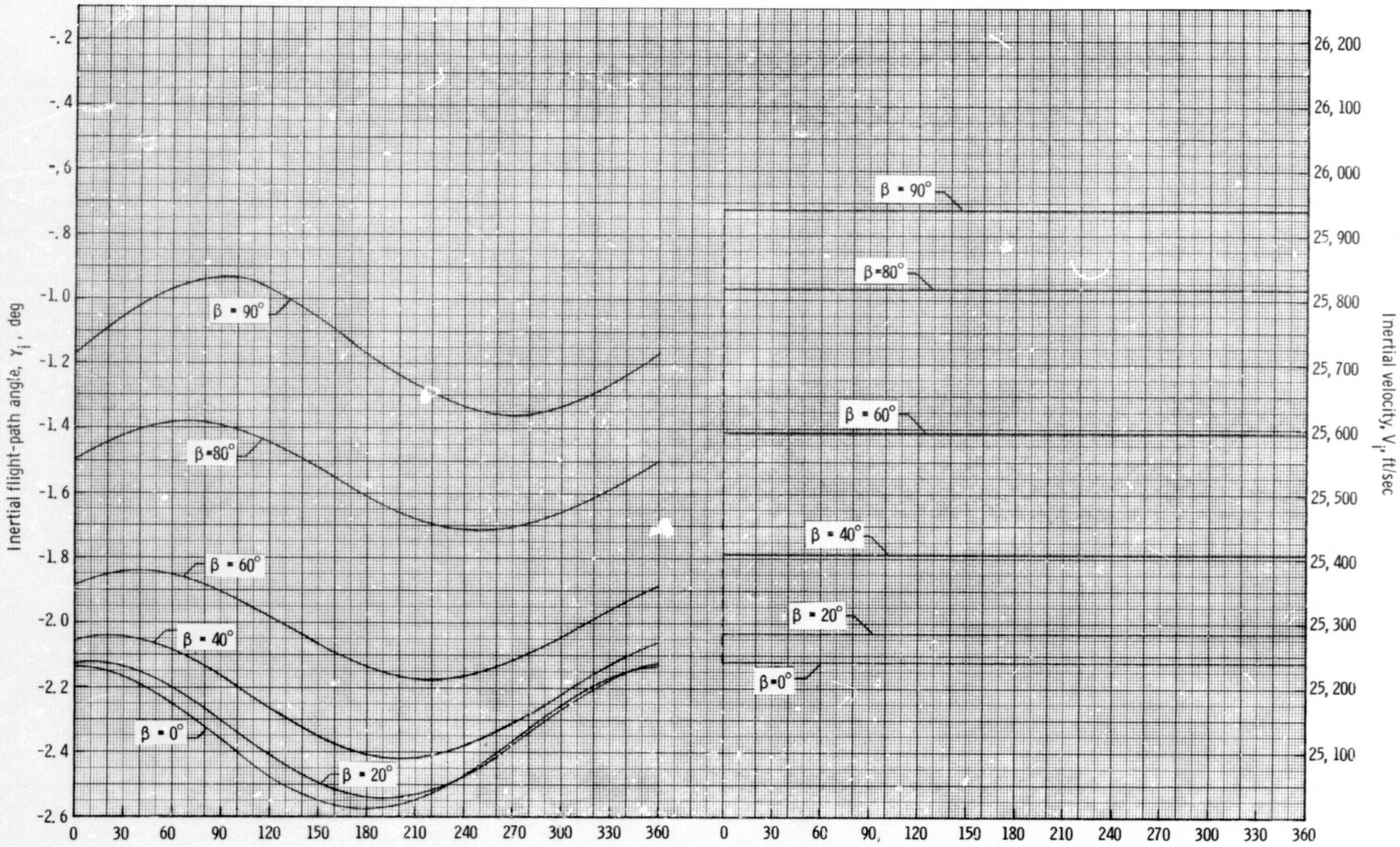

(c) ΔV = 700 fps

Figure 19. - Concluded.

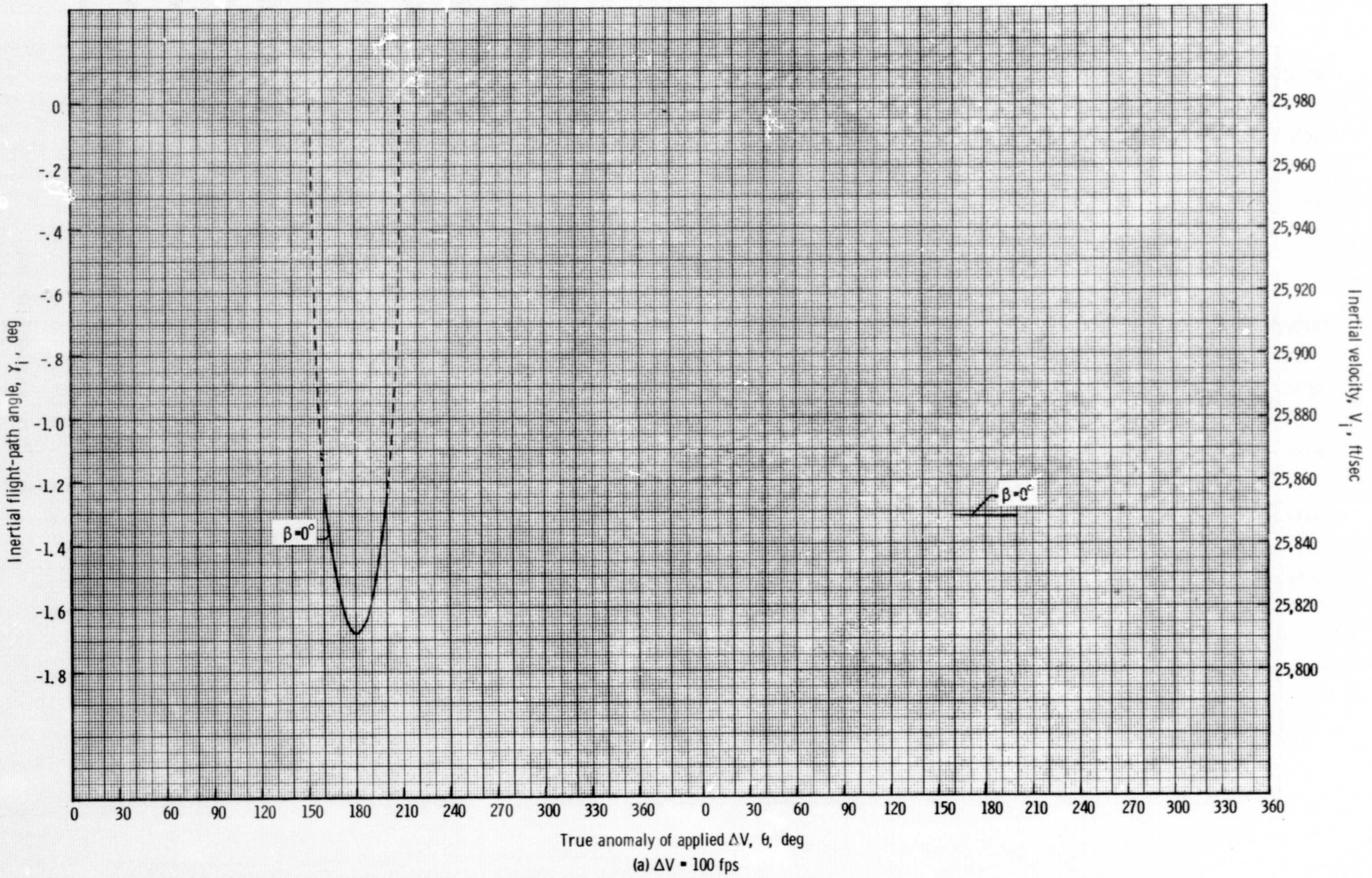

(a) ΔV = 100 fps

Figure 20. - Inertial flight-path angle and velocity at 400 000 feet as a function of retrograde true anomaly and a constant ΔV for an elliptical orbit where h_p = 120 nautical miles and h_a = 150 nautical miles.

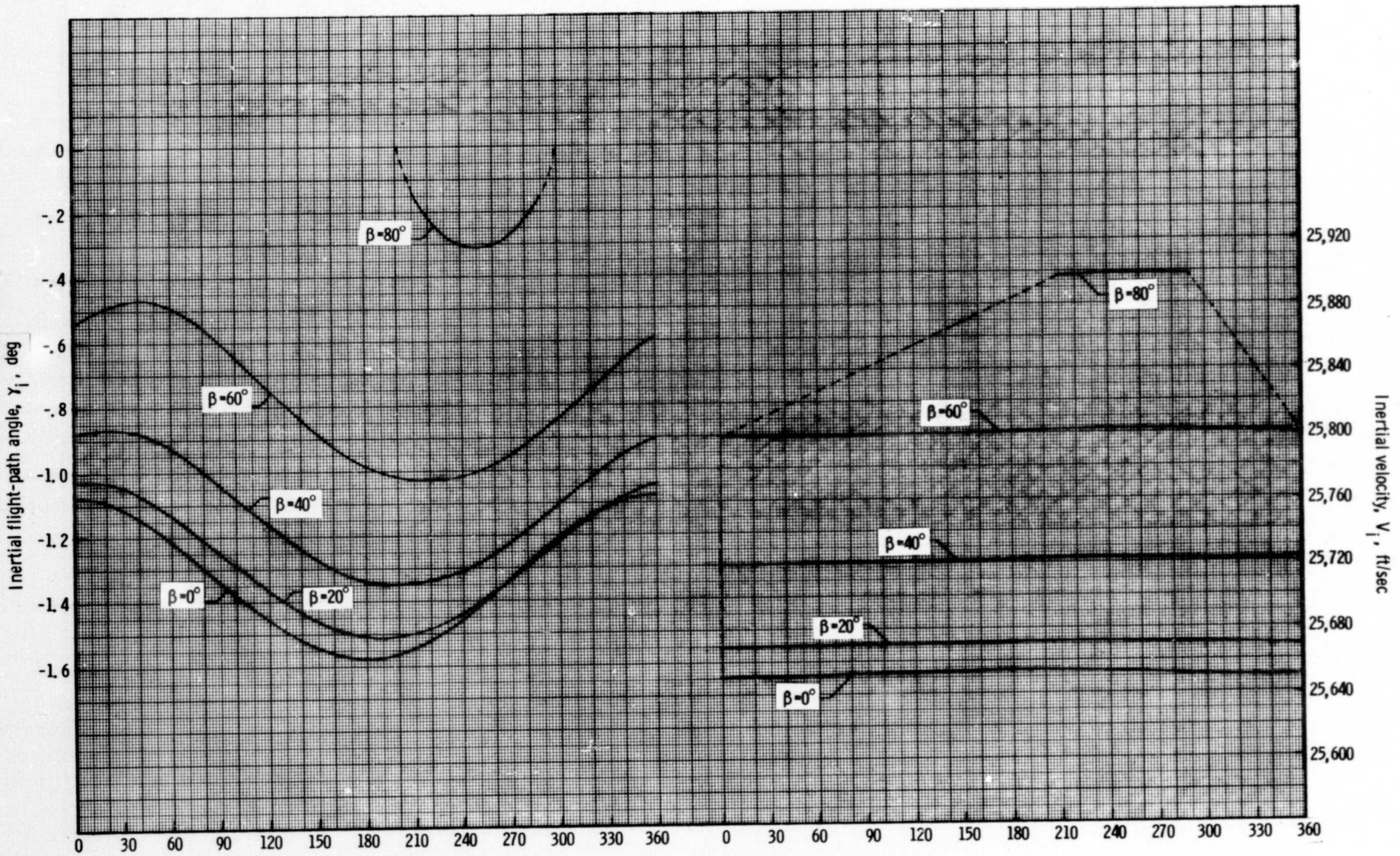

(b) ΔV = 300 fps

Figure 20. - Continued.

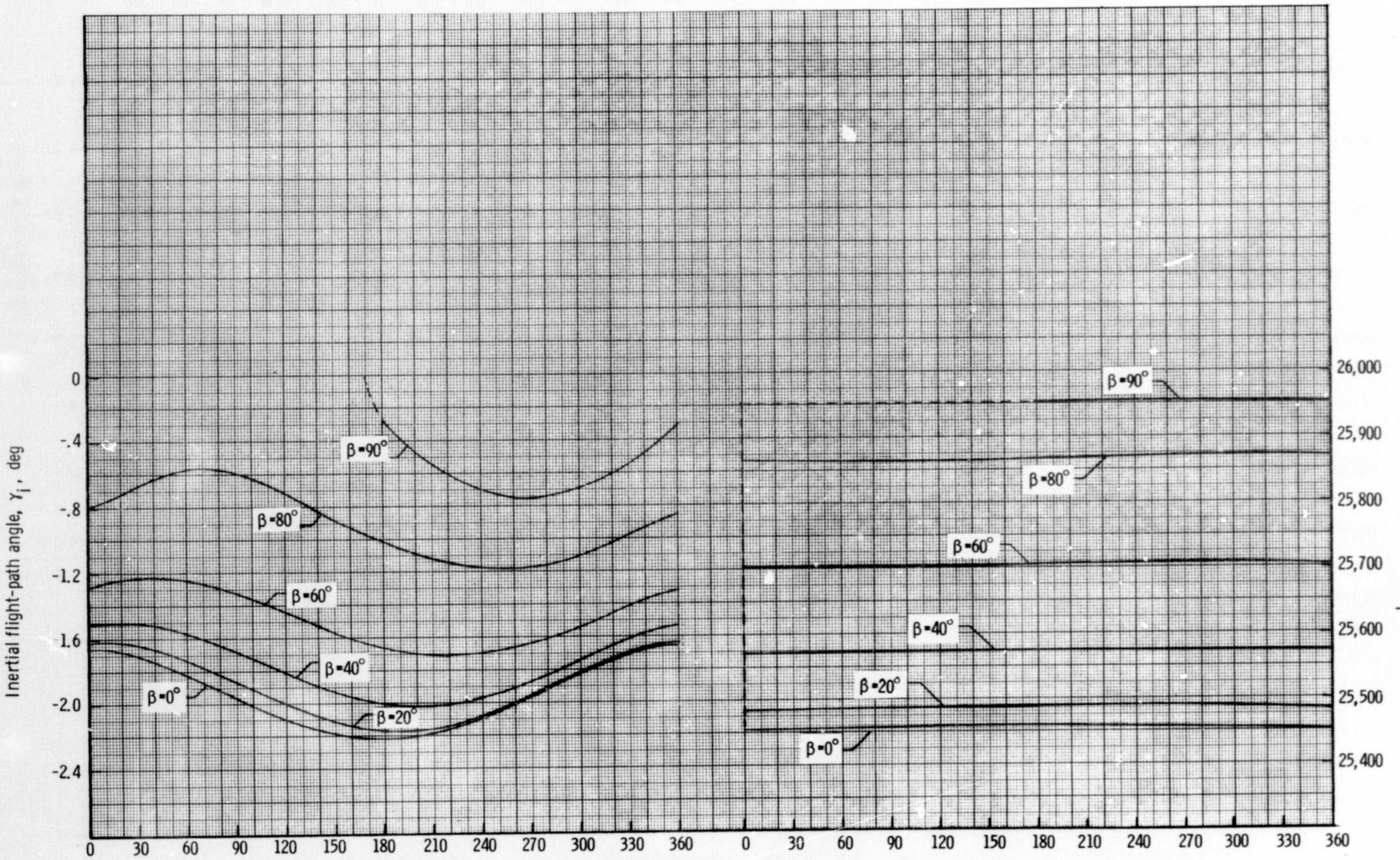

(c) ΔV = 500 fps

Figure 20. - Continued.

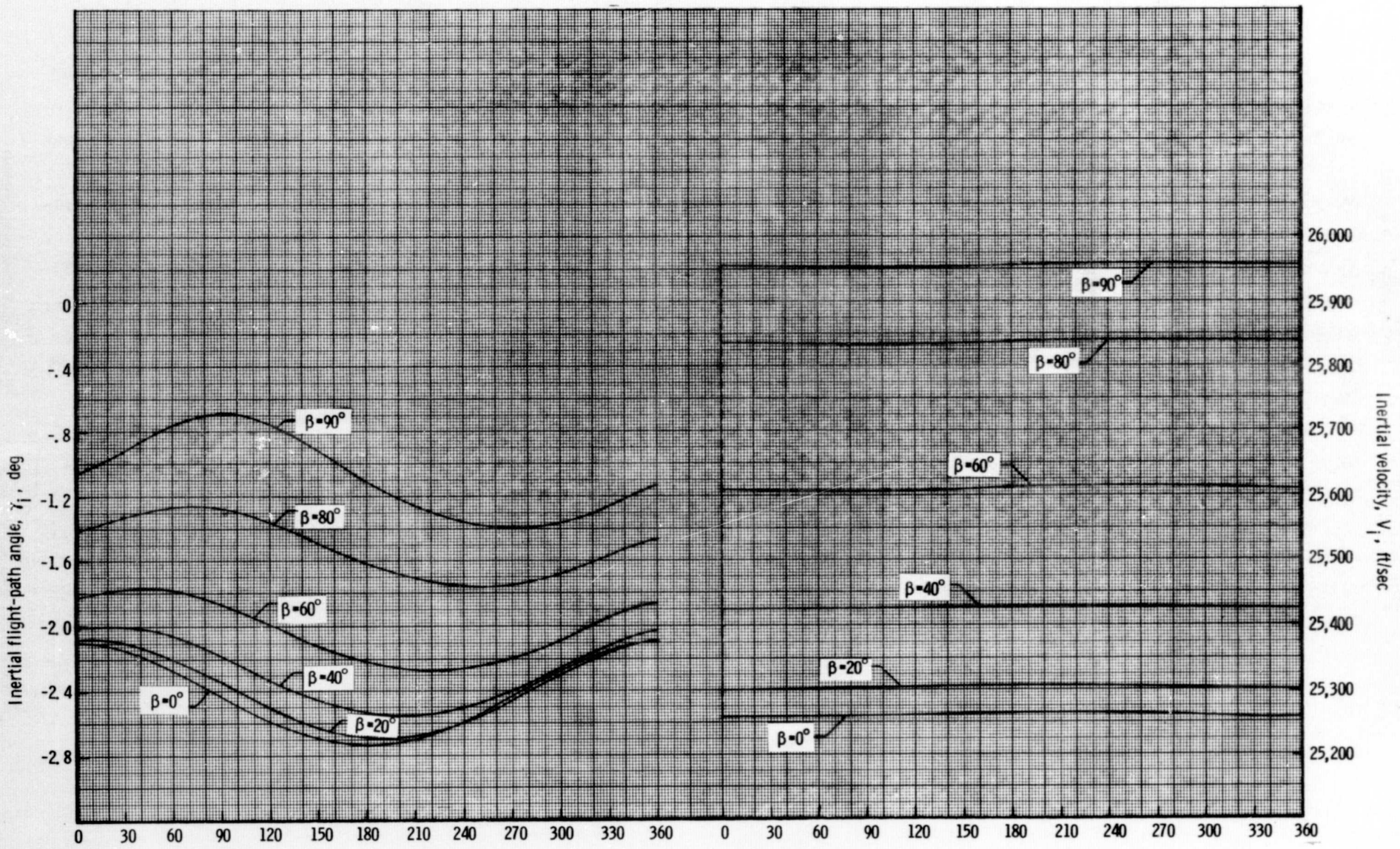

(d) ΔV = 700 fps

Figure 20. - Concluded.

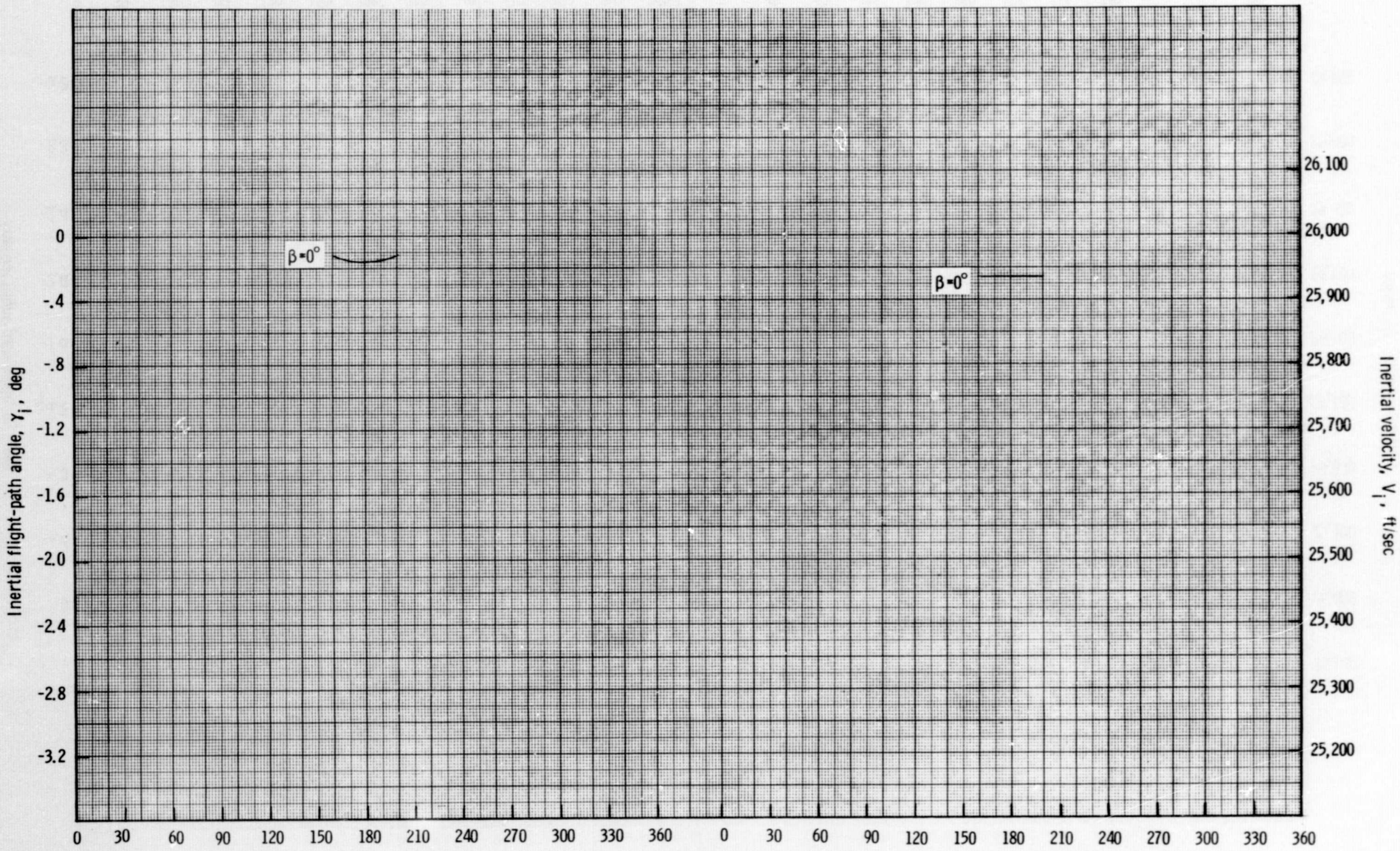

(a) ΔV = 100 fps

Figure 21. - Inertial flight-path angle and velocity at 400 000 feet as a function of retrograde true anomaly and a constant ΔV for an elliptical orbit where h_p = 120 nautical miles and h_a = 200 nautical miles.

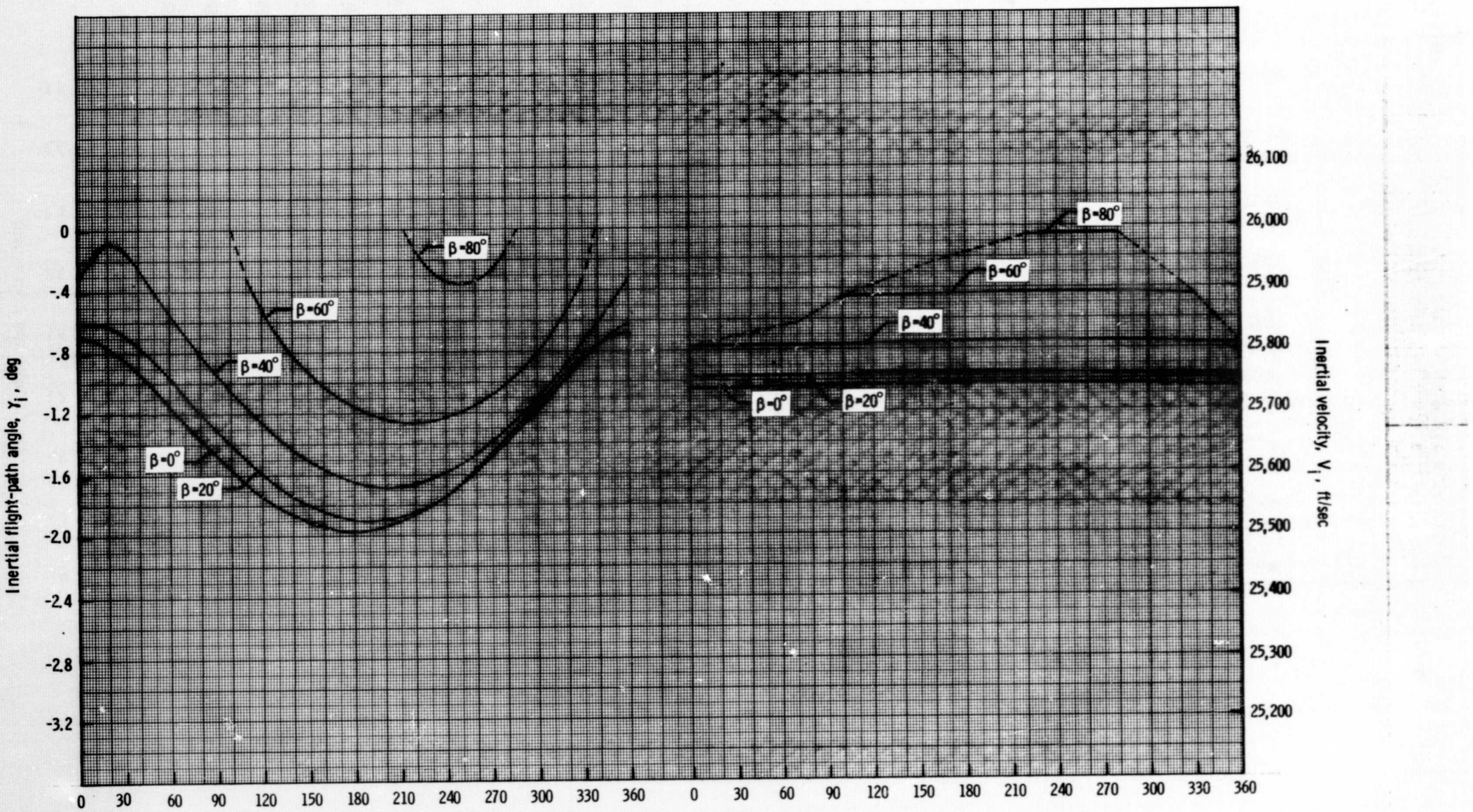

(b) ΔV = 300 fps

Figure 21. - Continued.

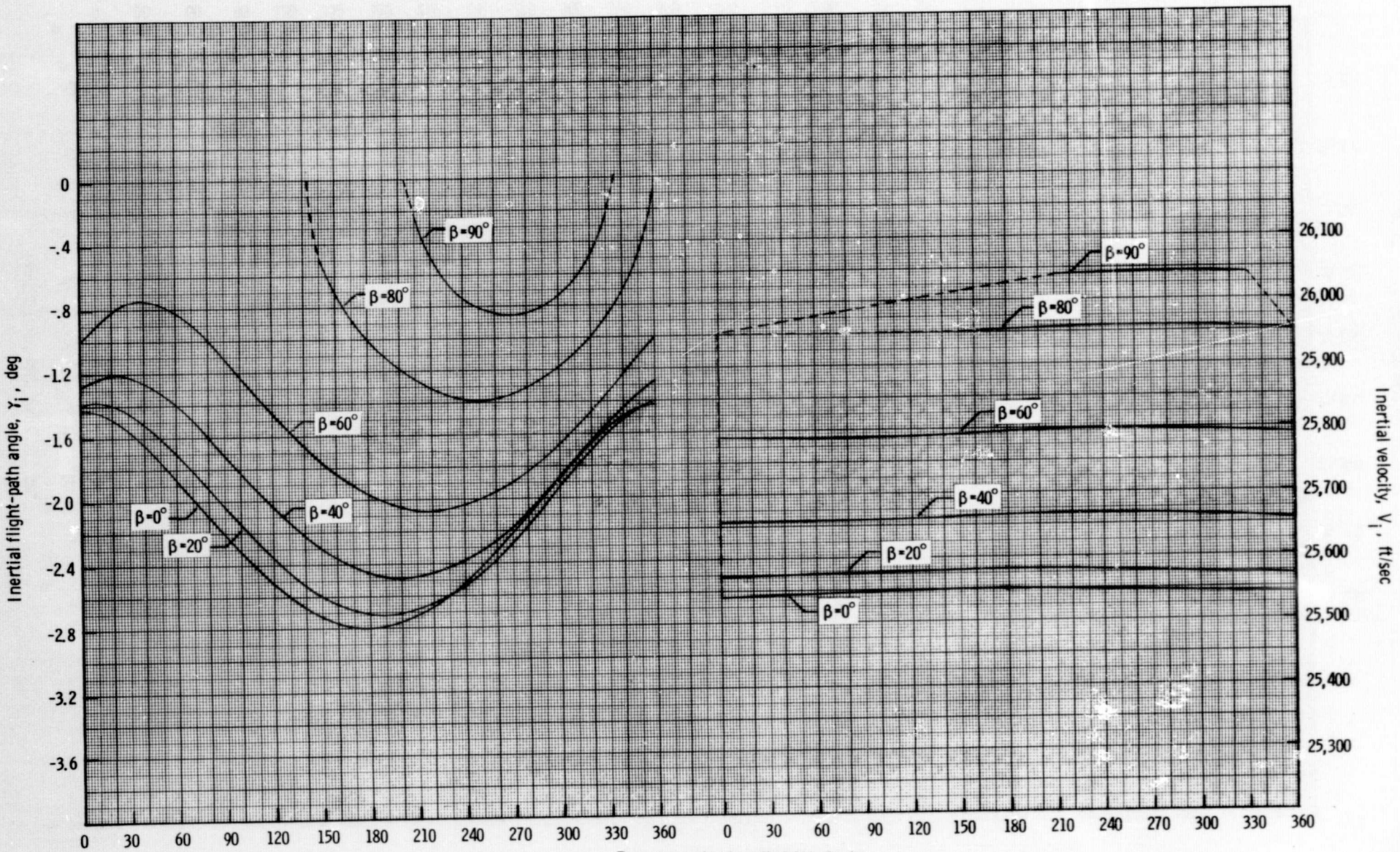

(c) ΔV = 500 fps

Figure 21. - Continued.

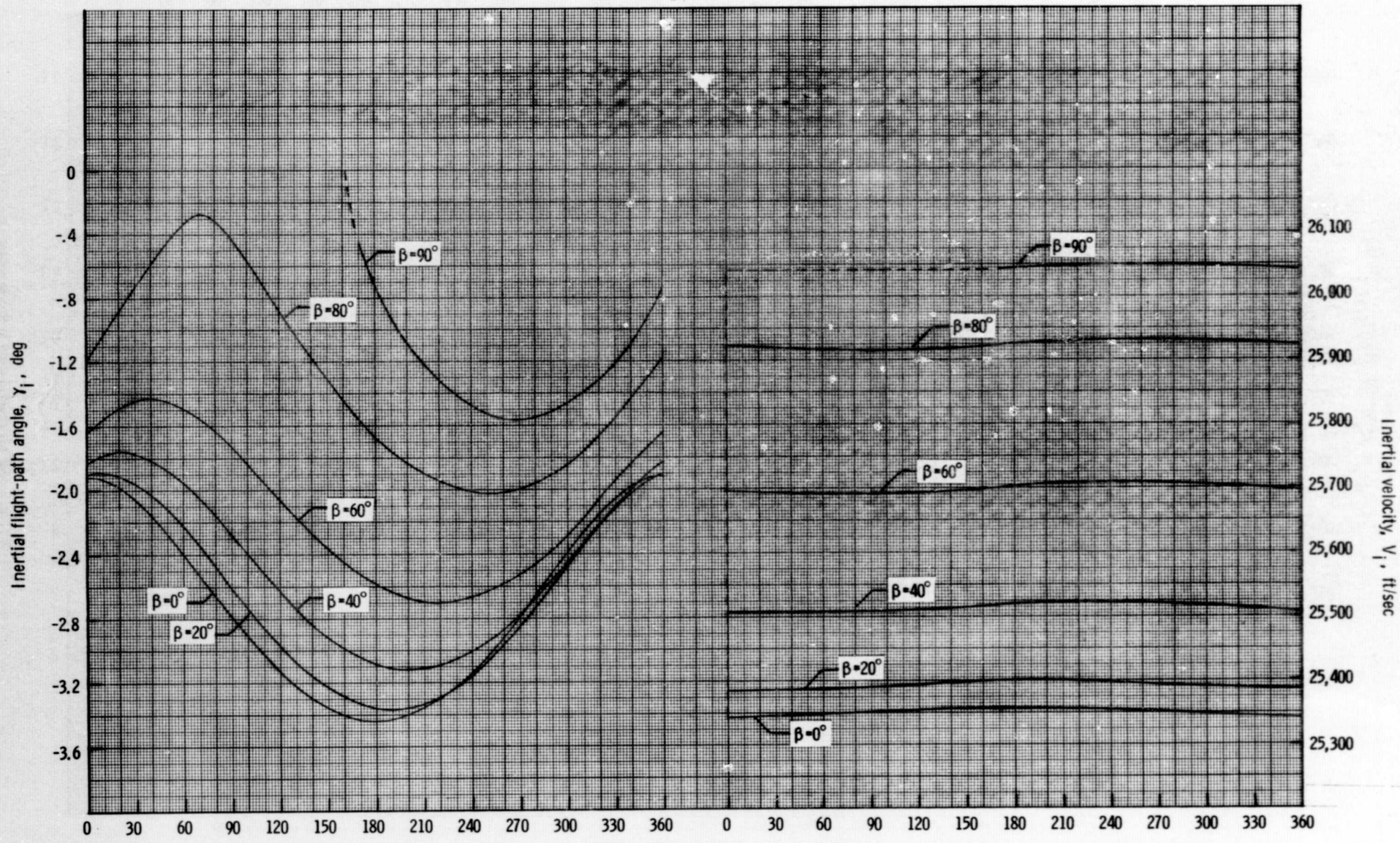

(d) ΔV = 700 fps

Figure 21. - Concluded.

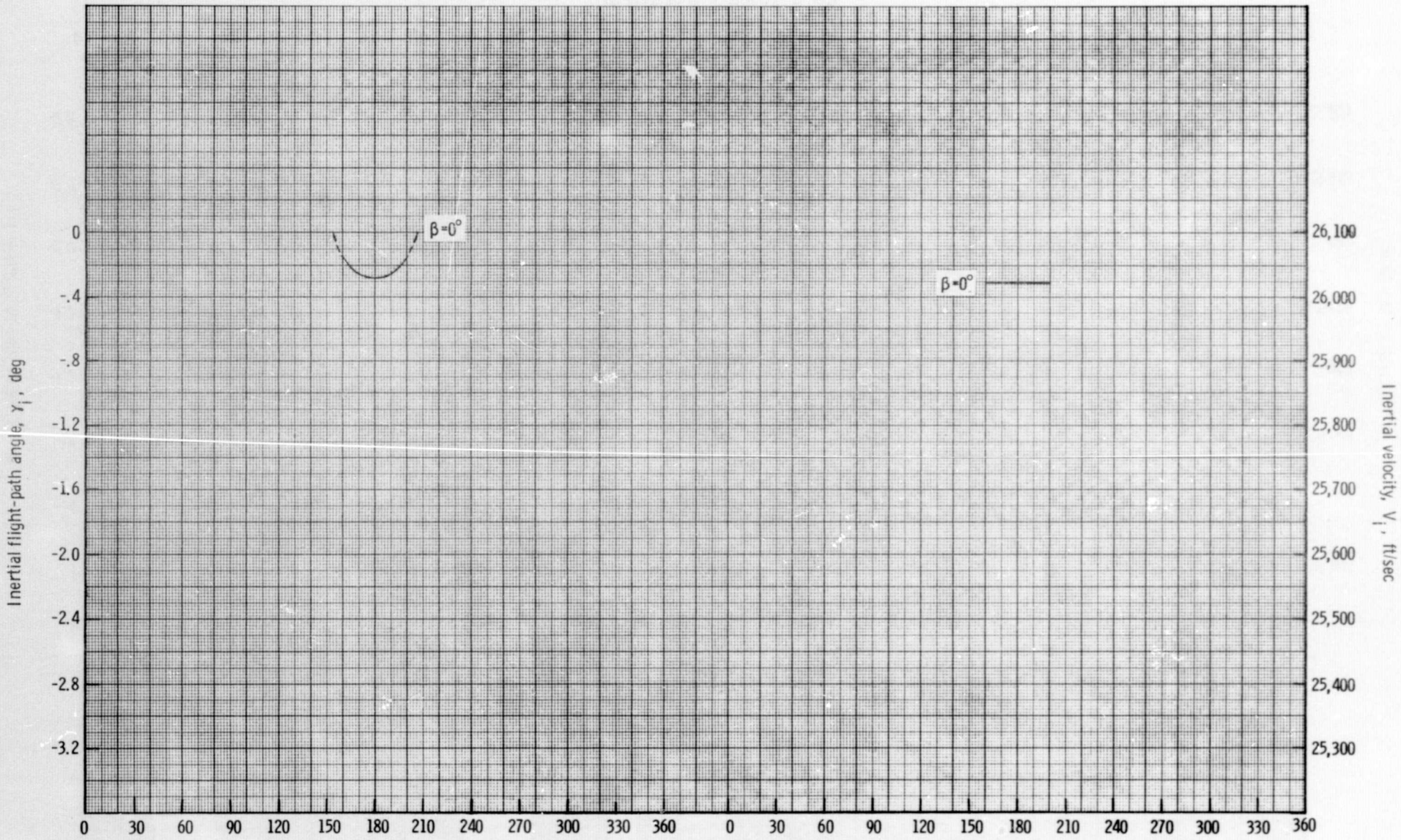

(a) ΔV = 100 fps

Figure 22. - Inertial flight-path angle and velocity at 400 000 feet as a function of retrograde true anomaly and a constant ΔV for an elliptical orbit where h_p = 120 nautical miles and h_a = 250 nautical miles.

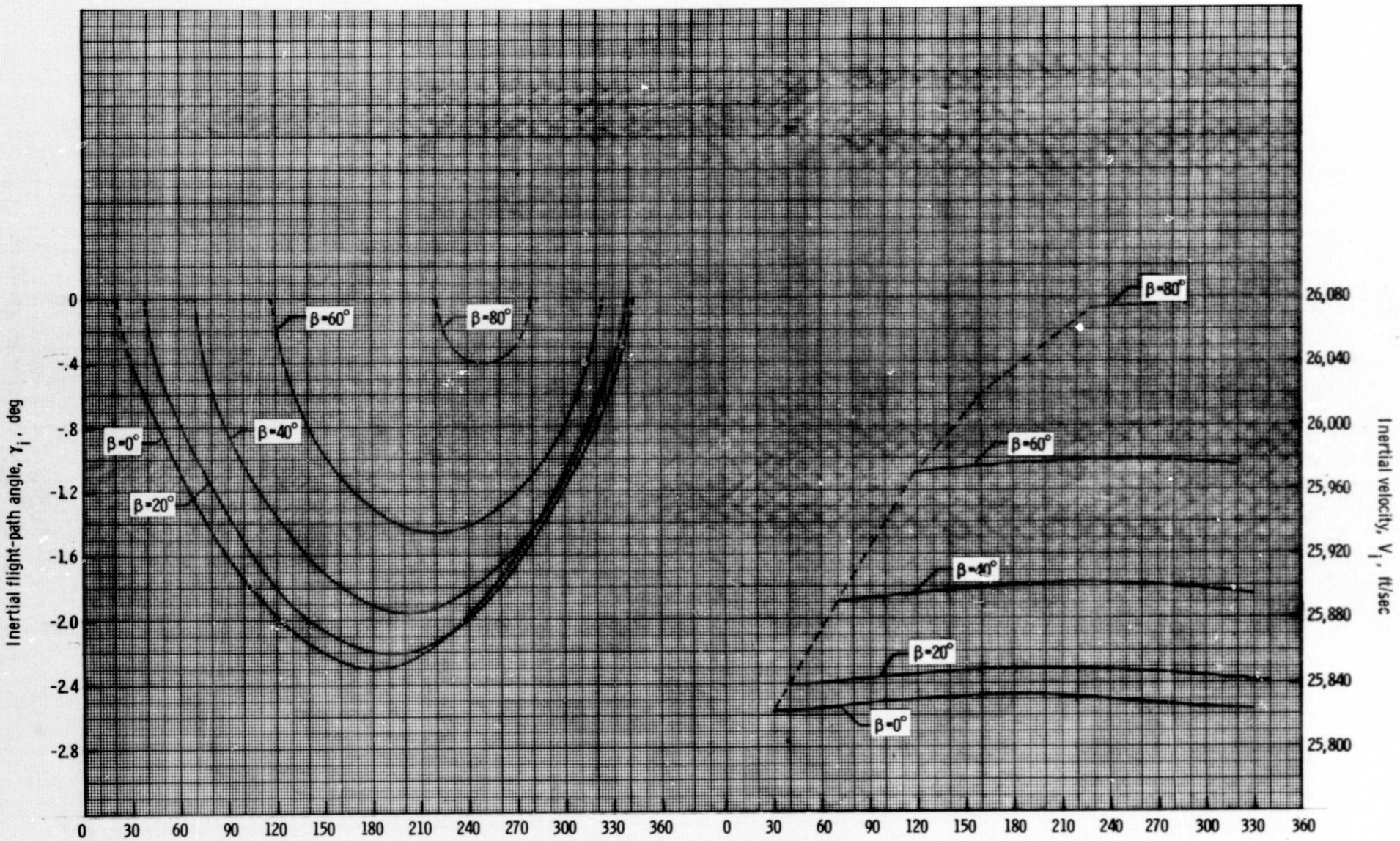

(b) ΔV = 300 fps

Figure 22. - Continued.

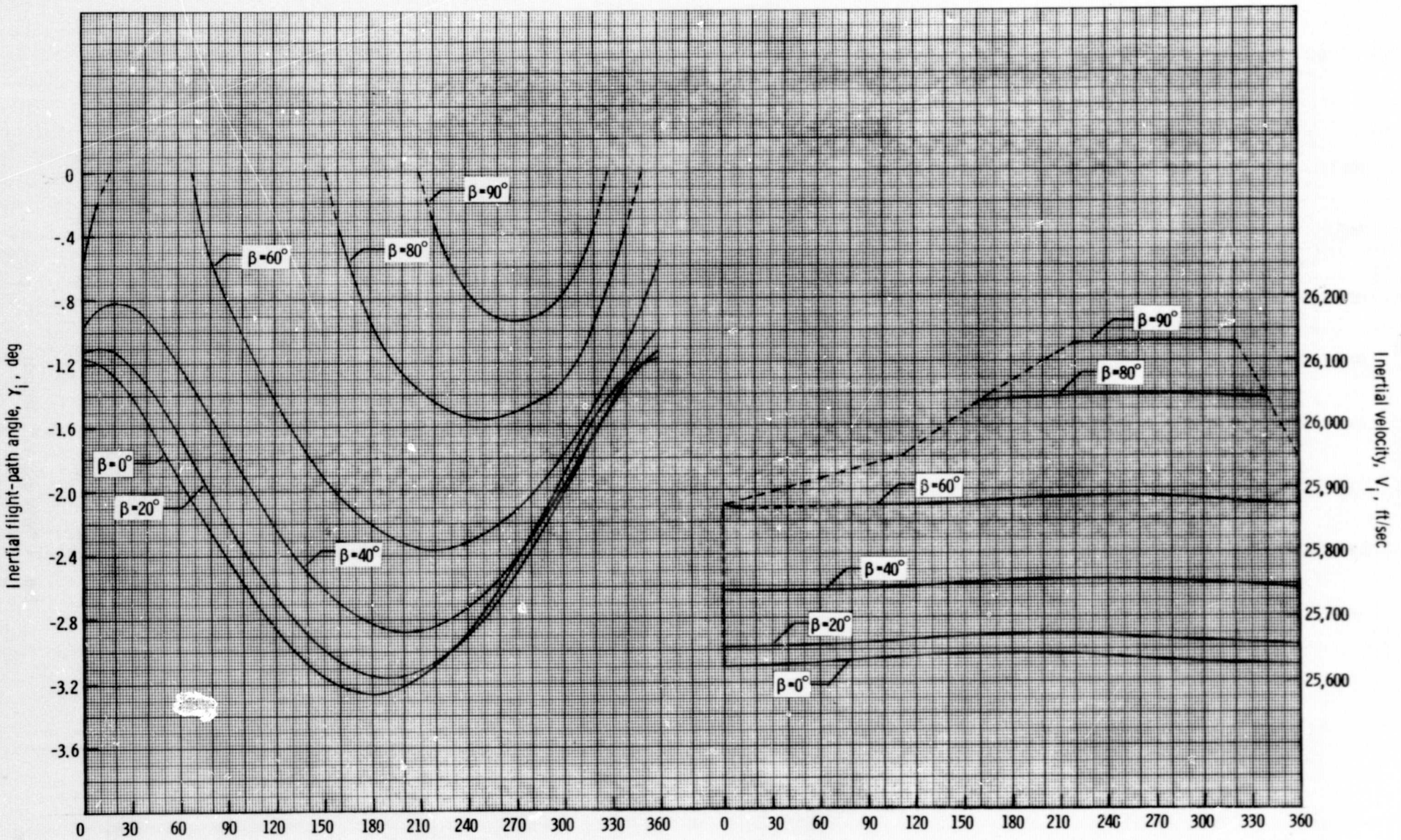

(c) ΔV = 500 fps

Figure 22. - Continued.

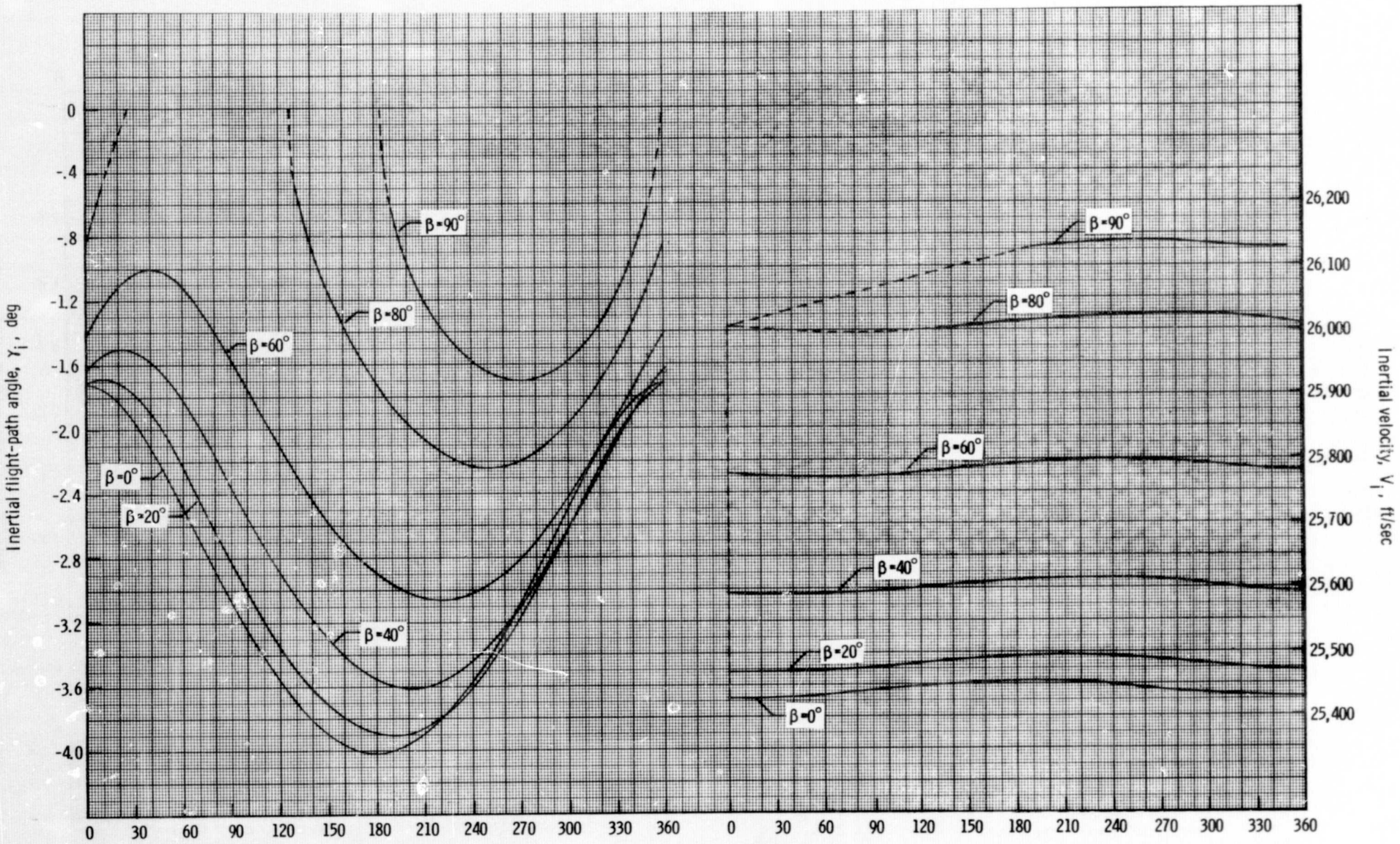

(d) ΔV = 700 fps

Figure 22. - Concluded.

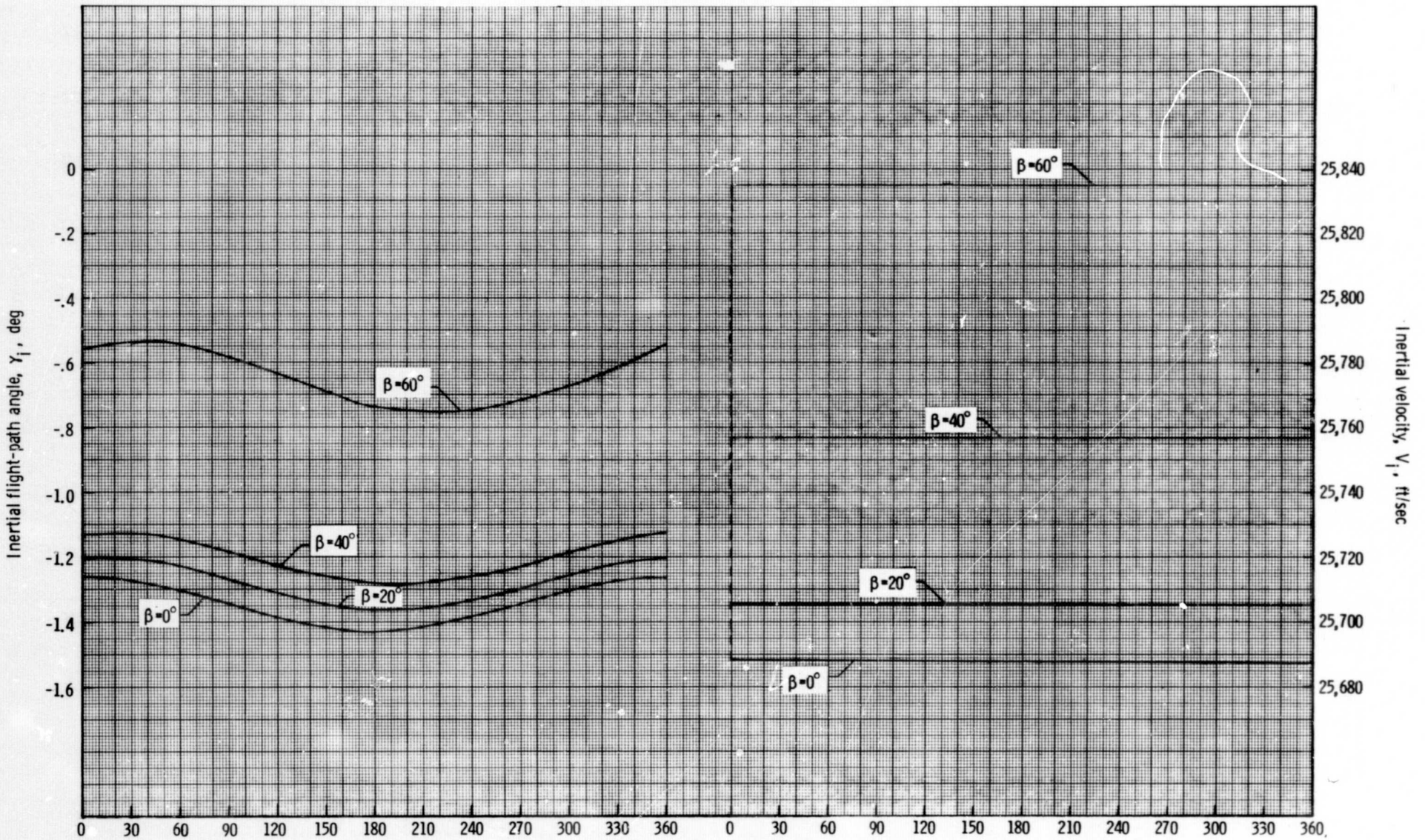

(a) ΔV = 300 fps

Figure 23. - Inertial flight-path angle and velocity at 400 000 feet as a function of retrograde true anomaly and a constant ΔV for an elliptical orbit where h_p = 140 nautical miles and h_a = 150 nautical miles.

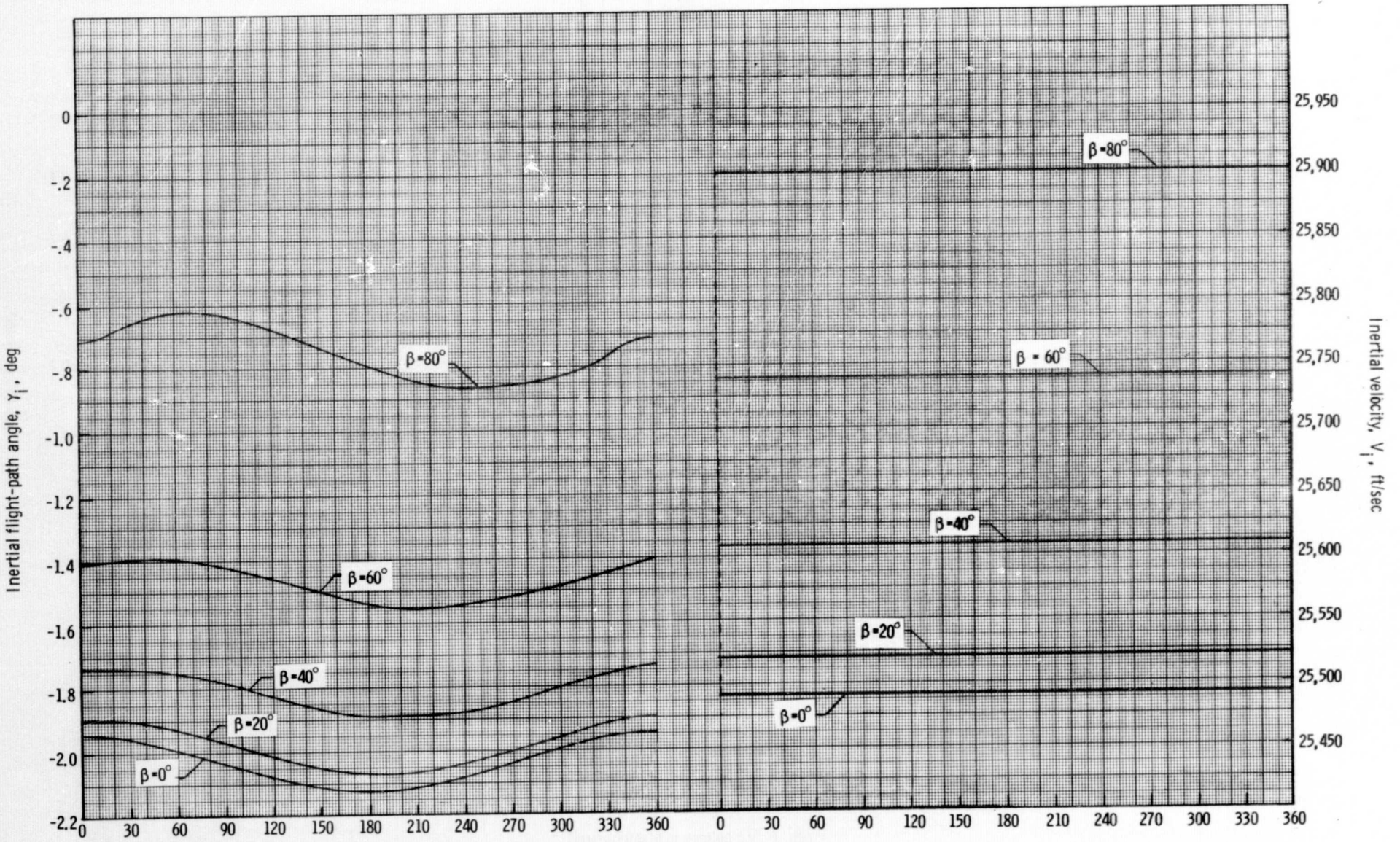

(b) ΔV = 500 fps

Figure 23. - Continued.

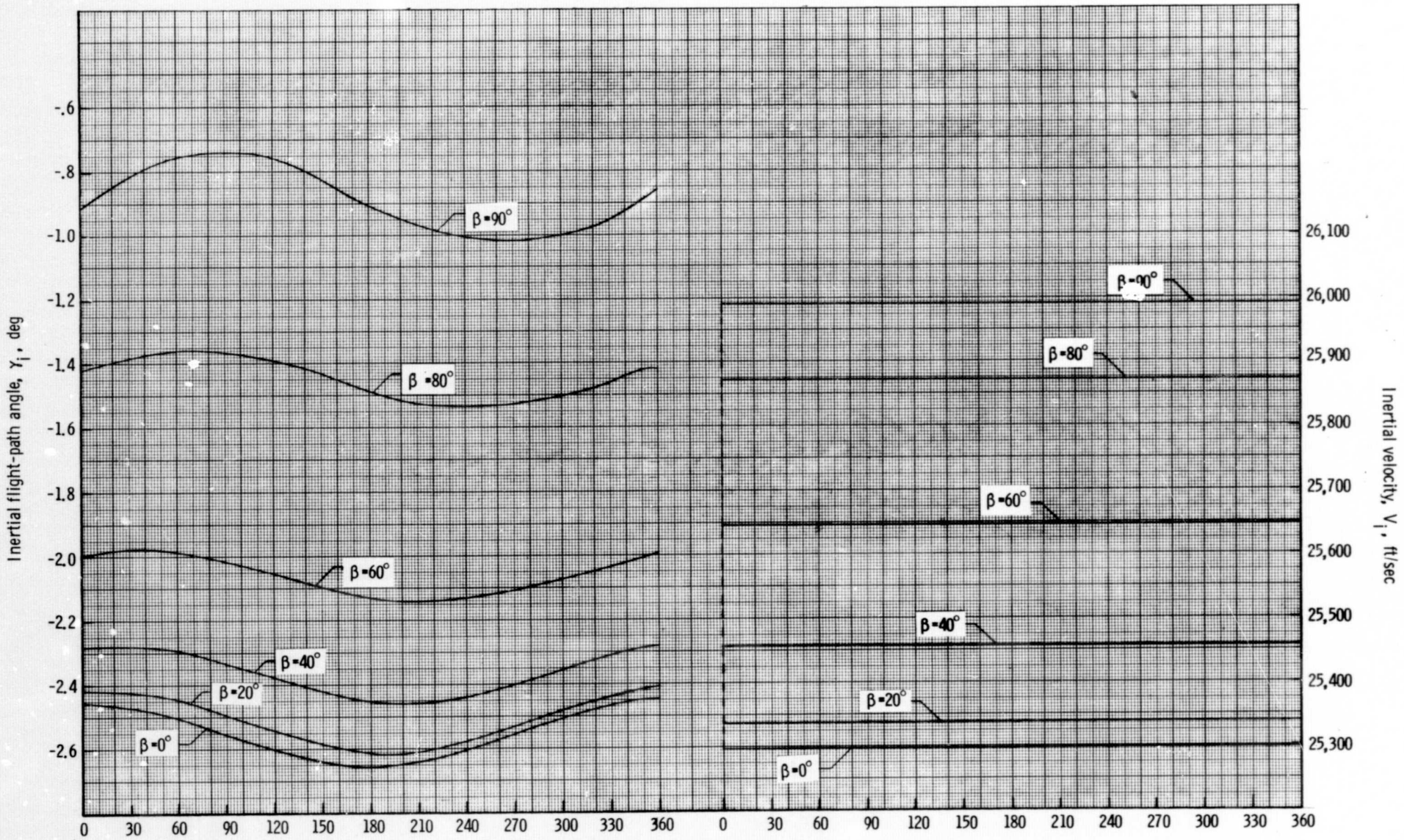

(c) ΔV = 700 fps

Figure 23. - Concluded.

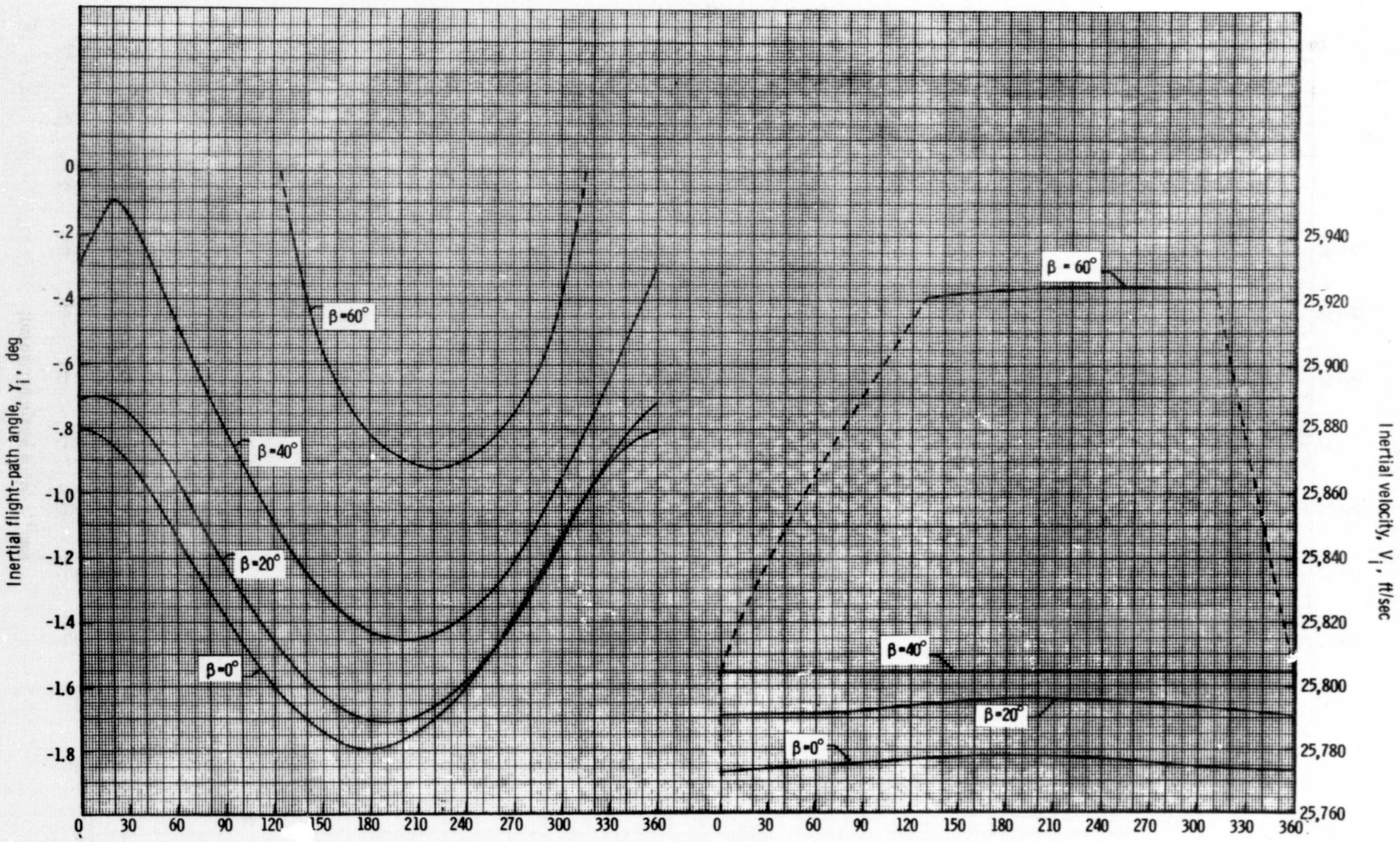

(a) ΔV = 300 fps

Figure 24. - Inertial flight-path angle and velocity at 400 000 feet as a function of retrograde true anomaly and a constant ΔV for an elliptical orbit where h_p = 140 nautical miles and h_a = 200 nautical miles.

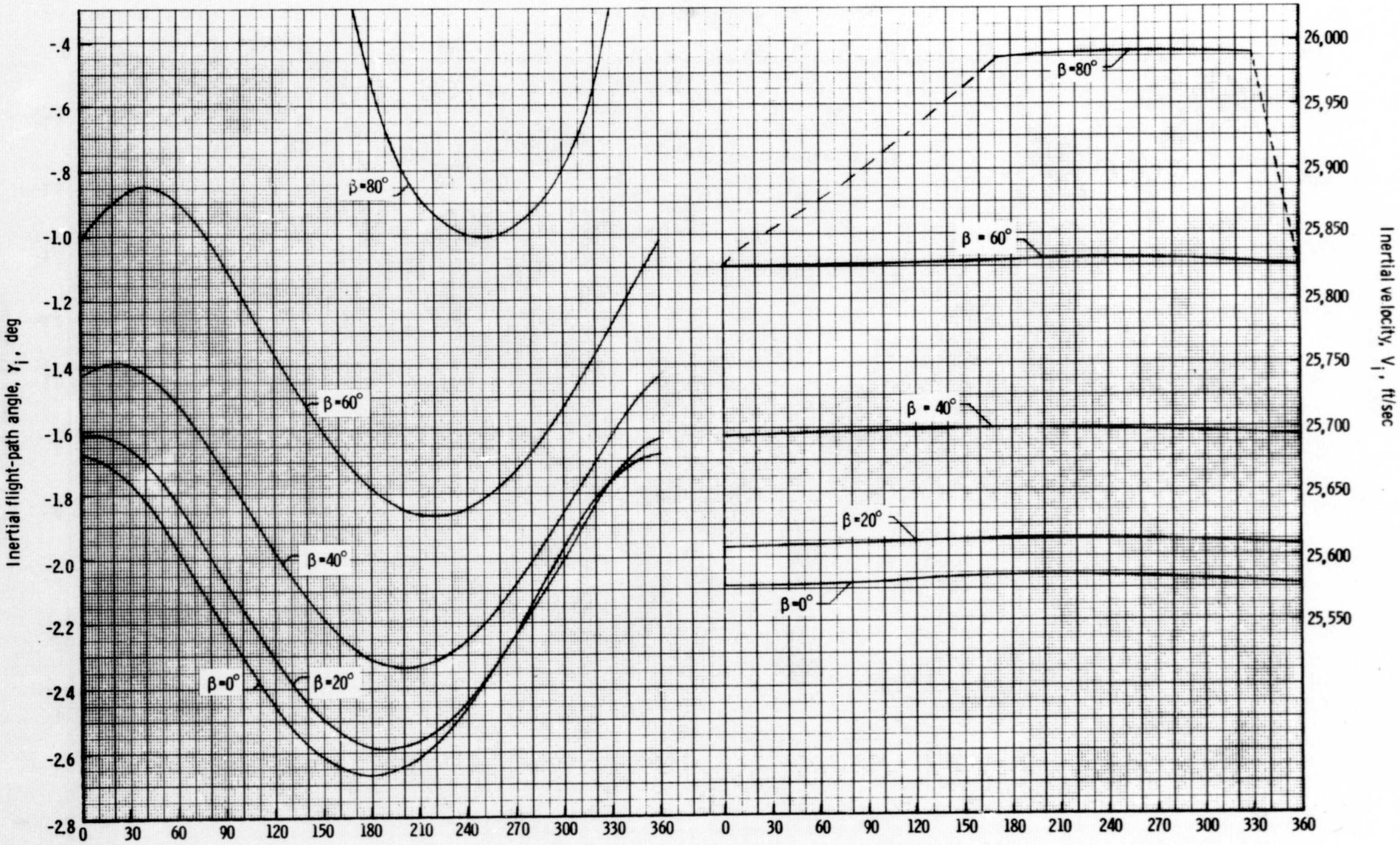

(b) ΔV = 500 fps

Figure 24. - Continued.

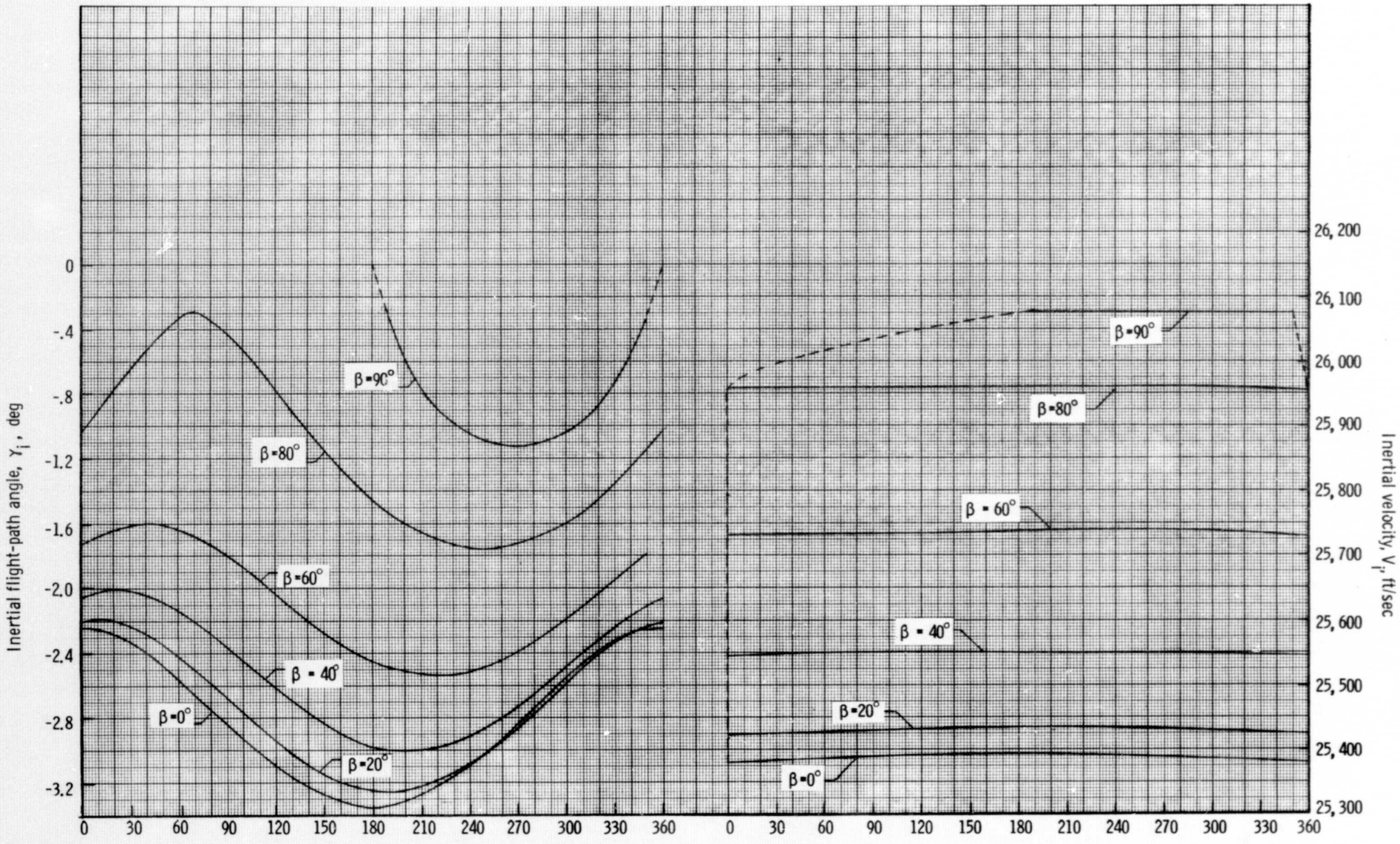

(c) ΔV = 700 fps

Figure 24. - Concluded.

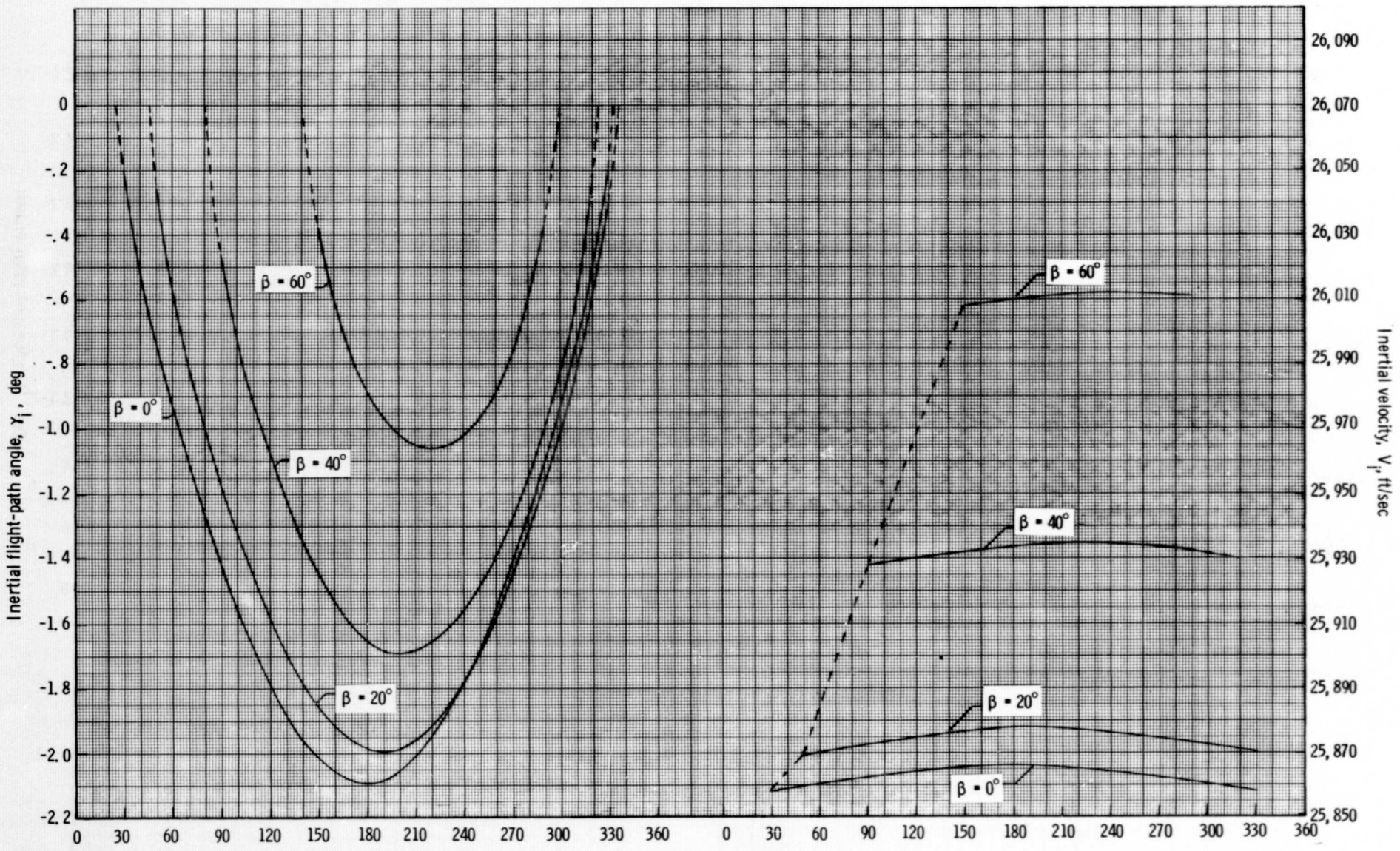

(a) ΔV = 300 fps

Figure 25. - Inertial flight-path angle and velocity at 400 000 feet as a function of retrograde true anomaly and a constant ΔV for an elliptical orbit where h_p = 140 nautical miles and h_a = 250 nautical miles.

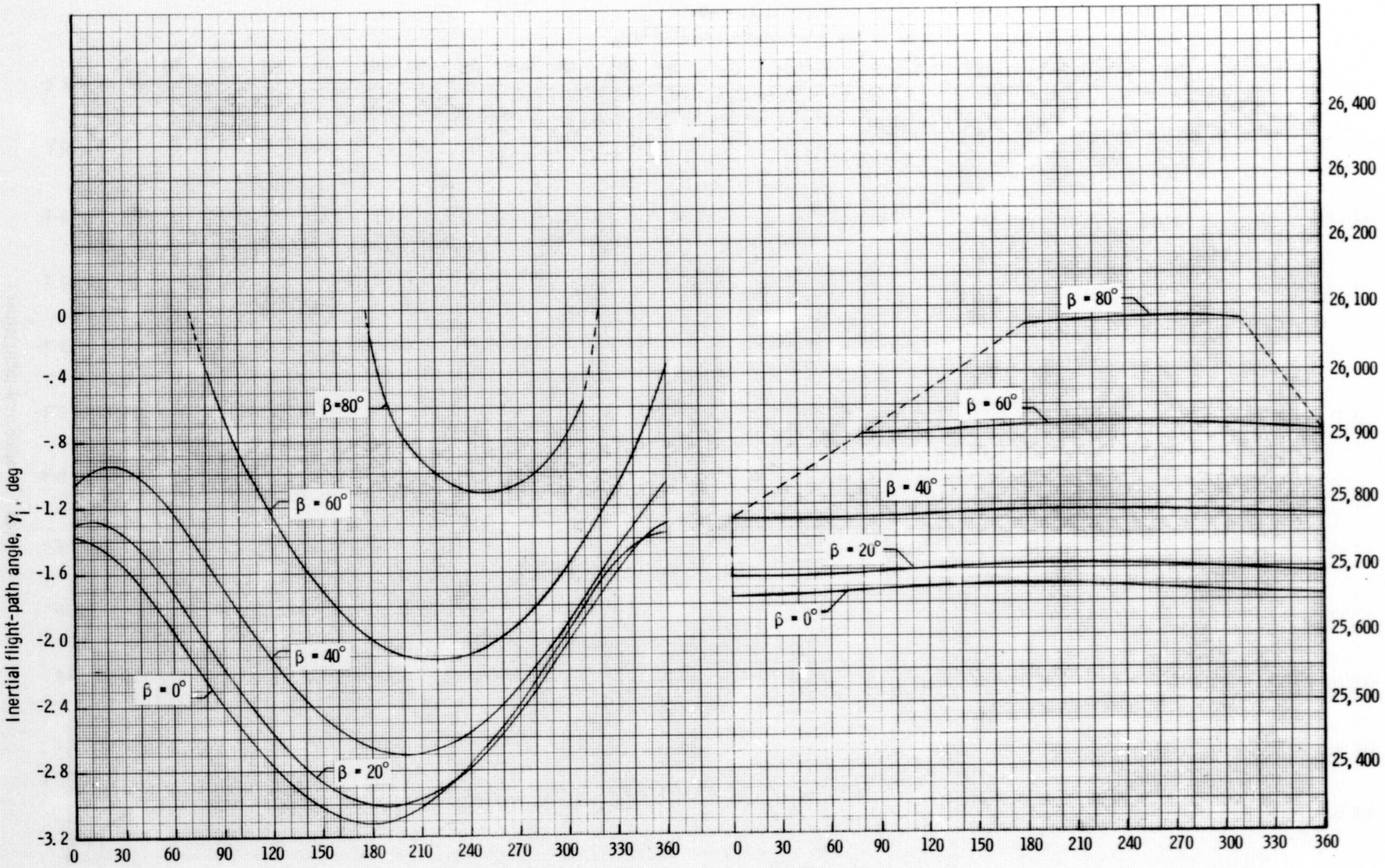

(b) ΔV = 500 fps

Figure 25. - Continued.

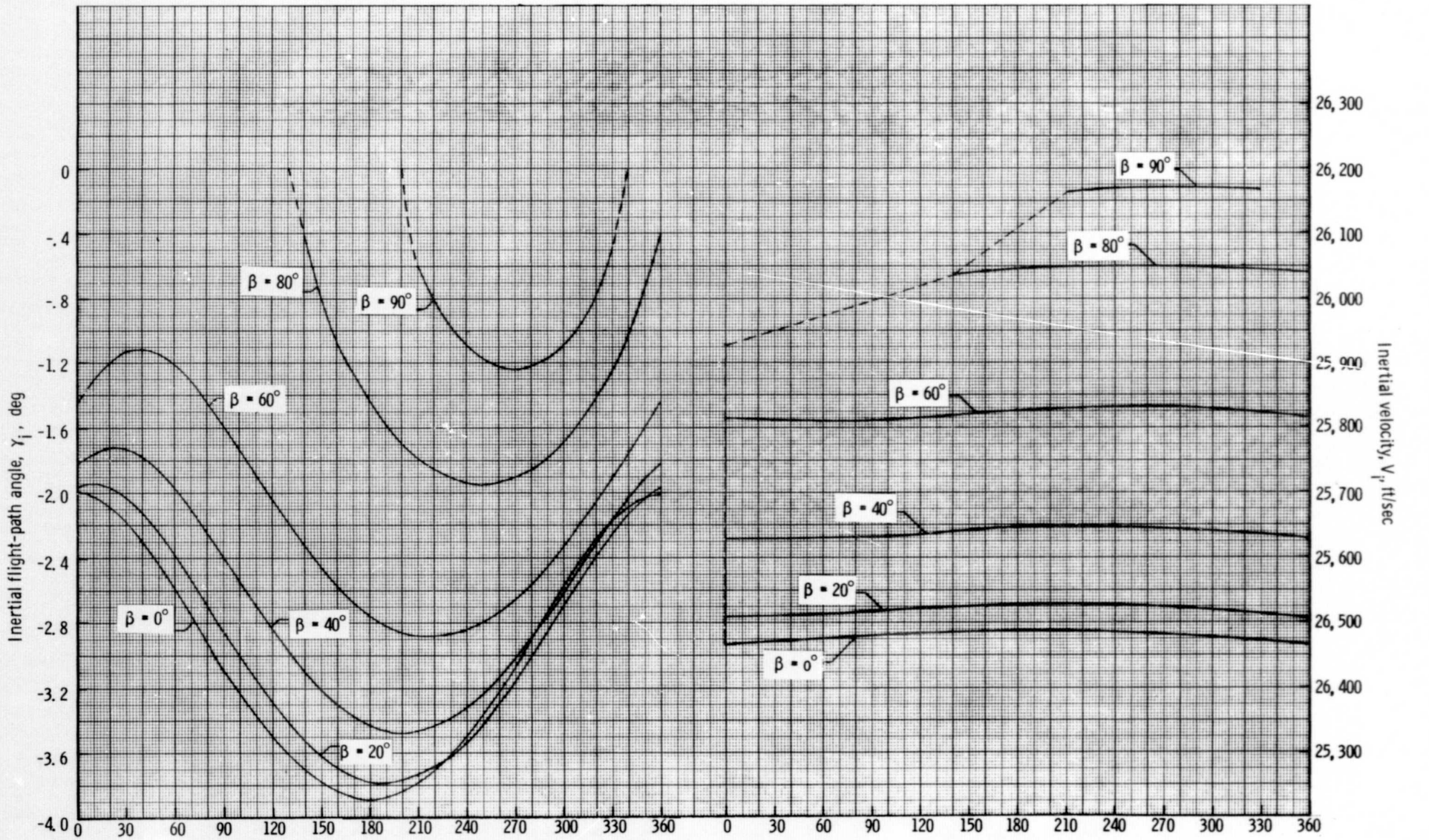

(c) ΔV = 700 fps

Figure 25. - Concluded.

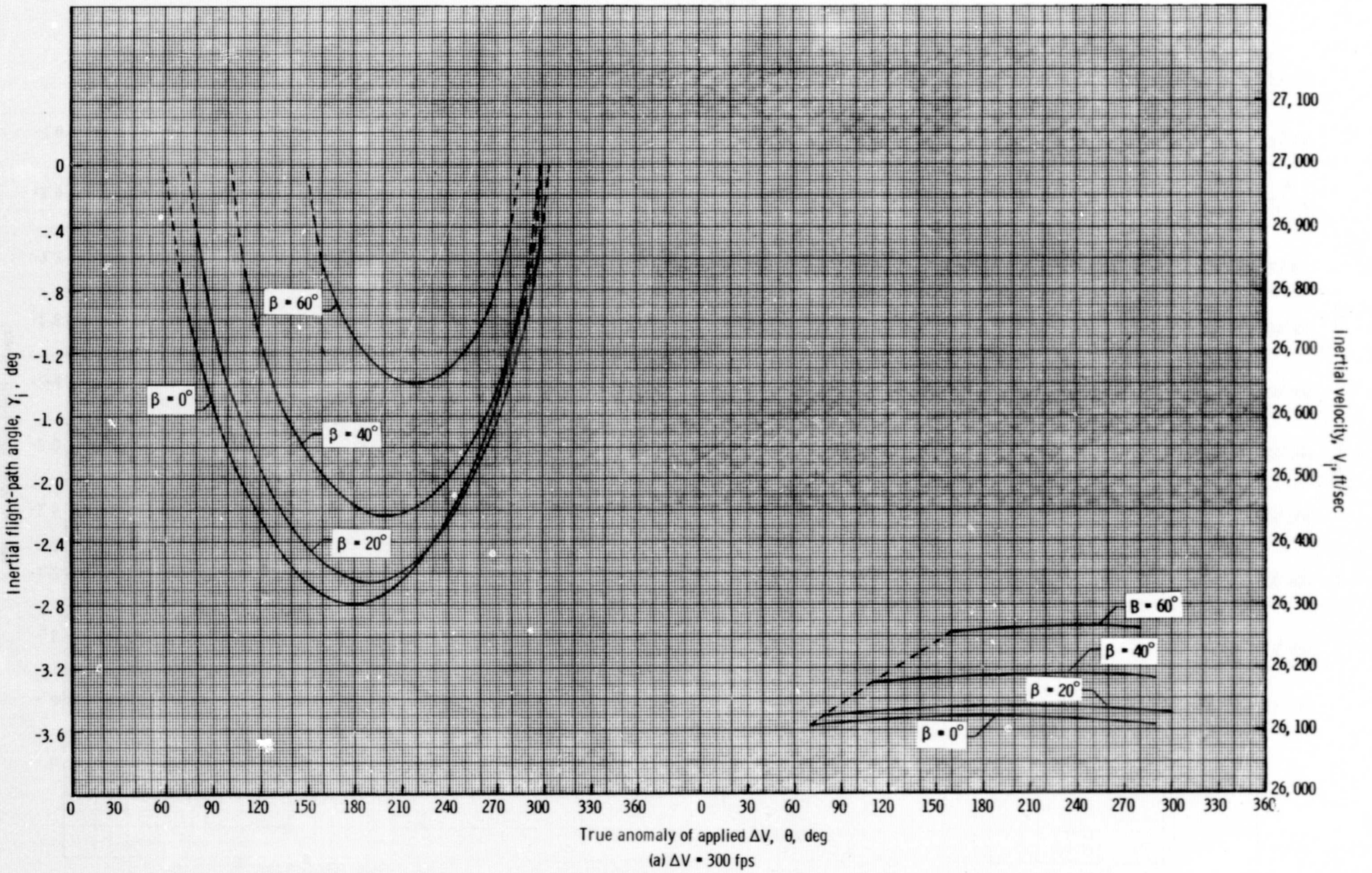

(a) ΔV = 300 fps

Figure 26. - Inertial flight-path angle and velocity at 400 000 feet as a function of retrograde true anomaly and a constant ΔV for an elliptical orbit where h_p = 140 nautical miles and h_a = 400 nautical miles.

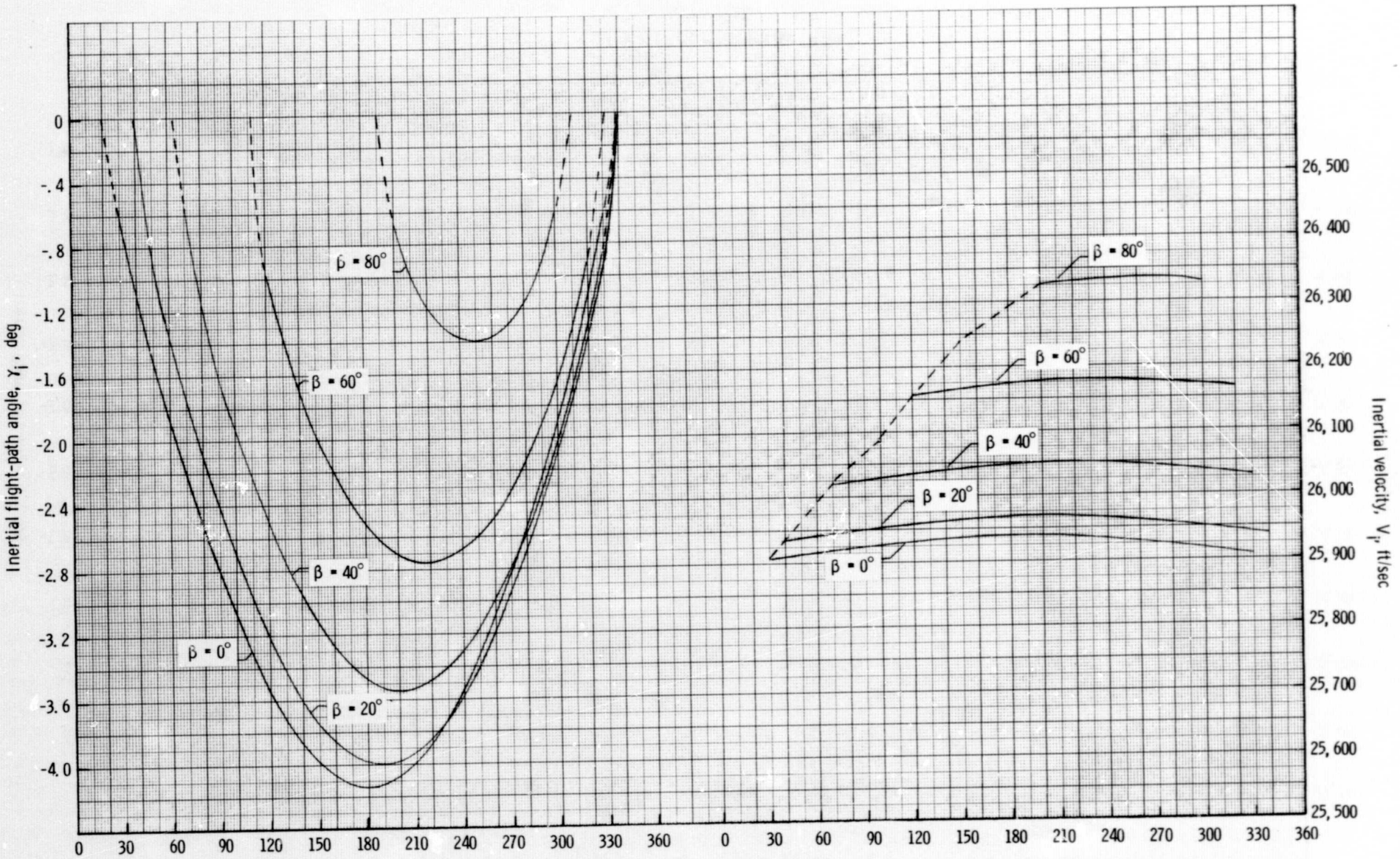

(b) ΔV = 500 fps

Figure 26. - Continued.

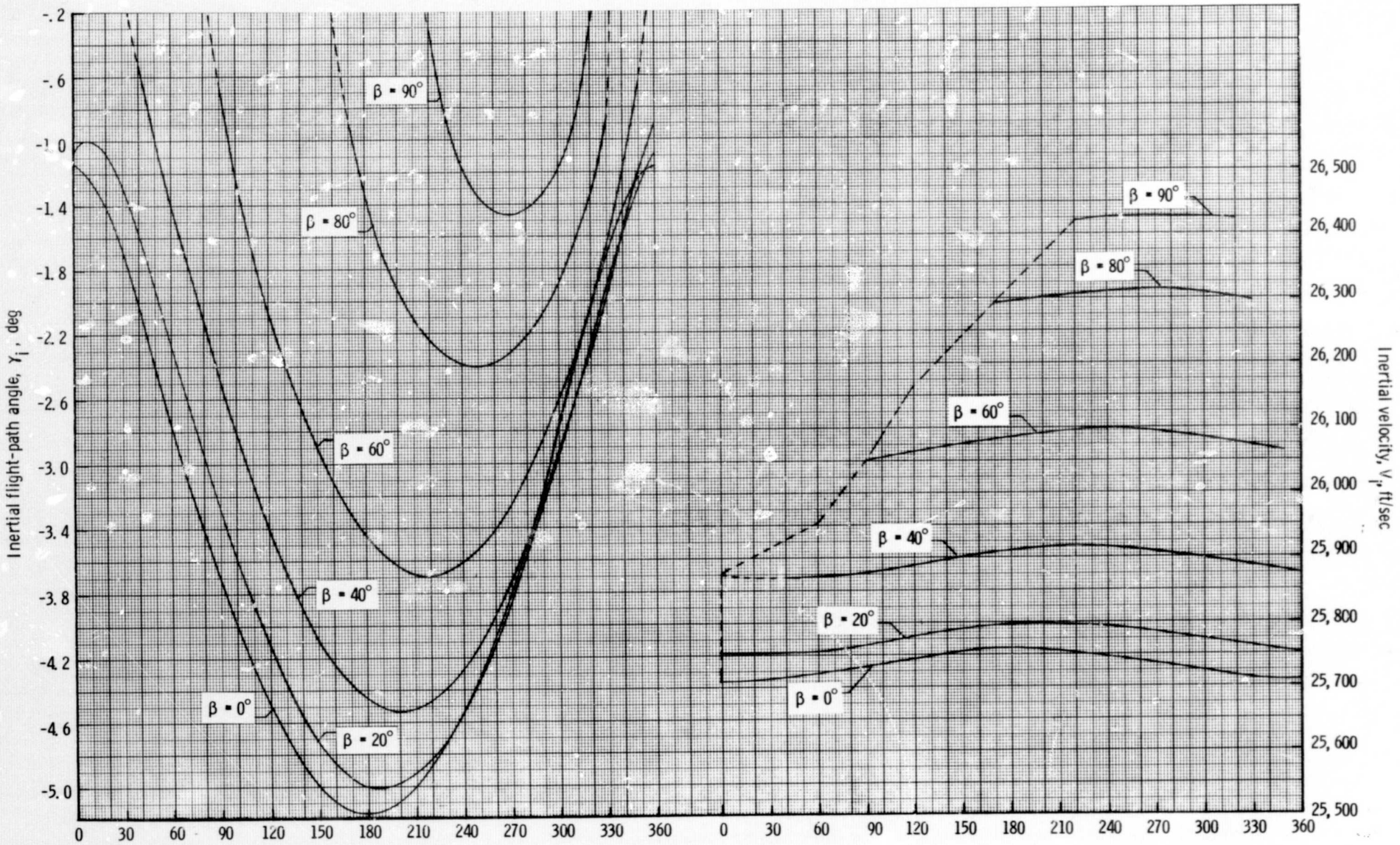

(c) ΔV = 700 fps

Figure 26. - Concluded.

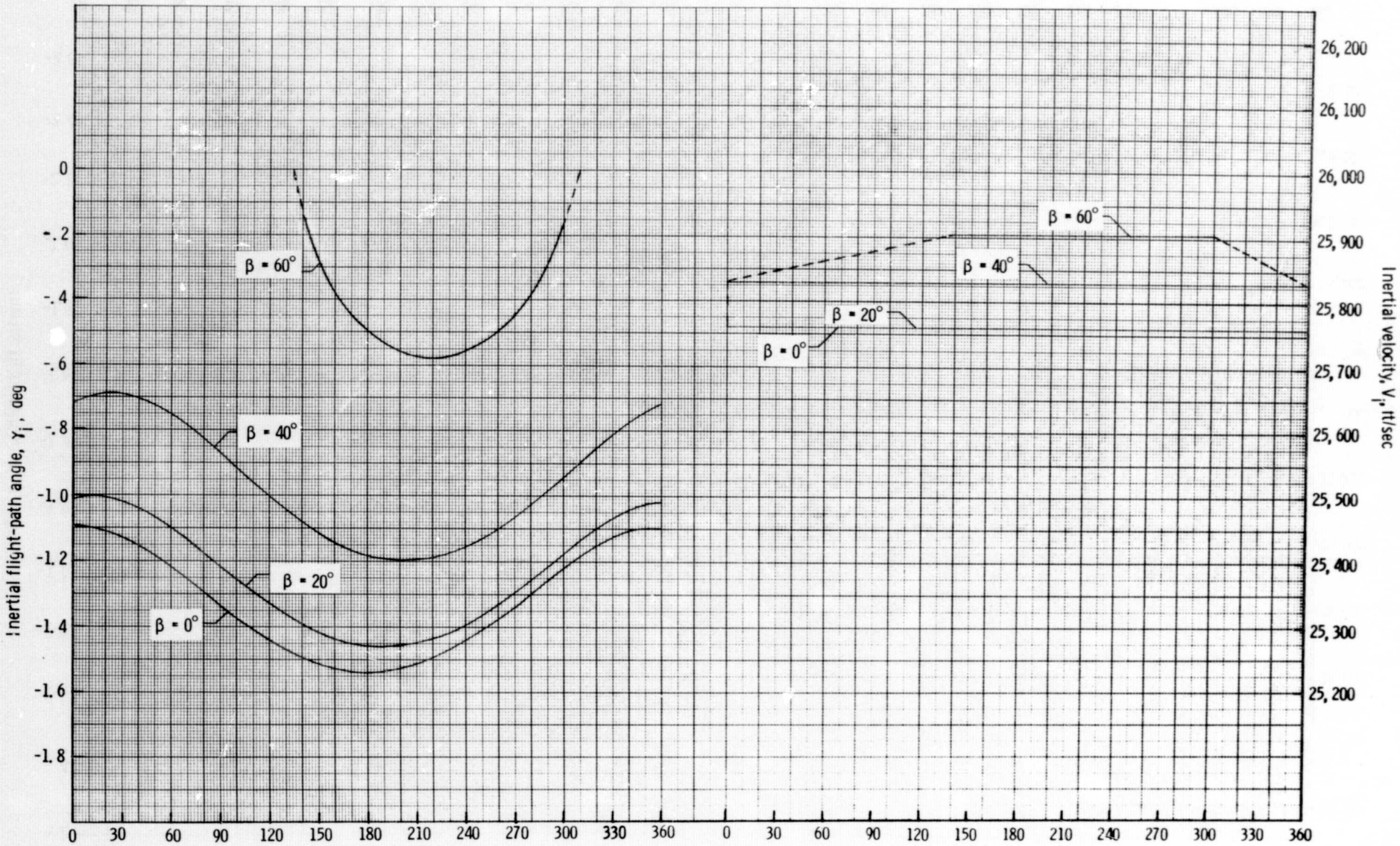

(a) ΔV = 300 fps

Figure 27. - Inertial flight-path angle and velocity at 400 000 feet as a function of retrograde true anomaly and a constant ΔV for an elliptical orbit where h_p = 153 nautical miles and h_a = 180 nautical miles.

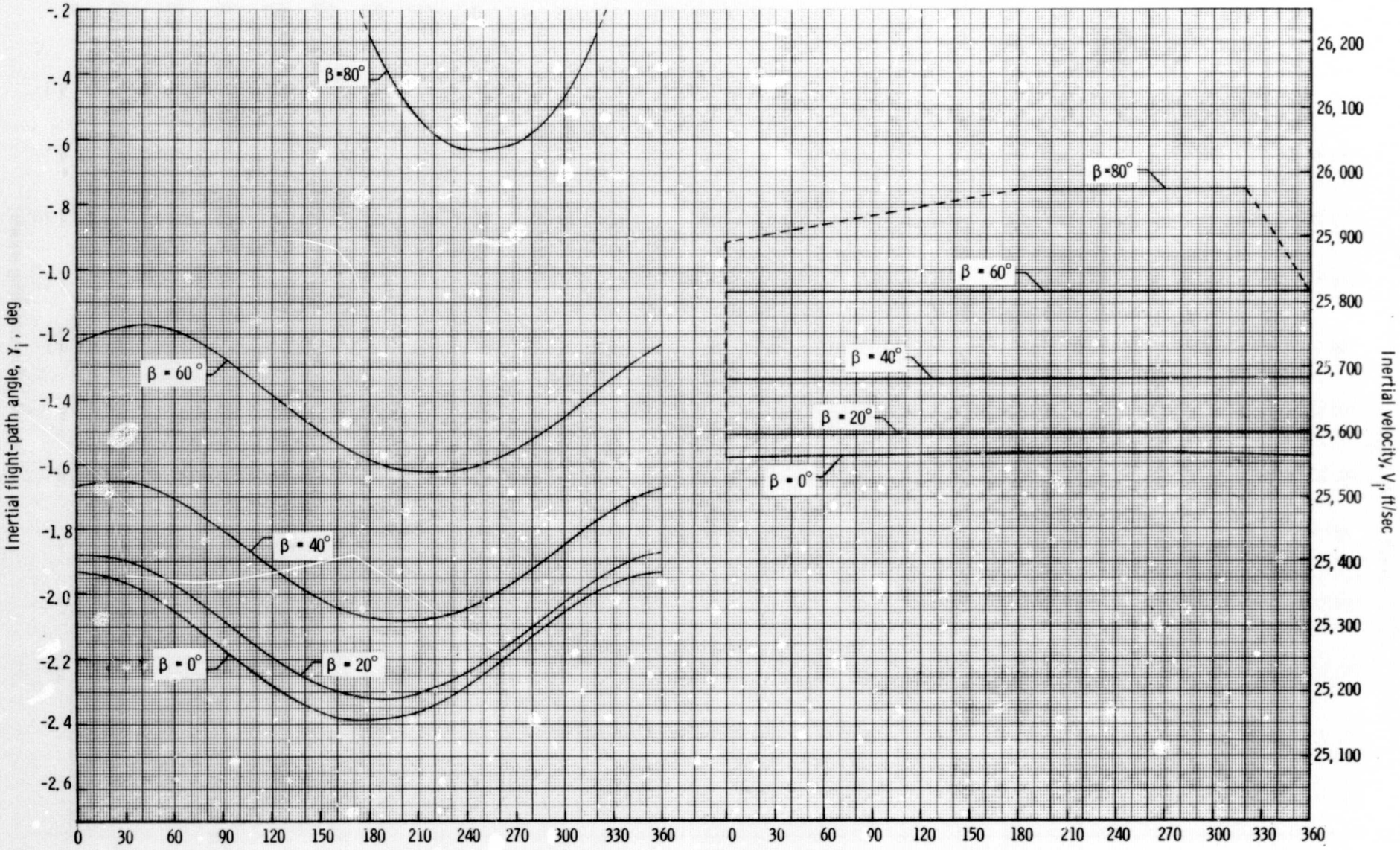

(b) ΔV = 500 fps

Figure 27. - Continued.

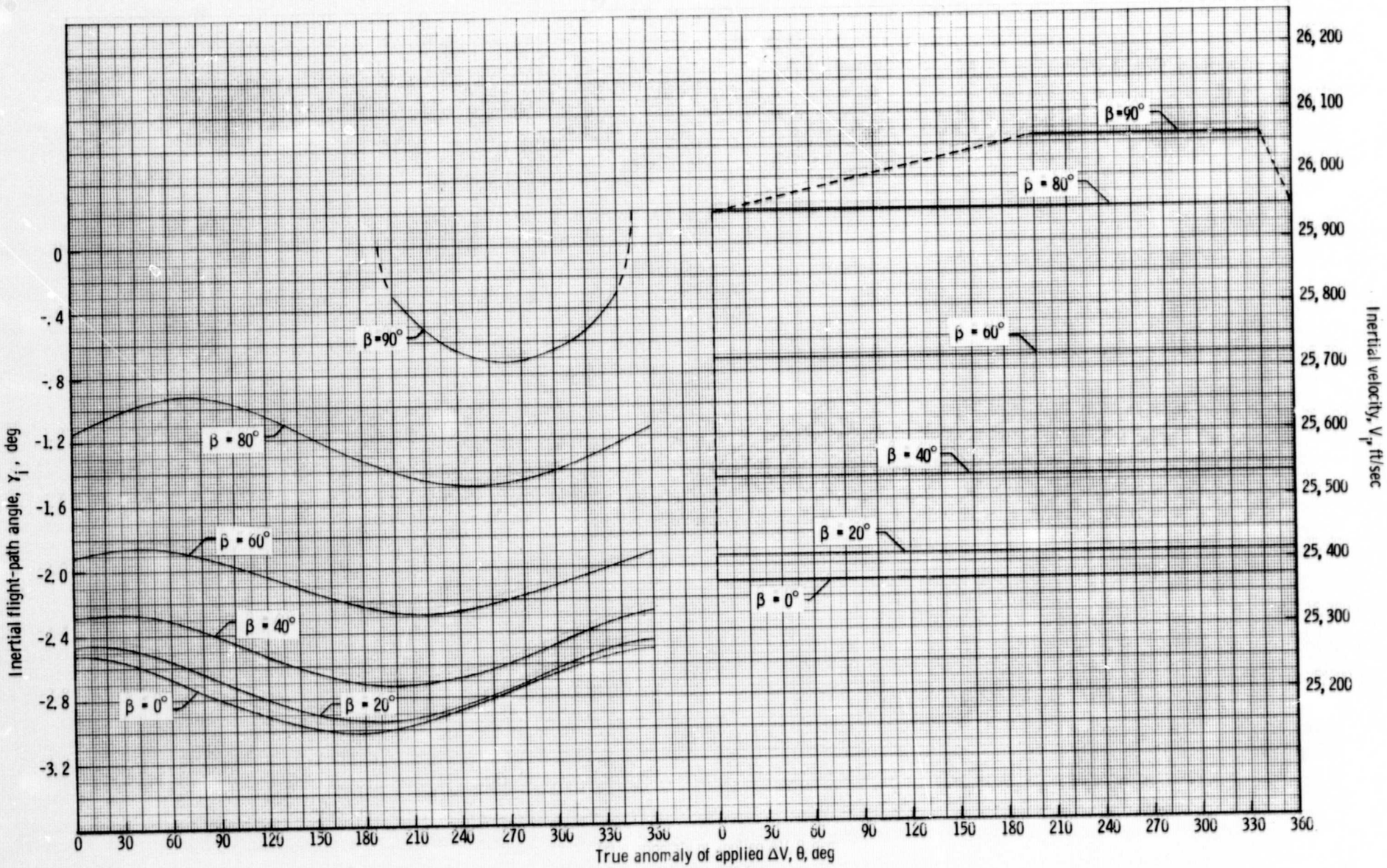

(c) ΔV = 700 fps

Figure 27. - Concluded.

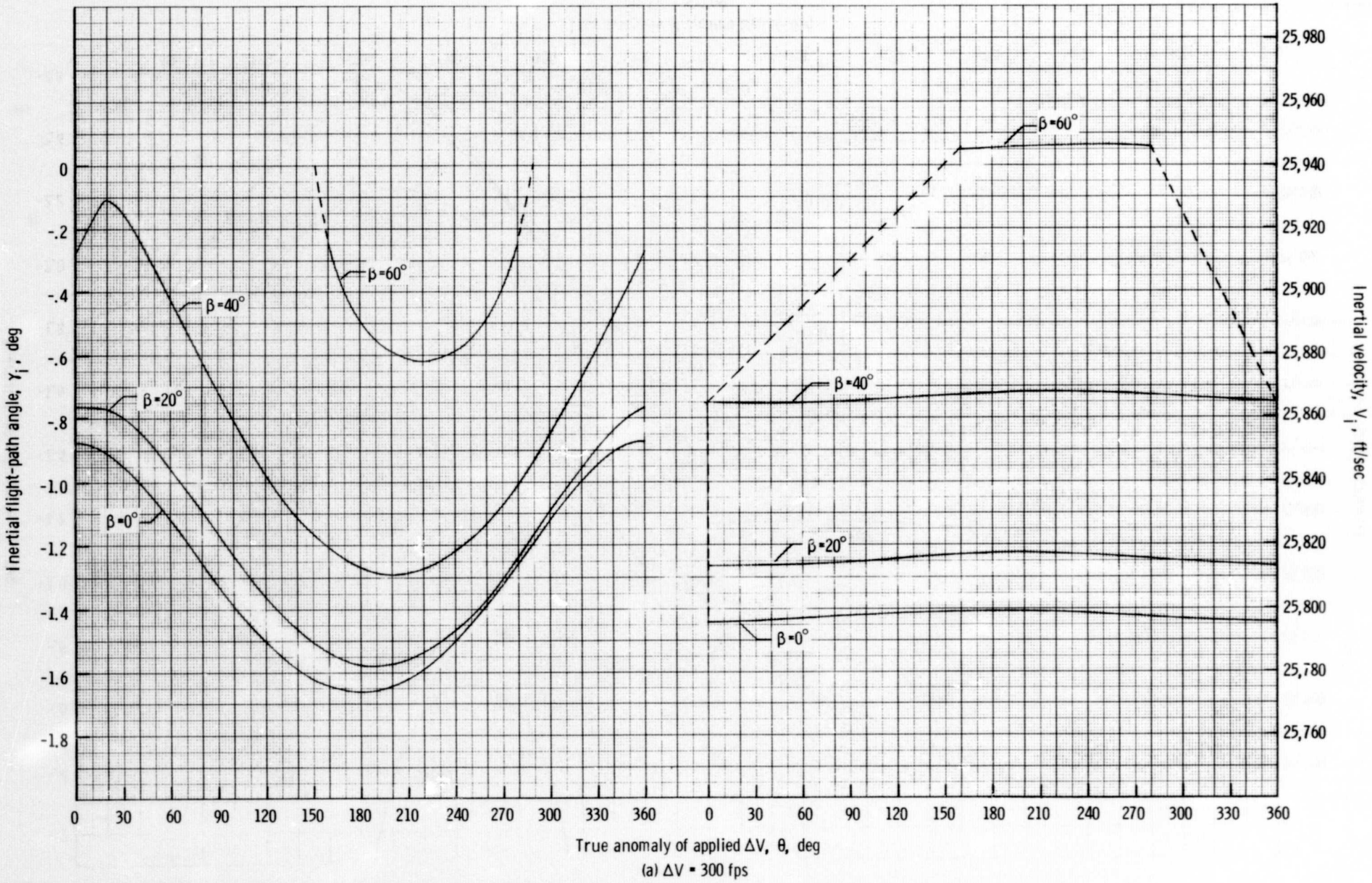

(a) ΔV = 300 fps

Figure 28. - Inertial flight-path angle and velocity at 400 000 feet as a function of retrograde true anomaly and a constant ΔV for an elliptical orbit where h_p = 153 nautical miles and h_a = 200 nautical miles.

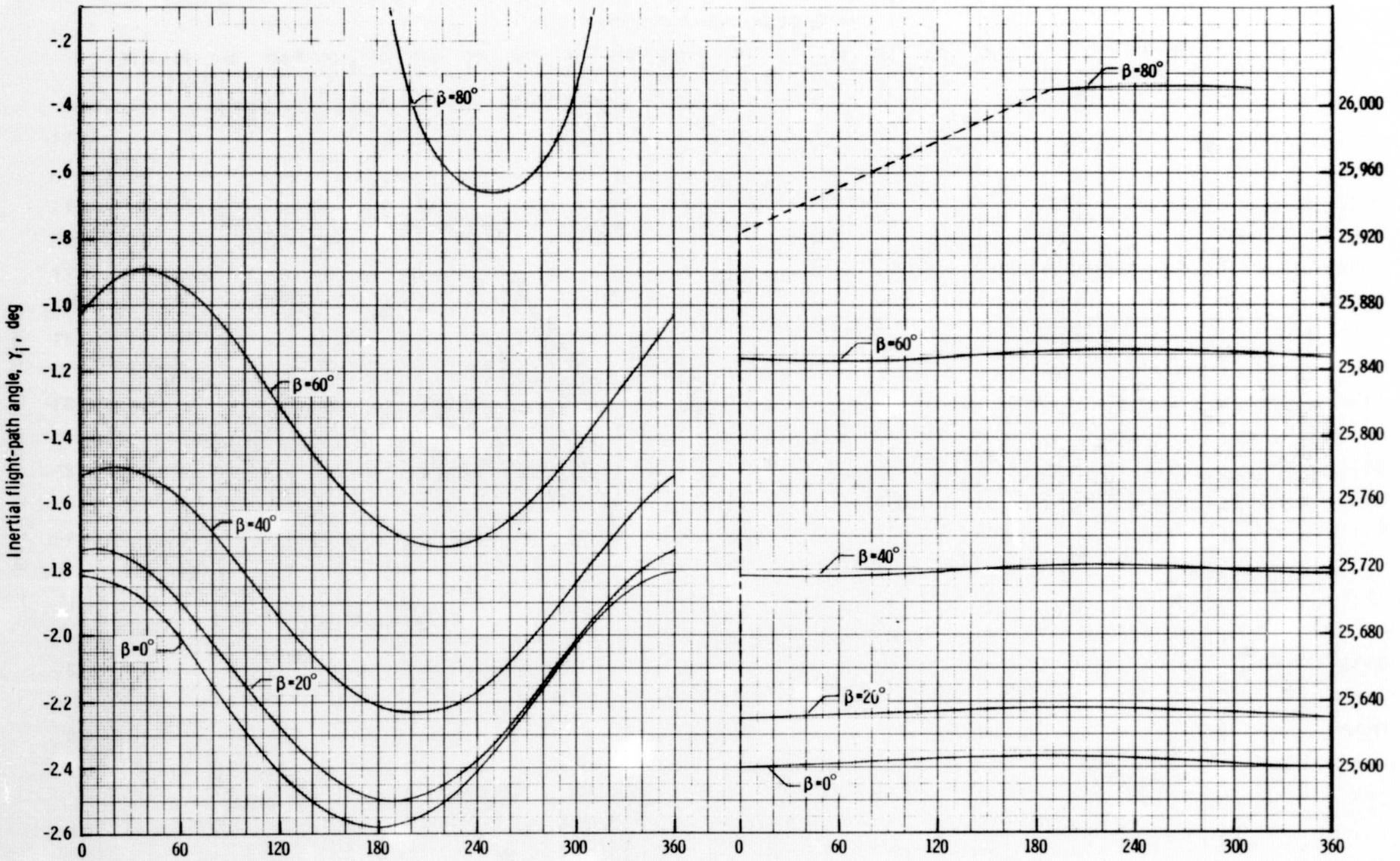

(b) ΔV = 500 fps

Figure 28. - Continued.

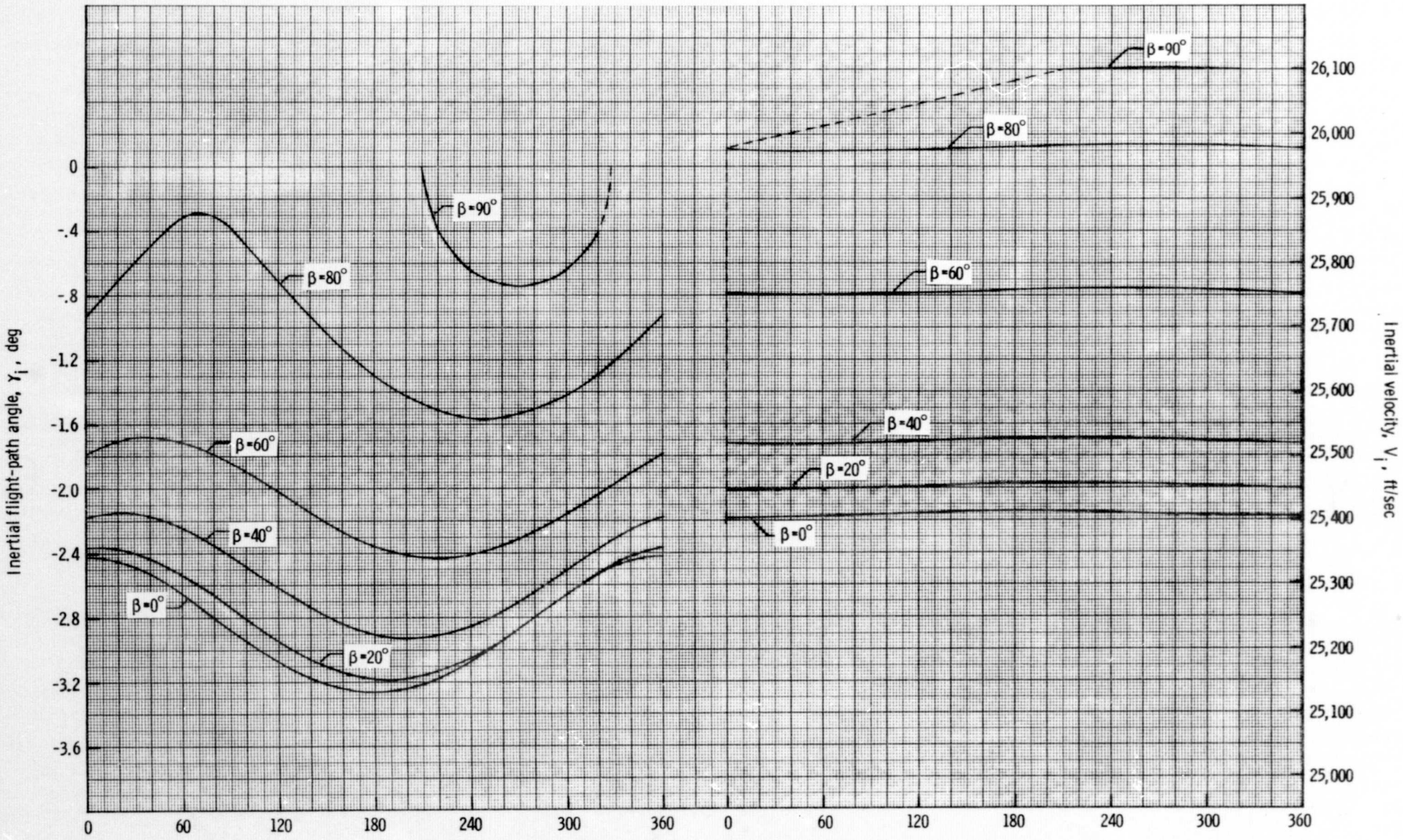

(c) ΔV = 700 fps

Figure 28. - Concluded.

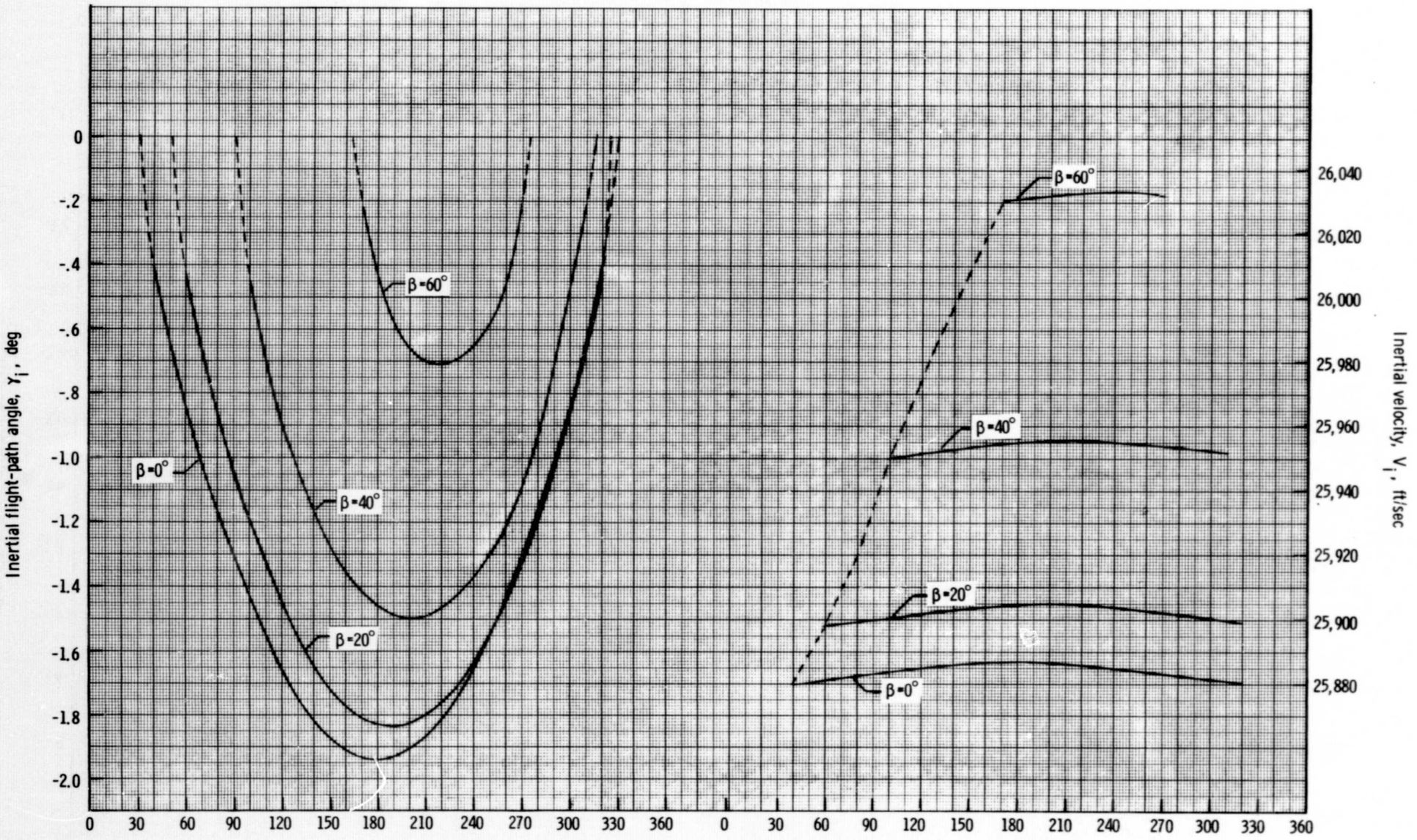

(a) ΔV = 300 fps

Figure 29. - Inertial flight-path angle and velocity at 400 000 feet as a function of retrograde true anomaly and a constant ΔV for an elliptical orbit where h_p = 153 nautical miles and h_a = 250 nautical miles.

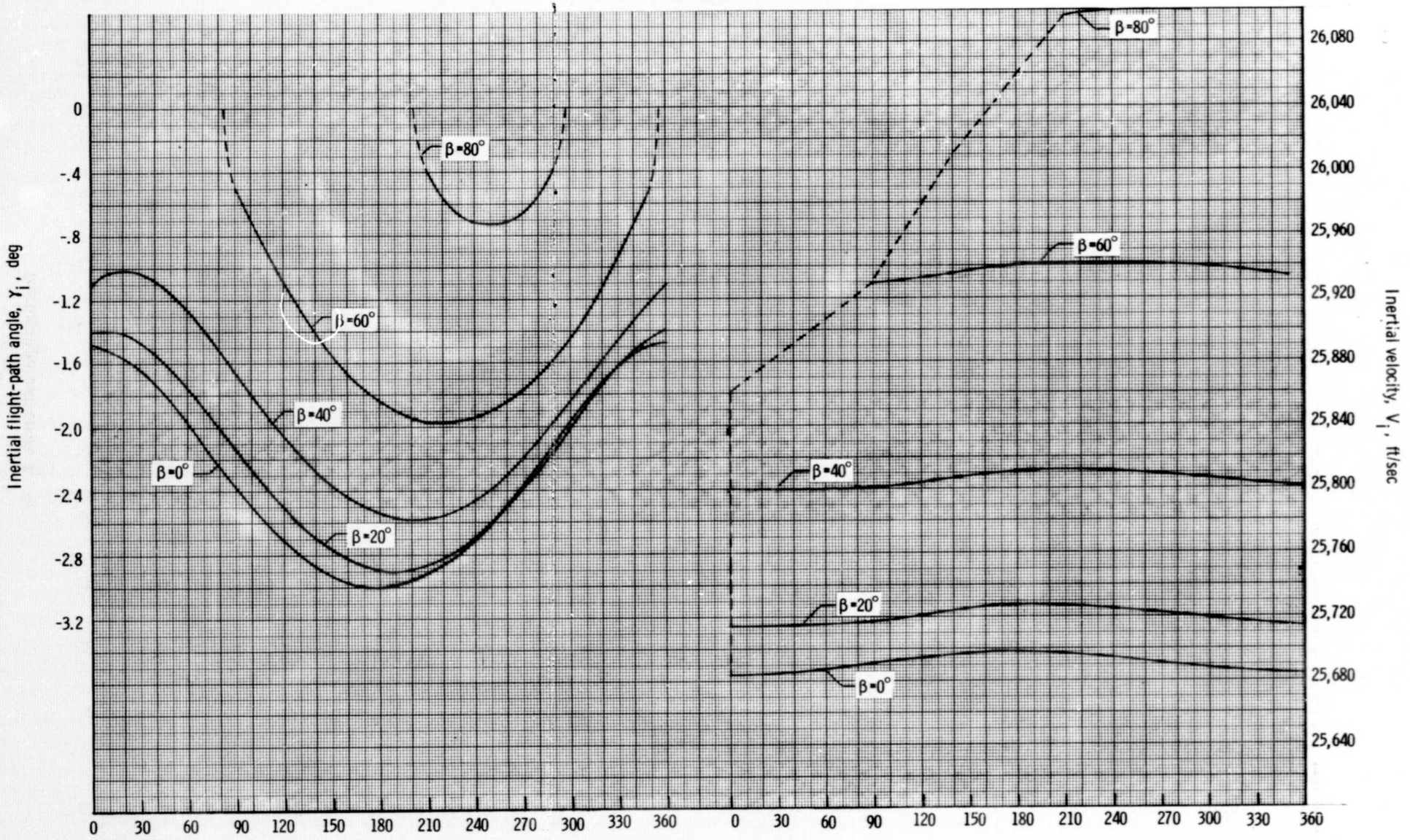

(b) ΔV = 500 fps

Figure 29. - Continued.

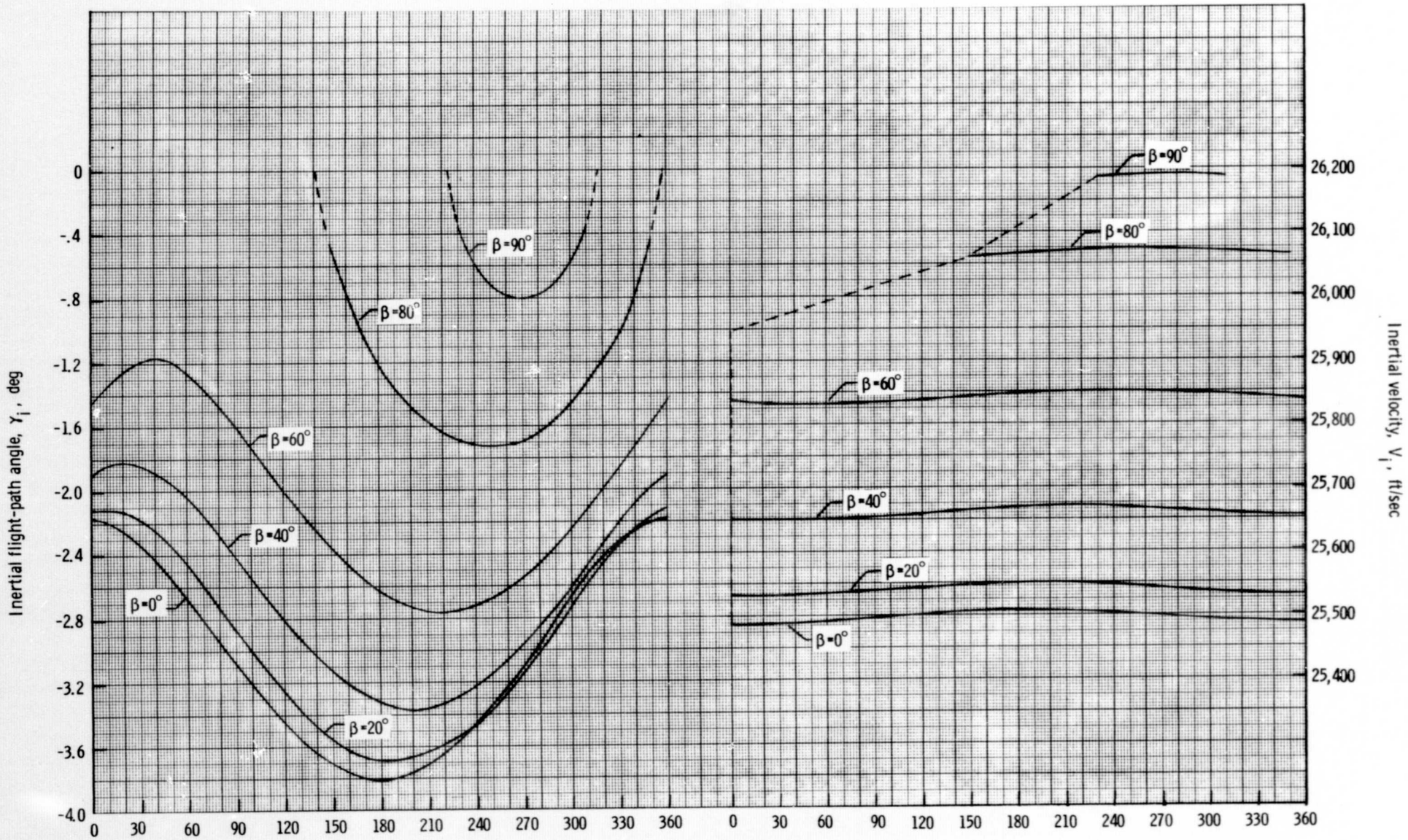

(c) ΔV = 700 fps

Figure 29. - Concluded.

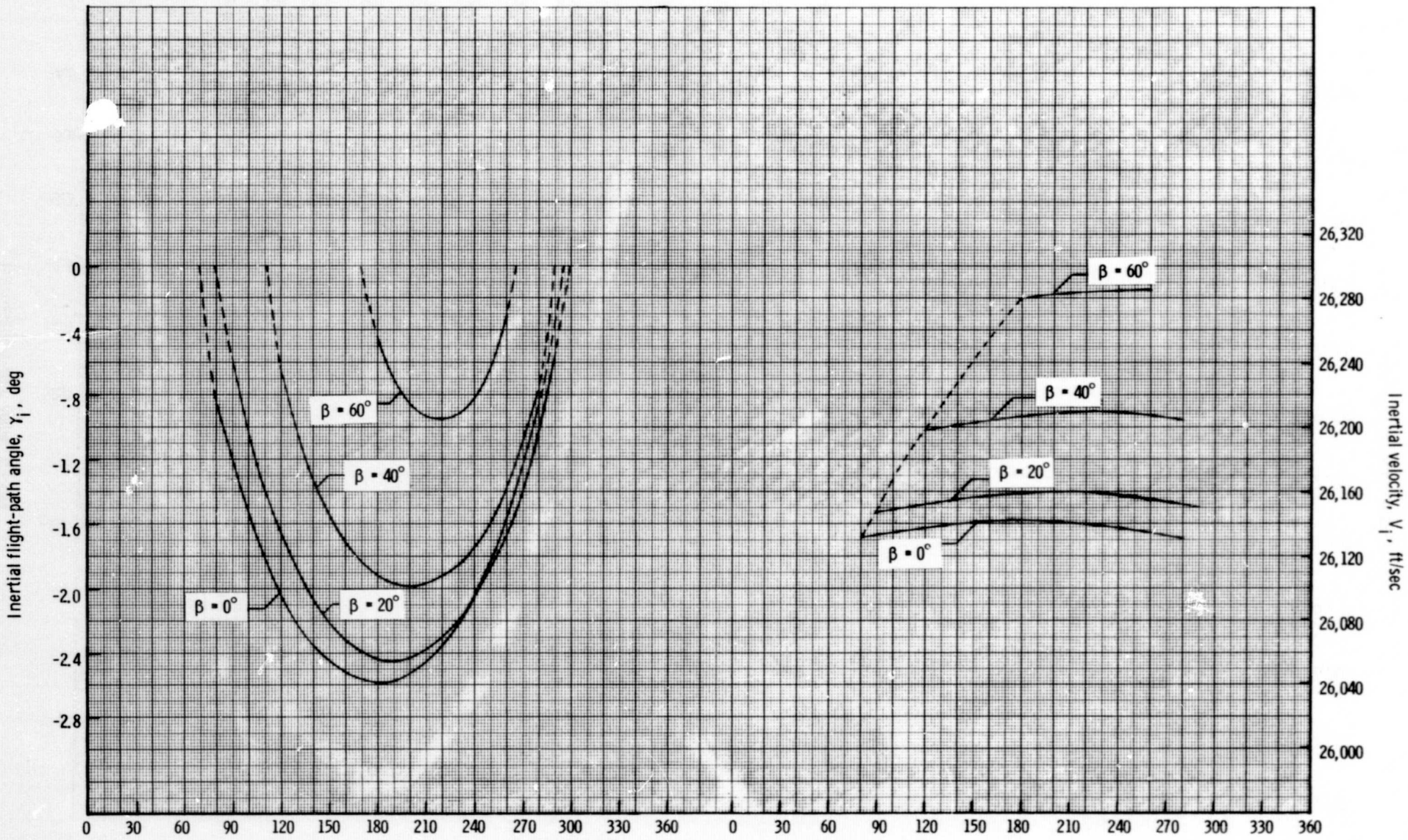

(a) ΔV = 300 fps

Figure 30. - Inertial flight-path angle and velocity at 400 000 feet as a function of retrograde true anomaly and a constant ΔV for an elliptical orbit where h_p = 153 nautical miles and h_a = 400 nautical miles.

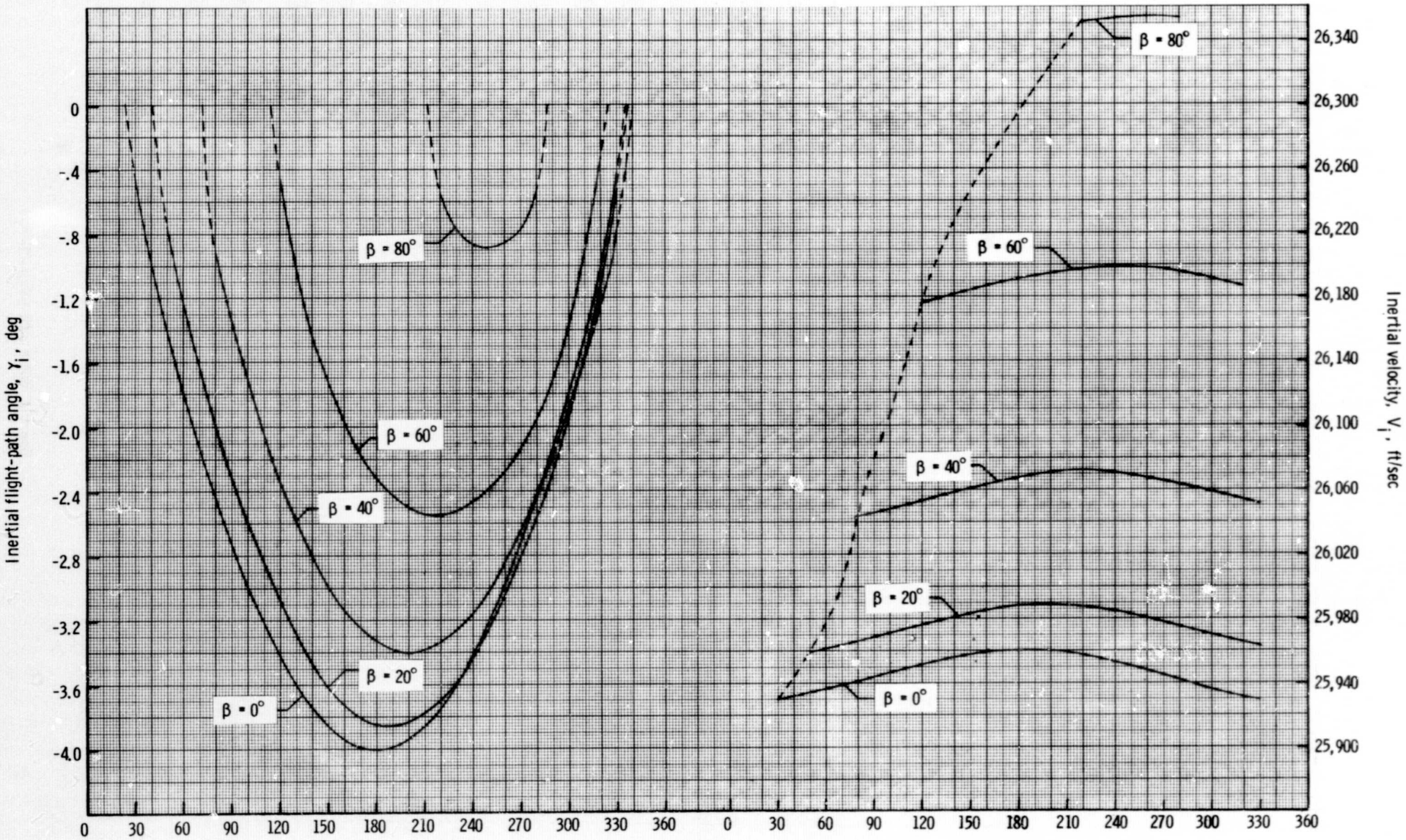

(b) ΔV = 500 fps

Figure 30. - Continued.

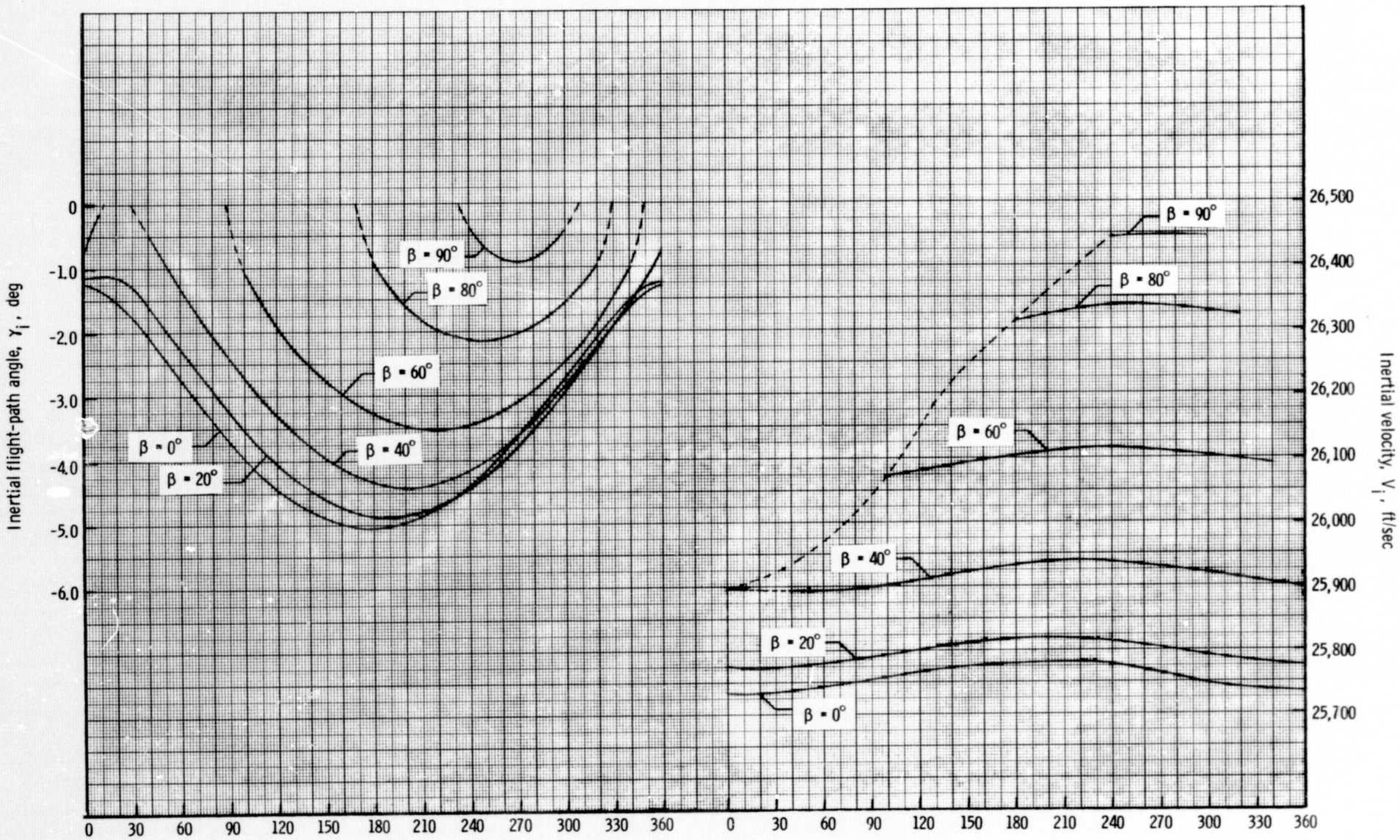

(c) ΔV = 700 fps

Figure 30. - Concluded.

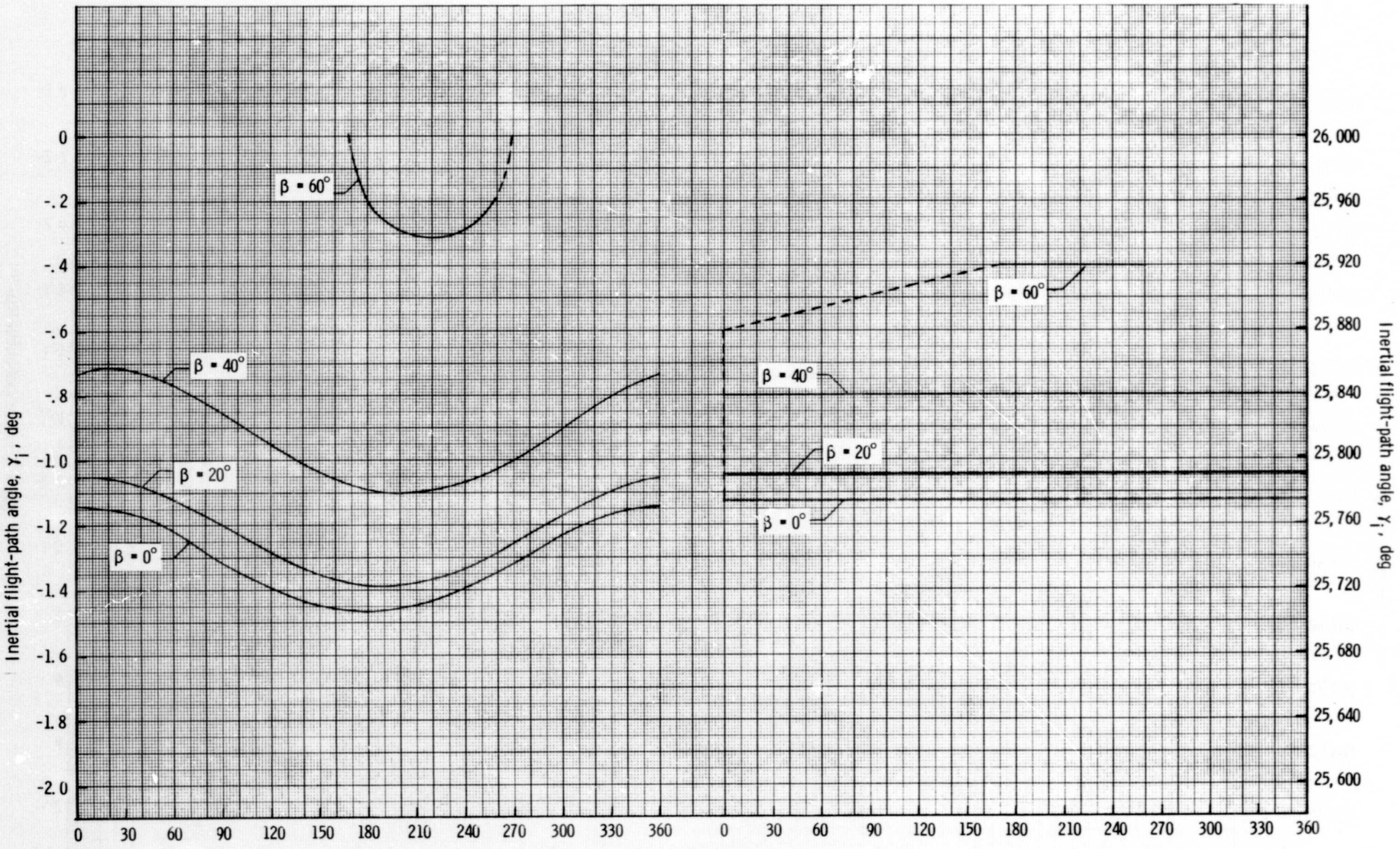

(a) ΔV = 300 fps

Figure 31. - Inertial flight-path angle and velocity at 400 000 feet as a function of retrograde true anomaly and a constant ΔV for an elliptical orbit where h_p = 160 nautical miles and h_a = 180 nautical miles.

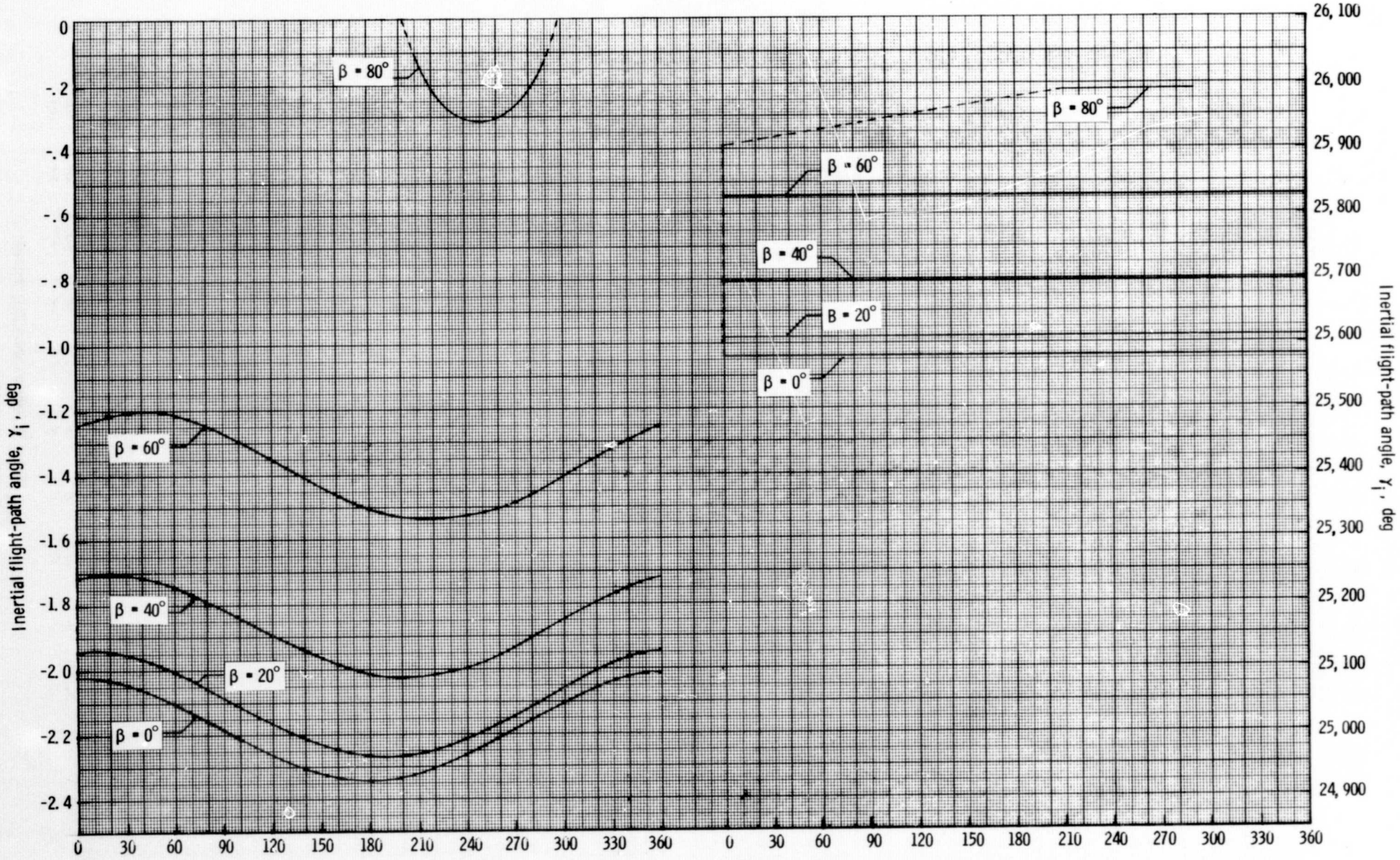

(b) ΔV = 500 fps

Figure 31. - Continued.

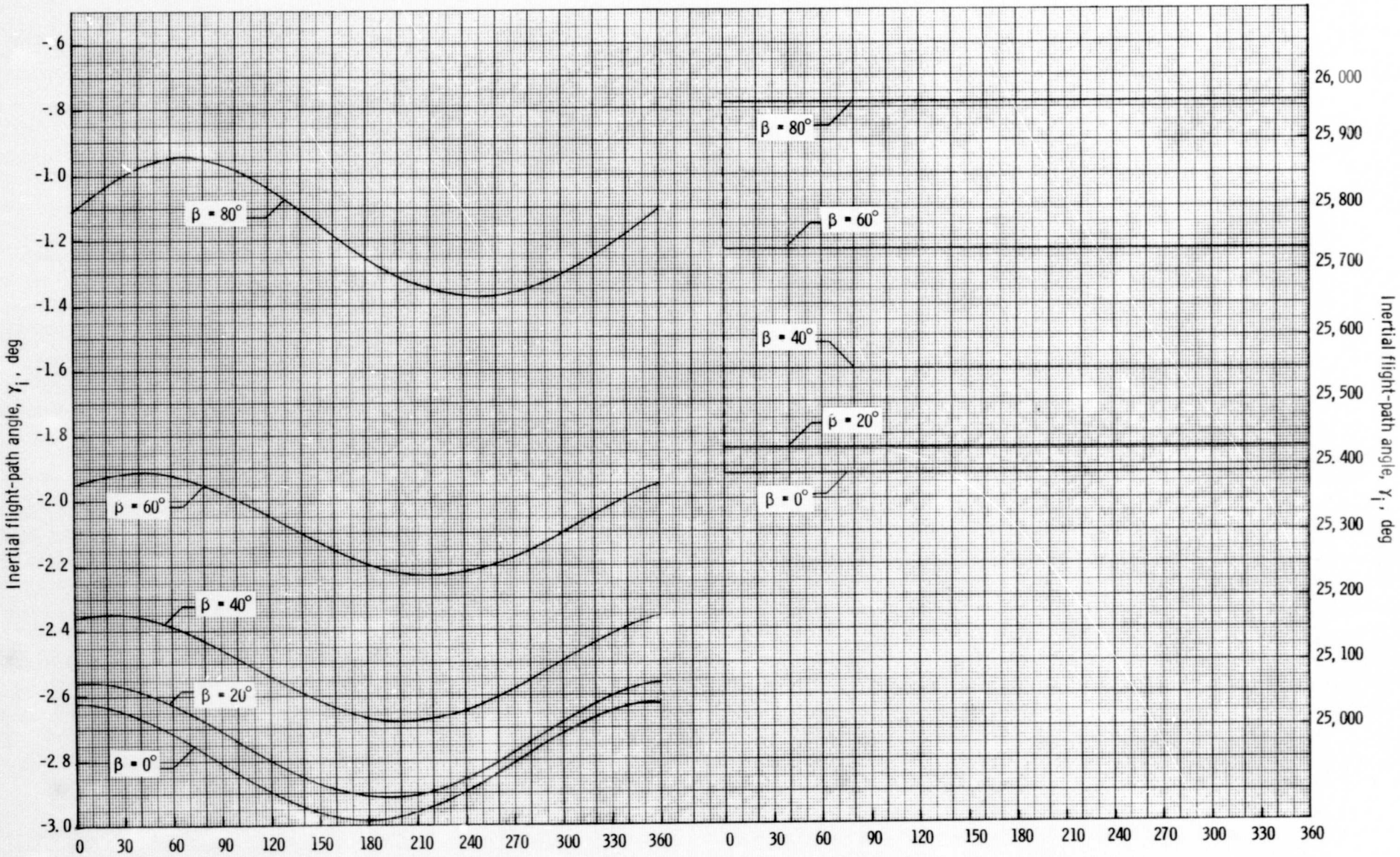

(c) ΔV = 700 fps

Figure 31. - Concluded.

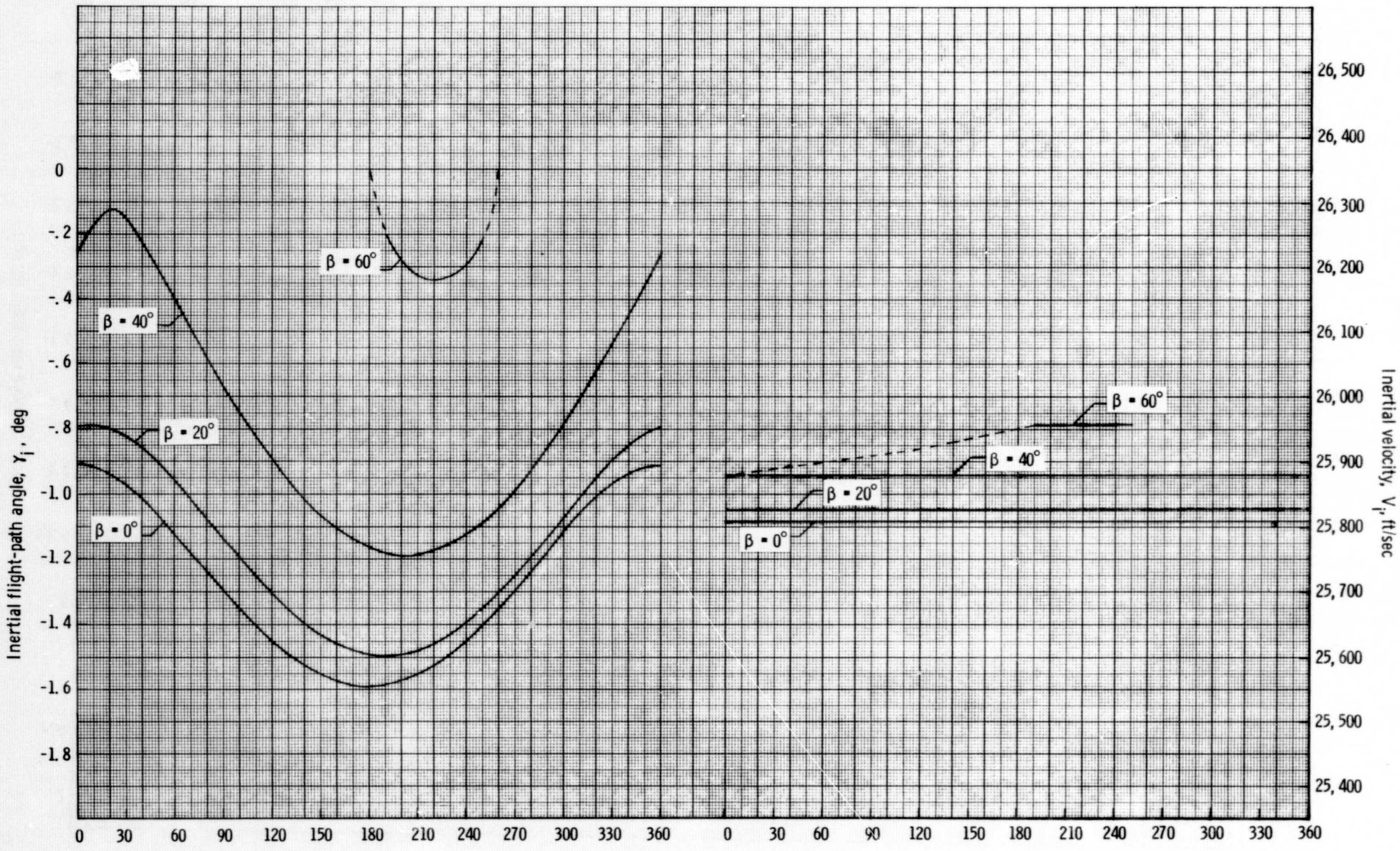

(a) ΔV = 300 fps

Figure 32.- Inertial flight-path angle and velocity at 400 000 feet as a function of retrograde true anomaly and a constant ΔV for an elliptical orbit where h_p = 160 nautical miles and h_a = 200 nautical miles.

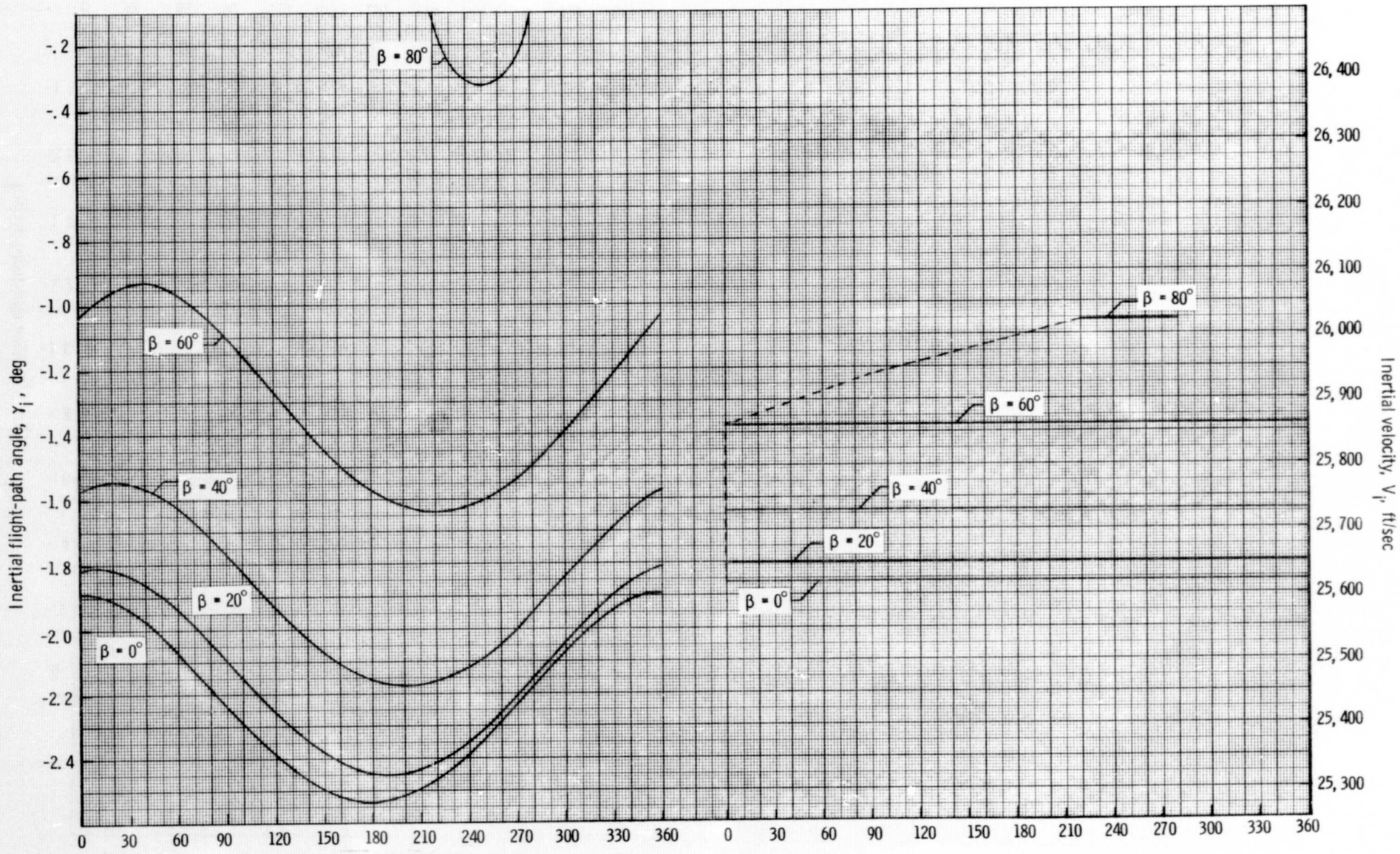

(b) ΔV = 500 fps

Figure 32. - Continued.

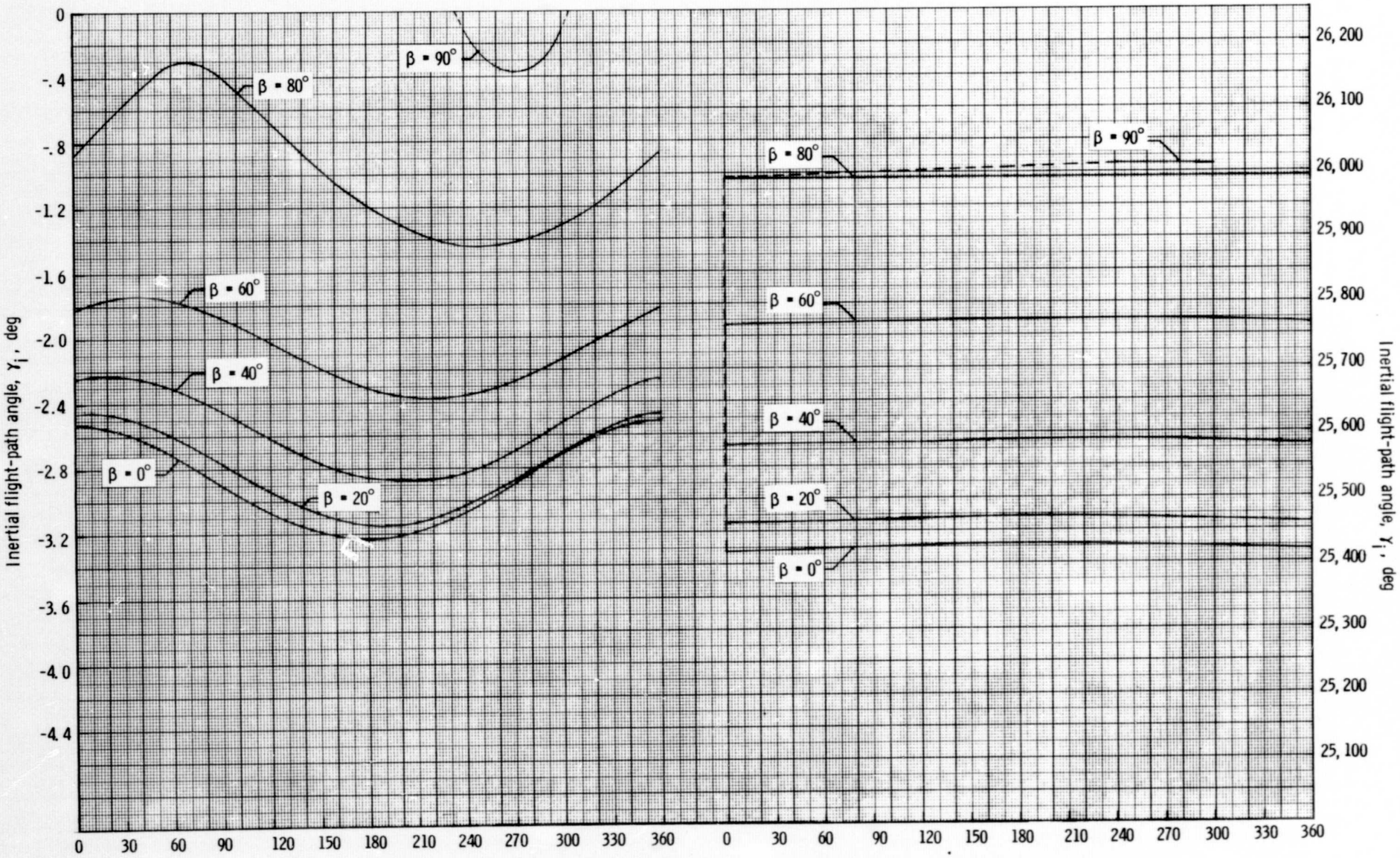

(c) ΔV = 700 fps

Figure 32. - Concluded.

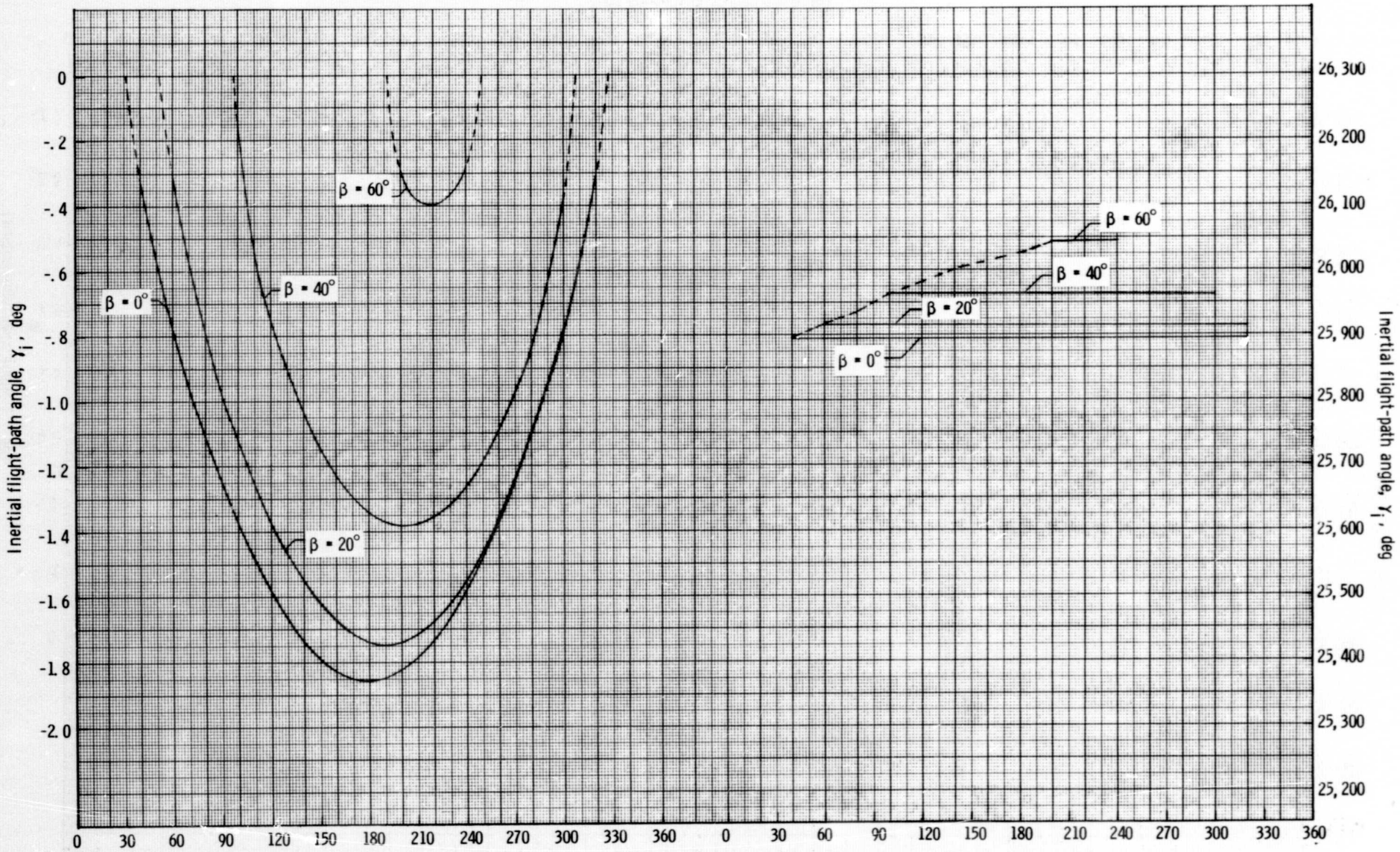

(a) ΔV = 300 fps

Figure 33. - Inertial flight-path angle and velocity at 400 000 feet as a function of retrograde true anomaly and a constant ΔV for an elliptical orbit where h_p = 160 nautical miles and h_a = 250 nautical miles.

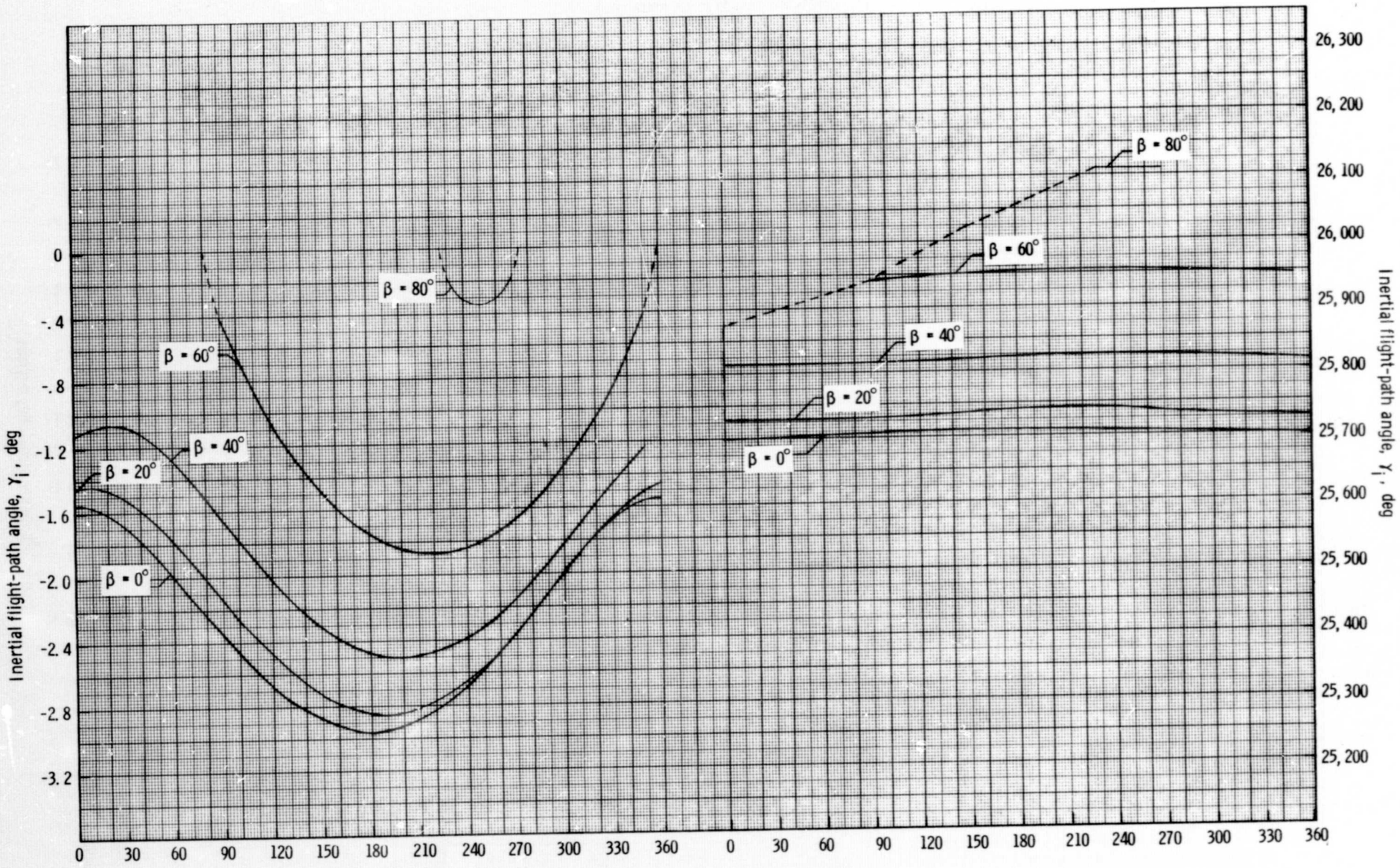

(b) ΔV = 500 fps

Figure 33. - Continued.

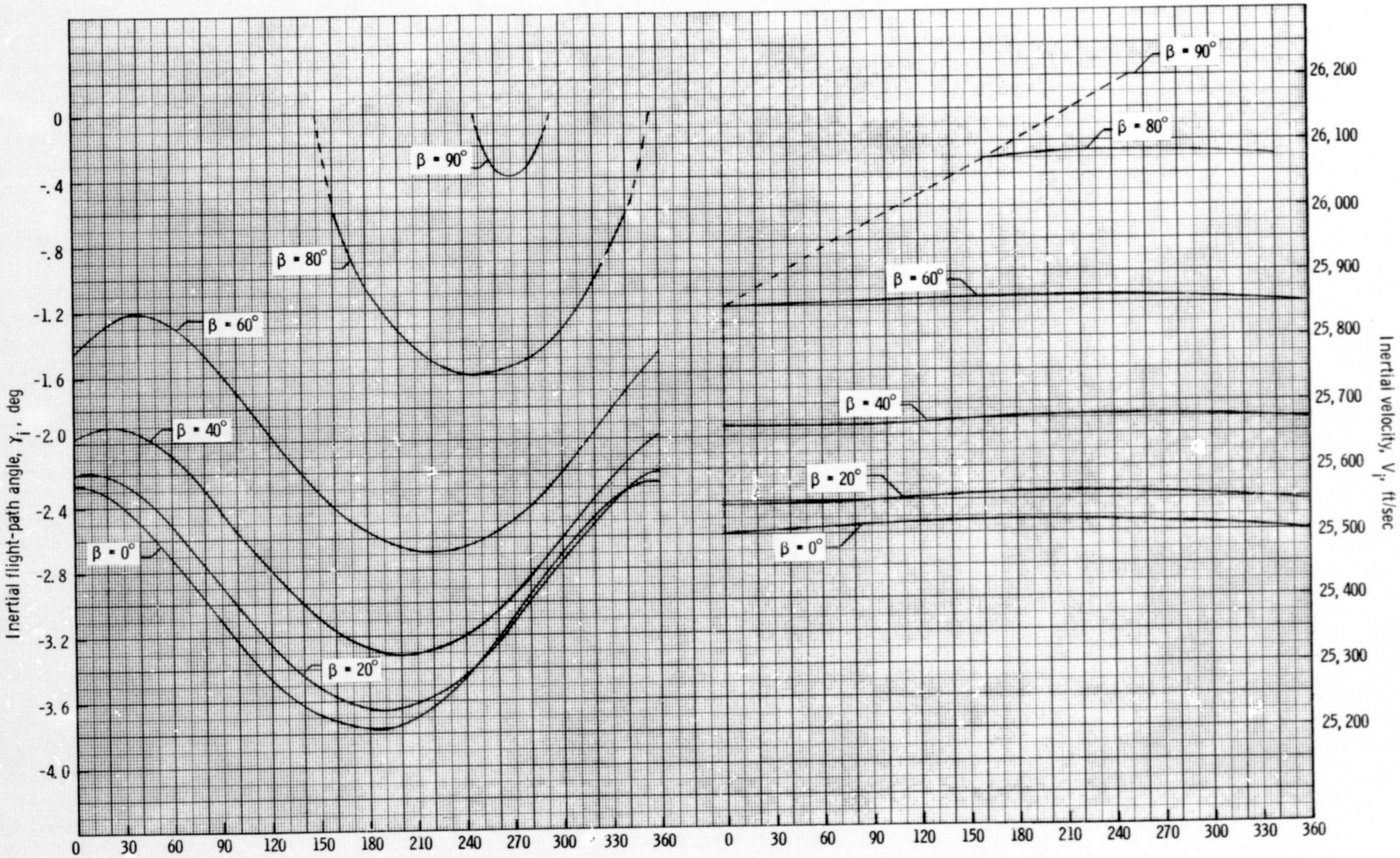

(c) ΔV = 700 fps

Figure 33. - Concluded.

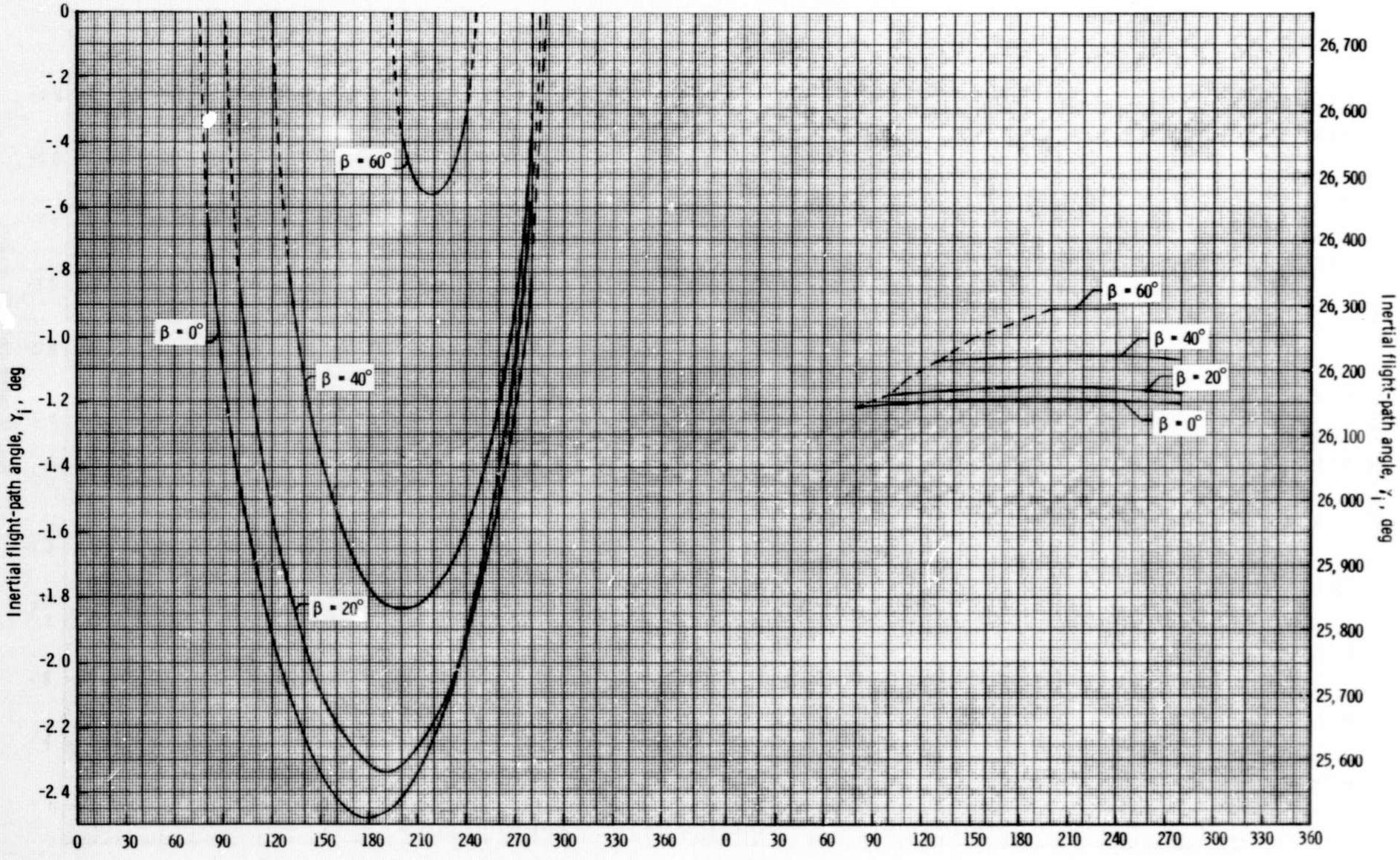

(a) ΔV = 300 fps

Figure 34. - Inertial flight-path angle and velocity at 400 000 feet as a function of retrograde true anomaly and a constant ΔV for an elliptical orbit where h_p = 160 nautical miles and h_a = 400 nautical miles.

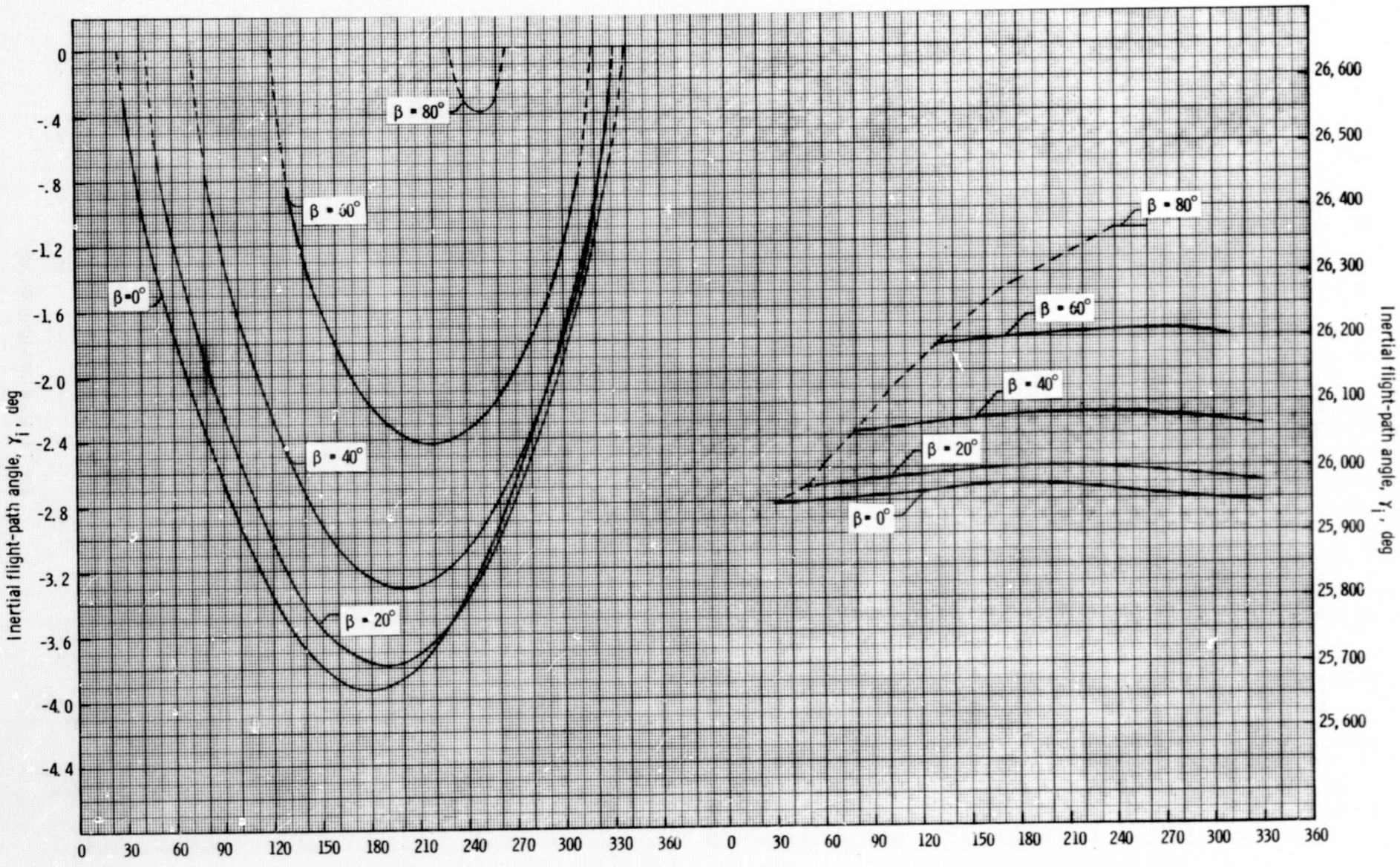

(b) ΔV = 500 fps

Figure 34. - Continued.

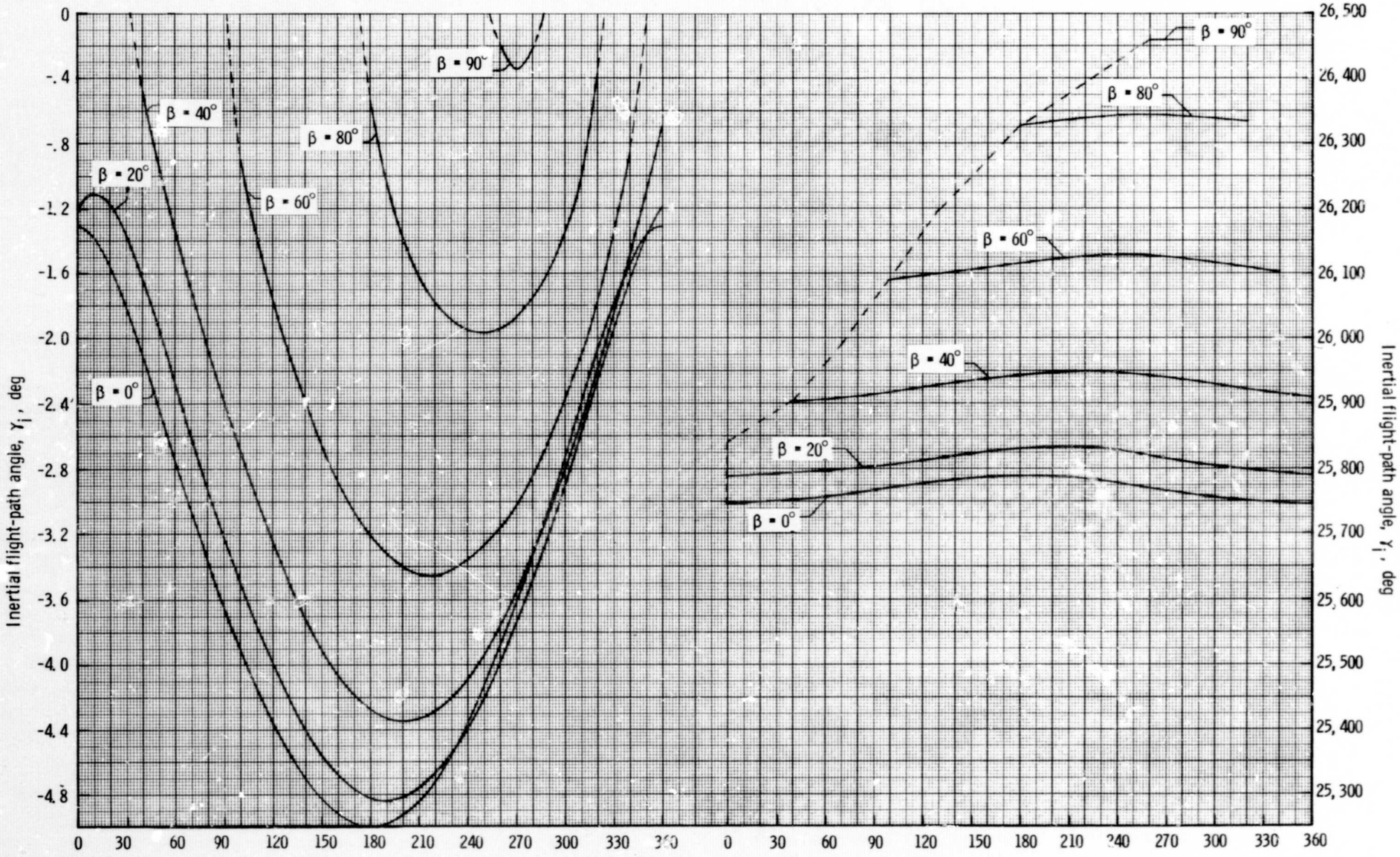

(c) ΔV = 700 fps

Figure 34. - Concluded.

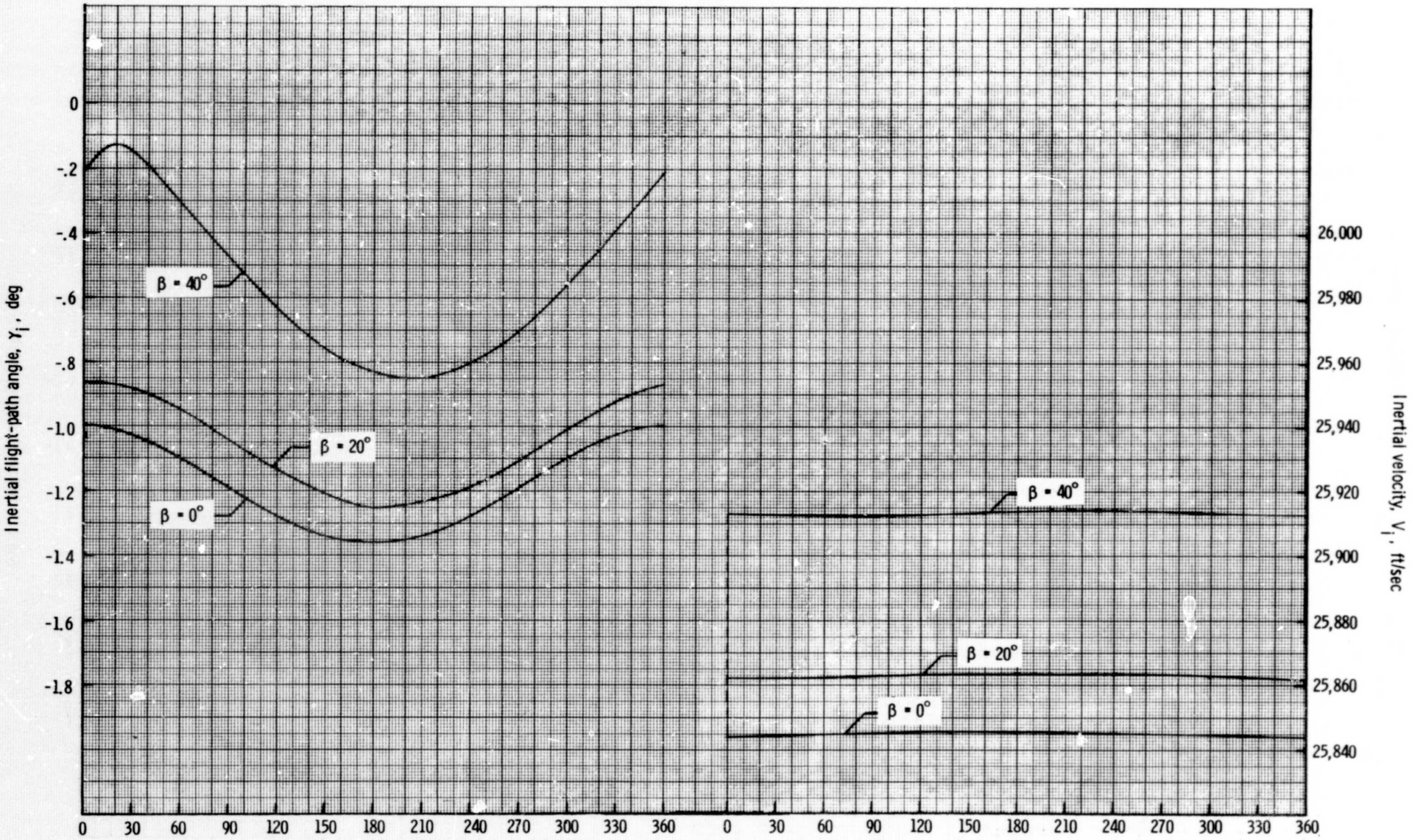

(a) ΔV = 300 fps

Figure 35. - Inertial flight-path angle and velocity at 400 000 feet as a function of retrograde true anomaly and a constant ΔV for an elliptical orbit where h_p = 180 nautical miles and h_a = 200 nautical miles.

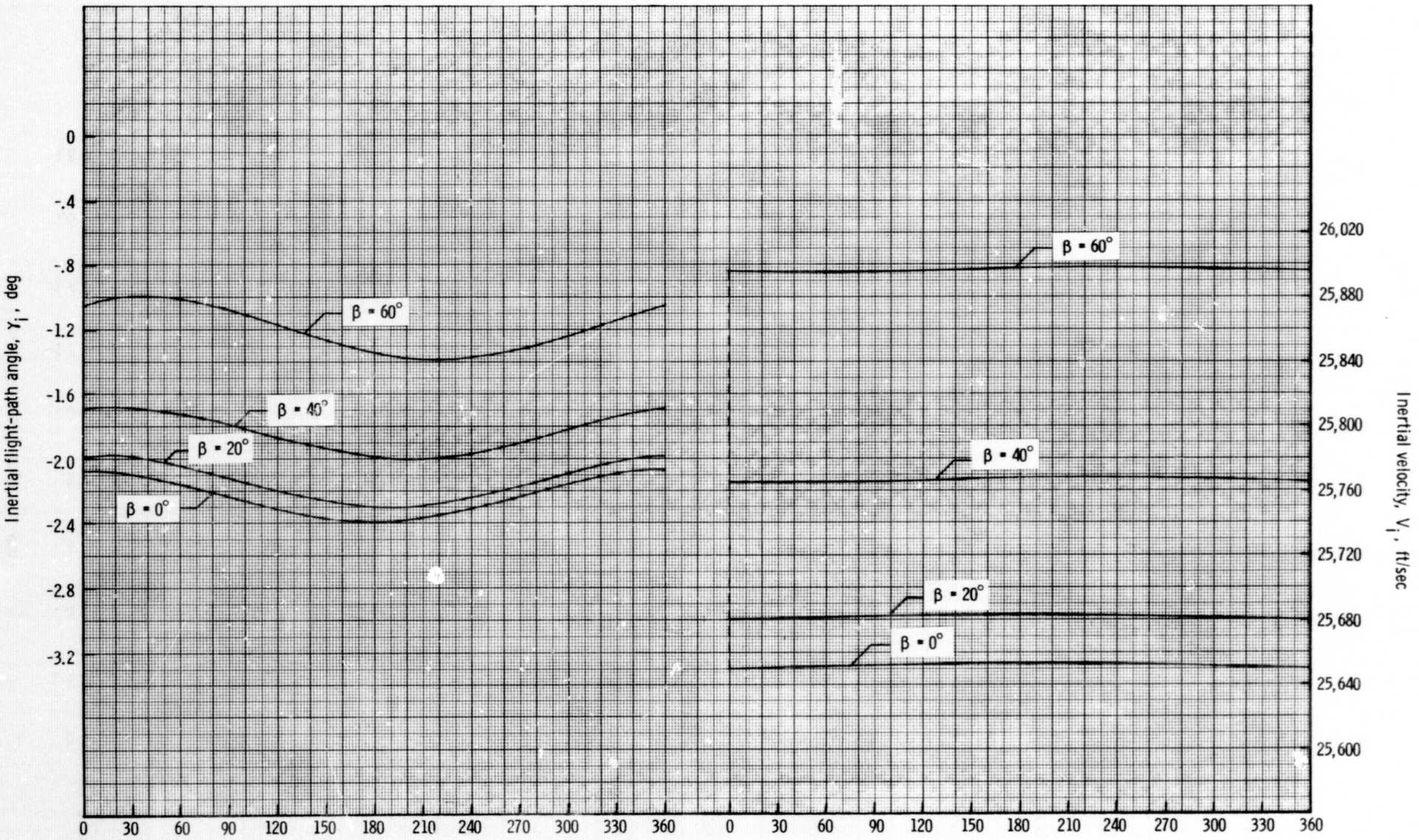

(b) ΔV = 500 fps

Figure 35. - Continued.

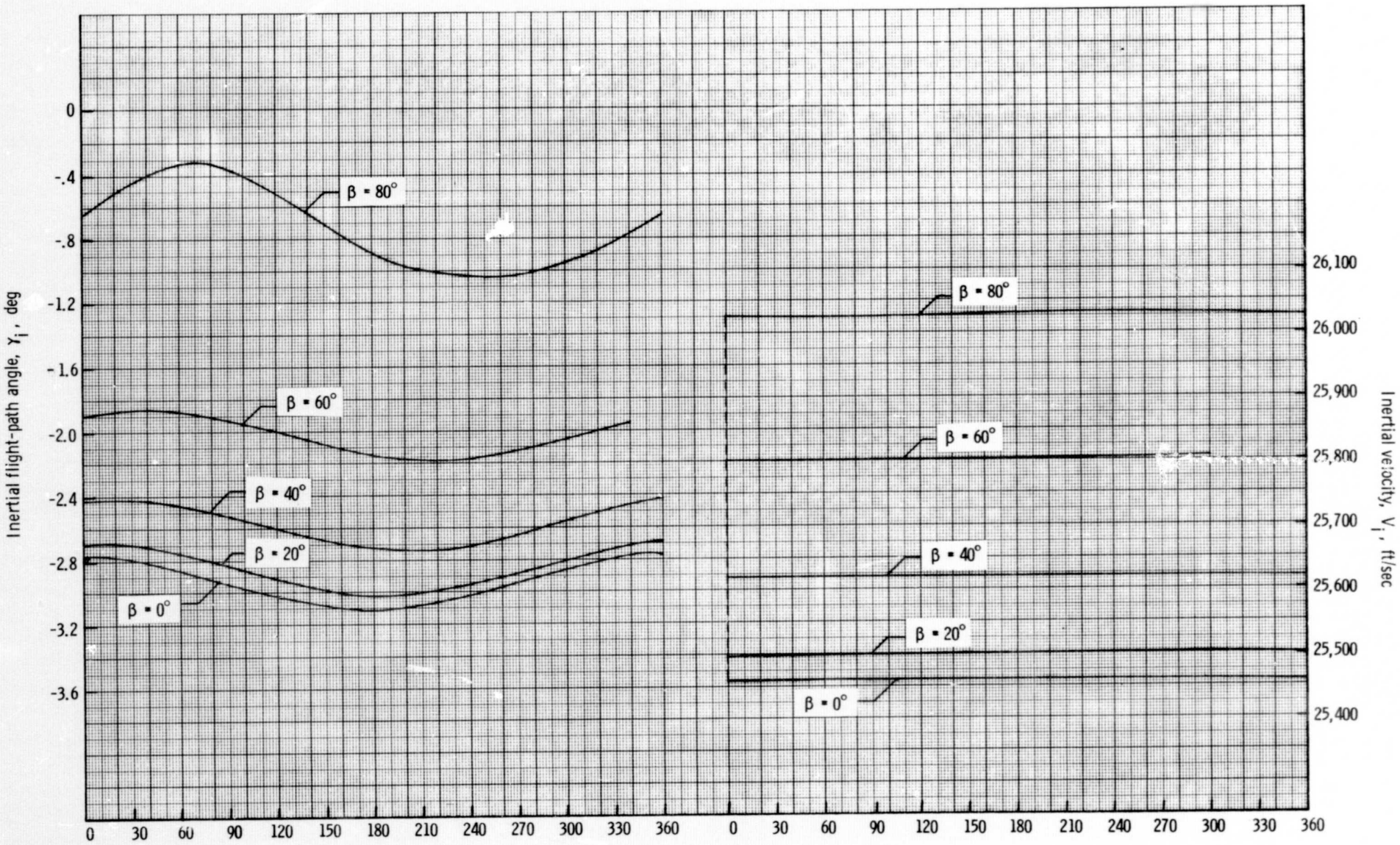

(c) ΔV = 700 fps

Figure 35. - Concluded.

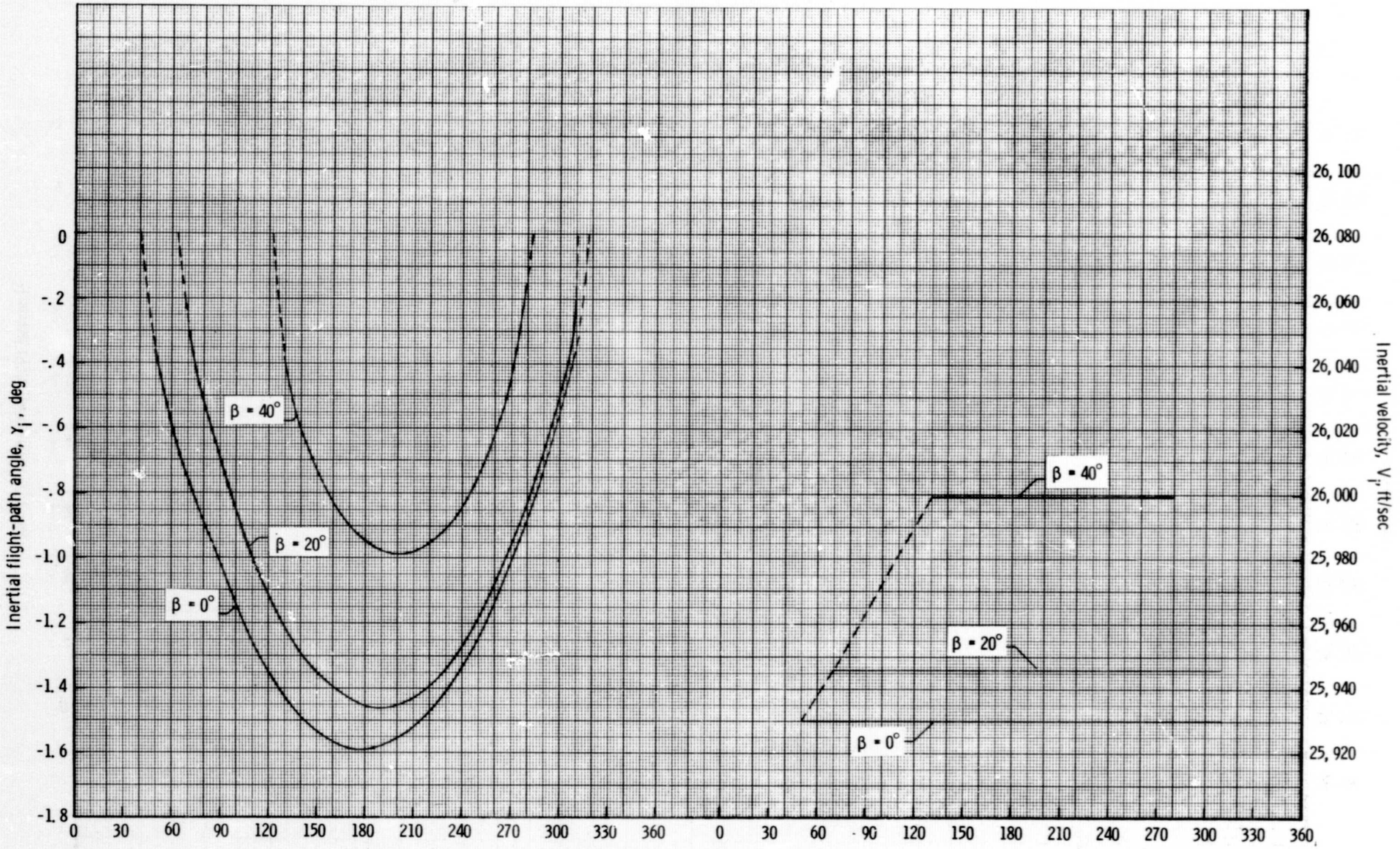

(a) ΔV = 300 fps

Figure 36. - Inertial flight-path angle and velocity at 400 000 feet as a function of retrograde true anomaly and a constant ΔV for an elliptical orbit where h_p = 180 nautical miles and h_a = 250 nautical miles.

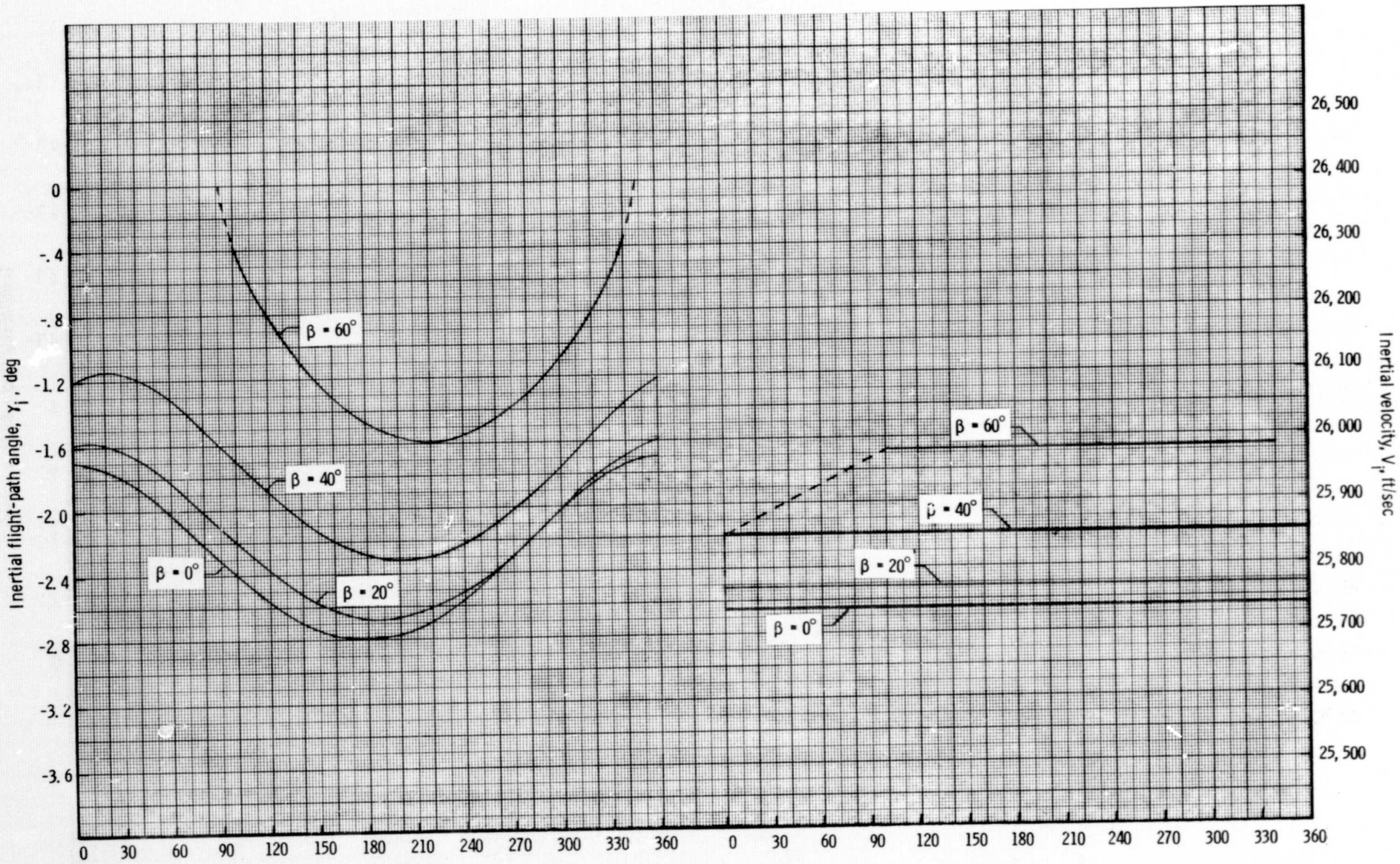

(b) ΔV = 500 fps

Figure 36. - Continued.

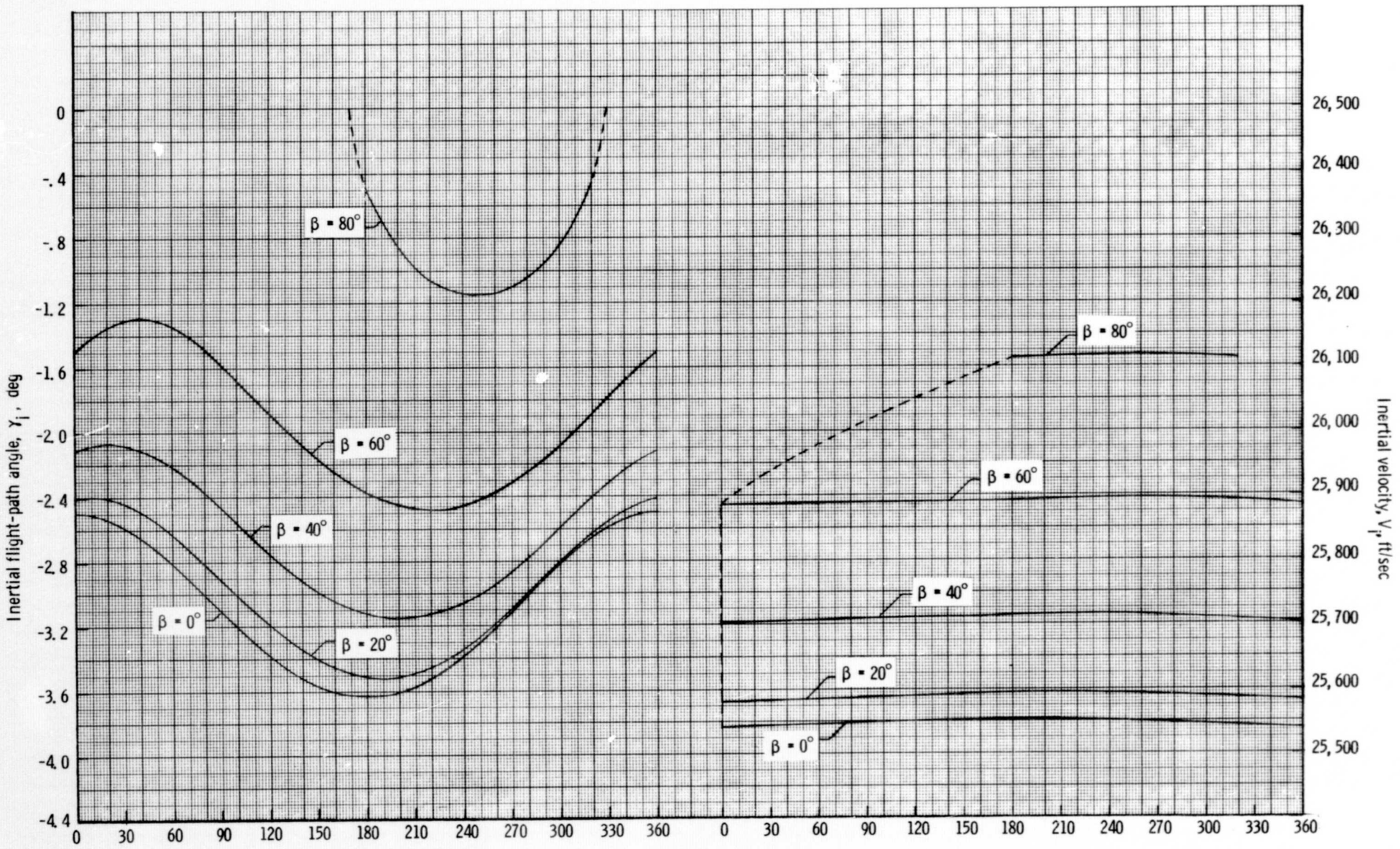

(c) ΔV = 700 fps

Figure 36. - Concluded.

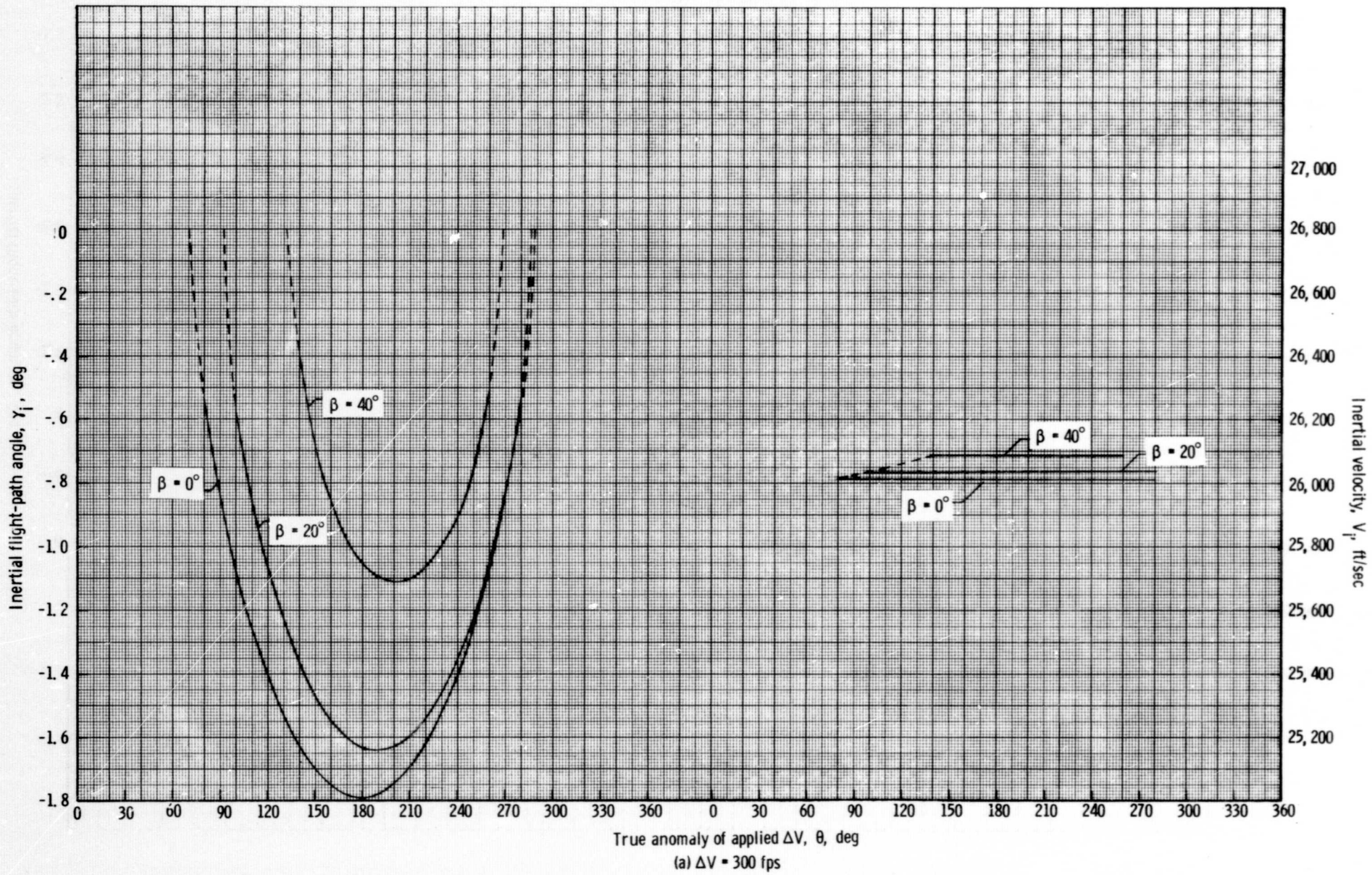

(a) ΔV = 300 fps

Figure 37. - Inertial flight-path angle and velocity at 400 000 feet as a function of retrograde true anomaly and a constant ΔV for an elliptical orbit where h_p = 180 nautical miles and h_a = 300 nautical miles.

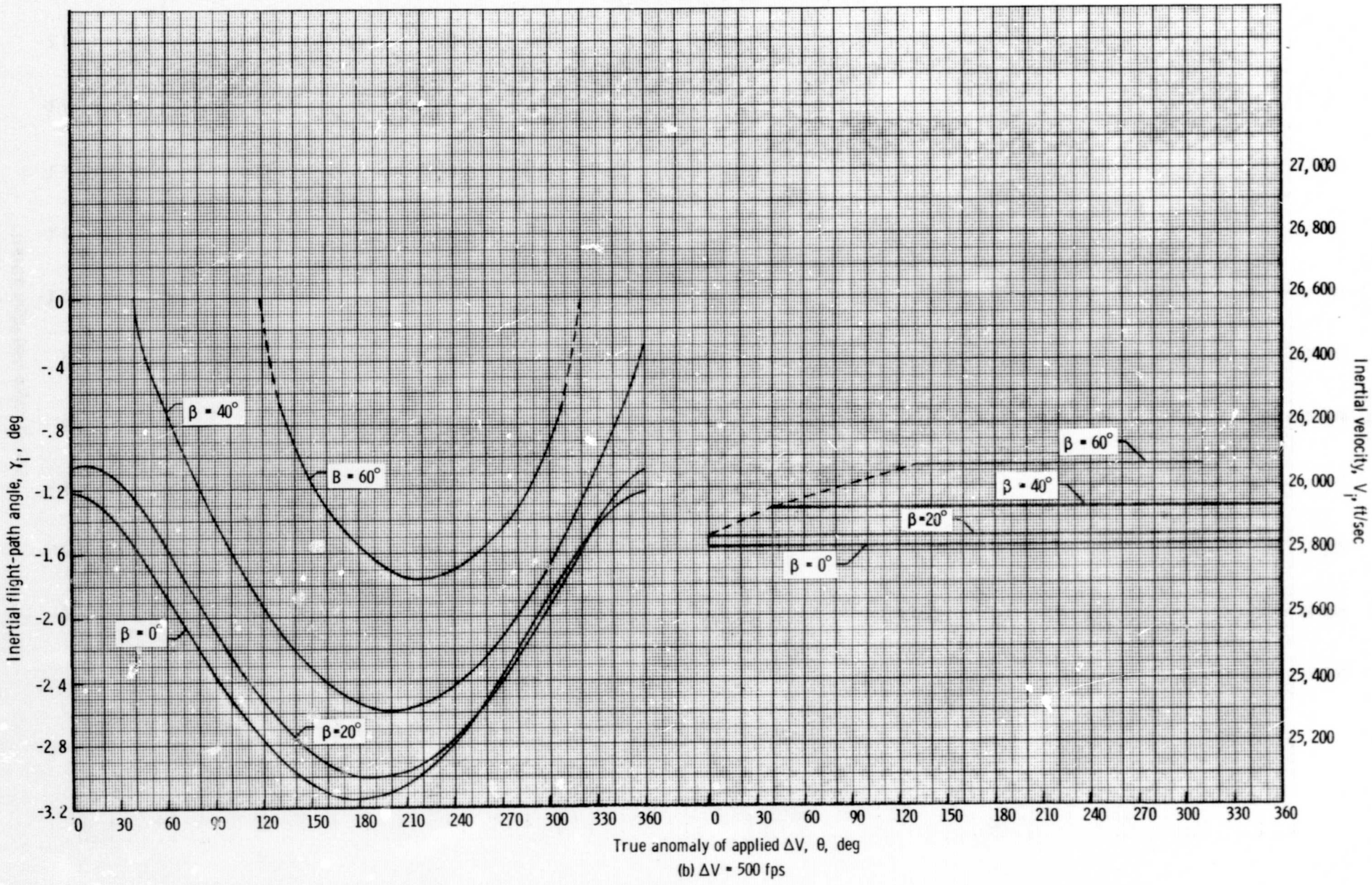

(b) ΔV = 500 fps

Figure 37. – Continued.

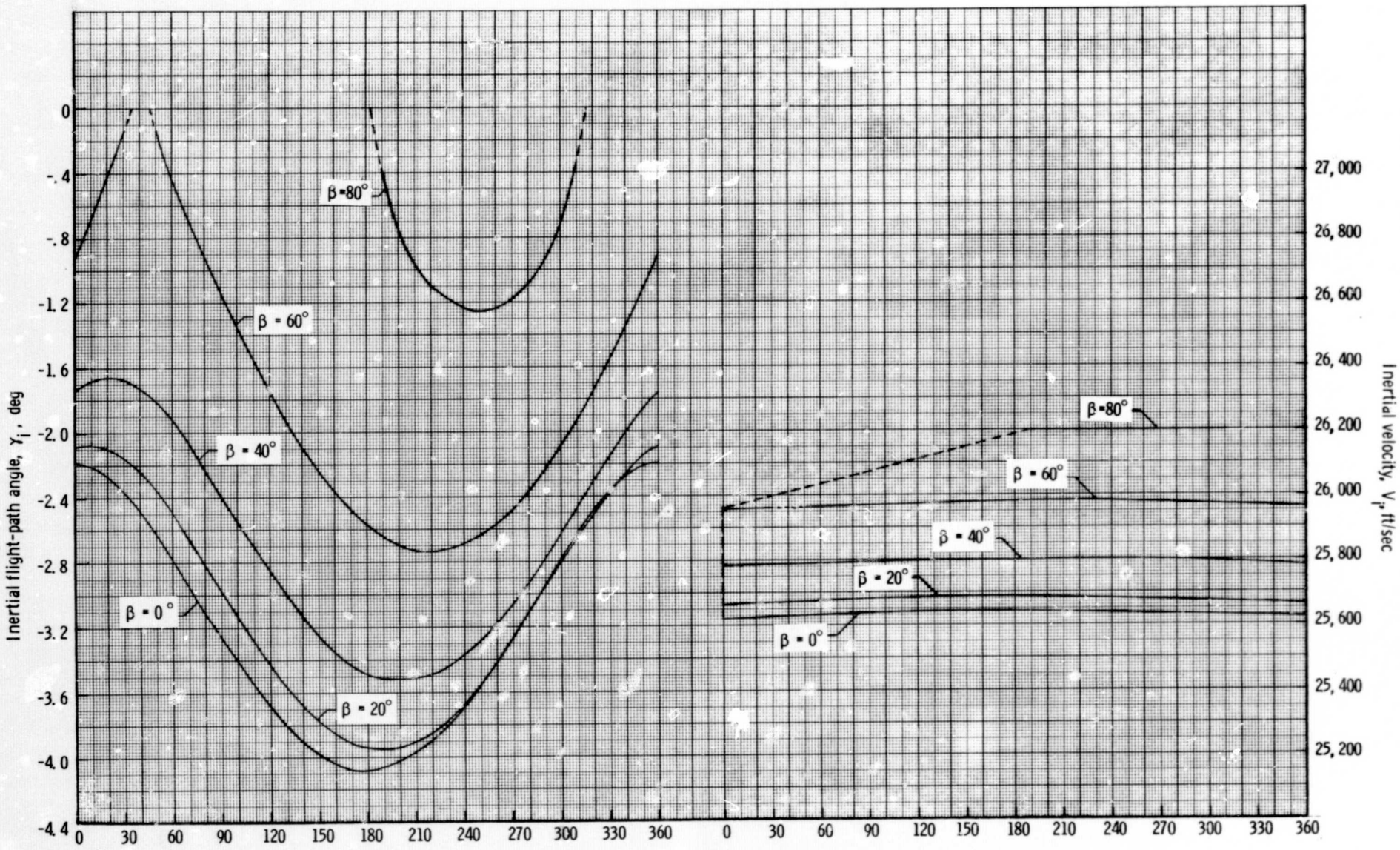

(c) ΔV = 700 fps

Figure 37. - Concluded.

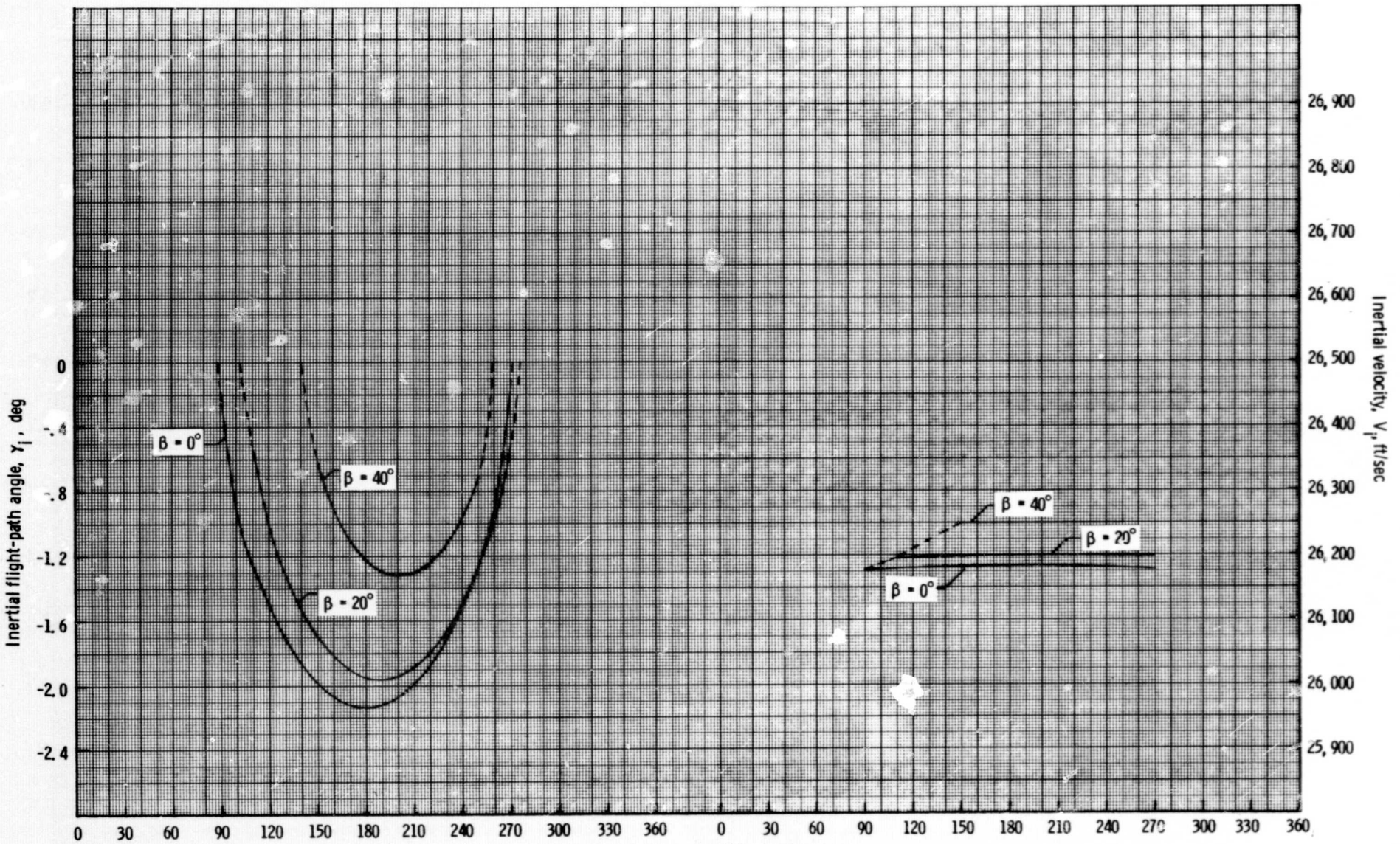

(a) ΔV = 300 fps

Figure 38. - Inertial flight-path angle and velocity at 400 000 feet as a function of retrograde true anomaly and a constant ΔV for an elliptical orbit where h_p = 180 nautical miles and h_a = 400 nautical miles.

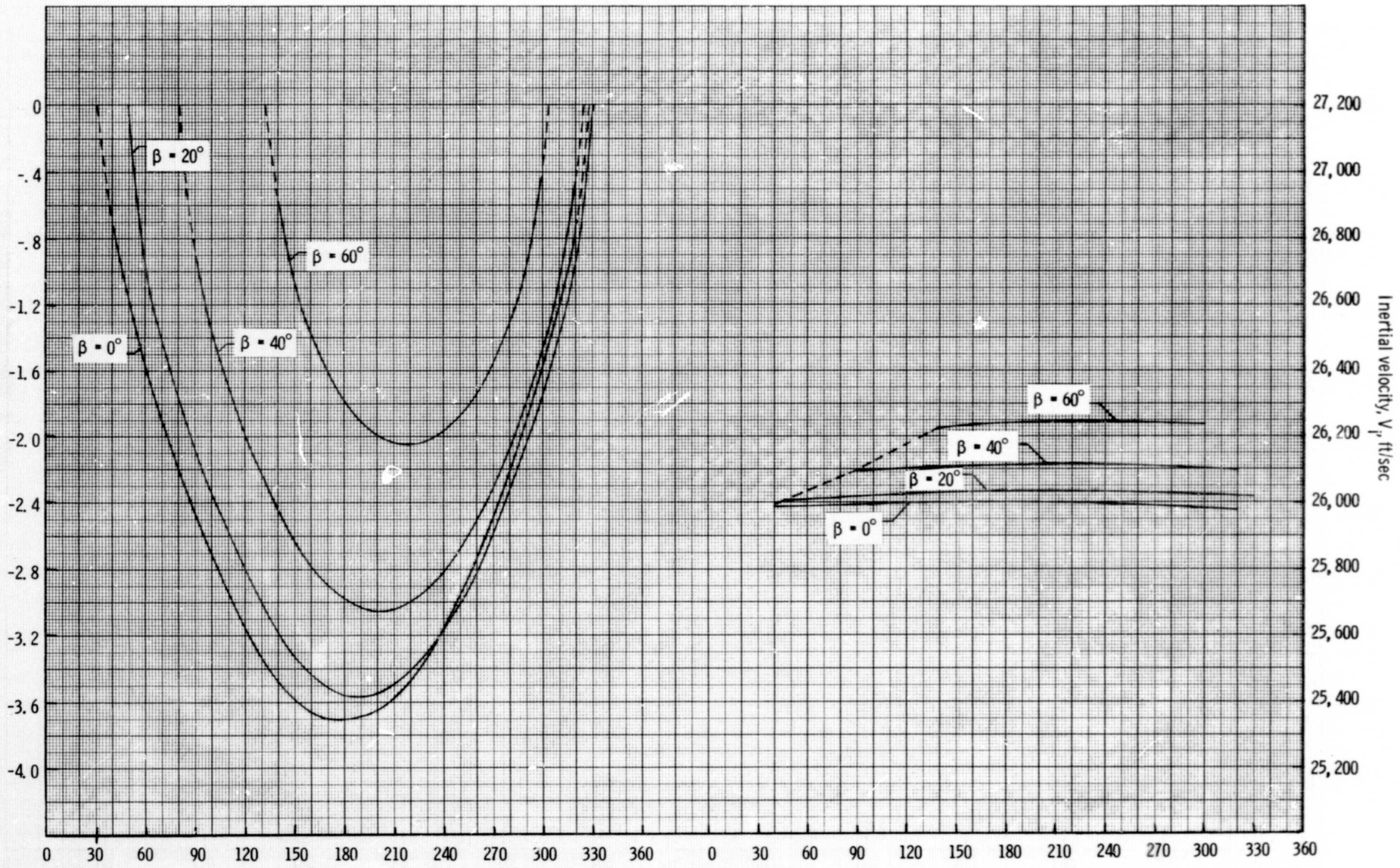

(b) ΔV = 500 fps

Figure 38. - Continued.

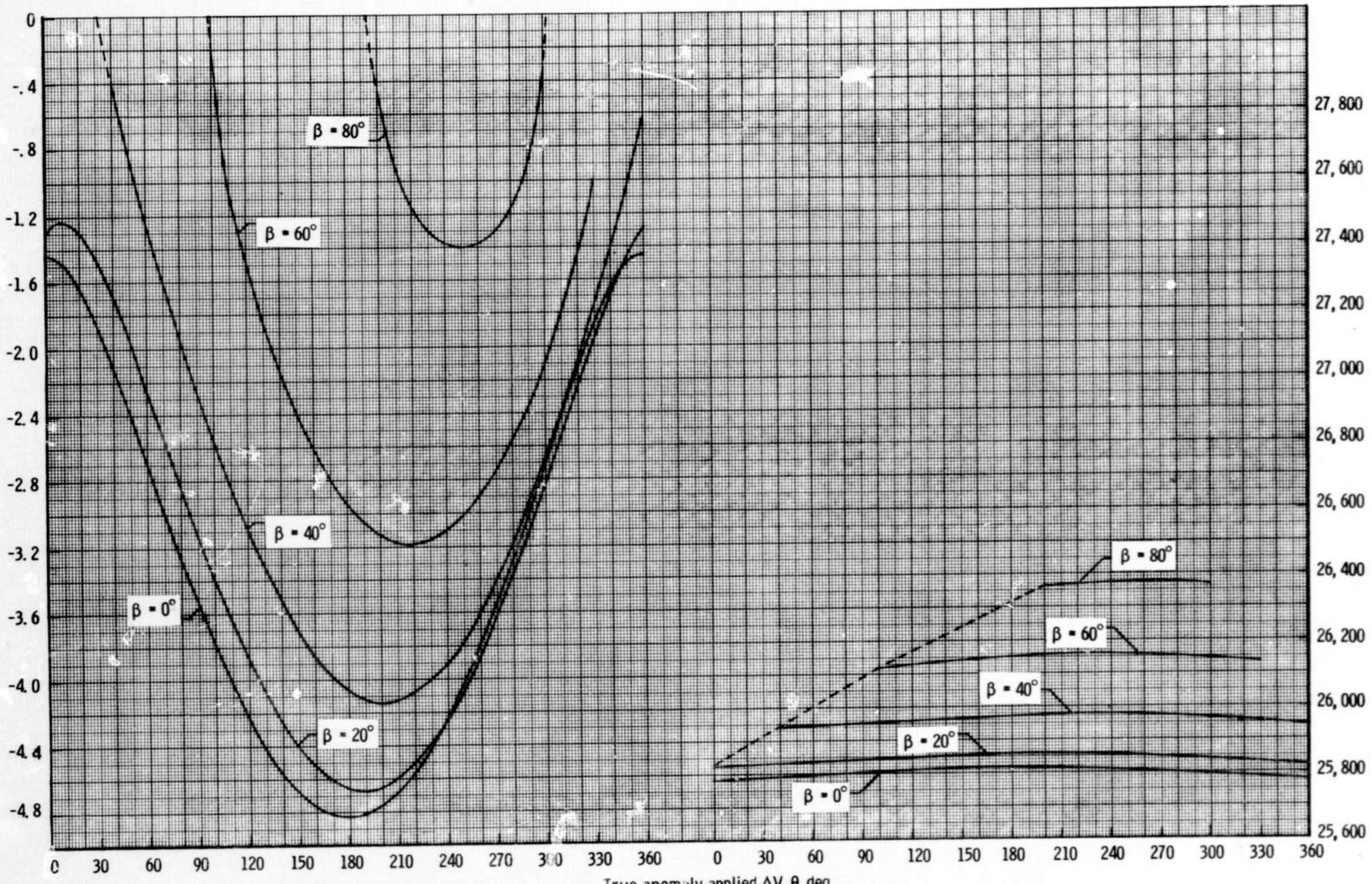

(c) ΔV = 700 fps

Figure 38. - Concluded.

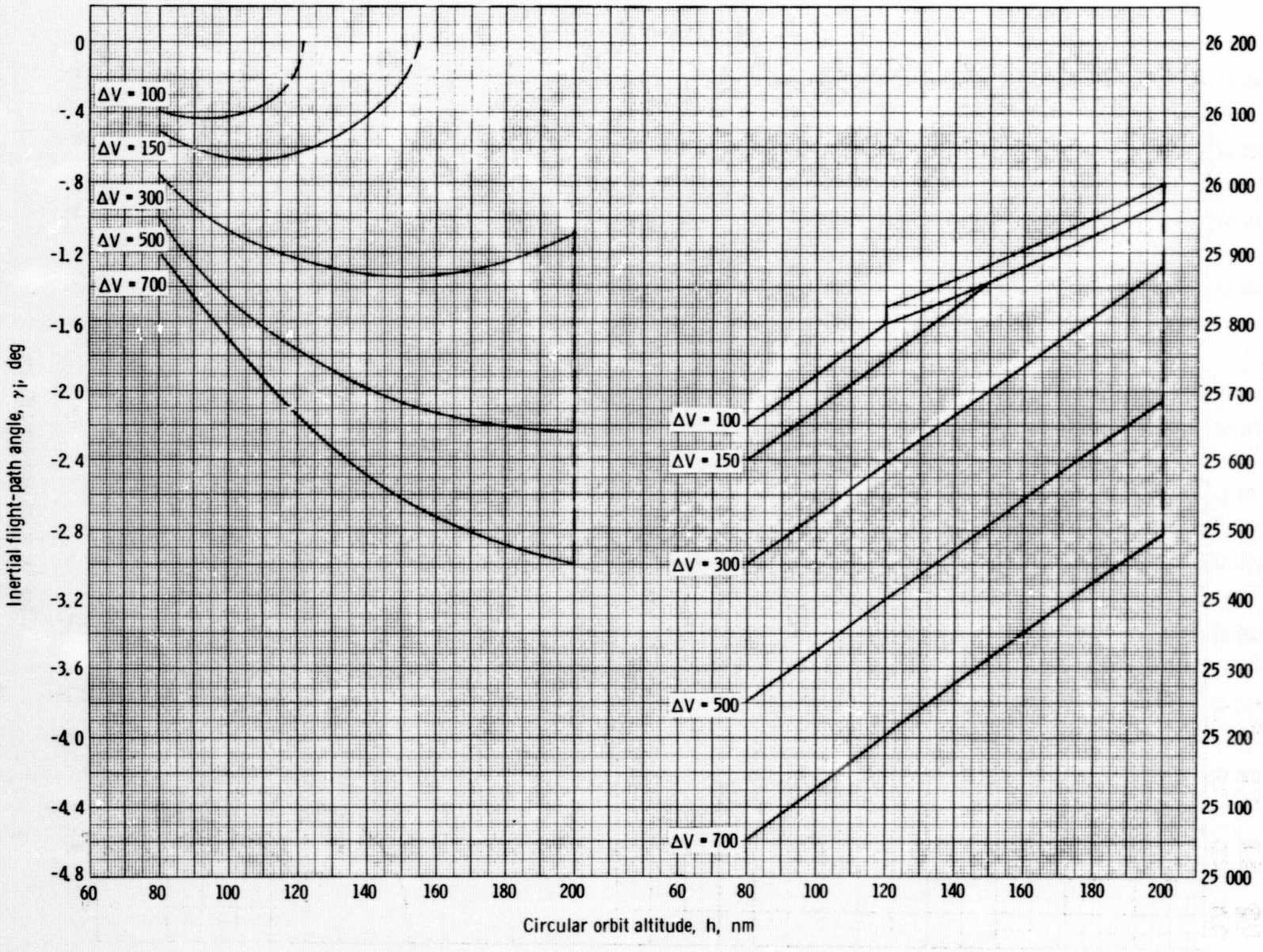

(a) Retrograde pitch angle, $\beta = 0^\circ$

Figure 39. - Reentry conditions at 400 000 feet after retrograde from circular orbits.

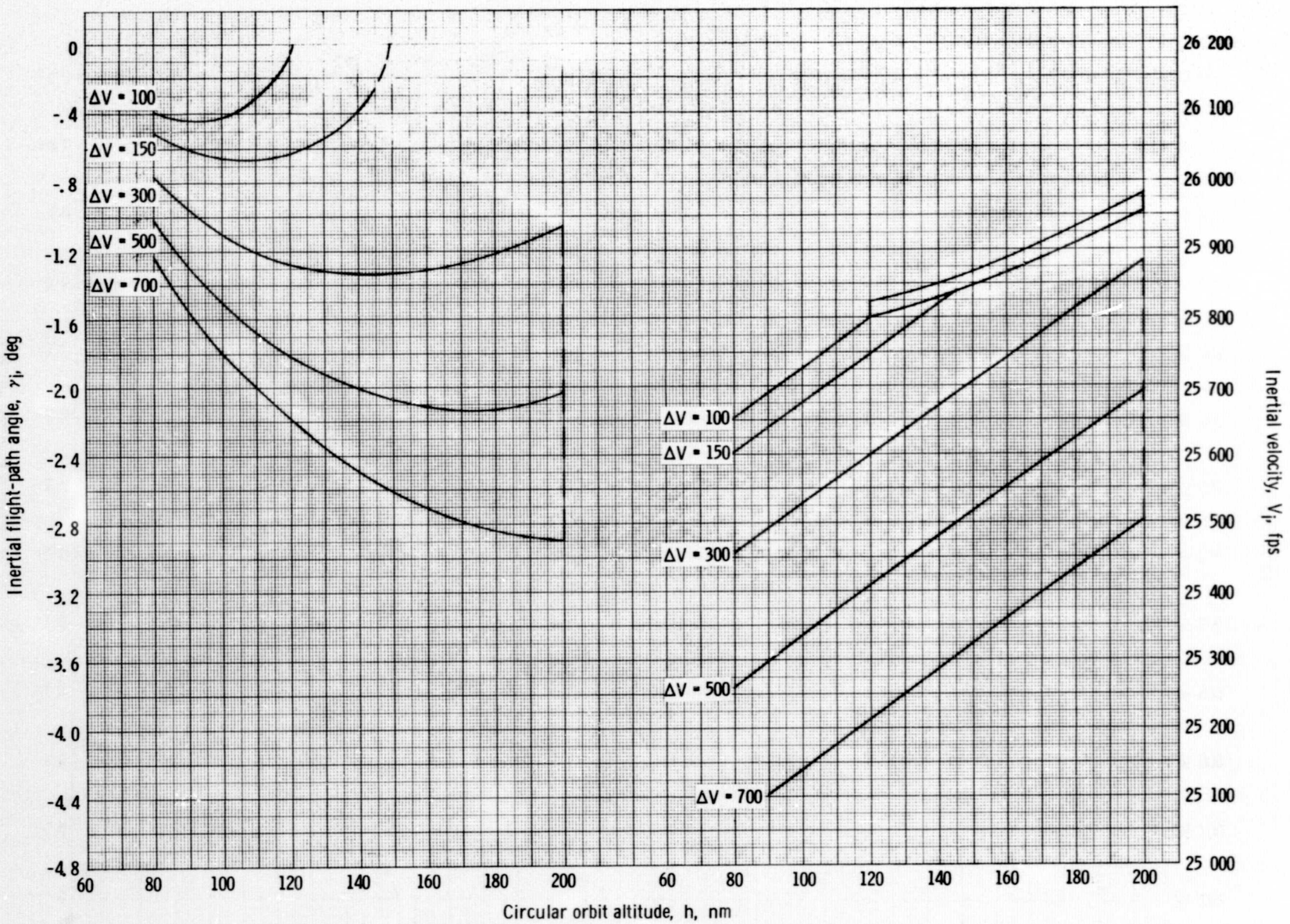

(b) Retrograde pitch angle, $\beta = 10^\circ$

Figure 39. - Continued.

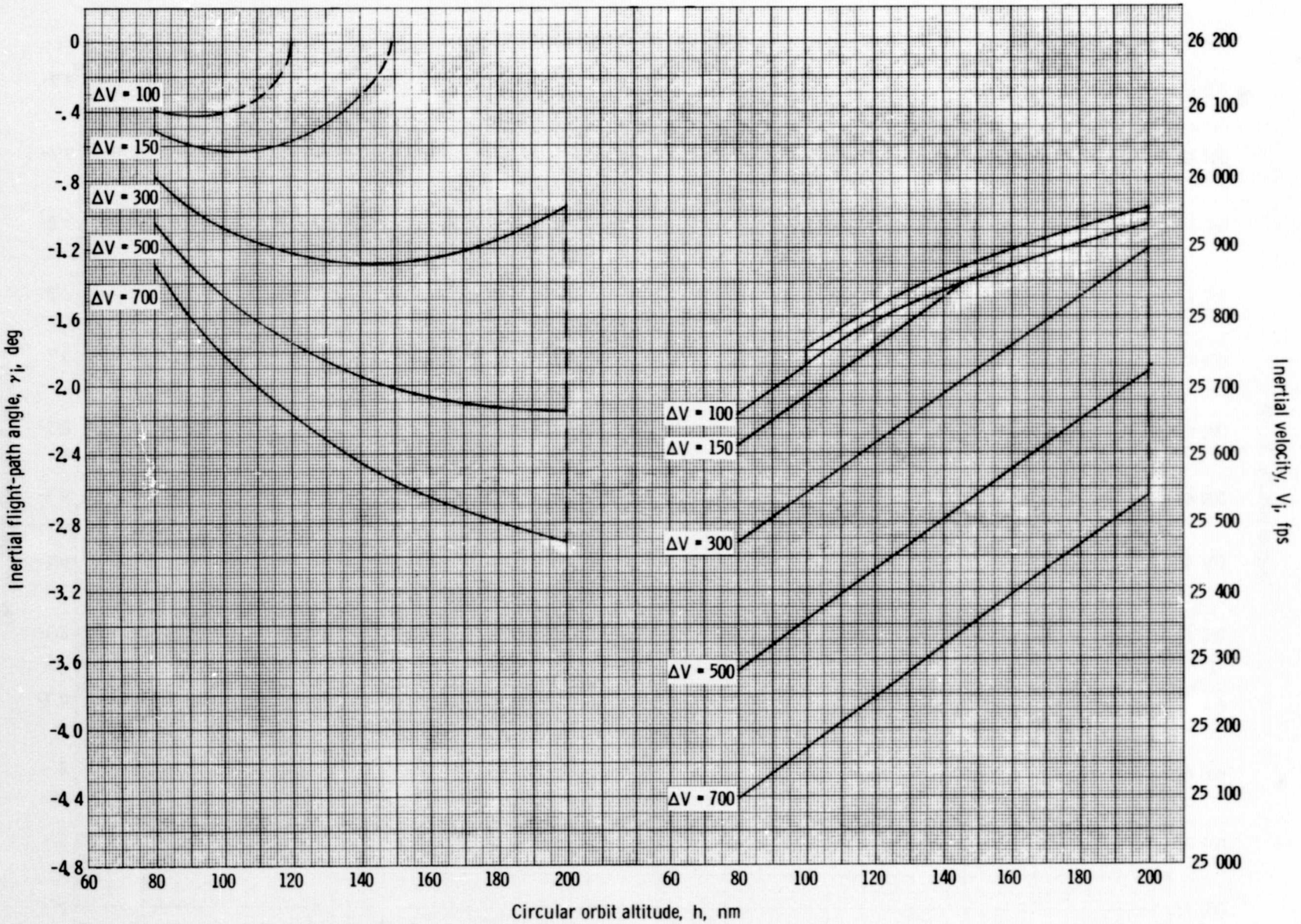

(c) Retrograde pitch angle, $\beta = 20^\circ$

Figure 39. - Continued.

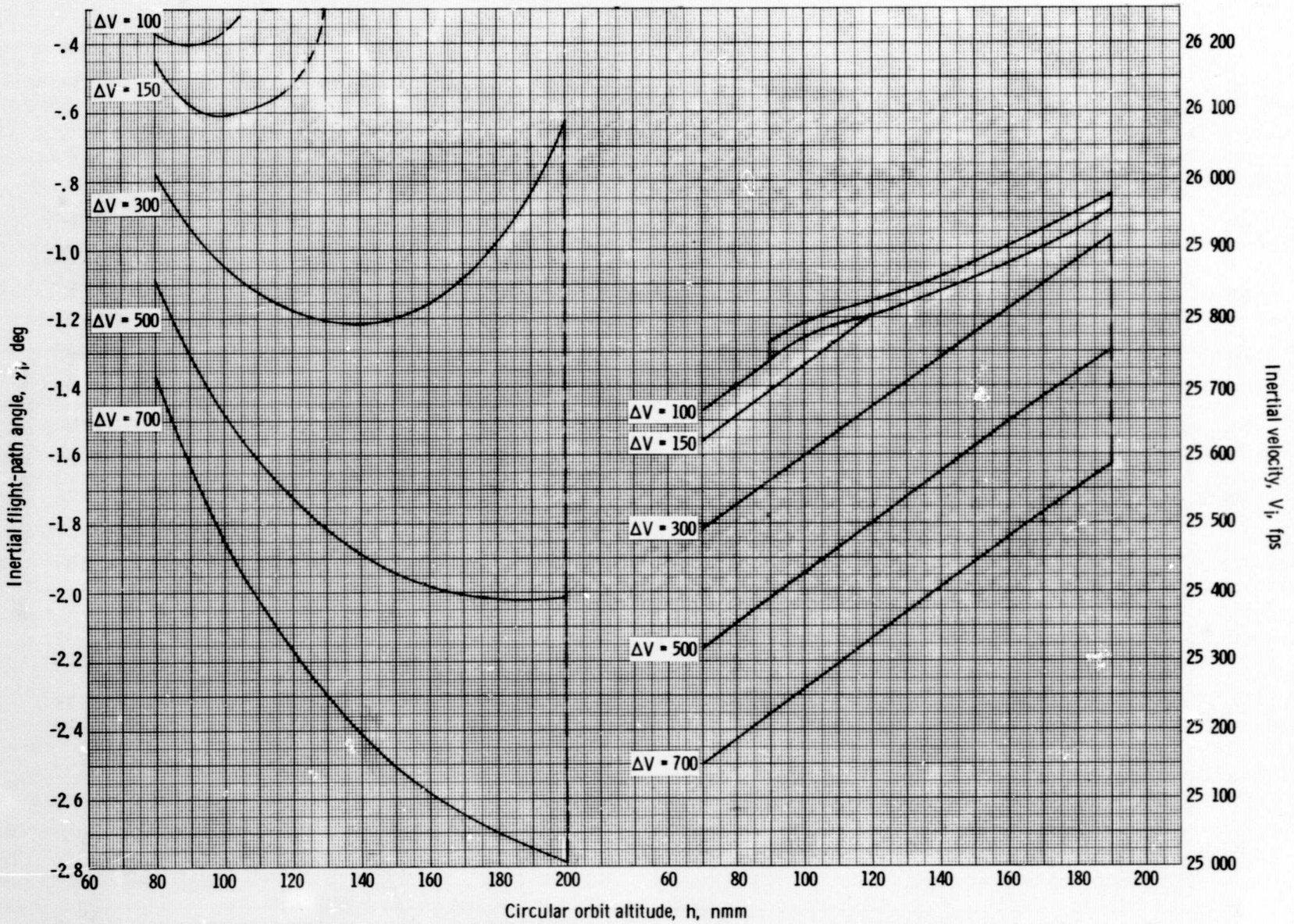

(d) Retrograde pitch angle, $\beta = 30^{\circ}$

Figure 39. - Continued.

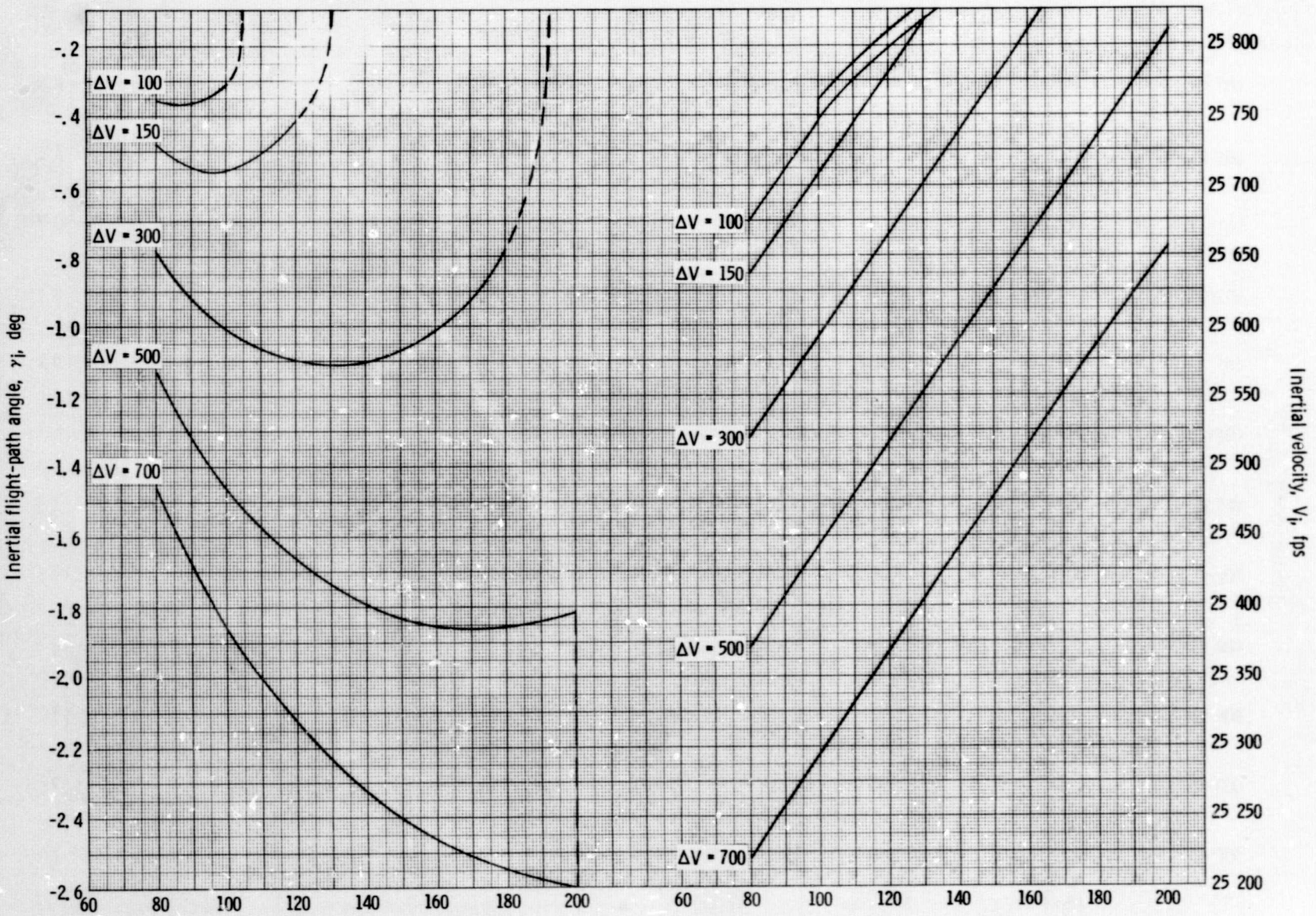

(e) Retrograde pitch angle, $\beta = 40°$

Figure 39. - Continued.

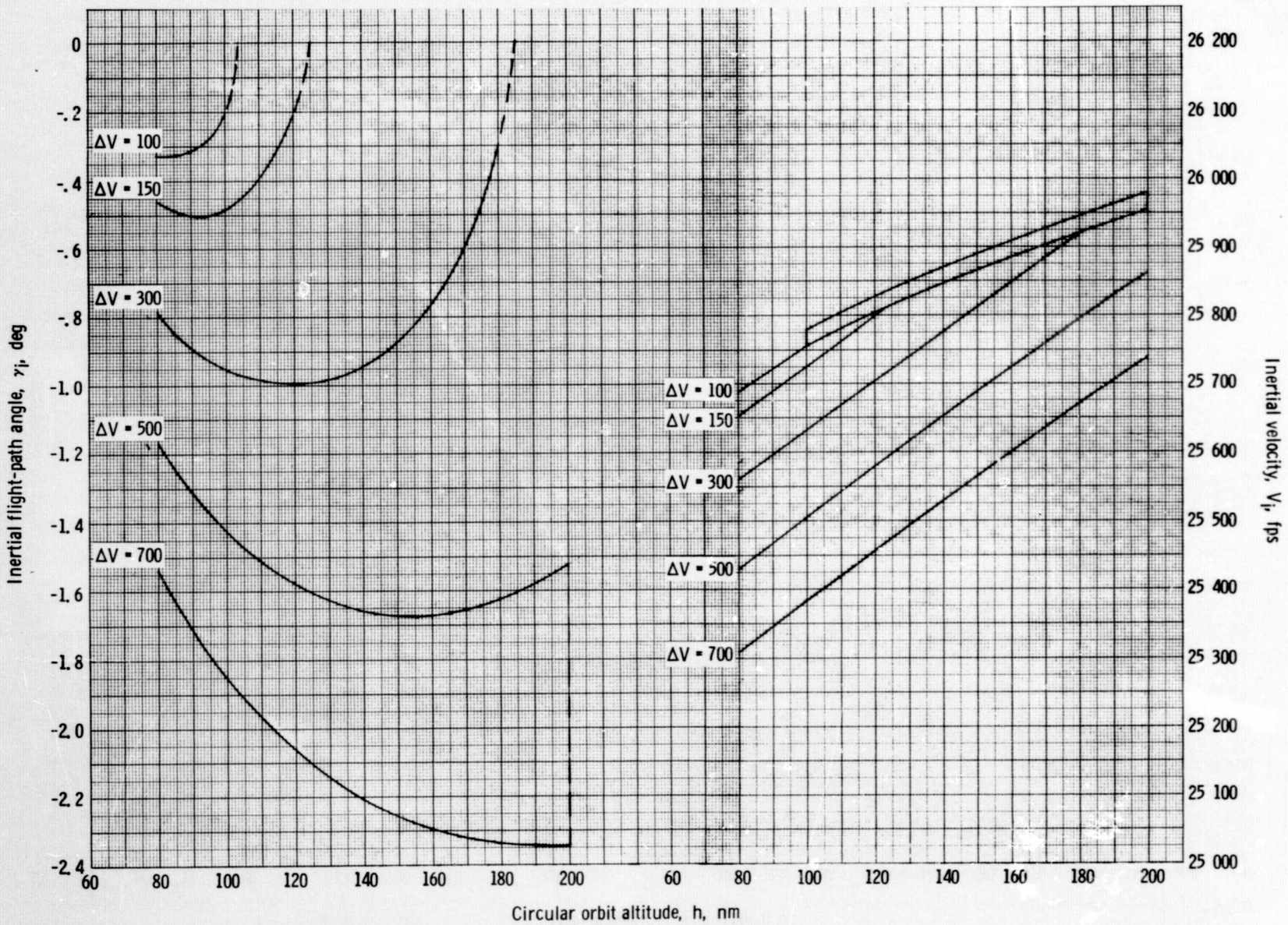

(f) Retrograde pitch angle, $\beta = 50^\circ$

Figure 39. - Continued.

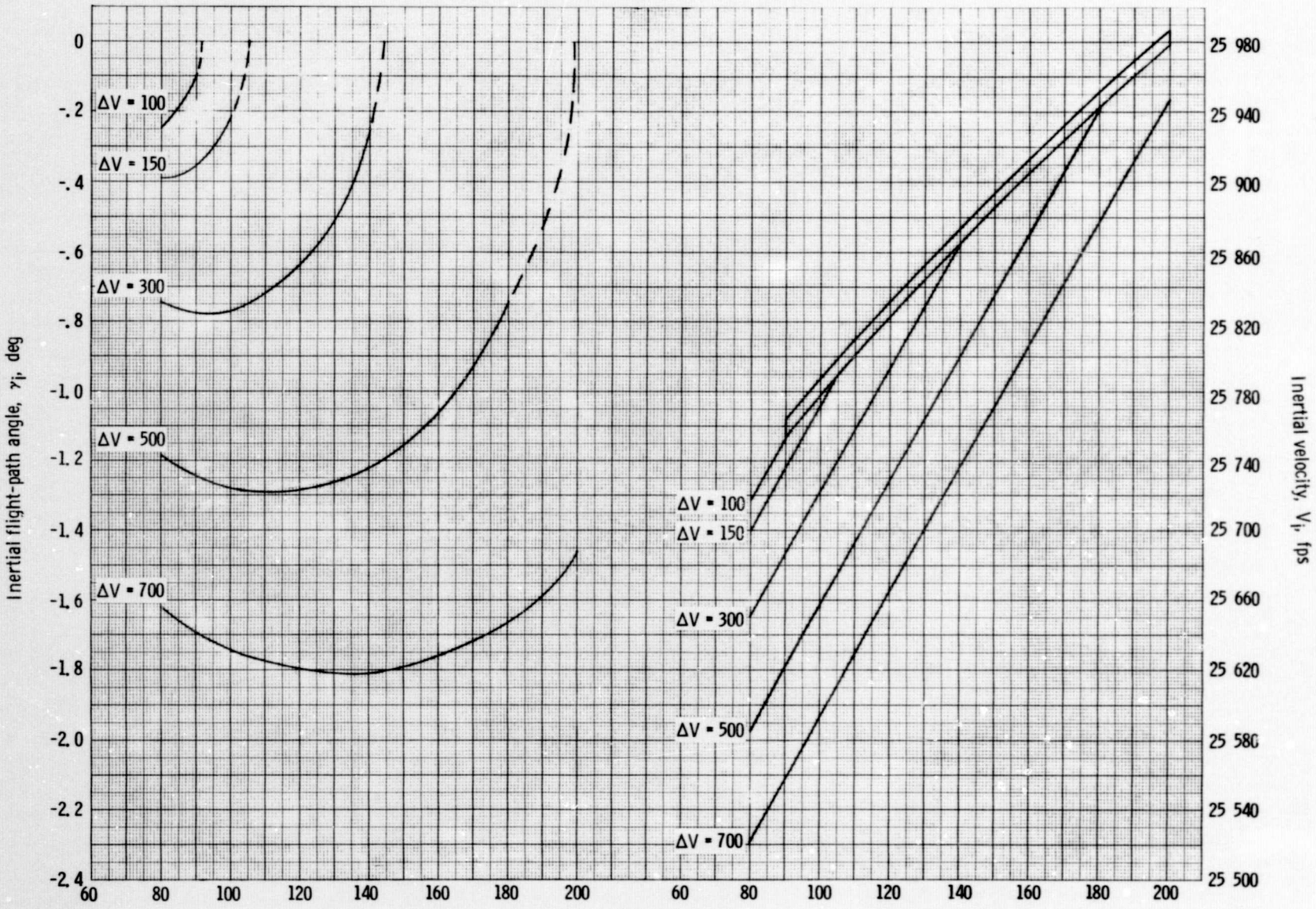

(g) Retrograde pitch angle, $\beta = 70^\circ$

Figure 39. - Concluded.

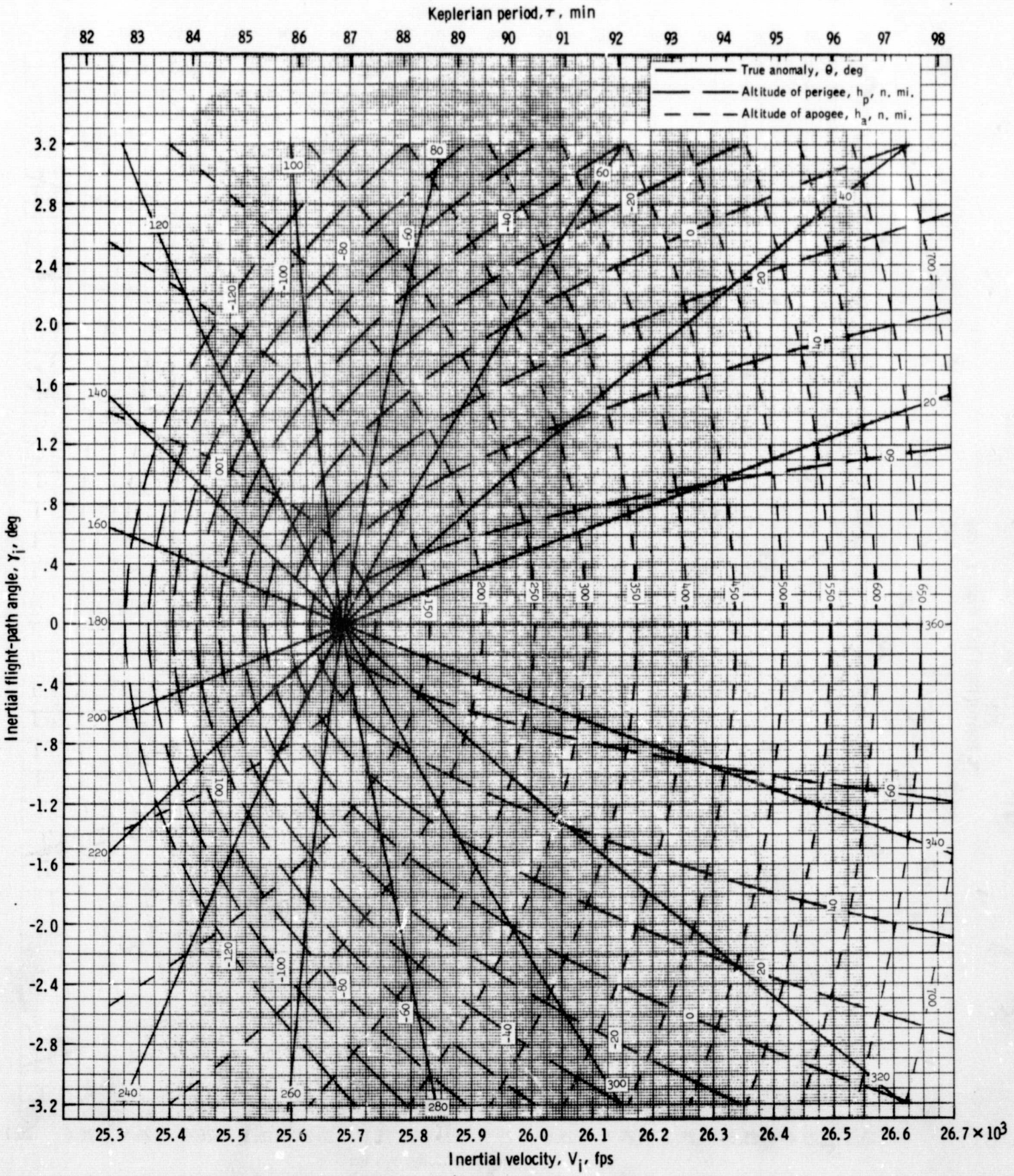

(a) 70 nautical mile altitude.

Figure 40.- True anomaly, apogee altitude and perigee altitude as a function of inertial velocity and inertial flight-path angle for various altitudes.

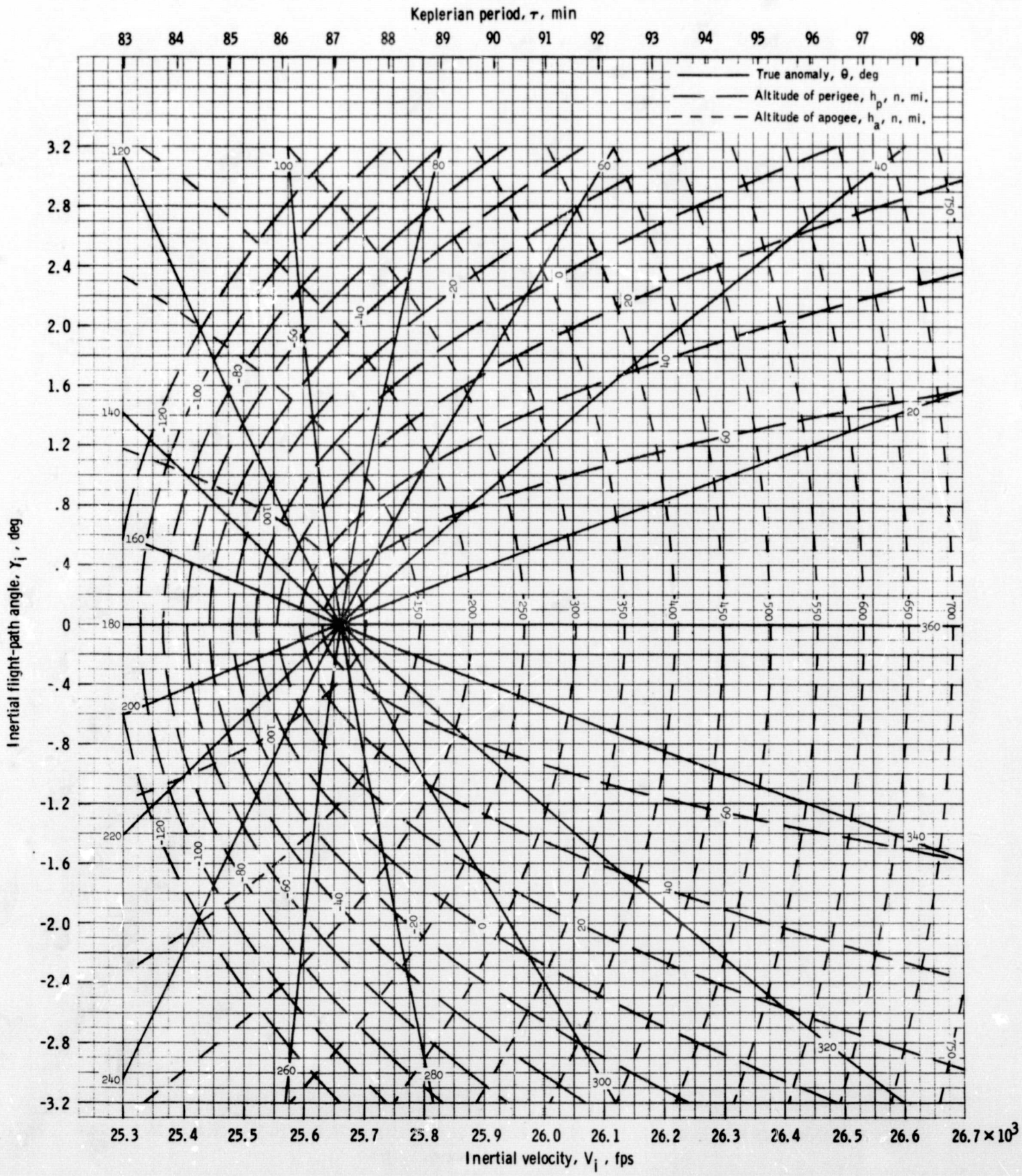

(b) 77 nautical mile altitude.

Figure 40. - Continued.

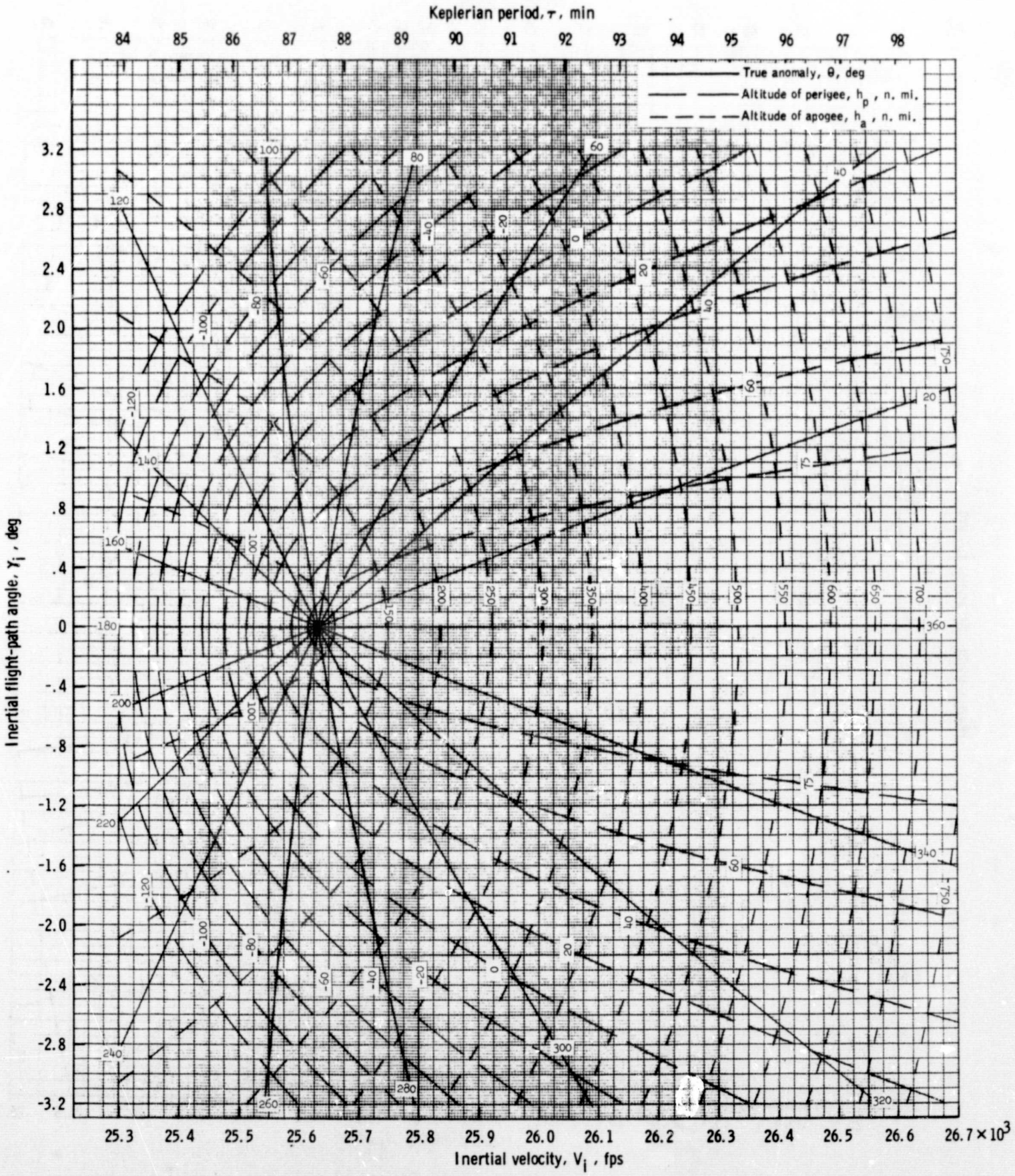

(c) 85 nautical mile altitude.
Figure 40. - Continued.

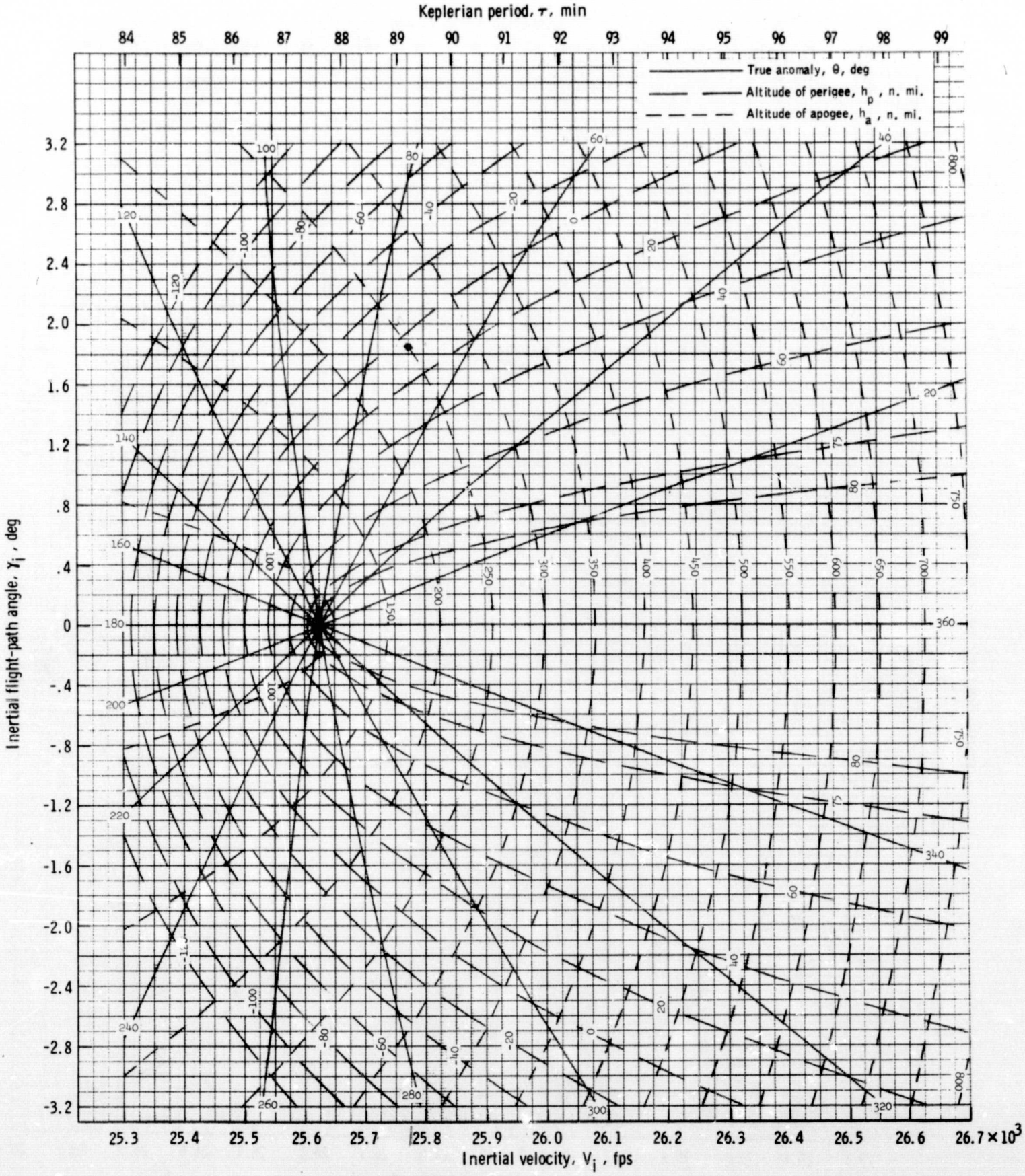

(d) 87 nautical mile altitude.
Figure 40. - Continued.

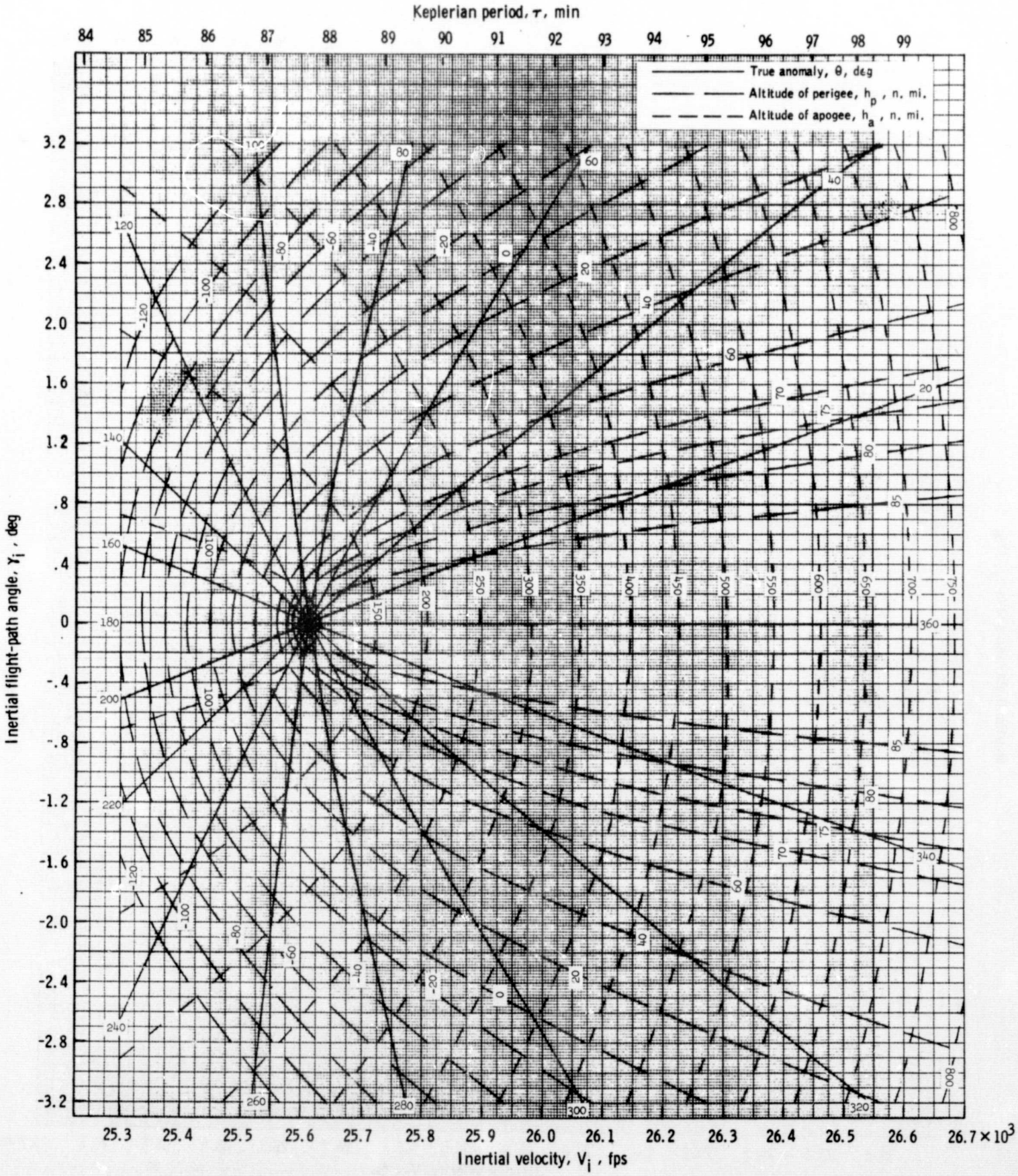

(e) 90 nautical mile altitude.

Figure 40. - Continued.

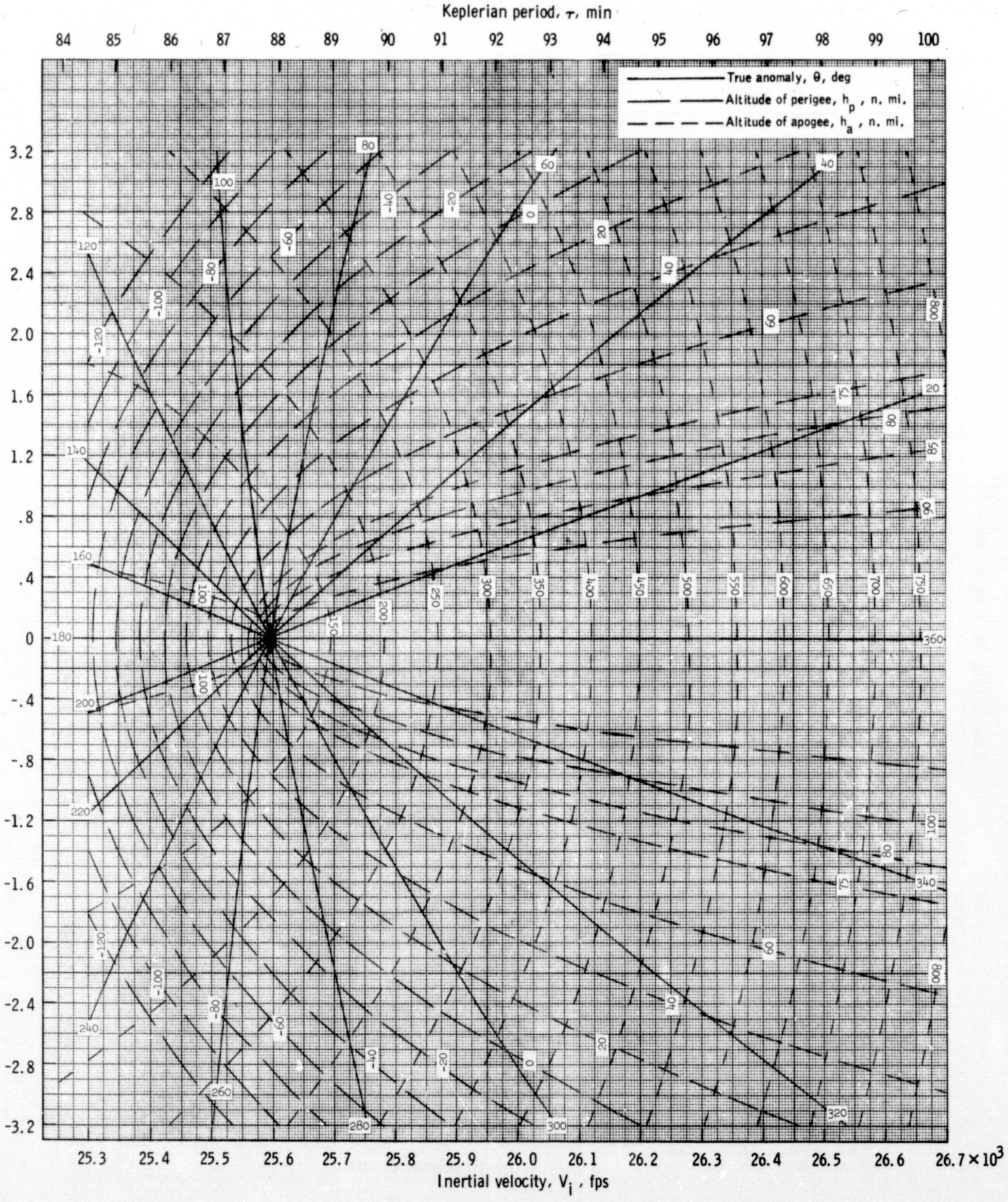

(f) 95 nautical mile altitude.

Figure 40. - Continued.

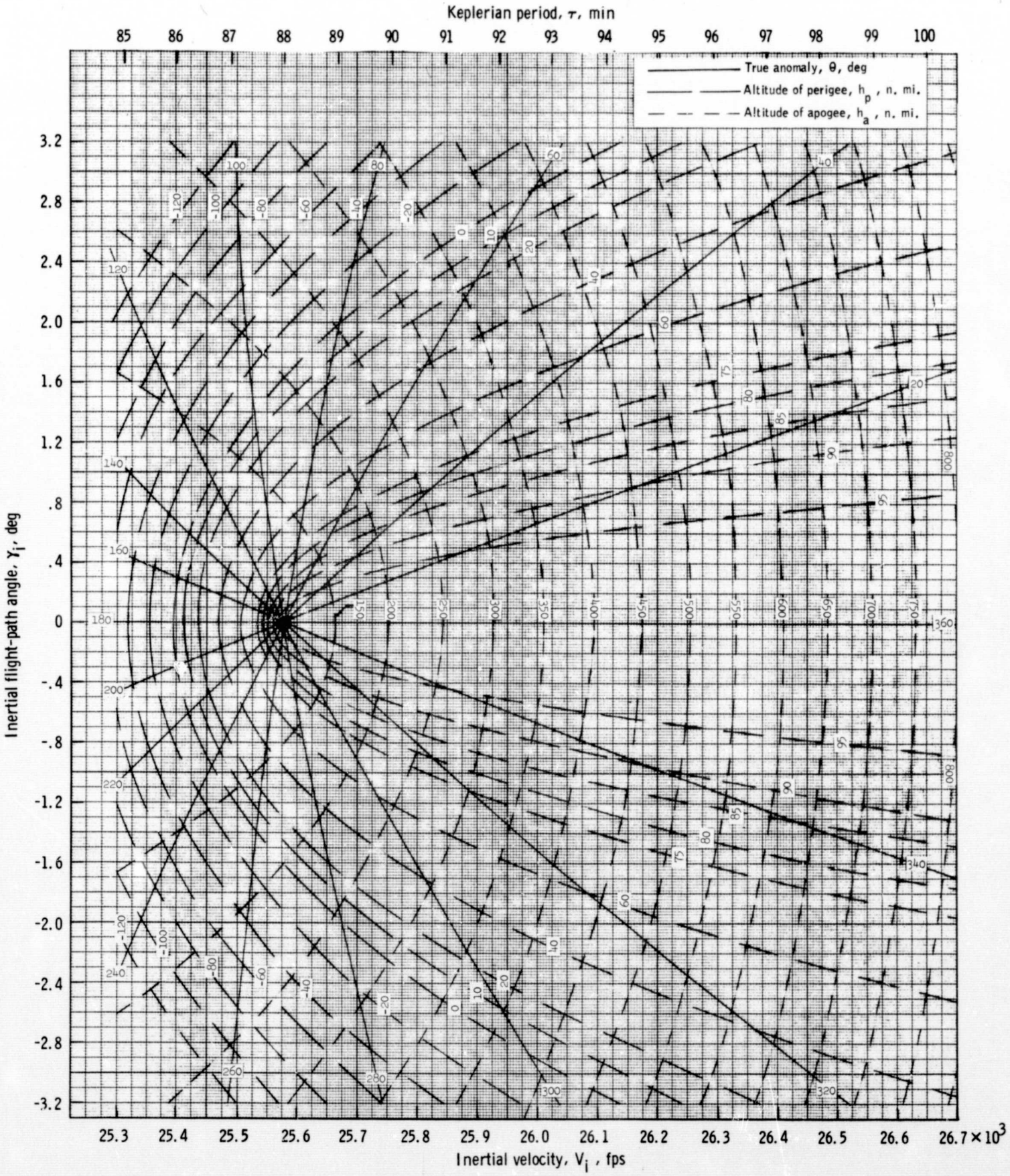

(g) 100 nautical mile altitude.

Figure 40. - Concluded.

6.0 ACKNOWLEDGMENT

The author acknowledges the assistance of Mr. C. R. Huss and Mr. W. R. Pruett for their support of this paper and the assistance of the Computer Operations and Math Aide Section of the Mathematical Physics Branch.